UNIVERSITY OF NOTTINGHAM

DOCTORAL THESIS

Automated Liquid Handling Systems for Microfluidic Applications

Author:

Solomon Idinyang

Supervisors:

Noah Russell

Sara Goodacre

A thesis submitted in fulfilment of the requirements
for the degree of Doctor of Philosophy
in the

Electrical Systems and Optics Research Group

School of Engineering

February 2017

Declaration of Authorship

I, Solomon Uri Idinyang, declare that this thesis titled, ‘Automated Liquid Handling Systems for Microfluidic Applications' and the work presented in it are my own. I confirm that:

- This work was done wholly or mainly while in candidature for a research degree at this University.
- Where any part of this thesis has previously been submitted for a degree or any other qualfication at this University or any other institution, this has been clearly stated.
- Where I have consulted the published work of others, this is always clearly attributed.
- Where I have quoted from the work of others, the source is always given. With the exception of such quotations, this thesis is entirely my own work.
- I have acknowledged all main sources of help.
- Where the thesis is based on work done by myself jointly with others, I have made clear exactly what was done by others and what I have contributed myself.

Signed:

_____

Date:

_____

“It started and so it must end"

SOLID

Abstract

Advances in microfluidic research have improved the quality of assays performed in micro-scale environments. Improvement of liquid handling techniques has enabled efficient reagent and drug use while minimising waste. The requirements for the applied techniques vary with applications and a custom integrated liquid handling solution was developed to accomplish some of these applications with minimal changes to the system. It is desirable to employ this technology to neuroscience research that requires a fluidic system that can test theories of reinforcement learning in neuronal cultures. An integrated system is therefore required to implement transport and manipulation of media and drugs loaded in a microfluidic device.

One requirement for such an integrated system for liquid handling is a transport mechanism to deliver reagents and nutrients to cultures. A liquid flow control system is required to allow precise and timely control of flow rates through a microfluidic device. This can be extended to enable more sophisticated drug delivery approaches like gradient generation, spatial drug distribution and high temporal resolution of the drugs delivered. Another requirement for an integrated system is a liquid loading system that is capable of inserting specified drugs into the flow line. Such a loading system would allow any number of drugs to be loaded during an experimental process to the microfluidic device containing cells as part of an assay. The integration of these systems will allow researchers take advantage of the combined systems. Software development process should also be undertaken to improve the modularity of the integrated system so that hardware changes have marginal effects on the system operation.

The project scope was the development of these liquid handling systems as well as their integration in hardware and software to enable their spatio-temporal drug delivery to neuronal cultures in microfluidic devices. The approach was to optimise

performance of custom liquid handling system which was developed to realise fast flow rate changes within 1 second interval.

Macro- and micro-scale solutions have been investigated in order to realise effective off-chip liquid loading capabilities. Emphasis has been placed on ease of use, modularity, rapid prototyping and precision. A commercial autoloader was identified as a starting point for sequential drug delivery. This was characterised for suitability and the constraints with this setup was used to identify additional requirements for the development of a novel sequential liquid injection system. The design process of the novel liquid injection system was unable to realise a working system due to mechanical and operational challenges encountered. A modular on-chip liquid manipulation system has been investigated and proposed to realise the sequential injection requirements. Rapid prototyping techniques that can promote ubiquitous microfluidic applications have been identified and verified.

An integrated liquid manipulation system has been developed using the commercial autosampler that enables sequential loading of agonists into the microfluidic device as well as reliable chemical signalling of the loaded drugs by switching flow rates of the inputs to the device. This system will be beneficial towards research of other cell types within other research fields requiring similar functionality.

Acknowledgements

I acknowledge God's presence in my journey throughout the PhD project for the strength, wisdom and perseverance given to push through the obstacles on the way.

I would like to appreciate my Parents throughout this period; for the financial support, prayers and encouragements that pulled me through to the end.

I would like to acknowledge the official sponsors of this PhD: The Niger Delta Development Commission (NDDC); and The Engineering and Physical Sciences Research Council (EPSRC).

I acknowledge my supervisors Dr Noah Russell and Dr Sara Goodacre who have contributed in support and guidance to the project development, project completion and thesis writing.

I also thank my fellows in the Nerophotonics Laboratory Research Group who have helped out with their time, assistance support, advice they have provided over the years and the collaborative efforts we have engaged in. Special thanks to Alexander Johnstone for his support and advice in device fabrication and COMSOL modelling. Many thanks to Hala Dhowre, Houda Sahaf for being good friends, keeping me sane through the years and the future plans for world domination.

Finally, a big thanks to my friends who have also encouraged me and kept me motivated throughout the period.

Contents

List of Figures

List of Tables

Abbreviations

AP	membrane separating the brain from the vascular environment
BPRS	Shipley BPR™ positive photoresist, used here to create gold patterns on glass
CAD	Computer Aided Design
CO_2	Carbon Dioxide (typically gas)
COMSOL	A multiphysics modelling software
DAQ	Data Acquisition (card), a signal processing unit permitting parallel computer control of laboratory apparatus
DI / dH_2O	Deionised / distilled water
DIV	Days *in vitro*, time cultured cells have been growing post-removal from the original organism
.dxf	Drawing Exchange Format, an image file type
FEM	Finite Element Modelling
FEP	Fluorinated Ethylene Propylene, a plastic
FITC	Fluorescein isothiocyanate, a fluorophore
FWHM	Full Width Half Maximum
G-SIS	Gatling-styled Sequential Injection System
GPTMS	(3-Glycidyloxypropyl) trimethoxysilane, an epoxysilane
HEK	Human Embryonic Kidney (cell line type)
HPLC	High Pressure/Performance Liquid Chromatography
Hz, kHz, MHz	Hertz, kilohertz, megahertz (frequency)
IPA	Isopropyl Alcohol, a solvent
IPSP	Inhibitory Post-Synaptic Potential
K^+	Potassium ion
LabVIEW	Laboratory Virtual Instrument Engineering Workbench, a visual programming language
LED	Light Emitting Diode
LTD	Long Term Depression
LTP	Long Term Potentiation
mA	milliamp
mbar	millibar, a pressure unit
MEA	Micro-Electrode Array
mg, µg	milligram, microgram: masses
MIF	Metal Ion Free
MPTS	(3-mercaptopropyl) trimethoxysilane (MPTS), a ligand
mPa	milli-Pascal, a pressure unit
mL, µL, nL, pL	millilitre, microlitre, nanolitre, picolitre: volumes
mm, µm, nm	millimetre, micrometre (micron), nanometre: lengths
mM, µM, nM	Millimolar, micromolar, nanomolar: molecular concentrations
ms	Millisecond
mV	milliVolt
MWCO	Molecular weight cut-off
N_2	Nitrogen (typically gas)
Na^+	Sodium ion
NTC	Negative Temperature Coefficient
O_2	Oxygen (typically gas)
OSTE	*Off-stochiometry thiol-ene*, a thiol-allyl polymer
PCB	Printed Circuit Board
PCTE	Polycarbonate

PDMS	poly(dimethylsiloxane), an elastomer
PE	Polyester
PEEK	Polyethylethylketone, a plastic
PEI	Polyethylenimine, a ligand
PET	Polyethylene Terephthalate, a plastic
PID	Proportional-Integral-Derivative, a feedback control method
PDL / PLL	Poly-D-Lysine and Poly-L-Lysine, cell attachment lignads
PS	Polystyrene
PVA	Polyvinyl Alcohol
PWM	Pulse Width Modulation
RMS	Root mean square
ROI	Region of Interest (in an image)
RPM	Revolutions per minute
SH-SY5Y	Human-derived cell line (often called ‘sushi’)
SiN	Silicon Nitride
SiO_2	Silicon Dioxide
SLAB	Simple Living Artificial Brain
SLM	Spatial Light Modulator
SNR	Signal to Noise Ratio
SPR	Surface Plasmon Resonance
STD	Standard Deviation
STDP	Spike Timing Dependent Plasticity
Ti	Titanium (element)
TiN	Titanium Nitride
UV	Ultraviolet, wavelengths in the range 100 to 400nm
VI	Virtual Instrument, a LabVIEW program element

1. Introduction and Literature Review

1.1 Thesis Overview

Precise control of fluid handling is a key requirement for many biomedical applications. A great many of these involve the controlled delivery and removal of substances such as agonists that interact with cultured cells to induce behaviour (like GABA or Carbachol), or to highlight their activity (example calcium imaging) and nature (example is protein specific staining). Precise volumes of media containing particular agonists can not only be delivered to the cultured cells, but can later be removed and sampled in order to assess what molecules the cells have excreted in response to their environment. Delivery of substances and subsequent sampling are respectively referred to in this work as 'upstream' and 'downstream' operations.

Automating these processes in a manner that permits the same software and equipment to perform many different types of fluid handling interaction with precision would be of considerable value to biological researchers.

Upstream loading operations will allow delivery of different agonists to the cell cultures to perform chemical stimulation or inhibition of cellular activity These loading operations will also enable protocols such as calcium imaging to be performed in addition to immunocytochemical assays and live-dead staining of cells. The automation process will reduce variability and increase repeatability of the procedures.

Downstream automated fluid sampling could enable mass spectrometry analysis to be performed to identify consumed or secreted molecules. Another potential example of downstream analysis is characterisation of the transcriptome. This can be performed by isolating, amplifying and identifying RNA molecules from the sampled fluid. This procedure can give information on levels of genes expression within the cell culture.

Such experiments can be of long duration and wasteful of reagents if performed using standard cell culture equipment, and also may have unintended discrepancies due to slight variation in manual preparation by the experimenter. This is particularly true of open bath applications where the delivery is reliant upon diffusion of the applied agonist and where the initial volume of buffer may be fractionally different for each culture.

Thus a system capable of ensuring that a repeatable volume of agonist is delivered into a cell culture region of known, fixed volume on a repeatable timescale is extremely valuable. Such a system that delivers minimal volumes and requires minimal supervision from the experimenter will allow many more experiments to be completed in less time and using fewer resources.

The adoption of microfluidic approached in biomedical research has contributed to advances in the repeatability and quality of long term assays. The confinement of biological cells to microscale environment allows efficient reagent utilisation due to the reduced volumes required.

Microfluidic technology can also allow long term observation of cultured cells in the device by providing constant perfusion of media, drugs and reagents to the cells without interrupting the flow or disrupting the cultures. It is difficult to achieve precise agonist-exposure manually without introducing air bubbles into the device or disrupting the flow, thus, the need for an automated fluid handling system.

Of particular interest to the Neurophotonics Laboratory (NPL) at the University of Nottingham, is both up- and down-stream precision fluid handling for cultured neuronal networks. Deciphering how the brain encodes and stores information, and how networks of cells can dynamically alter the signal pathways between cells in response to external cues, is crucial to understanding behaviour and learning. Figure

1-1 shows the overview of the real-time system for long term conditioning, stimulation and monitoring of neuronal cultures.

Neurons exchange neurotransmitters at synapses to communicate and when enough incoming synaptic signals arrive at one neuron an action potential is induced. The ability to dynamically stimulate, inhibit and modulate this information transfer is key to further understanding the how complex information is encoded in the signals in neuronal networks.

A liquid handling system is required therefore and must be integrated with other sensing and recording technologies. The fully integrated liquid handling system should allow perfusion of growth media to these cultures. This system will also need to allow sequential delivery of different agonists required during the study. This system will also be required to enable real-time dynamic control of chemical stimulation patterns and chemical gradient patterns to these cultures.

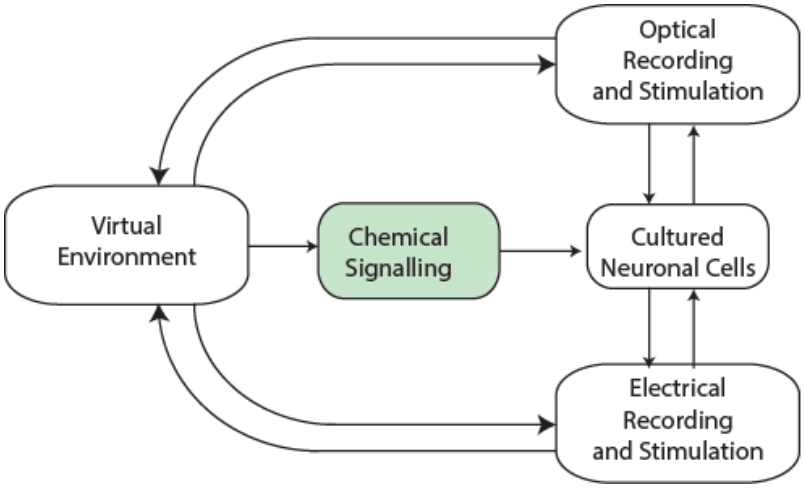

Figure 1-1: Real time neuronal culture monitoring system with incorporated chemical stimulation
The needs of the Neurophotonics laboratory for long term monitoring of neuronal cells requires a nutrient and drug delivery system capable of dynamic control of spatiotemporal drug deliver in a microfluidic device..

1.2 Aims and Objectives

The primary objective of this thesis is to implement a robust, scalable and modular and highly integrable automated fluid handling system (AFHS) for microfluidics application and to apply the AFHS to demonstrate upstream and downstream applications for cell cultures. This involves the development of a system capable of very precise spatiotemporal control of drug delivery, and in particular the application of this to cultured neurons, which due to the complex problem of in vitro neuronal culture, explained in detail later, are a particularly difficult cell type to work with in vitro.

This research will integrate a liquid handling system with a microfluidic device that will enable long term upstream loading operations and downstream sampling operations from the cells. Nutrients from the media are consumed and signalling molecules are secreted by the cells in the microfluidic device.

The research will achieve the aims by developing the liquid handling system, integrating the system and applying the system in exemplar applications that demonstrate both its functionality and precision.

The development objectives are to assess and/or build a mechanism that is capable of inserting micro litre liquid samples into another flowing liquid; develop a feedback control system to regulate the flow of the transported liquid; design a computer control interface for user manipulation of flow rates and sampling operations; evaluate the accuracy and precision of the sampling and volume delivery functionalities.

Integration of the system will combine this flow control system, injection and sampling with a microfluidic system; quantify fluid dynamic properties and the characterise the effects of the flow on the effective drug concentrations at the device; assess stability

of the system and flow disruption due to system operation; optimise flow control system to meet requirements of the temporal and spatial drug delivery.

The larger scope for the application of a robust liquid handling solution in neuroscience to enable researchers carry out experiments that could provide information on information coding in the brain is justified. The use of microfluidics technology in life science research to facilitate this type of research will be discussed in more detail and will be comprised of the development of devices and fabrication techniques. This will then be succeeded by discussion on fluid dynamics in in microscale. Liquid handling systems for microfluidic applications will be treated with emphasis given to macro-scale systems. Example applications that could be performed with such systems are also presented. More information is provided on the technological requirement for effective integration of developed liquid handling components in hardware and software.

1.3 Microfluidics for Life Science Research

The ability to deliver agonist volumes to micro cultures on effective timescale requires an accurate and precise automated system that allows the experimenter to transport growth media to these cultures and replace these media with drugs and reagents when required in the experimental protocols. Advancements in liquid handling technology has improved research in life science and pharmaceutical research (Hung, Lee et al. 2005). High throughput assays can be performed using multiplexed devices like array bioreactors and microtiter plates. The limitations of these systems include high system cost and difficulty integrating with other laboratory functions such as long term culture maintenance, custom sensors, real-time observation and analysis (Ho and Tai 1998, Stone and Kim 2001, Squires and Quake 2005). An example is the long term neuronal culture maintenance, stimulation and

recording electrodes for neuronal culture monitoring. This has sparked research into improved liquid transport and manipulation for research involving *in vitro* cell analysis using microfluidic technology (Quake 2007).

Microfluidics is a well-established field (Whitesides 2006) combining engineering, nanotechnology, biotechnology, fluid dynamics, chemistry to develop practical systems and applications for manipulation of fluids in low volumes, typically in micrometre scale devices (Tabeling 2005, Nguyen and Wereley 2006, Volpatti and Yetisen 2014). The application of microfluidics approaches extend to fields such as chemical engineering where chemical assays can be performed in small scale; development of microelectromechanical systems (MEMS) for development of miniature sensors, actuators and micro structures. The biomedical field has also benefited from microfluidic technology where reducing macro-scale cultures to microscale environments for improved liquid handling and efficient reagent utilisation and reduced waste.

Advances in the field spanning twenty years has resulted in varied applications such as suitable environment for growing and maintaining cell cultures. It has also provided new technologies that enable researchers perform automated bioassays efficiently on these maintained cultures (Teh, Lin et al. 2008, Ng, Uddayasankar et al. 2010). This is typically realised through the application of fluid control components with macro and micro-sized liquid manipulation components; liquid sampling techniques (Whitesides 2006, Xiao, Niu et al. 2012) and complex microfluidic chips. This incorporation of fluid handling and analysis capabilities for microfluidic chambers is commonly termed “lab-on-a-chip” or “miniaturised total analysis system - μ-TAS”. The attractive advantage is the ability to replace bulky laboratory equipment with easily disposable lab-on-a-chip systems in biomedial and pharmaceutical research (Timoney and Felder 1999, Neuži, Giselbrecht et al. 2012).

One advantage of these microfluidic systems is the ability to implement perfusion of media and drugs to cells in the devices (Leclerc, Sakai et al. 2003, Hung, Lee et al. 2005). It has been established that transport of media and growth factors into the microfluidic devices is required to maintain the housed cells just as is required in petri-dish cultures where regular media change is performed. A study was performed to assess mammalian cell activity in microfluidic devices maintained two sets of microfluidic devices, both with liver cells, but only changed the media to one set. It was found that cells without media change died “rapidly” (Leclerc, Sakai et al. 2003). Another study using HeLa cells claims that the cells in the device without perfusion died and detached from the device substrate after 4 DIV (Hung, Lee et al. 2005). The study also showed that flow orientation affected cell growth. Typical flow rates recommended for perfusion in microfluidic devices cannot be compared directly as due to varied device geometry. Wildly different flow rates have been quoted such as HeLa cells with 120nl/min (Hung, Lee et al. 2005) and 5000-20000nl/min were suggested for hepatocarcinoma cells (Leclerc, Sakai et al. 2003). The flow rate may be given as a function of induced wall shear stresses on the cells and the channel dimensions where these values are given (Wang, Jedlicka et al. 2014). A detailed formulation for velocity in a microfluidic channel which accounts from interfacial stresses has been derived (Barbati, Fang et al. 2013). Lower flow rates have also been reported as linear velocities over the cells in the channel such as 49 μm/s (2.45pL/s) in a device with unspecified dimensions (Kumamoto, Kitahata et al. 2015). This device, however, bears striking resemblance to a commercial chip (SND 450, Xona Microfluidics). Another study recorded 1.6 – 14 $\mu m.s^{-1}$ flow rates in a channel with width x height (0.033 x 0.046) which equals to volume flow rates of 0.0024 – 21 $nL.s^{-1}$ (Millet, Stewart et al. 2007).

These wide gaps in recommended flow rates may also be dependent on the cell type. Cells that require regular media change in static cultures should be maintained

at higher volume flow rates during perfusion in contrast to cultures requiring less nutrient change (Kim, Toh et al. 2007).

Applications of microfluidic devices include cell separation for single cells analysis (Wang, Yang et al. 2000, Kuczenski, Chang et al. 2011), high throughput analysis and mass spectrometry (Kamholz and Yager 2001). These devices are useful for drug discovery in pharmaceutical and biomedical research (Stone and Kim 2001). Its increasing use in research communities stems from the ability to construct these devices within laboratory environments (Whitesides 2006).

A microfluidic device confines the area for cell presence to few mm^2 (Balagaddé, You et al. 2005, Quake 2007) Considering the typical sizes of cells (10-20um diameter) the area required for hundreds of cells to grow is no more than 4 mm^2. Due to the small reaction space in microfluidic devices, there is a reduction in the volumes required for bio-analysis and reactions occur faster. This further reduces waste of costly reagents used (Beebe, Mensing et al. 2002). Another advantage of this micro devices is the preferred laminar flow of culture medium to the cells (Soe, Nahavandi et al. 2012).

A disadvantage to microfluidics is the need to re-evaluate volume densities, perfusion media consumption rate, development rate for cell lines where this data is unavailable (Halldorsson, Lucumi et al. 2015). Most of the other disadvantages revolve around the use of polydimethylsiloxane (PDMS) for fabrication. This material as will be discussed is preferred for its optical, non-toxic properties but its disadvantage lies in its potential for non-bio-compatibility, molecular absorption formation of artifacts due to interactions occurring in cultures as well as formulation used during device fabrication (Wang, Douville et al. 2012). Surface treatment is often required to mitigate these unwanted challenges to bio-compatibility and molecular absorption. Its gas permeability is also a challenge to its use as CO2 and O2 levels in the cell environment must be checked to ensure they are appropriate

levels. PDMS is known to swell when exposed to typical solvents and this effect is more pronounced with high-solubility solvents like Benzene and Pentane (Lee, Park et al. 2003). These disadvantages, though localized to PDMS, further affects the increased use of microfluidics in biological applications (Halldorsson, Lucumi et al. 2015).

Despite the advantages from using microfluidic technology, there is still a small scale adoption in laboratories that do not specialise in microfluidic technology. A typical study showed that only 9% of publications using microfluidic technology in 2011 were products of biomedical research (Sackmann, Fulton et al. 2014). Factors responsible for this low adoption include biocompatibility issues with the materials used; complexity of fabricating intricate microfluidic device designs and control equipment to realise advanced liquid handling in these devices (Araci and Brisk 2014, Sackmann, Fulton et al. 2014). Another factor is the lack of standardisation of custom solutions for interfacing and fluid handling (Becker 2010). Many researchers are aware that microfluidic technology only improves on well-established macro scale techniques and require a similar level of operational complexity to jump on the moving microfluidic wagon. A list of companies that provide established and custom microfluidic devices are presented in a study (Halldorsson, Lucumi et al. 2015).

Development of microfluidics based systems for life science research requires understanding of the fluidic dynamics in microscale as well as the materials and fabrication techniques used to develop these micro-scale systems.

1.4 Fluid Dynamics

Fluids can be defined as materials that undergo deformation due to an applied shear stress (White 2008). The term typically describes liquids and gases. They can be either compressible or incompressible, referring to the relative volume change of the

fluid with an applied pressure. Incompressible fluids have a linear relationship between the applied stresses and the flow rates (Boon, Yip et al. 1988, Kundu, Cohen et al. 2012).

The equation for incompressible flow are derived from a solution of Navier-Stokes equations given in Equation 1.1. The equation represents conservation of momentum and are solved with the continuity equation that represent the conservation of mass.

If we define an arbitrary volume stationary within a fluid flow as illustrated in Figure 1-2, we can say the mass flow into the volume less the mass flow out of volume is equal to the time rate of change of the mass within the volume shown in Equation 1.2. Fluid flow depends on the fluid properties, the forces acting on the fluid and the flow channel properties (White 1991).

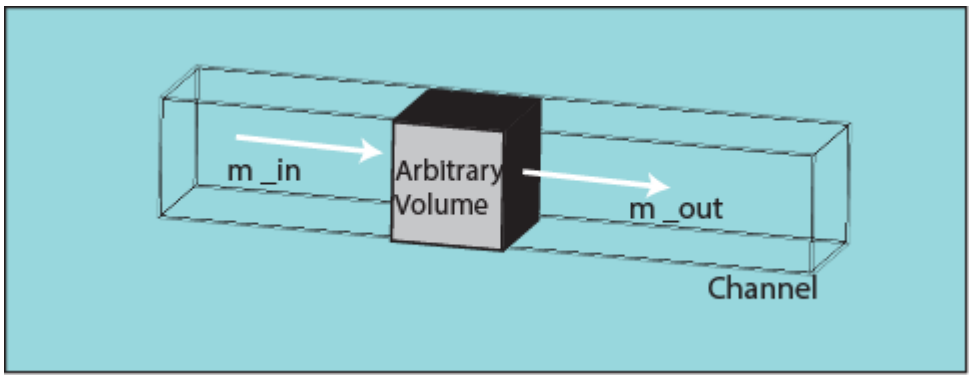

Figure 1-2: Arbitrary volume within a fluid flow

$$m_{in} - m_{out} = \frac{dm}{dt}$$ Equation 1.1

$$\rho\left(\frac{\partial u}{\partial t} + u.\,\nabla u\right) = -\nabla p + \nabla.\left(\mu(\nabla u + (\nabla u)^T) - \frac{2}{3}\mu(\nabla.u)I\right) + F$$ Equation 1.2

Inertial forces = pressure forces + viscous forces + external forces applied to the fluid

Where:
- u = fluid velocity
- p = fluid pressure
- ρ = fluid density
- μ = dynamic viscosity
- I = Identity matrix
- F = external forces applied to the fluid

The fluidic resistance is derived from the solution to the set of governing equations for fluid flow (Beebe, Mensing et al. 2002). These solutions are described in Equation 1.3 for fluid flow and Equation 1.4 for fluidic resistance in fluidic channels. For flow in fluidic channels, the fluidic resistance is dependent on the cross-sectional area, viscosity μ; and the length of the channel which shows fluidic resistance for a circular tube with radius, r. The solution is different for rectangular channels with different aspect ratios. Low aspect ratios where the width is almost equal to the height (w ≈ h) have the solution presented in Equation 1.5 and for rectangular channels (w << h or h << w) with high aspect ratio, the fluidic resistance is defined in Equation 1.6 (White 1991, Kovacs 1998, Beebe, Mensing et al. 2002). This may have implications for microfluidic channel designs as well as tubing used in microfluidics.

$$Q = \frac{\Delta P}{R}$$ Equation 1.3

$$R_c = \frac{8\mu l}{\pi r^4}$$ Equation 1.4

$$R_{low\ a.r} = \frac{12\mu L}{wh^3}\left[1 - \frac{h}{w}\left(\frac{192}{\pi^5}\sum_{n=1,3,5}^{\infty}\frac{1}{n^5}tanh\left(\frac{n\pi w}{2h}\right)\right)\right]^{-1}$$ Equation 1.5

$$R_{high\ a.r} = \frac{12\mu L}{wh^3}$$ Equation 1.6

Where:
- ΔP = pressure drop in the channel;
- Q = flow rate;
- L = channel length;
- R = Fluidic resistance in the channel;
- μ = fluid viscosity
- r = radius of the circular channel
- R_e = fluidic resistance in a circular pipe
- $R_{low.a.r}$ = fluidic resistance in a low aspect ratio rectangular channel

$R_{high\ a.r}$ $R_{high.a.r}$ = fluidic resistance in a high aspect ratio rectangular channel

w = width of the channel
h = height of the channel

Flow in a pipe or channel can also be characterised by the velocity and viscosity properties of the fluid. The Reynold's number is used to characterise the flow as turbulent or laminar flow. Turbulent flow regime exists above Reynold's number, higher than 2400 (Avila, Moxey et al. 2011), characterised by higher fluid velocities and larger channel geometries while laminar flow dictates the properties of the flow below the threshold.

Laminar flow is illustrated in Equation 1.7 where there are no cross-currents, eddies or fluid swirls and all the particles move parallel to the channel walls (Douglas, Gasiorek et al. 1979, Douglas 2005, White 2008, Kundu, Cohen et al. 2012). The fluid flows in parallel streamlines (or layers) without lateral mixing. This is the characteristic flow in microfluidic devices (Lin, Yu et al. 2012). Laminar flow effects includes Poiseuille flow, Taylor Aris dispersion which affects the behaviour of loaded volumes in a microfluidic device.

$$R_e = \frac{D_h v \rho}{\mu} \qquad \text{Equation 1.7}$$

$$D_h = \frac{4A}{P} \qquad \text{Equation 1.8}$$

Where:
D_h = diameter of the tube
v = mean fluid velocity (m/s); not to be confused with kinematic viscosity, ν
ρ = density of the fluid (kg/m^3)
μ = fluid dynamic viscosity (Pa.s)
A = cross sectional area
P = wetted perimeter of the cross section

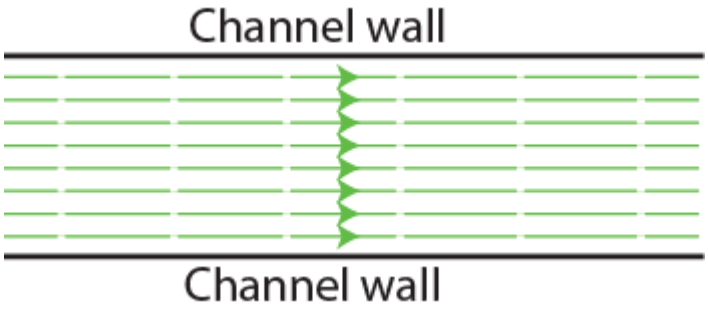

Figure 1-3: Illustration of parallel streamlines of laminar flow within a channel.
The streamlines shown do not interact with each other and stay parallel all through the pipe length.

1.4.1 Poiseuille flow

The linear profile of a volume in a pipe will be referred to as a plug for the throughout this thesis. Ideally, a flat interface exists at the boundaries of this plug that will be maintained when while the volume is under flow. The fluid velocity is assumed to be constant across the pipe cross-section.

One characteristic effect of laminar flow includes Poiseuille flow named after Hagen–Poiseuille, who showed that there is a non-uniform pressure drop across the cross section of a fluid flowing in a channel (White 2008). As the fluid progresses along a channel, the speed is faster at the centre of the tube cross section than at the walls. This results in the development of a parabolic flow profile of the fluid as it travels through the pipe. This is illustrated in Figure 1.4 (Douglas, Gasiorek et al. 1979). The equation for Hagen–Poiseuille flow shown in Equation 1.9 can be used to show the developed parabolic velocity profile for a fluid that has travelled a distance through a pipe.

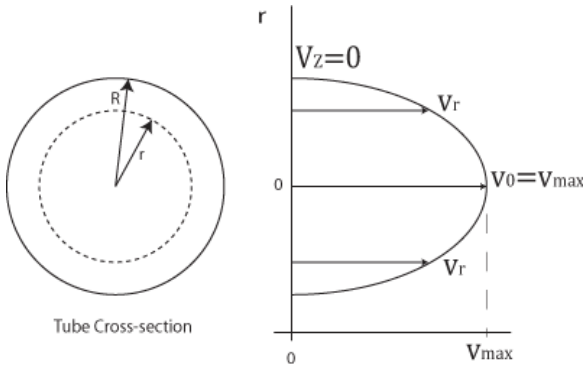

Figure 1-4: Velocity profile for laminar flow in cylindrical channel
Fluid flow in a cylindrical pipe is shown with non-uniform velocity attributed to the non-uniform pressure drop across the pipe's cross-section.

$$v_z = \left(-\frac{dp}{dz}\right)\frac{1}{4\mu}\left(R^2 - r^2\right) \qquad \text{Equation 1.9}$$

Where: v_z = fluid velocity

dp = pressure drop

dz = change in distance

μ = fluid viscosity

R = tube radius

r = radius of interest

1.4.2 Taylor-Aris Dispersion

Diffusion is a random motion of molecules in solution which results in movement of solute particles from a region of high concentration to low concentration (Bruus 2007). The parabolic flow profile combined with diffusion causes the solute in a section of fluid with different composition concentration to spread along the channel (Taylor 1953). This effect is illustrated in Figure 1-5 where a solution of specific concentration C_s is injected into a flow channel with zero concentration of the solute like water. As the plug of liquid travels down the channel, it is affected by non-uniform pressure which causes the parabolic profile. The concentrated sections then mix with the sections where there is no solute to form a uniform concentration at the cross-section. The effect of these combined phenomena is the broadening of the drug plug with reduced concentration at the boundary of the plug. A thorough derivation of the diffusion equations due to Taylor dispersion results in an effective diffusion coefficient D_{eff} (Aris 1956). Taylor Aris dispersion equation that shows the time taken to broaden the width of a sample by length (w) is given in Equation 1.10.

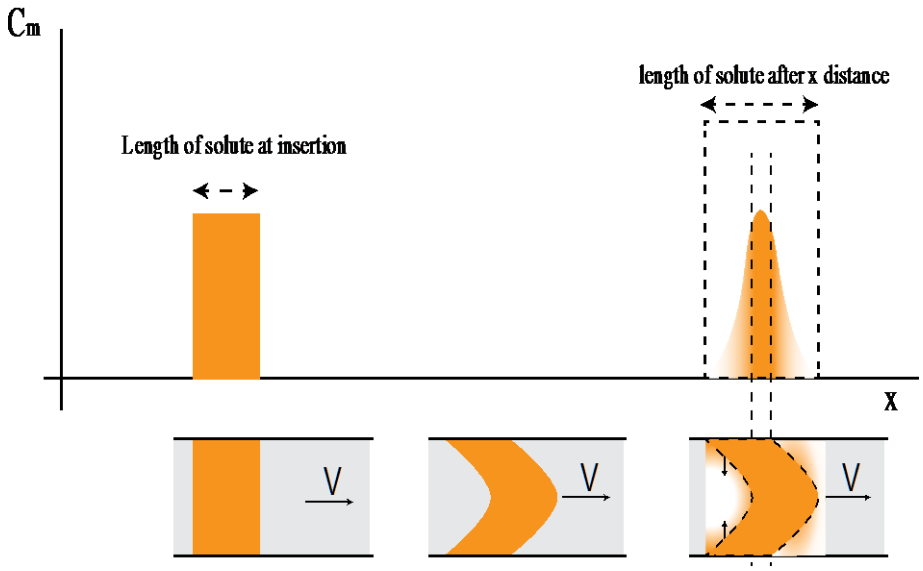

Figure 1-5: Change in concentration profile of a solution flowing inside water
The plug is inserted with a flat concentration profile. The mean concentration Cm across the length of the plug is constant and gradually a parabolic profile emerges due to Poiseuille flow. Convection and diffusion produce Taylor dispersion that affects the concentration of the plug of fluid. A Gaussian concentration profile is formed as a result.

$$\tau_{Taylor} = \frac{w^2}{D_{eff}} = \frac{D}{48V_0^2}\frac{w^2}{a^2}$$ Equation 1.10

The ultimate implication of Taylor dispersion is a reduction in concentration of drugs and reagents delivered to microfluidic devices with cell cultures.

Other forces that become more dominant at the microscale are surface tension and capillary forces. Surface tension is the reduction of a fluid's free energy by contracting to achieve the smallest possible surface area. It is caused by the higher cohesion between liquid molecules than adhesion between liquid and air molecules. This causes the surface to act as a single elastic membrane and is responsible for capillary effects, which increase with reduced channel dimensions. The capillary effects describe how fluid flows through a small orifice in a narrow tube or porous membrane. These forces are more dominant at the microscale, causing fluids to flow in opposition to gravity, and are the basis for applications such as capillary electrophoresis. They are, however, limiting factors for passive flow control and gravity driven flow systems within microfluidic devices.

1.4.3 COMSOL Simulation

The effects of fluid manipulation at microscale like Laminar flow, Hagen–Poiseuille flow and Taylor dispersion all contribute to the delivered agonist profiles. These effects can be observed experimentally and have been defined theoretically with characteristic equations that can be used to model the fluid behaviour. Solving each of these equations for a variety of applications can be performed using Computational fluid dynamics (CFD) software like COMSOL to visualise the effects of these systems (Andersson, Andersson et al. 2011). COMSOL as a CFD software breaks the fluid dynamics problem into a mesh of small discrete finite element sizes. The fluid dynamics equations that relate diffusion and flow are applied to the elements to produce results for the elements which are then recombined to obtain a solution for the large system. COMSOL simulations allowed quick examination of flow effects in different geometries without requiring the physical device. Mesh settings may need to be optimized to obtain more accurate results if the margin of error with course mesh sizes is too large.

While these effects are mostly detrimental to the applications requiring deterministic chemical signalling patterns, it is also possible to exploit these defects for some signalling applications. An example is a an gradient interface formed when two concentration volumes are flowed in parallel (Lin, Yu et al. 2012).

1.5 Materials for Microfluidics

Microfluidic devices for cell cultures are made from materials with good optical, electrical, mechanical, chemical and thermal properties. These materials include glass, silica, elastomers, and thermoplastics. (Ren, Zhou et al. 2013)(Waldbaur, Rapp et al. 2011). It is useful to briefly overview the advantages and disadvantages

of these materials in microfluidics while looking at examples cases where they have been adopted for use.

1.5.1 Glass and other inorganic materials

The optical transparency, chemical inertness and electrical insulation of glass have made it common place in microfluidics development. One wide spread application is its use as substrate layers for the microfluidic devices. Other applications of glass in microfluidics requiring channel fabrication typically involves chemical etching which may be a costly and dangerous process using chemicals such as HF. Further limits to use of glass are the requirement for clean room facilities for high temperature and high pressure bonding of glass devices. Other materials used include silicon and quartz. Fabrication techniques include soft-lithography; additive methods like deposition of chemical vapour and thermal oxidation; and subtractive methods like wet and dry etching (Nguyen and Wereley 2006, Guckenberger, de Groot et al. 2015). Fabrication methods for use with glass and silicon materials are mostly expensive and require specialised tools and technical expertise (Sackmann, Fulton et al. 2014). Fabrication methods for use with glass and silicon materials are mostly expensive and require specialised tools and technical expertise (Sackmann, Fulton et al. 2014). This prompted development of devices using materials that maintain the advantages gained with glass but is easy to fabricate.

1.5.2 Elastomers

Elastomers are materials with cross-linked polymer chains and are able to temporarily deform during the application of an external force. Poly(dimethylsiloxane) (PDMS) is the most pervasive elastomer in microfluidics (McDonald and Whitesides 2002). It is cheap and easy to fabricate in comparison with glass fabrication. Liquid

PDMS can be cast over molds with features and allowed to thermally cure at temperatures above or equal to room temperatures. Curing occurs at shorter durations with higher temperatures. PDMS can be temporarily or permanently bonded with itself or other materials like glass for reversible or irreversible sealing. Contact bonding allows the PDMS to seal when conformal contact is made with another material for a reversible seal. The PDMS surface can be oxidized using plasma treatment for irreversible bonding with glass or other substrates. PDMS also has the added advantage of being elastic, which has prompted research into its use in the fabrication of microvalves discussed subsequently in the on-chip development section.

Soft lithography is the preferred quick, inexpensive fabrication technique where a two-part polymer called polydimethylsiloxane (PDMS) is cured over a reusable mold. The mold may consist of microstructures that are imprinted on the hardened polymer to form the fluidic channels and features in the device (Iliescu, Taylor et al. 2012).

The disadvantages of PDMS are widely reported (refs) as gas permeable and incompatible with organic solvents. Small molecule absorption into PDMS channel walls has also been reported with few results in the attempts at mitigating this absorption.

1.5.3 Thermoplastics

Thermoplastics like Teflons are very inert to chemicals and solvents. They are also optically transparent and have elastic properties that allow the fabrication of microvalves from them (Grover, von Muhlen et al. 2008). Others like PMMA, Polycarbonate (PC), Polyethylene terephthalate (PET) are more compatible with solvents than PDMS but are not able to withstand most organic solvents like ketones.

Thermoplastics are generally not gas permeable which may be an advantage where gas losses are undesirable. They are excellent for commercial production of cell microchips but not very useful for rapid prototyping techniques discussed subsequently. They are also more suited for use as substrates in place of glass for composite microfluidic devices. They are easier to bond using thermal bonding than glass and do not require as high a temperature or pressure and can be done without the need for a clean room facility.

Fabrication methods for plastics also includes micromilling(Guckenberger, de Groot et al. 2015), injection molding (Attia, Marson et al. 2009, Tanzi, Matteucci et al. 2013), hot embossing(Becker and Heim 2000, Abgrall, Low et al. 2007), and stereolithography (Au, Lee et al. 2014) (Waldbaur, Rapp et al. 2011). Injection molding involves casting a molten form of the material into a mold cavity that has a template of the microfluidic features. The molten material conforms to the template features and is cooled down to harden it. Hot embossing also requires a template but the template is pressed against the plastic at high temperature to transfer the features onto the plastic. Stereolithography is a 3D printing process to develop the microfluidic features one layer at a time.

1.5.4 Material Selection and Fabrication for Microfluidics

Material choice for microfluidic devices is typically influenced by the properties expected for the desired device. Properties such as chemical inertness, optical transparency and biochemical compatibility play a huge role in the material selection process but it is ultimately a choice of what offers the best balance. Other properties like implementation and ease of reproduction affect the fabrication process adopted.

PDMS, for example, offers a good balance between its advantages and disadvantages. Its fabrication technique, referred to as soft-lithography is a far easier process to replicate than glass or thermoplastics. The interconnection of PDMS devices to the outside lab is also a factor to be considered in the development

process. PDMS elastic and hydrophobic properties make it more desirable to glass when considering connections as it is easy to press-fit tube connections into PDMS that maintain a liquid sealing (Beebe, Mensing et al. 2002).

The type of microfluidic device developed is dependent on the functionality required of the chip (Kim, Toh et al. 2007). A simple chip design allows scientist to culture cells on the chip while liquid control is maintained by external systems. More advanced chips can be developed that incorporate liquid handling functionality and analytical sensing. These options classify microfluidic systems into Chip in a Lab and Lab-on-a-chip respectively and affect the ease of chip replication and the wide spread adoption of the developed solutions.

1.5.5 Lab-on-a-Chip vs Chip-in-a-Lab

Microfluidic design has taken several approaches which vary in complexity and ease of fabrication. Simple microfluidic designs consist of cell cultures and fluidic paths that allow fluid interaction, and all liquid manipulation is performed by external pumps and loaders that interface with the device. This simple chip-in-a-lab design simplifies fabrication methods used since there are fewer constraints on the type of material or the bond strength of the fabricated device.

The device is only required to be leak free while flowing under considerably low flow rates (0 – 100 $nL.s^{-1}$) which is within the low end of typical values for cell cultures in microfluidic devices and represents three orders of magnitude $\log_{10}$ (flow rate) which will be a starting point to develop liquid handling solutions. Standard protocols can be developed for liquid handling since the control system is developed off-chip and does not change operation when used with other chips.

Another generation of designs implements liquid handling systems and/or analytical detection systems on-chip together with the micro-culture environment (Ghallab and

Badawy 2004, Bodén, Lehto et al. 2008). The integrated liquid handling system poses more constraints on the fabrication process since the device must be able to withstand high pressures required for fluid actuation without leaking (1 – 4 Bar air pressure) (Huang and Lee 2007, Quake 2007, Rohde, Zeng et al. 2007, Cole, Desai et al. 2011, Fordyce, Diaz-Botia et al. 2012). Miniaturised total analysis systems (μ-TAS) requires advanced sensor integration and compatible fabrication techniques which adds constraints to the development of these systems.

This ability to integrate one or more laboratory tools in a single chip for automation is termed “lab-on-a chip”. The advantages includes system compactness; ability to perform highly parallelised functions and high-throughput analysis; increased process control due to faster system response; shorter diffusion distances leading to faster response times and analysis; and low fluid volume consumption since all the required volumes are contained on the chip. One disadvantage is the novelty of the technology and need for new research to establish standard operational protocols for cell lines which could be reproduced. Another disadvantage is the complex fabrication techniques required which pose challenges for laboratories that do not specialise in microfluidic technology. While these devices perform liquid handling on-chip, they also require off-chip manipulation equipment like pressure control systems and advanced logic operations to implement interesting fluidic control (Grover, Ivester et al. 2006, Jensen, Grover et al. 2007, Devaraju and Unger 2012, Fordyce, Diaz-Botia et al. 2012)

Selecting a simple cell culture microfluidic device is key to developing simple tools and applications that could improve on the work in neuroscience as it will use simple fabrication techniques that may be easily adopted and apply macro-scale systems that can be developed with greater ease than microstructures found in microfluidic devices. Practical considerations such as bubble formation (Garstecki, Ganan-Calvo et al. 2005, Sung and Shuler 2009), shear stress (Chung, Flanagan et al. 2005) and

fluid dynamics must be accounted for in selecting an ideal microfluidic device as well as flow control methods (Kim, Toh et al. 2007). The fluid dynamics in the microscale is dominated by laminar flow characteristics and the effects of these forces on flow in this scale are described to give an understanding of the major issues with microfluidic liquid handling.

1.5.6 Fast prototyping Multi-Layered Devices

There is a disparity between the rates of emerging microfluidic system development techniques and the adoption of microfluidic systems life science or biomedical research especially when those research environments are not core-microfluidic laboratories (Langelier, Livak-Dahl et al. 2011, Scott, Au et al. 2013, Sackmann, Fulton et al. 2014). This could be due to a gap between the microfluidic technology production and end users in the field or aggressive patenting of microfluidic devices which limits industrial contribution and development (Bange, Halsall et al. 2005, Yetisen and Volpatti 2014). A significant investment is required for entry into microfluidics research and in-house device fabrication is the go-to option for research groups venturing into microfluidics. In-house multi-layered microfluidic device fabrication typically includes any of the following:

- SU-8 master molds for the feature transfer to PDMS;
- Milling, etching and laser ablation of polymeric substrates and glass;
- Hot embossing and injection molding;

as these techniques guarantee precision of the features (Thompson, Ouyang et al. 2015). High resolution mold fabrication methods are preferred in literature since several features can be developed on the small surface area. However, the significant investments and technical expertise required to undertake this in-house system development presents another obstacle to the widespread adoption of microfluidic technologies (Iliescu, Taylor et al. 2012). Technical expertise, from

training, practice and experience is required to manage the complicated work stations during the fabrication process. Suitable equipment as well as clean-room facilities are required further pushing the development option out of the reach of new entrants into microfluidics. A further disadvantage of these standard mold fabrication techniques is the long turn-around time per device which is more disadvantageous when the mold requires corrections. The same is true if the mold development process is outsourced to companies such as MIT foundry.

The development process encountered some of these challenges faced by standard laboratories when investigating microfluidic technology for liquid handling. As such the development process pursued rapid prototyping techniques that could potentially deliver on the liquid handling requirements with minimal strain on available resources.

An early adoption of rapid prototyping techniques used a flexible plastic in place of PDMS as the actuating membrane for the valve (Yuen, Kricka et al. 2000). The devices were fabricated with doormat style valves but the system was limited by the high pressure liquid flow required to actuate the plastic membrane for liquid flow (1 – 7 bar).

More recently, the rapid-prototyping train has taken off showing rapid prototyping techniques as a method for developing single layered devices with the typical example of a craft-cutter in a method called Xurography (Bartholomeusz, Boutté et al. 2005). Multilayered devces have also been developed using the rapid-prototyping techniques but the reference to rapid-prototyping has also been made in situations where the methods used have been anything but. Methods like glass- etching, embossing, laser ablation or 3D-printing have been documented as rapid-prototyping methods. It goes to say that any method of device fabrication that excludes SU-8 mold replication has been termed rapid-prototyping.

This research redefines rapid-prototyping techniques by excluding methods that do not allow quick turn-around time on feature development for multi-layered devices. It also restricts the development to methods that use Xurography.

High-resolution craft cutters have been used to develop features for on-chip valves and applied for on-chip liquid handling solutions. Studies showed lack of development in the fabrication of on-chip liquid manipulation components using low resolution features (~500 μm feature and above) such as is obtainable with low-resolution craft-cutters. It may be that the low resolution of the features from simple craft-cutters make it difficult to realise these components but there has been no evidence to support or contrast this claim. The typical fabrication techniques have been based on the scaling advantages gained when using small features to develop on-chip liquid manipulation components (Cosson, Aeberli et al. 2015).

It was therefore, more beneficial to attempt the development of simple modular on-chip components using a simple craft-cutter to demonstrate the possibilities for realising an integrated liquid handling system. Another objective for pursuing low cost fabrication techniques is the added potential for wider appreciation and adoption in biomedical research. PDMS was selected as preferred material for the research due to its widespread adoption for its optical, inert, plumbing and soft lithography properties.

The use of Tape has increased the speed at which microfluidic devices can be fabricated as the tape provides adhesion and can be cut into the features for the different layers. However, simple tape adhesion has been found to be an unsuitable bonding technique for multi-layered devices fabricated in PDMS material due to the weak bonds formed between PDMS and the tape layer with the onset of Taylor fingers in the tape layer at high pressures (Thompson and Abate 2013). Variation to simple tape adhesion using clamps as well as chemical adhesion of mutil-layered devices were investigated for developing multi-layered devices using xurography and

soft-lithography techniques. A PDMS-to-PDMS bond is also investigated as they are able to provide very strong bonds while the challenge of the moulds is solved using a tape/plastic combination.

1.5.6.1 PMMA-assisted Tape Adhesion (Additional clamping pressure)

Tape bonded devices have been used in a wide variety of applications with limited flow pressures. The advantage of tape bonds is the availability of materials to produce the features. A craft cutter is often used to excise geometries from a piece of double-sided silicone tape that is then brought in contact with two layers on either side to form a complete device (Bartholomeusz, Boutté et al. 2005). Multiple layers can be made by repeating the steps. Silicone tape has been seen to perform better at sticking to PDMS than other types. It is also well known that PDMS adheres poorly to tape due to its low surface energy and hydrophobicity (Kim, Surapaneni et al. 2009) which affects its application in multi-layered Lab-on-a-chip devices. Some on-chip valves have been shown to require high actuation pressures (P = 2bar) which is beyond the bond strength of tape to PDMS adhesion. Figure 1-6 shows the onset and progression of Saffman-Taylor fingers in tape-bonded devices under low pressures (P = 1 bar) obtained in the lab during a trial run. This is due to weak adhesion of PDMS to the tape.

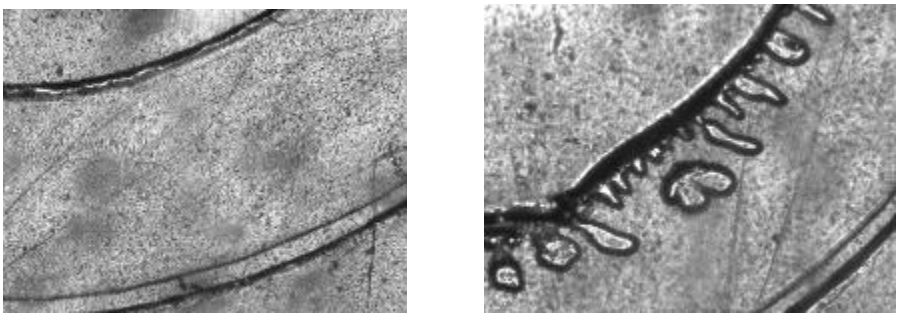

Figure 1-6: Saffman-Taylor Fingers progressing in a tape bonded microfluidic device without clamps *Before pressurisation, the tape layer is intact (left image) but parts of the* layer start to form the fingers during pressurisation (right image)

PDMS offers a quick and effective solution to meet the thin membrane requirement and facilitates external tubing connections for fluid flow which makes it a better material for fabrication. A solution to this weak bond between tape and PDMS can be solved by adding a spring or screw clamp mechanism to the device (Lamberti, Sacco et al. 2011, Temiz, Lovchik et al. 2015). This can improve chip longevity in high pressure applications and has been demonstrated in non-tape bonded devices where the leakage pressure increased to 0.6 bar when a clamp was used (Chen, Li et al. 2013).

1.5.6.2 Chemically Bonded Devices

Chemical bonding techniques have been proposed as a reliable method for fast prototyping multi-layered microfluidic devices (Tsao and DeVoe 2008, Lee and Chung 2009). These methods were developed in response to the need for bonding techniques that take advantage of the quick turnaround brought about by xurography. Typically, patterns are excised in plastics to act as actuation or liquid layers which are then chemically bonded to PDMS

A technique based on covalent chemical bonding between PDMS and thermoplastics has been demonstrated (Tang and Lee 2010). This used APTMS and GPTES for the additional functionalization of PDMS and plastic surfaces respectively that had undergone oxygen plasma treatment. The procedure requires initial oxygen plasma treatment of the PDMS and plastic at 50-60W for one minute. The treated surfaces are immersed in 1% (v/v) aqueous solutions of the APTES and GPTES for 20 minutes. There are then thoroughly washed and dried. The surfaces are then brought together and kept in contact for 1 hour. A leak test was performed to determine the bond strength and a pressure test was also performed. It was seen that the bonds were maintained for an average pressure of 5.10 Bar for PMMA; 5.79 Bar for PC; 5.79 Bar for PET; and 6.07 Bar for U-PET.

An alternative approach (Aran, Sasso et al. 2010) showed chemical bonding using one silane on a single surface. 5% aqueous solution of APTES was heated at 80 degrees while the plastic was plasma activated. The plastic was then immersed in the APTES solution for 20 minutes and left to dry. The surface was brought in contact with plasma activated PDMS layer for 20 seconds. The bond is described as instantaneous for PCTE and PETE plastics. The bonded devices bond stayed intact at pressure of 2.2 Bar which was the limit of the pressure sensing equipment used. The attraction of this method is the ability to bond the functionalised plastic to glass in situations where the substrate is glass.

A “one-step” chemical bonding procedure which does not require specialist skill or training was also proposed (Wu and Lee 2014) as a simpler procedure over the other methods. This is a single step modification process using an amine-PDMS linker to functionalise different plastic sheets for 20 minutes. The sheets are sonicated in IPA solvent for 1 minute to remove the excess amine-linker. They were then exposed to a corona discharge to activate the surfaces and the bond is formed when the surfaces are brought in contact to PDMS. This procedure was found to give approximate bond

strength of 4.28 Bar 3.6 Bar and 4.3 Bar for the polycarbonate, poly(ethyleneterephthalate) PET and PVC sheets used respectively. The use of the corona lamp significantly reduces the technical requirement for special Plasma generator systems as these lamps could be obtained for significantly less and do not require vacuum conditions or precise gas control. This method is most promising for replication since it requires far less steps and can be done with relatively less cost (Wu and Lee 2014).

1.5.6.3 PDMS-PDMS Bonding

Plasma generator or corona discharge lamp requirements for hydroxylation steps of the chemically bonded microfluidic devices limit the ease of fabrication for the method. The number of steps required for bonding the devices increases the risks of error due to bad bonds or misalignment. PDMS-to-PDMS bonding was reviewed as an alternative method for rapidly prototyping the devices.

The use of uncured PDMS as a glue in the stamp-and-stick method (Satyanarayana, Karnik et al. 2005); and the contact of two partially cured PDMS pieces together for subsequent full thermal curing (Eddings and Gale 2006) have been presented as options for PDMS-to-PDMS bonding.

The PDMS stamp-and-stick method is performed by spinning uncured PDMS to obtain a thin layer of PDMS which is then transferred to a PDMS layer that is brought in contact with it. The PDMS layer with the thin uncured PDMS film is then placed on another pre-cured PDMS piece and the assembly is left to cure under temperature. Typical spin speeds depend on target film thickness. In one application, for example, a 1.5 μm film was obtained by spinning at 8000 rpm for 8 minutes (Satyanarayana, Karnik et al. 2005).

The partial cure alternative is a method where the layers are brought in contact with each other after a partial cure process (70^{o}C for 25 minutes). They layers are then cured for a longer duration (Fordyce, Diaz-Botia et al. 2012).

This use of uncured PDMS glue has been reported to produce strong bonds with less variability in the bond strength with average burst pressure of 6.7 Bar with small difference of 1.4 Bar between the minimum and maximum burst pressure reported (Eddings, Johnson et al. 2008). This was significantly better than partial-cure bond method which showed higher variability (~ 3.2 Bar) between the operating range of the device. These high bond strength values reported make PDMS an ideal rapid prototyping technique in addition to the ease of assembly with no requirement for technical expertise.

The limit to this technique is the mold fabrication process. The fabrication of SU-8 molds for feature transfer was ruled out as it does not fit the rapid prototyping objectives of the development process. Laser cutting (Samuel, Thacker et al. 2014) and xurography (Pinto, Faustino et al. 2014, Martínez-López, Betancourt et al. 2017) has been used previously to develop features for microfluidic devices. Features are first cut out of the tape and backing layer combination. The backing layer is removed from the parts of the cut piece where the feature is expected. This will leave some parts with the backing tape still on it. The whole piece is transferred to a petri dish where the PDMS will be cast together with the parts with backing tape left on. This ensures that the cut patterns maintain their position in the layer. The part with the backing tape is removed from the petri dish and the layer features remain adhered to the petri-dish.

1.6 Liquid Handling for Microfluidic Systems

Different materials for and prototyping techniques have been presented for the development of microfluidics systems. Liquid handling is required to accomplish flow of nutrients and chemical agonists to the microfluidic devices to maintain and perform assays on cultures within the devices. The different types of fluid handling mechanisms for biomedical microfluidic systems can be grouped into:

- The flow control system that manages the transport of fluid to the devices; and
- Volume injection system that enables an agonist volume plug or volume sequence to be injected into the device for drug-response and analytical assays.

Further analysis on secretions from cultured cells may also be required. This can be achieved by sampling of the fluids downstream of the microfluidic device. The flow control, liquid injection and sampling subsystems can be developed as off-chip macro scale systems or on-chip micro-scale systems.

1.6.1 Liquid Transport

Transport of cell culture media, drugs, reagent and analytes are required in microfluidic devices for long term maintenance and analysis. Majority of flow control developed for microfluidics are pressure driven flow systems or electroosmotic flow systems (Author 2008). Others include gravity-driven flow, bubble-driven flow, and capillarity. The disadvantages to electroosmotic flow, such as unrepeatability, dependence on fluid properties, and electrochemical reactions; make it an unsuitable choice for precise, highly scalable liquid transport mechanism. Only pressure-driven flow systems and gravity driven flow will be considered as they can provide consistent flow characteristics that are independent of fluid properties.

On-chip and off-chip flow control are illustrated in Figure 1-7 and Figure 1-8. In both classifications, liquid is transported from a reservoir to the microfluidic device by actuation mechanisms. On-chip flow control has been mostly developed as an integrated lab-on-a-chip solution that requires advanced fabrication techniques (Jang, Hancock et al. 2011). The fabrication methods are difficult to realise in a non-specialised microfluidic laboratories. The method of flow control illustrated in Figure 1-8 requires pressurized liquid at the sample inputs while the on-chip valves allow flow on that path or restricts it. This simple on-off system requires off-chip hardware to pressurize the liquid. Liquid transport can also be realised by the generation of peristaltic pumping of on-chip valves arranged in a sequence (Melin and Quake 2007). This method does not have any feedback system for accurate flow control and does not meet the requirements for the target liquid handling system. As such, the simple on-off system will be investigated further for on-chip liquid manipulation.

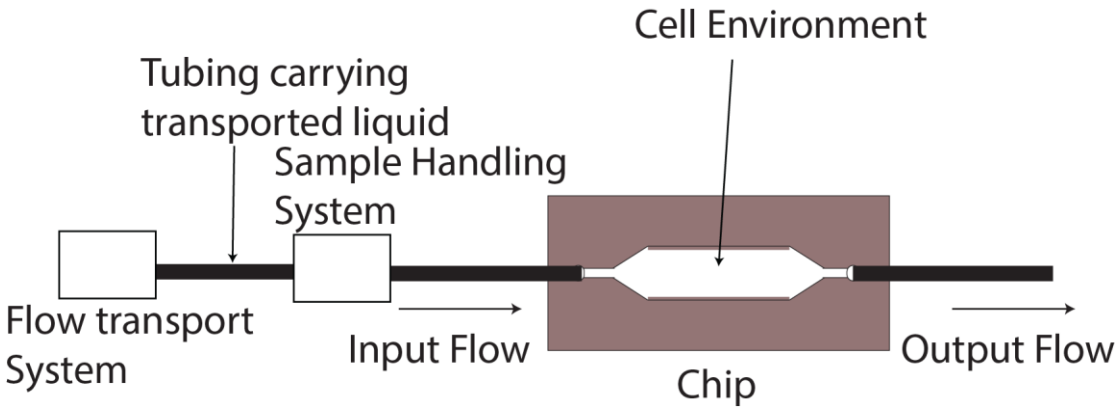

Figure 1-7: Simple Microfluidic Device with off-chip liquid handling
The use of a simple microfluidic device with off-chip liquid handling maintains the architecture regardless of the changes made to the chip design. The system objectives to the microfluidic chip always remains the same – to transport samples to the chip. All liquid manipulation is done by systems capable of performing required tasks.

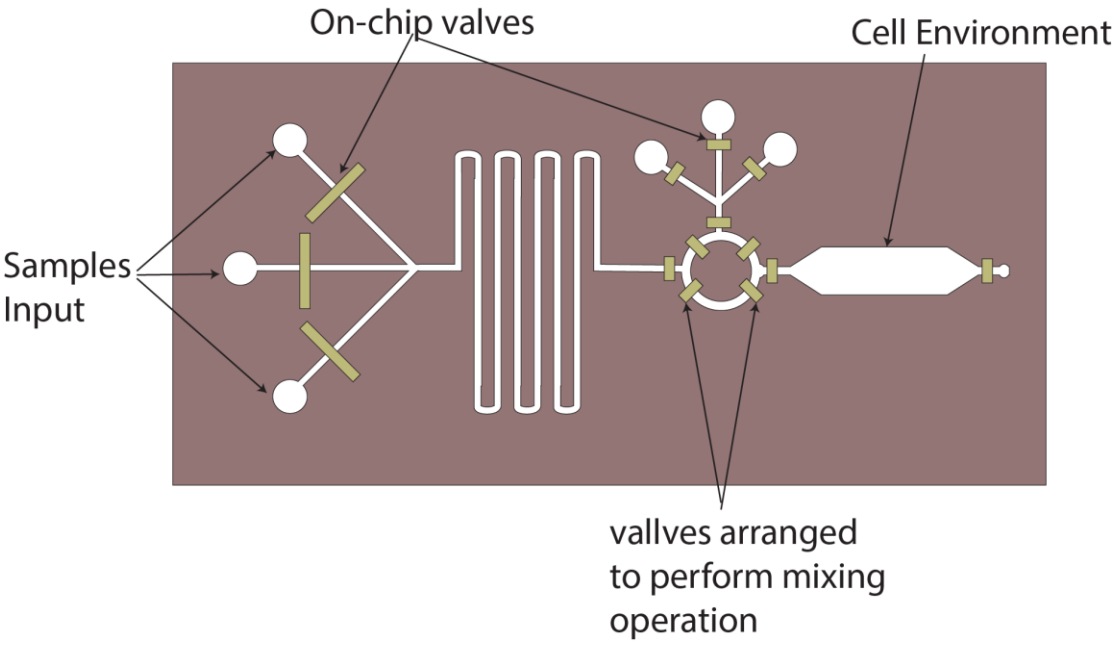

Figure 1-8: Integrated Microfluidic Chip with On-Chip Valves Performing Liquid Handling
On-chip valves perform Liquid handling requirements on the chip. This method reduces the space required to keep macro-sized liquid handling systems but requires extensive fabrication methods.

Off-chip liquid actuation solutions that can be used to realise liquid transport in microdevices induce pressure-driven flow. These solutions include gravity-driven arrangements, syringe drivers, peristaltic pumps, and pneumatic pumps. Valves can be used as assistive flow control technology with any of these mentioned techniques to allow flow or halt flow in a liquid channel. These solutions may be applied to achieve i) positive flow actuation where flow direction is away from the actuating device; or ii) negative flow actuation where the fluid is transported towards the control system.

Manually controllable flow control techniques are not considered since they obviate critical automation requirements.

1.6.1.1 Gravity-Driven flow

Gravity flow can be induced when there is a difference in hydraulic head Δh (m) in reservoirs causing liquid to move in the direction of lower height. The advantage of

gravity-driven flow is the flow rate consistency that can be achieved if the height difference is maintained. Real time flow control is achievable by mechanical equipment setup to actively alter the hydraulic head by altering the height of the reservoir (Kenis, Ismagilov et al. 1999, Takayama, Ostuni et al. 2001). Alternatively, the fluidic resistance can be changed by pinching the tube for flow control but this is best suited to small liquid reservoirs and requires manual pressure modifications (Kim, Kuczenski et al. 2009). A mechanical system was developed to dynamically change the fluidic resistance and fluidic capacitance in the microfluidic network(Kim, Kuczenski et al. 2009). The achieved flow rates were not stated but the device was able to perform an interface shift operation in 0.2s in a 500μm wide channel. This method of pumping is more suited to long term perfusion of media to cells since they are less noisy and these applications do not require dynamic flow rate control (Tehranirokh, Kouzani et al. 2013). However, the method is vulnerable to flow rate changes due to bubbles causing changes in resistance.

1.6.1.2 Peristaltic Pumps

A peristaltic pump applies positive displacement for pumping a variety of fluids. This flow control applies a continuous compression and translation force on an elastic tubing containing the fluid from a connected liquid reservoir. This is illustrated in Figure 1-9 with three rollers that rotate to cause the liquid flow. Peristaltic pumps have previously been applied to provide flow for microfluidic devices (Feng, Yang et al. 2011)

Peristaltic pumps create pulsed flow and will not be suitable for applications where flow perturbations are undesirable because they can cause boundary shifts that expose the cells to agonists. The constant pinching and motion by the rollers will quickly degrade the flexible tubing which will require regular replacement.

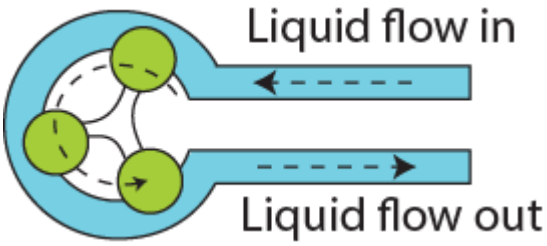

Figure 1-9: Schematic of peristaltic pump
Peristaltic pump is comprised of rollers, a flexible tubing housed inside a hard casing. The rotor rotates the rollers to cause a pinch of the tubes. This continuous rotation forces the liquid to be pushed through the tube till it exits the device.

1.6.1.3 Syringe Pumps

Syringes use a plunger to create positive liquid displacement when pushed and negative liquid displacement when pulled illustrated in Figure 1-10. Commercially available syringe drivers have been used extensively to control volume flow rates for long term experiments.

The rate of volume displacement is equal to the flow rates in the channel though it has been seen that this flow may deviate throughout the course of experiments with syringe drivers. A noisy flow rate has also been observed which is typical to simple syringe drivers and has been shown to be caused by the pump's mechanical oscillations (Li, Mak et al. 2014). It has also been shown that the pump's mechanical frequency increases with increasing flow rates (Zeng, Jacobi et al. 2015). The use of high quality syringe pumps like those manufactured by Kloehn, Cavro Scientific Instruments (Chien and Parce 2014) can mitigate the noise and provide high accuracy. These are more expensive setups and represent significant investment when compared with regular laboratory syringe drivers. Laboratory experience showed that the syringe quality also played an important part in maintaining consistent flow. Stalling of the syringe plunger was found to be more common in plastic syringes were found to be less smooth in operation compared to glass syringes.

This noisy performance of syringe drivers are difficult to mediate since the pumps do not have feedback control which makes it difficult to monitor and reliably control the flow rates with dynamic precision. Syringe drivers can cause pressure build up if the flow path is blocked momentarily. This is because the syringe driver continues to push the plunger and the pressure builds up while flow rate is zero. The high pressure setup during the obstruction can cause damage to microfluidic devices and fluidic components that cannot tolerate these pressures. This makes it highly unsuitable for injection systems where the flow path may be temporarily blocked during the injection phase sending pressure shock waves to the cultures. Another disadvantage of syringe drivers is the continuous flow when flow is terminated in the control interface. This is due to the built up pressures in the system and can be minimised by using inline valves to abruptly stop flow when desired. The hysteresis in the syringe also prevents rapid flow rate changes.

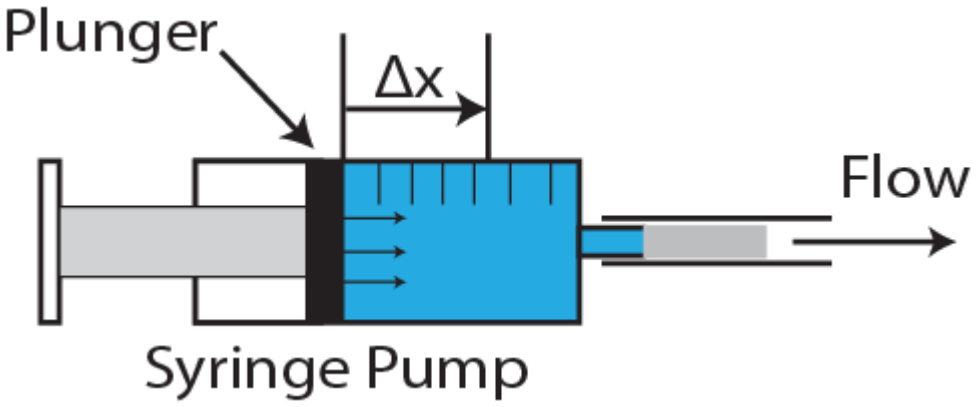

Figure 1-10: Syringe Illustration.
The plunger in the syringe allows the displacement of volumes by its linear motion. The volume that is displaced per second ($m^3.s^{-1}$) is the product of the cross sectional area - πr^2 (m^2) and the linear velocity of the plunger – $\Delta x/t$ ($m.s^{-1}$).

1.6.1.4 Pneumatic Pumps

A positive (or negative) pressure difference may be applied across a microfluidic device. Gas can be supplied from a pressure source to a partially filled, sealed liquid reservoir causing the liquid to flow through an immersed tube in the liquid reservoir. Figure 1-11 shows a schematic for a positive pressure pump with a pressure source,

optional pressure regulator used to regulate the input pressure to a value more suited for micro volume applications and a partly filled liquid reservoir. Figure 1-12 shows an example schematic of components for a pneumatic regulator. The regulator illustrated is a two-valve system where the interoperation of two valves for pressurisation and depressurisation of the system.

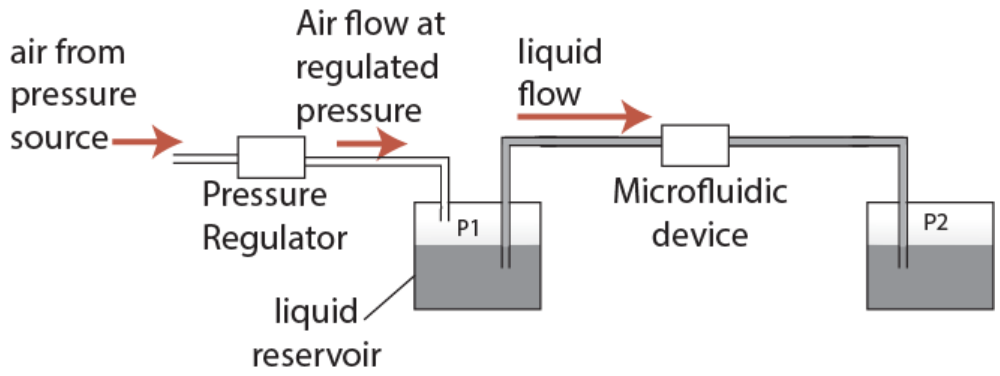

Figure 1-11: Pressure-driven pump system
The pressure-driven pump system is comprised of a pressure source, pressure regulator and liquid reservoir. The pressure above the liquid forces the liquid to flow through the connected tube. The flow rate is determined by the fluidic resistance experienced in the tube and the optional back pressure.

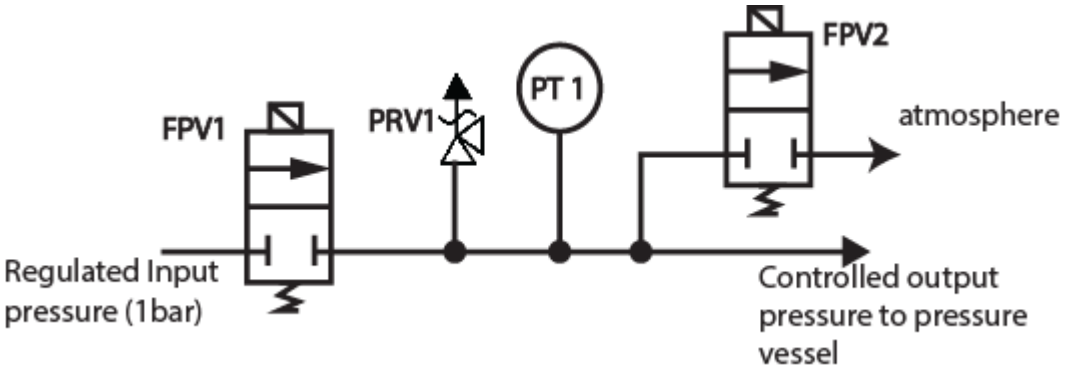

Figure 1-12: Pneumatic Pump Schematics.
The schematic for the pneumatic pump above is comprised of an input source; two Valves (FPV1 and FPV2), a Pressure Relief Valve (PRV); a Pressure Transducer (PT1); an output connection to the reservoir and an orifice for venting to atmosphere. The pressurisation valve (FPV1) controls air flow into the system that is sensed by the PT1. PRV1 is set to relieve pressure in the system by venting to atmosphere when a threshold pressure is exceeded. This is used to protect the pressure transducer. The depressurisation valve (FPV2) controls the air flow to atmosphere which depressurises the system quickly at high flow rates or vice versa. The combined action of the pressurisation and depressurisation valves determine the total pressure maintained in the system and present at the liquid reservoir.

Alternatively, a vacuum pump can be used to draw liquid from the liquid reservoir through the microfluidic device. This method is limited by the ability to dynamically control the pressure difference since the pumps are on-off mechanisms. An in-line

proportional valve could regulate the pressure from the pump but there is limited control over the stability of the partial pressure. Another disadvantage is that constant vacuum pump operation may damage it.

Pneumatic pumps were preferred for the continued development of the liquid handling station as they could be developed to provide consistent, pulseless flow and less likely to damage microfluidic components due to pressure build-up. Flow sensors may be required to improve accuracy and precision of liquid flow control.

The preferred liquid transport system will be connected to a volume injection system which will insert samples into the flow line that will be transported to the microfluidic device. Accomplishing this task will require an understanding of volume injection systems and the integration of liquid handling systems.

1.6.2 Volume Injection

Off-chip solutions for volume handling were preferred for microfluidic application development to reduce the complexities of chip design and provide a tool that was well within the reach of typical laboratory users. The use of pneumatic pumps was also selected to achieve volume transport to the microfluidic devices. The sample manipulation part of the liquid handling system lies between the flow transport and micro-device and enables users to load volumes into the channels.

Liquid Injection systems are usually used to insert volumes of drugs or reagents into flow lines to microfluidic devices for analytical experiments where a volume of reagent is placed directly into a flow stream of liquid without interrupting the flow or introducing an air bubble. One of the goals of this project is to apply off-chip liquid injection systems for custom drug delivery in microfluidic systems. A suitable method of realising this goal is the use of flow injection systems that are used for flow injection analysis in analytical fields. This involves the transport of volume solution of

analytes to a target region where detection and analysis operations can be performed. These methods and systems have also been applied as tools for injecting agonist concentrations to cultures in microfluidic devices. The ideas are very much the same in that flow rate of a buffer or zero agonist concentration liquid is controlled by syringe drivers or pneumatic pressure controllers. Reagents are then inserted into the flow path by action of a switch. Typically, a sample plug in inserted into a flowing carrier stream for transport to the detection system but this can be used as a mechanism of transporting agonists to microfluidic cultures. More information on flow injection systems will provide more understanding to its application to microfluidic applications.

1.6.2.1 Flow Injection and Sequential Injection

Air segmented flow analysis methods were initially used as methods of delivering very small volumes for microfluidic devices. This method has been demonstrated using a vacuum pump to pre-load variable solution volumes (50 – 700 nL) into cartridges (Linder, Sia et al. 2005). The volume plugs were separated by air during the loading stage. This is not suitable for live cell culture microfluidic systems, however, since air bubbles are detrimental to cell survival (Meier, Hatton et al. 1999, Sung and Shuler 2009). Another problem with method is the issue of cross contamination, which occurs when preceding volumes leave residue on the channel walls that are picked up by succeeding agonists (Chen and Ismagilov 2006). Flow injection analysis (FIA) has been widely used as replacement for segmented flow analysis since the carrier liquid removes the residue on the channel walls and discrete analysis can be performed without affecting successive results (Miró and Frenzel 2004) which improves on air segmented flow analysis since no air is injected into the sample stream. This method will be more suited for cell cultures in microfluidic devices and has been established as a viable method of liquid delivery (Sundberg 2000).

In FIA, a carrier stream that is driven by a pressure pump is interrupted with a volume plug of reagent. The flow of the carrier liquid is resumed and propels the sample to a detector. This is commonly used in high performance liquid chromatography (HPLC) systems. FIA techniques have been implemented in microfluidic perfusion systems where the chip replaces the detector illustrated in Figure 1-13.

Advantages of FIA in analytical fields include the relative ease and low cost to setup; and the simple structure of the equipment, which can be integrated with many detection instrumentation. FIA offers ability to precisely and accurately delivery low volumes (10 – 100µl). This will be affected by dispersion in the channel but can be limited by reduced channel geometries. Another disadvantage of FIA is cross-contamination (Ranger 1981)

Sequential injection analysis (SIA) is an enhancement to FIA techniques (Economou 2005) and are also illustrated in Figure 1-13 where a multi-position valve is switched to allow single or sequential volume loading into a holding coil (or reaction column) and transport of loaded sequence to the detector. Ideally, the multi-switch valve should allow the coil to be loaded without affecting the flow of the carrier fluid to the target destination (Economou 2005). This can be achieved using injector valves where the coil is connected as a potential path between either of two flow paths as illustrated in Figure 1-14. Sample loading and carrier flow to the detector occur simultaneously due to internal fluidic connections in the injection valve.

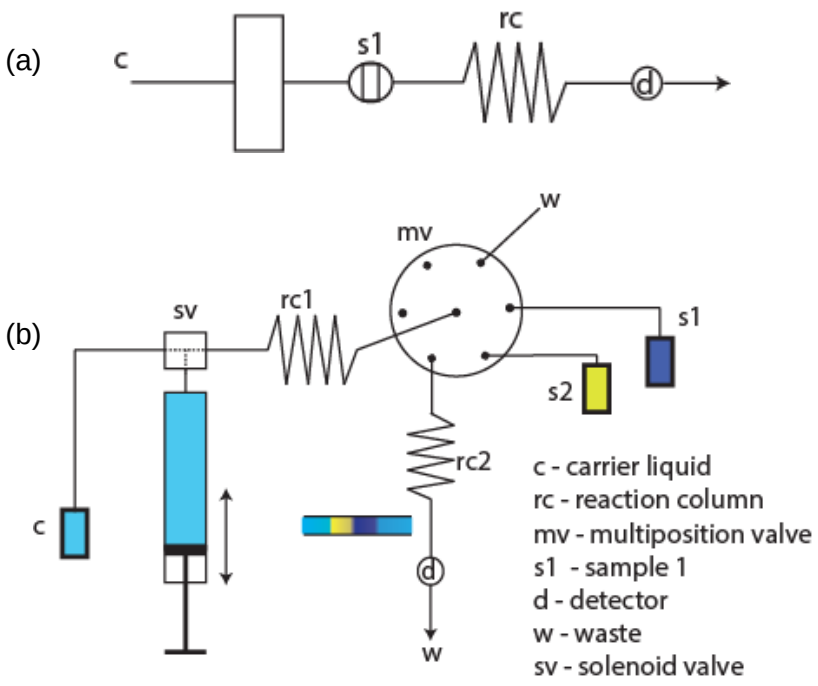

Figure 1-13: Flow Injection Methods

With the flow injection analysis method (a), the flow from the primary source was stopped and the flow in the secondary source was initiated in order to push the sample into the flow path. This was then stopped and the primary flow restarted to transport the reagent to the detection system. An improvement on this method used a multi-position switching valve in sequential injection analysis (b). Here the multi-position switch is used to select the sample to be aspirated into the reaction column1, the sample is then transferred to the reaction column 2 and the transport mechanism for the carrier liquid is used to transport the inserted plug(s) to the detector. This schematic shows an implementation where the transport mechanism to the detector is paused while loading the different samples into the reaction column. Typically, these reaction columns can be used as reservoirs to hold large volumes of the samples to be delivered or can be used in dilution operations.

SIA is also characterised by software control capabilities and can allow long term unsupervised assays to be performed which is beneficial to its application in microfluidic cell cultures. The SIA method can be applied using commercial autoloaders (Zotou 2012). Autoloaders may lack determinism in volume injection due to the number of push pull sequences that are required to load samples into the line. These sequences will also take longer time to realise for larger volumes. This is due to the fact that the syringe used to sample will have to load the samples at a constant rate for all volume samples and it will take 100 times as long to load 100 μL as it will take to load 1 μL.

The overall volume injection operation is comprised of volume loading and volume injection phases where the reagent is first loaded into a holding reservoir and a switching mechanism is actuated so that the reservoir is brought in-line with the carrier liquid. These operations move the sampled fluid through fluidic channels, each time increasing the dispersion effects (Taljaard and Van Staden 1998, van Staden 2015). The volume sampling step can be performed using a pneumatic pump to pressurise sample reservoirs (Foret and Kusý 2006). This was done in (Rane, Zec et al. 2012) where solenoid valves were gated to achieve very low sampling volumes (50 – 600 nL).

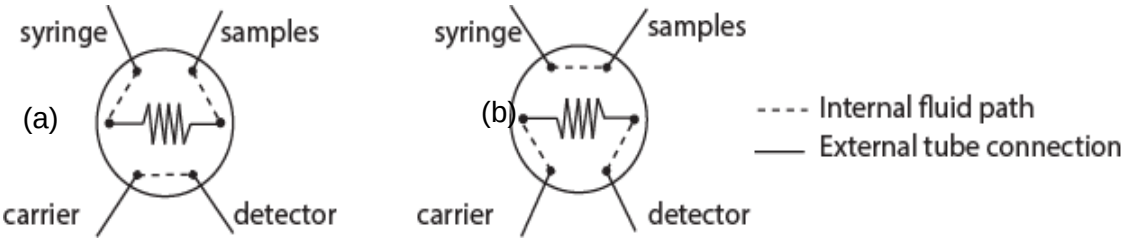

Figure 1-14: Two position injection valve system
A two-position injection valve used in sequential injection systems. The internal fluid paths can be altered by a switching mechanism to direct flow in either of the shown configurations. In position (a), the carrier liquid is directly connected to the detector system allowing loading operations to be performed simultaneously. In (b), the switch changes the internal fluidic configuration to enable transport of the loaded volumes.

This fluid transport and volume injection system is crucial for the intended application of this project outcome which is to facilitate the development of a real-time feedback system for neurons in a controlled environment in order to learn information processing patterns and behaviour in these neuronal cultures.

1.6.3 On-Chip Liquid Manipulation

The advantage of precise micro volume management has propelled research into microfluidic systems and the several devices with singular functions or integrated functions have been developed over the decades of research (Young and Beebe 2010, Streets and Huang 2013),

The introduction of on-chip valves (Unger, Chou et al. 2000), typically called Quake valves, has allowed researchers to replace macro-sized liquid manipulation components with micro-sized variants. The micro-sized liquid components realisable from quake-valves include solenoid valves (Kaigala, Hoang et al. 2008, Kim, Chen et al. 2009, Churski, Michalski et al. 2010, Au, Lai et al. 2011), pumps (Chang, Beaumont et al. 2008, Blanco-Gomez, Glidle et al. 2009), mixers (Nam-Trung and Zhigang 2005), and concentrators(Gao, Sin et al. 2011). These micro components can be assembled as building blocks for more lab-on-a-chip systems (Sin, Gao et al. 2011).

Passive components like reservoirs can be developed on chip as well. These on-chip components reduce drug delivery time, volume waste, dead volume and increases precision during volume injection (Bodén, Lehto et al. 2008).

On-chip valves are developed using multi-layered device fabrication techniques. An elastic membrane, like thin PDMS is typically used to seal the flow path which prevents liquid flow. On-chip valves can be normally-open or normally-closed where the active deflection of the membrane by an actuation means seals the liquid path or opens the path respectively. The actuation method is typically pneumatic pressure but has been demonstrated with liquid pressure.

1.6.3.1 Normally open (NO) valves

Normally open microfluidic on-chip valves have been the most utilised on-chip valve type (Huang, He et al. 2012) since their development (Unger, Chou et al. 2000). Designs for normally open valves exist in literature and best practices have been proposed to improve liquid flow cut-off and start times. Higher aspect ratio ($^{width}/_{height}$) of the liquid channel and longer valve length have been shown to improve performance (Fordyce, Diaz-Botia et al. 2012).

The assembled layers for a normally open valve are shown in a CAD design in Figure 1-15 while the schematic illustrated in Figure 1-16 (a) shows the side of the device; (b) shows the front view with the length of the liquid channel; and (c) shows the flexible membrane deflected to block the liquid channel.

The flexible membrane is usually made from PDMS and previous studies have shown that the thickness affects the valve operation and durability. The fluid layer is sandwiched by the bottom substrate and the thin flexible membrane layer. The actuation layer is above the membrane and is filled with pressurising fluid that deflects the membrane.

NO valves have been used extensively in microfluidic applications (Unger, Chou et al. 2000, Yuen, Kricka et al. 2000, Wheeler, Throndset et al. 2003, Go and Shoji 2004, Oh and Ahn 2006, Quake 2007) and typically require high pressures for actuation between 0.4 - 2 bar (Mohan, Schudel et al. 2011).

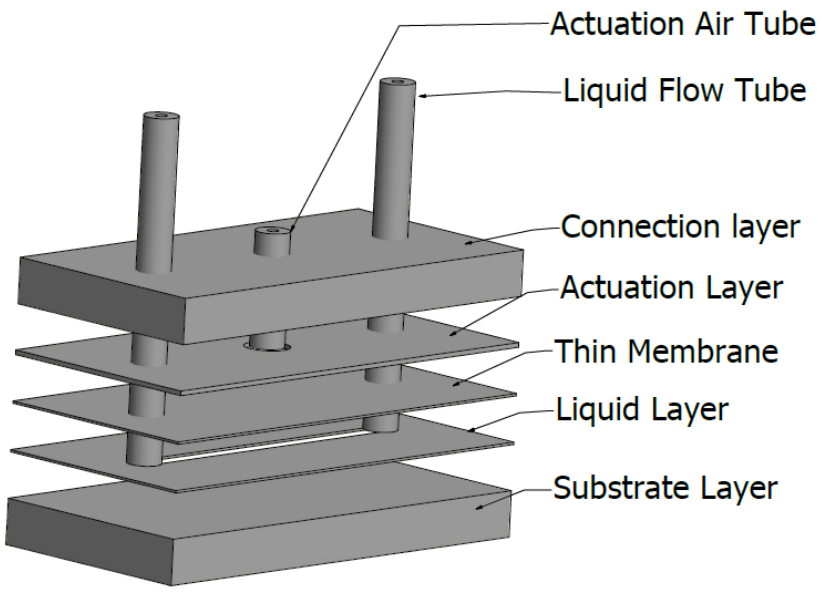

Figure 1-15: CAD Design for a Normally Open On-chip Valve
The CAD design shows the expanded view of an assembled microfluidic device with a normally open valve. The liquid channel in the liquid layer is not restricted during non-actuated periods. The membrane lies flat over the channel. At actuation, the gas is introduced into the actuation layer which deflects the membrane to restrict liquid flow in the liquid channel.

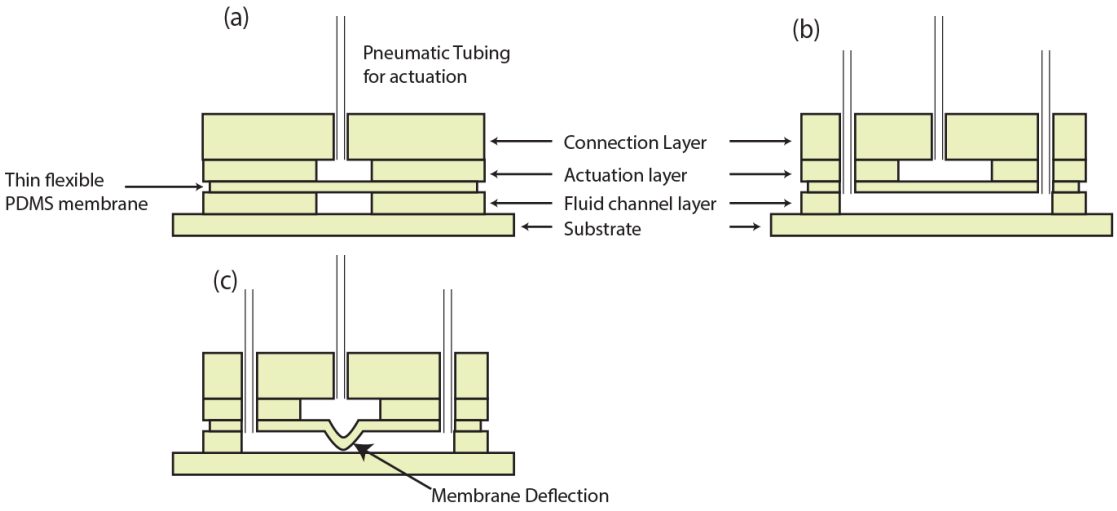

Figure 1-16: Layers for a normally open on-chip valve

a. Left to right view of the device. The thin membrane has not been actuated and remains flat allowing liquid to flow through the path in the fluid channel layer
b. The front view of the device shows the liquid and actuation layers
c. The thin membrane has been actuated and preventing liquid flow.

1.6.3.2 Normally closed (NC) valves

The major drawback of NO valves which is the requirement for high actuating pressure is addressed in NC valves. A section of the fluid channel is raised so that contact is made with the membrane when the device is assembled. This contact seals the liquid path when the membrane is not actuated and actuation is achieved by applying vacuum in the actuation layer which raises the membrane away from the raised section in the liquid layer. The CAD design shown in Figure 1-17 shows an expanded view of a microfluidic device with a normally closed valve. Figure 1-18 shows the schematic of NC valves where (a) shows the side view with the channel blocked by the raised feature that contacts the membrane layer shown in (b); and (c) shows the actuation of the membrane to permit liquid flow.

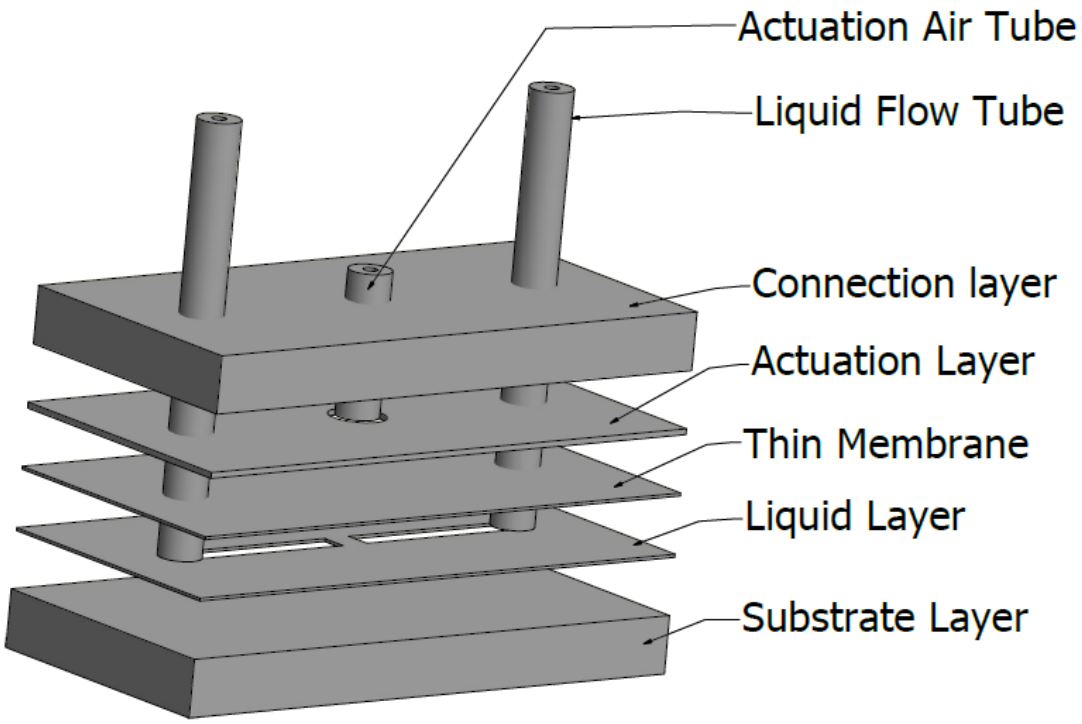

Figure 1-17: CAD Design for Normally Closed Valve

The liquid channel has a wall which stops liquid flow while the membrane is flat over the liquid layer. Vacuum pressure pulls the actuation membrane away from the wall allowing liquid to flow over.

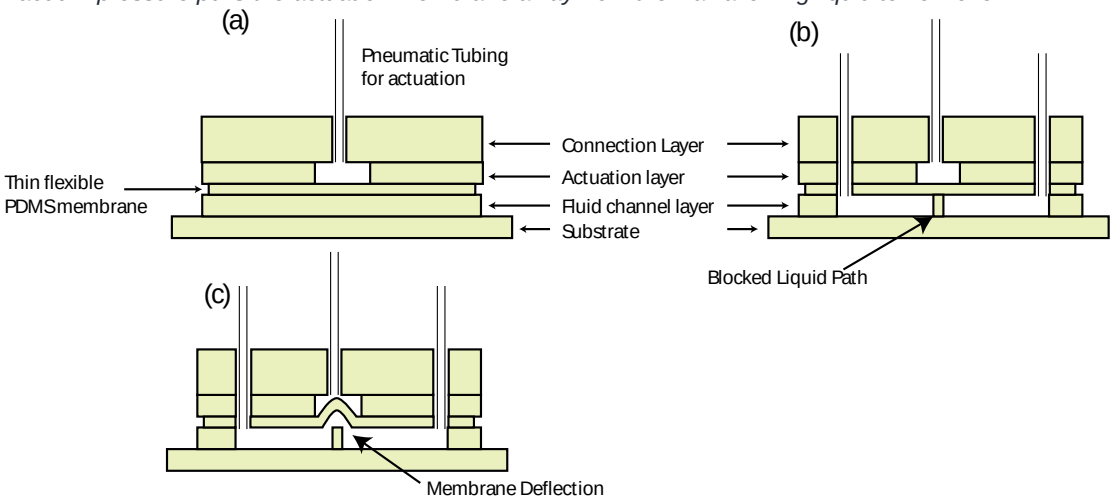

Figure 1-18: Layers of Normally Closed On-Chip Valves

a. *The thin membrane has not been actuated and remains flat blocking liquid flow through the path in the fluid channel layer*
b. *The front view of the device shows the liquid and actuation layers*
c. *The thin membrane has been actuated permitting liquid flow*

These devices have been shown to be more durable since the operating pressures are not high enough to damage the membrane or de-bond the multi-layered assembly. Detailed considerations have been documented on the development of

normally closed valves (Mohan, Schudel et al. 2011). There is good evidence that these valves require vacuum for actuation (Grover, Ivester et al. 2006).

Variants of the normally closed valves include the “doormat” and “curtain” designs. The doormat version has the membrane above the wall separating the micro channels (Kazuo and Ryutaro 2000, Li, Hsu et al. 2005, Cooksey, Sip et al. 2009). The curtain style version has the wall integrated with the flexible membrane. This is lifted off the channel layer when actuated with a vacuum pressure allowing liquid flow.

1.6.3.3 Doormats as Normally Open

The doormat valve can be used as a normally open valve where the liquid pressure forces a path for flow over the wall. This is possible when the liquid pressure is able to overcome the stiffness of the flexible membrane or the area of the actuation layer is significantly large (Samuel, Thacker et al. 2014). These valves are built such that the width of the actuation layer is larger than the width of the liquid channel. Doormat Valves as normally-open valves require significantly less pressure to close seal the flow path (< 0.3 Bar) (Samuel, Thacker et al. 2014). This offers a promising advantage over typical NO valves which may require higher pressures (up to 2 Bar).

Normally-open valves and doormat valves are preferred due to ease of use and practical considerations. Positive pressure sources and regulators are more readily available and may be more assessable to experimenters for application than sub-atmospheric pressure sources which provide vacuum conditions for normally closed valves.

1.6.3.4 Actuation

On chip valves could be actuated using an on/off solenoid air valve to allow or stop positive pressure or sub-atmospheric pneumatic pressure supply to the actuation

layer which results in the push or suction of the membrane layer. As described previously, a positive pressure is applied for NO valves to push the membrane to block the fluid path. Valves that are normally closed usually require sub atmospheric (vacuum) pressure to pull the membrane away from the liquid flow path.

1.6.3.5 On-chip reservoirs

The use of on-chip reservoirs are a further advantage to on-chip liquid handling. Reservoirs can be made by cutting out a cylindrical feature from the top bulk layer (Sin, Gao et al. 2011). This implementation further reduces the overall size of the liquid handling solution and has the added advantage of eliminating the need for external liquid reservoirs when loading smaller volumes in the order of 100 µL. Pipette tips and microvials have been directly connected to the chip to act as reservoirs to facilitate easy reagent dispensing.

The on-chip components can be assembled as fully integrated microfluidic devices with these on-chip components. However, the constraints in our design which include modular design will require a more modular approach to microfluidic chip design and this is further investigated. The on-chip liquid transport system can also allow for

1.6.3.6 Chip Modularity

The need for developing scalable and modular system can be extended to the on-chip manipulation system. This is a preferred alternative to a wholly integrated microfluidic chip design in line with the project objectives. The idea is to fabricate chips where the liquid handling functionality is separated from the cell culture environment. Some example chips have been fabricated previously that take advantage of the emerging need for modularity in microfluidics. These chips are developed as subcomponents for a microfluidic system like liquid transport,

manipulation and the target microfluidic device are subsequently assembled (Arora, Simone et al. 2010, Araci and Brisk 2014). Lego-styled plug-and-play microfluidics have been developed previously (Rhee and Burns 2008, Yuen 2008) and recently (Bhargava, Thompson et al. 2014, Hsieh, Yang et al. 2014), where microfluidic components are fabricated as independent blocks that can be fitted together to solve the liquid transport and manipulation problem independent of the microfluidic device target.

Modularity allows easily reconfiguration to the fluidic circuit as well as the points for manipulation and transport. This trend in microfluidics may improve the rate of adoption for microfluidic techniques in biomedical research since a plethora of applications are possible from reconfiguration of these components. A redesign is not required as all the components can been pre-fabricated allowing the experimenter to pick and choose which ones are required for the target experiment.

1.7 Integrated Liquid Handling Systems

Long term liquid flow and repeated drug delivery to microfluidic devices is sometimes required for applications in biology. One way to achieve this is to implement one of the flow control systems mentioned in the “Liquid Handling for Microfluidic Systems” section above. Adoption of a flow control method alone may only provide sufficient flexibility to perform long term perfusion but is not capable of sequential injection of various small volumes into the microfluidic devices. It may also be possible to improve the flexibility of fast signaling applications by enabling a wider choice of agonists with the integration of a liquid injection system. Commercial systems are usually configured for single applications and are not easy to integrate into the desired lab due to hardware incompatibility and proprietary software development which prevents custom development.

Other advantages of developing an integrated liquid handling system is the potential for modularity, if properly designed, that ensures the system can be integrated into other laboratory systems and protocols if developed with the aim of future integration. An integrated liquid handling system is typically custom design and/or built using off-the-shelf components or equipment that are best suited to the smaller functions required. This includes use of actuators like pneumatic valves, solenoid valves, pressure sensors, flow sensors, data acquisition systems, control interface typically PC; and control software.

A typical application requiring some of these properties of an integrated liquid handling system is an immunoassay described in the “Immunocytochemistry” section that requires precise low volume chemical delivery to avoid wasting expensive reagents. Co-flow applications where two or more flow inputs are directed to the device could be optimized using an integrated liquid handling system. These applications include boundary switching systems, gradient generation, drug concentration modulation and rapid interface sweeping applications.

Liquid handling systems are typically automated by custom or proprietary software developed for their specific control (Ly, Masterman-Smith et al. 2013). However, the integration of these components represents a non-trivial challenge to typical lab users, which further alienates the vast majority of researchers that could benefit from automating liquid handling operations. The integration of these components is treated in this project as hardware and software development processes undertaken to first develop liquid transport system and loading systems and then to integrate these systems into a working tool that allow fluidic operations in microfluidic devices. This will enable further research to utilise this integrated liquid handling tool to develop high level applications. It is, however, necessary to discuss immediate applications that can be performed using this system.

1.8 Example Applications of Liquid Handling

Sub-second agonist delivery and bio-assays like immunocytochemistry were identified as potential applications for liquid handling systems to facilitate neuroscience research into information processing in the brain. The system development process will also require the use of fluorophores to demonstrate and characterise the system capabilities. Fluorophores are also used to optically detect cell cultures in immunocytochemistry. More information on fluorescence theory will provide more insight on its application to microfluidic device verification and in vitro culture monitoring.

1.8.1 Fluorescence Theory

Fluorophores are fluorescent chemicals that can be used to localise specific target molecules in cell biology. They are an important tool in cellular analysis because they can identify molecules responsible for cellular functioning or used to identify the cell structure. For example, they can be used to enhance contrast in images of living and dead cells under microscope.

Fluorescence is a process involving absorption of a photon and an electron transition and the subsequent photon emission (Masters, So et al. 2009, Burry 2010). Light can be emitted and absorbed as photons that exhibit both particle and wave properties (wave-particle duality). As a particle, the photons have an energy and momentum that depends on its frequency, v (or its wavelength λ) and is related in Equation 1.11.

$$E = hv = \frac{hc}{\lambda}$$ Equation 1.11

where: h = Planck's constant = 6.626068 × 10-34 m2.kg.s-1
v = frequency (Hz)
λ = wavelength (m)

c = speed of light = 3.00×108 $m.s^{-1}$

When light of a particular wavelength (frequency) excites a fluorophore, photons are absorbed and electrons at a ground state are excited to a higher, unstable energy level. The electrons then lose a small amount of energy due to infra-red vibrational losses. Eventually, a photon is emitted at a longer wavelength (lower frequency) to this thermal loss. The difference in wavelength between excitation and emission photon is known as Stokes Shift. The transitions are illustrated using the Jablonski diagram in Figure 1-19. An optical filter can be used to separate the emission and excitation spectra because the wavelengths differ. A fluorescence microscope is typically required to excite the fluorophore and to collect the emitted fluorescence light.

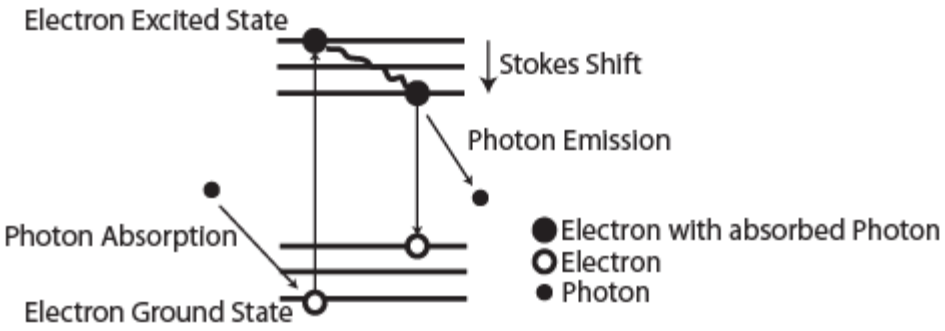

Figure 1-19: Electron energy transition during fluorescence
A fluorophore absorbs photons when incident light at its excitation frequency is applied. These photons excite the electrons at ground energy state to a higher excited level. The electrons lose energy due to infra-red vibrational losses (stokes shift) and rest temporarily at a slightly lower energy state. Thermal loss occurs and a photo is emitted at a longer wavelength which contributes to the collective fluorescence.

For example, Fluorescein is a commonly used fluorophore for optical illumination experiments. Fluorescein's peak absorption is for blue light at 470nm wavelength and its peak emission is green light at 550nm wavelength. Fluorescein spectrum is shown in Figure 1-20. Many fluorophores are now available with a wide range of excitation and emission wavelengths.

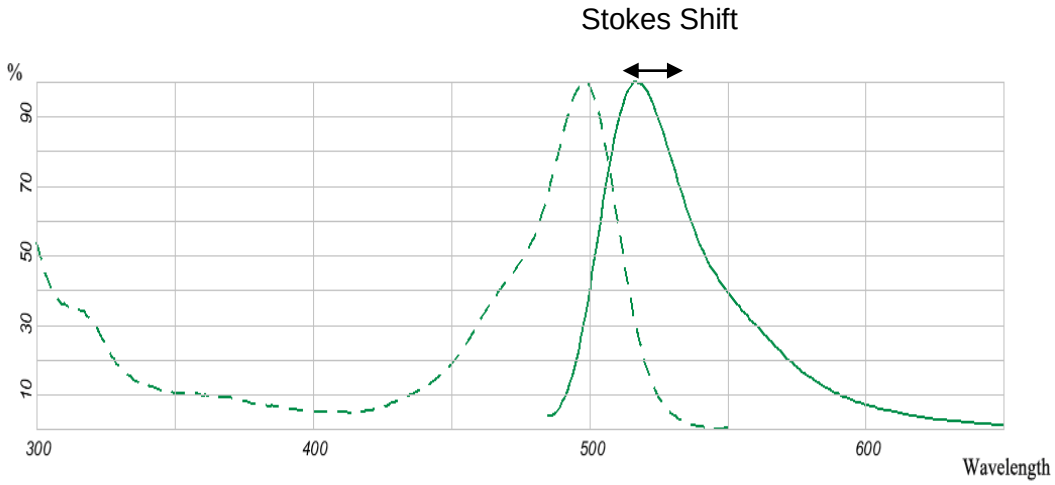

Figure 1-20: Fluorescein excitation and emission spectrum
Fluorescein is excited with light at 470 nm wavelength and emits its peak light intensity at 550 nm wavelength.

1.8.2 Immunocytochemistry

Immunocytochemistry (ICC) relies on the use of antibodies, produced by an animal's immune system (e.g. rodents such as mice, or larger mammals such as goats), to identify specific proteins in in vitro cell cultures.

An antigen is the foreign substance introduced to a body to trigger the production of antibodies. The antigens may be around a cell or on a structure contained in a cell. Antibodies, also known as immunoglobulins, are proteins produced by cells of the immune system in response to the presence of such foreign molecules. Antibodies bind specifically to the antigen and thus can be used to identify the presence of these molecules in ICC assays.

ICC may be performed using a direct approach where a fluorescent tag is attached to the antibody that targets the antigen directly. Another approach requires a primary (1°) antibody to bind with the target antigen and a secondary (2°) antibody that is covalently bound to a fluorescent tag subsequently binds to the primary antibody (Burry 2010). This indirect labelling method is used to amplify the fluorescent signal obtained since several secondary antibodies can bind to the primary antibody which

is attached to the antigen. This improves the sensitivity since weak signals are more difficult to detect, although it may also decrease accuracy through binding to incorrect targets. These approaches are illustrated in Figure 1-21.

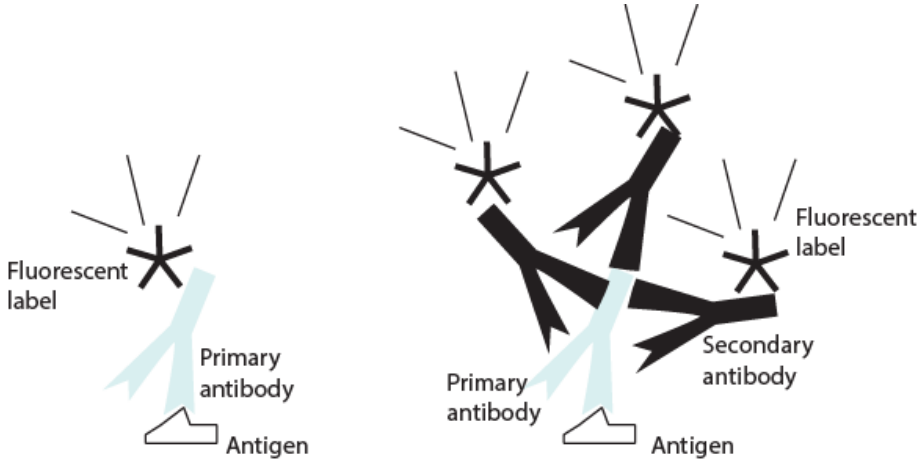

Figure 1-21: Direct and Indirect Antibody Labelling.
Direct labelling (left) uses an antibody tagged with a fluorescent marker to label target antigens while indirect labelling (right) uses secondary antibodies tagged with the markers to target the primary antibody that has bound to the target antigen. This amplifies the signal from the detectable fluorescence because the direct method provides fewer fluorescent tags per antigen molecule while several antibodies may bind to the primary antibody in the indirect method.

This review will focus on fluorescence labelling where fluorescent markers are attached to the antibodies that bind to antigens. ICC protocols are well established (Burry 2010, Skoog and Tani 2011). The general steps involved in the protocol are fixing of the cells, 'blocking' cells to reduce subsequent non-specific binding of antibodies, permeabilisation of cell membranes to allow perfusion of reagents, antibody incubation, imaging to localise antibody binding and interpretation of the data. Fixation is a crucial and mandatory step in ICC. Fixing is a method of maintaining the structure of the cells in a life-like form by creating a form of scaffolding within the cells (Burry 2010). Results of ICC protocol have been shown to be sensitive to the fixation method used (Skoog and Tani 2011).

Fixation can be performed by denaturing which utilises thermal or organic solvents like methanol; or chemical fixation which uses chemicals that bind to cellular components. The preferred chemicals contain aldehyde group and includes

formaldehyde, formalin and paraformaldehyde (Burry 2010). Chemical fixative may be advantageous because these not denature the cells (Vekemans, Rosseel et al. 2004, Burry 2010). In ICC research, the latter is used while formalin is more used in IHC for clinical analysis.

The chemical fixatives are carried in a buffer solution to where they are applied to the cells. During fixation, this buffer solution keeps the pH between 7.1 and 7.3 (Burry 2010). The method of application is critical due to the onset of necrosis at death of the animals. Vascular perfusion is the preferred method where the fixative is carried in the blood stream of the animal before death, thereby fixing the cells before they can necrose (Burry 2010). Alternatively, the tissue containing the cells can be placed in the fixative in a drop-in fixation method where the fixative is allowed to perfuse through the tissue. Finally, it can be performed by applying the fixative directly on the cells. This is difficult because there is a possibility of removing the cells from the cover slip by force when applying the fixative solution. There is also a possibility of drying of the cells when all the liquid is removed.

Permeabilization ensures that the reagents can penetrate the walls of the cells. For neuronall cultures, this is necessary as the target structures lie inside the cell walls. The wall is comprised of lipids so detergents are used to breakdown the cellular membrane to enable access to the internal structure.

Application of antibodies at this stage may bind to several sites where the antigen is not present. This “non-specific” binding is an unwanted condition that can be prevented by a blocking step that blocks sites absent of the target antigen(Burry 2010). Blocking agents prevent nonspecific binding and each possible site for incorrect binding requires a different blocking agent.

Current ICC procedures requires repetitive incubation of cell cultures in antibody solutions coupled with regular rinses. An automated system that streamlines the

sequence of reagent delivery to the neuronal cultures will add precision and accuracy to the results ensuring repeatable and comparable results across laboratories.

1.8.2.1 Automating Immunocytochemistry

The results from ICC assays can vary due to differences in the cell cultures or incubation time, as well as small differences in reagent concentrations used (Burry 2010). The inconsistencies are likely to be particular significant when volume sizes are small. This variability could be reduced from the automation of the ICC protocol that manages the control of the wash cycles and incubation steps with precision.

Reagents used for ICC are expensive and there is therefore a cost benefit to reducing the wastage due to unused reagents. A microfluidic approach could add a cost benefit to developing a system that automates immunocytochemistry. Constant supervision of the process can be eliminated, thus increasing productivity in the laboratory. Other advantages include reduced skill and labour required to perform the operation (Javois 1999). Research on automated immuno-staining tends towards immunohistochemistry - immuno-staining for tissues; but present the same ideas for precise control of the ICC procedure. The developed automated staining system should meet the following criteria (Javois 1999, Burry 2010):

1. Highly repeatable volume sampling. Errors in the volumes loaded into the flow line should be as small as possible,
2. Full automation of entire procedure. A lab technician should not be required to supervise the process.
3. Reagents carryover must be eliminated in the system and as such cleaning should form part of the operation of the system.
4. Inert materials must be used to avoid reaction with transported reagents.
5. A control system must be implemented in a user-friendly program

6. The system must improve the repeatability and reliability of the staining process over currently used methods.
7. The staining system must not add noise or interfere with other laboratory functions.

1.8.3 Co-Flow Applications

Parallel liquid volumes under laminar will maintain their independent streamlines as long as diffusive transport is not dominant. The flow rates of two liquid inputs can also be altered independently to affect the volume of each liquid present in a microfluidic device (Yamada, Katanosaka et al. 2009). Here, a Y-shaped microfluidic channel was used in a study to facilitate cell response analysis in response to the amount of the drug present in the device. This application made use of gravity driven flow and the heights of the liquid reservoirs were altered to change the flow rates. A faster interface shift can be achieved by rapidly switching the flow rates between the liquid inputs with one going high-low-high and the other low-high-low (Bae, Beta et al. 2009). These co-flow applications are generally performed with a single drug connected to one of the inputs of the device. An integrated liquid handling system could allow for long term, automated co-flow applications with varied drugs used within a single experiment. The big advantage to this flexibility is that all drug changes occur within the system without addition of air introduction which may occur while replacing the liquid in the reservoir for one input.

1.9 Hardware Development

The potential of microfluidic tools in Life Science research and the liquid handling systems that could help realise this potential has been established. The development of the hardware components can take the path of off-chip macro systems that

integrate with single-layered microfluidic devices which may have single-input or multi-input liquid channels. It may also follow on-chip development methods where the liquid handling components are established on microfluidic chips.

1.10 Software Development

The software development task for integration of laboratory equipment is complex. The primary challenge is the choice of development environment. Good software development of laboratory equipment should provide users a powerful software control of laboratory systems and a user friendly interface that improves on functionality achievable from manual control of the equipment. The ability to easily add functionalities to the developed system in software is a requirement for increased scalability. Highly scalable systems can handle a growing amount of work since they can be increased to (Bondi 2000). Any system that can improve performance, capacity or functionality with added hardware or software improvements is a scalable system (Hill 1990).

The challenge to ensure scalability of liquid handling system through efforts in software development is another technological gap that is addressed in this work. A good software design methodology must be adopted from start to finish to promote this integration. The choice of a programming language is the first step towards ensuring the development of a highly integrated and scalable system that is easy to maintain over time.

Text based languages such as C and C++ offer a versatile low-level environment for application development. However research has benefitted from the ability to quickly implement ideas using high-level languages because these languages provide considerable advantages over the low-level alternatives (Griswold and Griswold 1983). The use of LabVIEW programming interface from National instruments

provides a power tool for research and development of control systems (Cruz and Gutiérrez 2010). The graphical programming style allows the development of engineering ideas using a logical top-down development approach instead of a bottom-up design methodology.

LabVIEW is a versatile tool for developing high-level programs for increased modularity and improved readability. LabVIEW is expensive in comparison to open source programming languages like Python, C, and C++ but has key strengths in its high level design format, quick development time as well as the ease of code maintenance. LabVIEW abstracts the developer from low level challenges like memory allocation, multi-threading setup, GUI module additions and design. These key strengths along with the advantage of a large library of development kits for laboratory equipment makes LabVIEW the ideal choice for realising the software integration as well as laboratory equipment interfacing (Zurek, Marketos et al. 2007, Cruz and Gutiérrez 2010). The availability of development kits for laboratory equipment is critical for developing large scale applications with these systems but many of the kits that are currently available cannot be edited/adapted. As such their use is often limited in the integration efforts described. This forms another technological constraint towards realising the fully integrated liquid manipulation system that is addressed. A fully transparent software development process will be undertaken to provide researchers with useful plug and play libraries for integration of the developed liquid handling system.

Another consideration for development is the requirement for a sensing and control hardware that can convert commands from the high level programs into data acquisition and control signal generation functions. National Instruments provides a wide array of useful data acquisition systems ranging from real-time systems to multifunctional data acquisition systems. The advantage is the high level of support

obtainable with the equipment and high level of integration with the software as well as scalability.

The use of open source tools has been widely adopted for development of liquid handling solutions with increasing development of electronic prototyping tools and single board pcs like the Arduino and raspberry pi boards (Urban 2015). An Arduino was used for syringe pump control (See and Hauser 2014), solenoid valve control (Bogusz, Hantao et al. 2012), automated injection (Mai, Pham et al. 2013); and Raspberry Pi has been applied for peristaltic pump control (Ting, Hu et al. 2014). These tools have the advantage of removing licensing costs for the developed software applications. These applications are generally developed using low level programming coding languages that affords the user good control of low-level functions but sometimes requires high-level programming for user interfacing.

The bulk of software development efforts have been directed towards implementation in LabVIEW with an object-oriented design architecture.

1.11 Software Design Methodology

The long term goals of the overarching project – the implementation of a chemical reward system for neurons, was considered when developing software for the individual components of the system. It was necessary to abstract the specific high level applications from the low level functions of the liquid manipulation systems. It was also necessary to build scalable software that could be quickly updated to add functionalities. For example, software for applying interface switching and flow control can be updated to integrate another device such as the autoloader or a successfully implemented alternative. This scalable development process could have been achieved using any of the waterfall, spiral and agile software development approaches (Graham 1992, Cockburn and Highsmith 2001, Boehm 2006). However,

the choice would impact on the deliverables, user experience and realistic timescale for these deliverables (Chamberlain, Sharp et al. 2006, Kaur and Sengupta 2013).

i. Waterfall development process - where the overall aims and objectives are defined from the outset and the progress of development flows from the high level conceptual descriptions to initiation, design, construction, debugging, implementation and maintenance. This system is difficult to realise with limited knowledge of the future potential of the system and so was not used.

ii. Spiral development process – where the different aspects of development are reiteratively considered and used to modify the development process. This method treats the development as a series of smaller waterfall processes where the end of a sub waterfall process starts another one. This was a very extensive process that required several short term targets and multi-person development team catering to different aspects of the final program.

iii. Agile software development – where the immediate goals are first met and then incremental developments realise the final outcome. This method allows the system adaptable to changes in requirements and is more amenable to an evolving system.

The agile method was selected since it enabled quick deployment which was required for timely software development. The basic requirements for each component of the microfluidic system was identified and an initial software prototype was developed. The software was then deployed for use by other laboratory users who applied the system to solving immediate problems. Integration efforts were also carried out using the agile software methodology.

Overall, the design rules adopted were used to inform on more detailed choices made during the design process.

1.12 Design Rule Adopted

The usability of the software designed would impact its adoption and the user interface (UI) design, user experience (UX) design, documentation, readability were considered during development.

1.12.1 UI and UX Design

Software was designed to maintain a simple and efficient user interface where possible while achieving the user's goals for functionality. This is slightly different from the User experience design that refers to the experience during the use of the system which includes design graphics, interaction, information architecture and documentation/manual. Default LabVIEW front panel design controls and indicators were used throughout to maintain the same experience. LabVIEW tabs controls were used to hide advanced panels from the default users to maintain a clean minimalist design for typical users. Buttons were appropriately labelled to provide instant information to the users on the functions. Help tips were written for controls requiring detailed description.

The LabVIEW programming language aided the user interface and experience design with its readily available controls, indicators, and graphing objects which sped up the development process, allowing these choices to be made on the fly with minimal costs when modifying them.

This user experience and interface consideration is in line with recommendations for consistency and intuitive experience for the user when developing user interfaces robotic control software for microfluidic system integration (Kong, Yuan et al. 2012).

1.12.2 Code Readability

A big part of the system development was the consideration for future development (Blume 2007). Often time, the developers ignore design rules and disregard the impact of their coding style on further development. This is typical where the application only serves a single purpose and will not be used subsequently. It was crucial that core aspects of the code were readable to increase development time for further integration of system core code to larger systems. This is also tied to the documentation style adopted. Appropriate wire labels and module documentation was adopted throughout the code design process.

1.13 Thesis Structure

The thesis aims to answer two questions: (1) Can an integrated liquid manipulation system be developed that implements high spatial and temporal drug signaling patterns in tandem with sequential agonist delivery for long term assays?;

(2) Can we reliably integrate that liquid manipulation system with other equipment used to answer questions on the learning ability of neurons in vitro?

Chapter 2 describes the methods and tools used for microfluidic device fabrication, pressure control and sequential injection.

Chapter 3 treats the characterisation and optimisation of Liquid Handling Systems. The results from a previous attempt at developing a pneumatic pressure controller is characterised and optimised to improve on its performance limits for flow transport in microfluidic devices. This is then used to demonstrate the ability to achieve steady long term flow and instantaneous flow rate changes for high resolution drug signalling applications. This will also then be integrated with a commercial auto-sampler system to demonstrate the ability to sequentially load different agonists at varied concentrations.

Chapter 4 will discuss the development process for a novel liquid handling system. Due to limits identified before and during implementation of the commercial injection system, a novel system is designed that could further improve temporal resolution of sequentially delivered volumes with sampling capabilities. The developed system is expected to also boost efforts towards a scalable, modular liquid manipulation system. Constraints critical to the design process are set and a prototype is fabricated from the realised design.

Chapter 5 will pursue an alternative path towards developing a sequential injection system on a microfluidic device. An investigation is undertaken to determine if simple on-chip fluid manipulation systems could be developed using rapid-prototyping techniques which hinge on the use of craft cutter for making patterns used in microfluidic device development. This was carried out to improve on and potentially replace the commercial auto-sampler with the development of modular on-chip components offer flexible microfluidic devices for liquid handling.

Chapter 6 treats the system integration challenges for Liquid Manipulation Systems. The software requirements for the highly scalable liquid manipulation system is treated in this chapter and software design elements are applied towards realising custom user friendly interface for liquid manipulation. Example demonstrations and applications are also shown that use the results of the developed liquid handling hardware and software system.

Chapter 7 concludes with a Discussion on the outcomes of the research and the future work based on these outcomes. The research results are assessed in comparison with the original aims and objectives and the research question. Future work and further demonstration that is necessary is described as well as an appraisal of the position of this work in the field of liquid manipulation systems applied to neuroscience research.

2. Methodology

This chapter details the used materials, components, devices and experiments that were used during the development of the liquid handling system. A full list is presented in the Appendices.

2.1 Engineering Design Methodology

The bulk of the thesis is dedicated to developing a highly modular and scalable microfluidic system that could be adapted quickly to meet the immediate needs of the laboratory and be able to scale quickly to meet additional needs if required in the future. An Engineering design methodology was adopted to cater to the development challenge. The design process iteratively tackled the issues with development of hardware and software sections required to develop the highly integrable system. The problem definition was performed at a preliminary stage to identify the basic functions and specification of the components that will make up the liquid handling system and a larger microfluidic station that incorporates this liquid handling system. The feasibility of this system being realised was investigated through initial tests with some of the available components that make up the desired system. The components were put together, tested for functionality and characterised to identify strengths and failings in the design and system. An optimisation was undertaken through hardware and software design processes aimed at developing novel approaches and a blueprint that would be useful to achieving the desired microfluidic system.

2.2 Microfluidic devices and Interfacing

The single and dual-input devices shown in Figure 2-1 below have been made to demonstrate the application of the fluidic handling system for microfluidics. They have also been used to develop neuronal cell cultures using different substrates in experiments that validate the use of the liquid handling system. These devices allowed further development of the liquid manipulation system to continue with the understanding that these designs would form the basis of future systems used in the research laboratory. These designs were fabricated on plain glass substrates for demonstrating liquid injection and drug switching. Other collaborators utilised the same with plain glass as well as gold patterned glass substrates for characterising surface modification effects on neuronal cultures. They also incorporated these designs on an MEA substrate (glass) in an attempt to integrating rapid drug signalling, agonist delivery and neuronal culture monitoring.

Microfluidic devices were made using simple fabrication technologies that allowed rapid turn-around time for production. A combination of methods including soft-lithography, photo-lithography, stamp and stick, Xurography were used to realise these devices. These methods allowed flexibility in developing new designs for fabrication. They also used materials that are bio-compatible with the other processes that are part of the multidisciplinary research efforts such as surface chemistry for cell cultures. Rapid prototyping procedures like xurography and “stamp and stick” enabled the substrate surface to be chemically treated before bonding without damaging the chemical layer on the substrate.

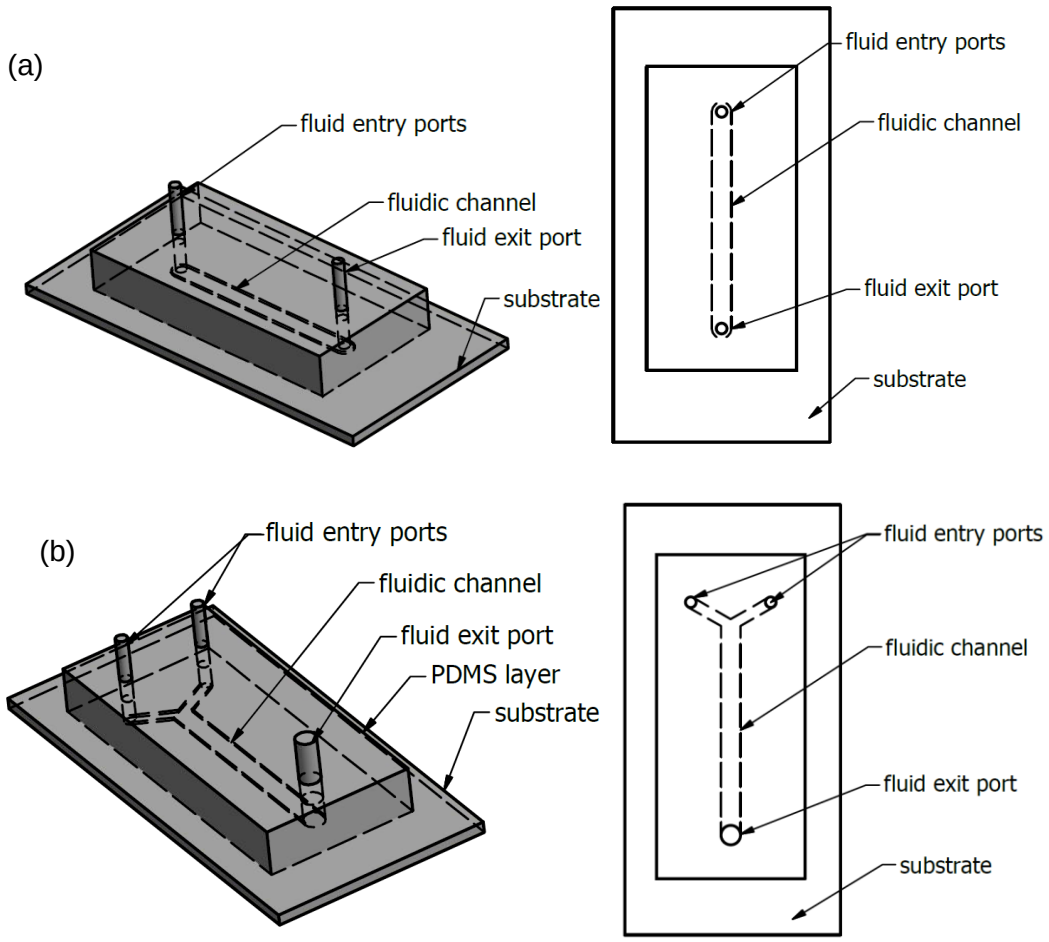

Figure 2-1: Microfluidic devices used to demonstrate fluid handling capabilities
The single input device (a) is used to demonstrate liquid loading capabilities that do not require high temporal resolution or spatial resolution of the loaded agonists. The dual input device (b) is used to demonstrate spatial and temporal resolution of fluid transport system.

2.2.1 Soft-lithography, Photolithography and Device Assembly

Device fabrication using PDMS was developed by Whitesides group and widely adopted for fabricating microfluidic devices (Whitesides 2006). It required the development of a master mold with features using photolithography and the application of a fluid elastomer over this mold to imprint the features on the elastomer which is cured.

2.2.1.1 SU-8 Mold and Photolithography

The photolithography step uses ultraviolet (UV) light to transfer a pattern from a mask to a photoresist on a substrate. SU-8 is a photoresist that becomes cross-linked when exposed to ultra-violet light. It is used as a negative photoresist to make high resolution molds by exposing some parts to the UV and washing off the remaining parts with a solvent.

The photolithography was undertaken by Mr. Alexander Johnstone of the neurophotonics lab as cleanroom training and access rights were required. A silicon wafer substrate (Pi-kem) is first cleaned with ethyl lactate and acetone, methanol (Sigma Aldrich), nitrogen dried and heated at 150 degrees for 30 mins in an oven (Memmert) to remove moisture and promote SU-8 adherence. The SU-8 is applied by spin-coating on the substrate at 2000 for 30 seconds to get layers of 75 μm thickness. The coated wafer is pre-baked on a hotplate at 65 degrees for 5 minutes followed by 95 degrees for 10 minutes to remove excess photoresist solvent and harden the sub photoresist.

The coated wafer is exposed to UV at 365nm 9mW/cm^2 for 30 seconds to crosslink the parts of the resist that has been exposed to the light. The wafer is heated again on a hotplate at 65 degrees for 5 minutes followed by 95 degrees for 10 minutes in order to achieve this rapidly and effectively. Once it is cooled down to room temperature, the wafer is exposed to ethyle-lactate with mild agitation while changing the developer solution every five minutes to refresh the solvent. The wafer is rinsed at the end of the development in ethyl lactate and is nitrogen dried.

The final step is the hard bake where the wafer is heated from room temperature to a 150 degrees for 30 minutes and then permitted to cool back to room temperature. This step renders the resist mechanically robust for use with soft-lithography which

will typically occur at less than 100 degrees. This master mold can then be used to mold features to an elastomer in a soft-lithography process.

2.2.1.2 Soft-lithography

This widely adopted method developed by Whitesides was preferred since it produces chemically inert devices with good optical properties. PDMS (polydimethylsiloxane) is formed from the thermal curing of a silicone elastomer mixture of base and curing agent. The Sylgard 184 kit (Dow Corning) is comprised of a base and curing agent that was mixed in a ratio of 10:1 respectively. This manufacturer recommended mix ratio was used as there was no added requirement for rigidity of the cast PDMS. The mix is then degassed using a vacuum pump (Becker, D42279) to remove trapped air. Trapped air could remain stuck in the PDMS during cure and affect the usability of the PDMS material. The mixture is poured over a flat surface or mold and left to cure at 60 degrees for 30 mins to 1 hour. The hardened PDMS can then be peeled off the mold or surface and used as a part of the assembled microfluidic device.

Thin layers (t = 20 – 85 μm) of PDMS were formed by spin coating the PDMS mixture over a featureless SU-8 wafer, made by a collaborator, using a spin coater (SPS Europe, Spin150) for 30 seconds. The same was done by replacing the wafer with a glass slab (50 x 50 x 2 mm). The thickness of the spun PDMS was measured for different spin speeds on the glass slab and is shown in Figure 2-2.

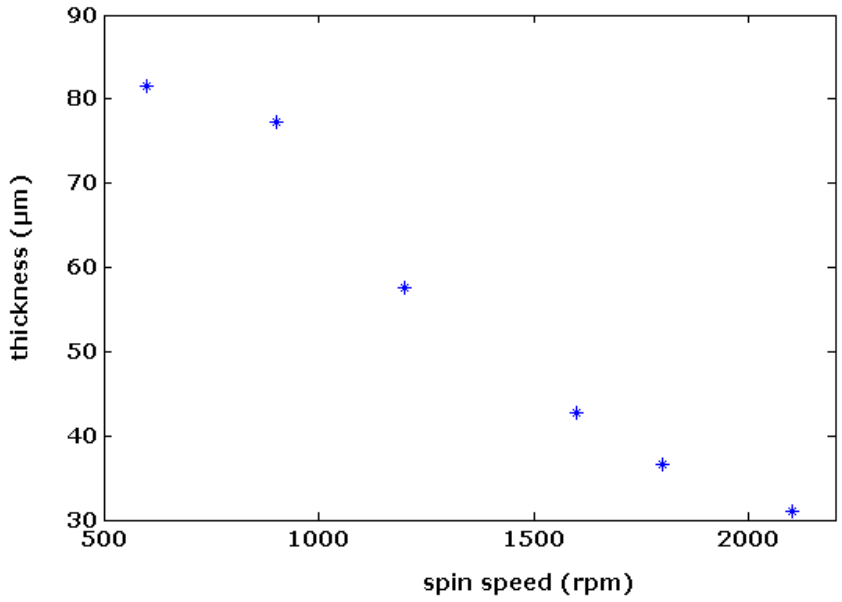

Figure 2-2: PDMS thickness with different Spin Speed
PDMS was spin-coated on a glass slab (50 x50 x2 mm) at 500 rpm for 10 seconds and then variable speed settings shown for 30 seconds. The slab is then placed on a hot plate at 80°C.

The final step in the assembly using this fabrication method requires a bond between the substrate and the channel-patterned PDMS cast. Either the Oxygen plasma bonding or a stamp and stick methods was used to close the device. A hole is first punched through the PDMS at the channel terminals using a bio-punch (Ø = 0.05 – 3 mm) to allow tube connections for fluid passage.

2.2.1.3 Device Assembly

Oxygen Plasma Bonding

A plasma oven (Diener product - Zepto) was used to activate surfaces of glass and soft-lithography PDMS for bonding. The pieces were placed on an aluminium slab with the contacting surface facing upwards. The slab was placed in the oven and the vacuum pump turned on for 10 minutes with the oxygen gas source set to zero pressure. This is to remove unwanted gasses in the chamber and to increase the percentage of oxygen present for plasma bonding. Oxygen gas was allowed into the

vacuum compartment when the pressure dial on the oven reached to 0.16mbar. The oxygen air flow was regulated to get the pressure in the chamber to between 0.26 and 0.28mbar. The plasma generator was turned on for 2 minutes at full 90W power. Literature recommends 60W but it was observed that this did not produce good bonding with the equipment. After the plasma activation, the activated surfaces are brought into direct contact. Methanol was not used to aid alignment since the substrate surface area was large enough to accommodate the smaller PDMS device. The bonded device was left on the hot plate at 80 degrees for 1 hour to improve the bond.

This method of bonding was inefficient when several devices needed to be fabricated since the devices needed to be brought into contact within 1 minute for reliable bonding. An alternative was used when large number of devices were required.

Stamp and Stick

A faster method used to bond PDMS soft-lithography layers to substrate was the stamp and stick method. The curing agent from the PDMS kit (Sylgard 184) was spin coated on a cover slip to produce a thin film (0.01 mm) on the cover slip. The PDMS from the soft-lithography was briefly brought in contact with the curing agent that stamped onto the extruded surface and not the channel geometry. The layer was then placed on the glass substrate and the assembly was placed on the hot plate at 80 degrees for one hour with a load (w = 2 Kg) on it.

2.2.2 Xurography

A disadvantage of soft-lithography was the rapid deterioration of the SU-8 mold with use. Another disadvantage is the lack of rapid prototyping flexibility. Small changes to the design will require development of new master molds with the modified designs. Xurography (established by (Bartholomeusz, Boutté et al. 2005)) provided an

alternative means of fast prototyping microfluidic devices. A craft cutter (Graphtec America product, silhouette cameo original) was used to cut patterns into a double sided silicon tape material placed on the cutting mat. Geometries were first designed in a CAD package (Autodesk Inventor professional 2013) and exported in DXF format. The dxf file was imported into the Silhouette studio software and the cut settings modified to match the material to be cut. Blade depth settings were adjusted to obtain through-cuts on different material types for different materials. Double cuts were required for harder materials such as PET. For this process, the layer is placed on the cutting mat and held in place with scotch tape to prevent movement during the cut. The cut is initiated and the patterns are excised from the layer when completed.

2.2.3 Tape-layered Microfluidic Devices

Silicon based adhesive transfer tapes of thickness 125 μm (3M product 96042) are provided with a PET primary release liner and were attached to a secondary release liner to maintain the tape integrity during the cut process. Geometries were imported into the silhouette design software for the tape cutter as described above.

PDMS is mixed and cured as described previously to a thickness of 5mm. the secondary release liner was removed and the tape was brought into contact with the PDMS. Access ports were cut and cleaned as described using a biopsy punch. The 125 μm tape is made of a 25μm PET film sandwiched between two 50μm tapes which makes it difficult to create access ports for multi-layered devices. The ports had to be cut on the other layers using the cutter to avoid damaging the tape and the biopsy punch. The primary liner was then removed and the tape was brought into contact with glass. The device was left at room temperature for several days or cooked at 45 degrees for a day to improve the bond.

The selected microfluidic devices were connected to macro liquid handling systems using commercially available High Performance Liquid Chromatography (HPLC) tubes and connectors.

2.2.4 Tubes and Interconnects

The macro-to-micro fluid connections allowed integration of macro sized liquid handling systems with the selected microfluidic devices. The tubing used were selected based on material properties and dimensions that enhanced the objectives of the project. Fluid dead volume, tubing compliance, fluidic resistance, chemical inertness and gas permeability properties were considered in selecting the tubing used.

The dead volume, which is determined by the tube diameter and length, affects reagent transport time, volume replacement time and the volume of samples consumed. Larger tubing diameters result in larger volume per length. The tubing length were selected to bridge the system components with minimal tension and small internal diameter tubing (ID = 0.15 mm) was preferred over the alternatives (ID = 0.25, 0.5, 1.0 mm) when developing interfacing the macro-to-micro components. Another advantage of small diameter tubing is that Taylor dispersion effects are minimised for sample injection applications where drug concentration may be critical. Taylor-Aris generalised solution in Equation 2.1 shows that a longer time duration is required to broaden a sample plug by the same length (w) in smaller tube diameters (a). Doubling the internal diameter will increase the broadening time by a factor of four.

$$\tau_{Taylor} = \frac{w^2}{D_{eff}} = \frac{D}{48V_0^2}\frac{w^2}{a^2} \qquad \text{Equation 2.1}$$

Where w = linear length extension of sample width

D_{eff} = effective diffusion coefficient
D = molecular diffusion coefficient of the sample
a = pipe radius

Another advantage of low tube diameters is the high fluidic resistances they provide. This is important for pneumatic pressure-driven flow to ensure that low changes to the pressure from noise does not translate to high noise in liquid flow rate during perfusion in microfluidic systems (Stone, Stroock et al. 2004).

The tubing compliance relates to the elasticity of the tubing and can cause undesirable flow effects (Meyvantsson, Warrick et al. 2008) by altering the pressure-flow relationship (Kim, Chesler et al. 2006). Consistent tube dynamics was required to ensure precise and steady flow control (Fiering, Mescher et al. 2009). PEEK (Polyether ether ketone) and FEP (Fluorinated ethylene propylene) tubes were used in the development process.

Typical perfusion systems for cell cultures requires the infusion of soluble CO_2 gasses in the media delivered to the cells. Little consideration was given to gas permeability of the tubing to limit the loss of these soluble gasses during perfusion. PEEK tubing was used to connect most of the devices to microfluidic devices due to its gas impermeability and high fluidic resistance which allowed flow rates to be controlled more effectively. It was expected that future development efforts towards gas exchange at the microfluidic chip would obviate the need to consider gas permeabilisation through microfluidic components. FEP (Fluorinated ethylene propylene) tubing was also used in experiments requiring properties like transparency, lower fluidic resistance and flexibility.

The use of PDMS for microfluidic device fabrication removed the challenge of connecting tubes to the devices. A biopsy punch (Harris Uni-Core; diameters - 0.5, 1.5, 3.0 mm) was used to punch holes in the PDMS that allowed tubes to be connected to the device using the “press-fit” method (Christensen, Chang-Yen et al.

2005). The conformal nature of PDMS allowed connection of 0.35 mm diameter tubes in 0.5 mm punched holes.

Small HPLC (high performance liquid chromatography) PEEK tubes (Thames Restek) with dimensions (ID = 0.15 mm; OD < 0.25 mm) were used for most connections due to its small internal diameter. These tubes could not be “press-fit” into the PDMS due to the punch size available (0.5 mm) and high flexible of the tubes. These tubes were sleeved using larger internal diameter peek tubing (ID = 0.25 mm; OD = 0.35 mm). A silicone glue was applied to the smaller tube before pulling through the sleeve to prevent leaks. This “sleeving” process is illustrated in Figure 2-3.

It was found that the PEEK tubes caused tears to the PDMS when inserted. This was solved by using 23G steel tube connectors (Elveflow, steel connector OD = 0.5mm, h = 20mm) that were bridged to the PEEK tubes using pieces of Tygon tubing (ID = 0.5 mm) steel connectors. This is also illustrated in Figure 2-3.

PEEK Luer adapters (Thames Restek) and connectors and were used to connect syringes to the tubing and FEP tubes were also used in some instances requiring larger internal volumes were required.

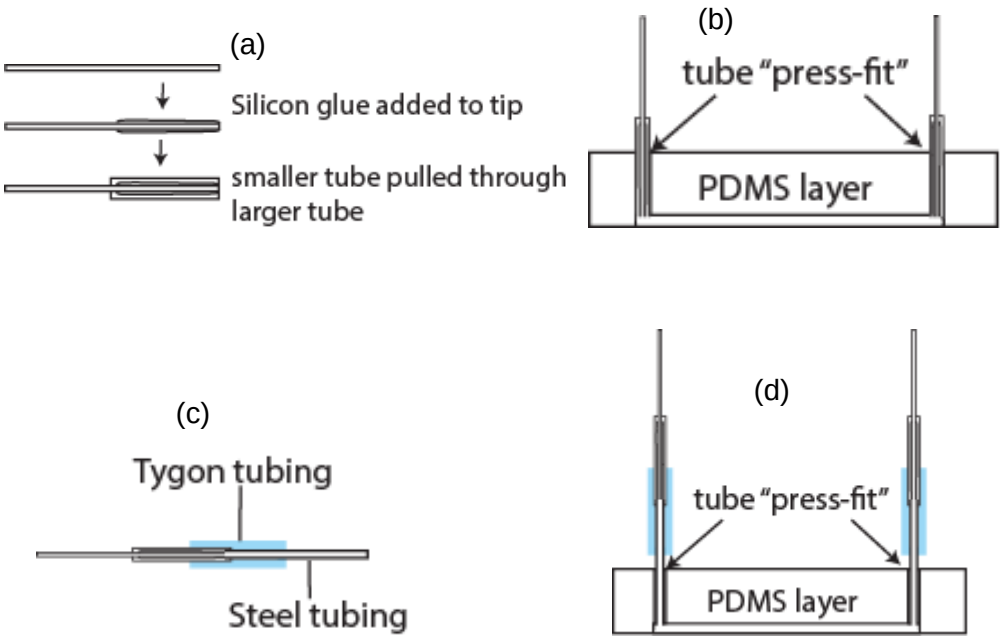

Figure 2-3: Sleeving small outer diameter tubes and connection to PDMS for fluidic interfacing
"Sleeving" was used extensively to adapt smaller outer diameter tubes for use with large bore HPLC connectors and connection with PDMS layer of microfluidic devices. (a) Silicon glue was added to the section of the small tube to be sleeved to prevent leaks. (b) The tube was then passed through a larger diameter tubing and the sleeved unit would be "press fit" to the PDMS layer. (c) To avoid ripping the PDMS layer, steel tubes were preferred for connection. Tygon tubing was used to were bridged to the sleeved tubing with the steel tube for connection with the PDMS layer (d)

The tubing and interconnections selected were used to connect fluid flow systems and liquid injection systems as well as interfacing these systems to the microfluidic devices. Fluid transport was implemented using syringe driver controls and pneumatic control systems.

2.3 Fluid Flow Control

This section describes the components and devices used to achieve fluid transport which include syringe drivers and pneumatic pressure-driven flow control.

2.3.1 Syringe drivers

Flow control using syringe drivers (Cole-Parmer, 789210C) was demonstrated using a custom software written in LabVIEW that further demonstrated the software integration efforts. The application allowed the two-syringe driver system used to simultaneously deliver contents of the syringes to more than one target microfluidic device so it could be used in applications that simultaneously characterised the cell cultures in multiple devices. Syringes (1, 2, 2.5, 5, 10, 20, 50 mL) were configured into the software so the user is able to choose the one in use at run time. A computer cable for Series 75900 pumps (Cole-Parmer) was used to adapt the RJ11 port to 9-way d-sub connection for RS232 communication and an RS232 to USB adapter (FTDI Chip) was used to provide the pc with an RS232 connection for interfacing with the syringe driver. Multiple syringe drivers were controlled by connecting them in a chain illustrated in Figure 2-4. A LabVIEW software was written to control the syringe drivers in a continuous mode and single operation mode. The single operation mode starts a configured operation when executed while the continuous mode allows the user to make changes to the operation during the operation.

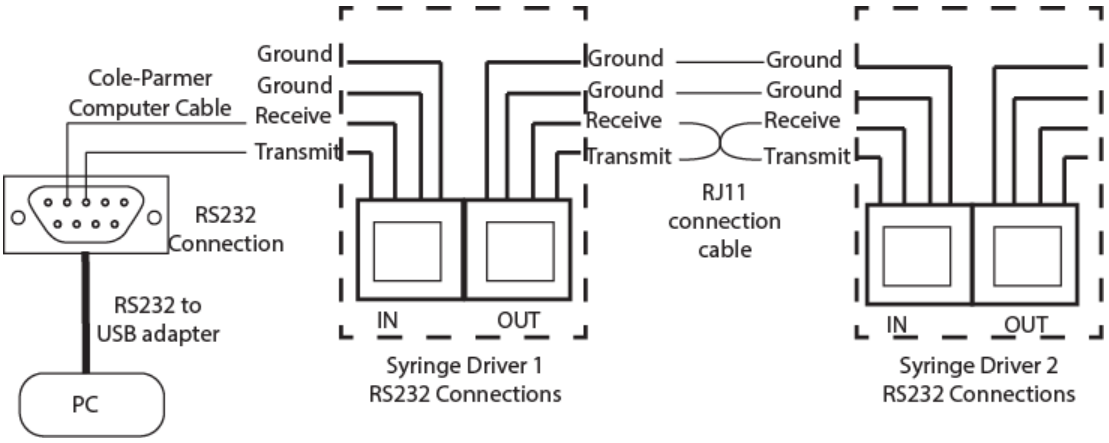

Figure 2-4: PC control of daisy-chained syringe drivers
RJ11 connection sockets on Cole-Parmer syringe driver for RS232 communication with PC and other daisy-chained syringe drivers. The RJ11 is interfaced with the PC using a communication cable supplied by Cole-Parmer and an RS232 to USB adapter. The other syringe drivers are daisy chained by connecting the "OUT" on the last connected driver to the "IN" on the next in the chain using RJ11 communication cables.

The flow inconsistency obtained while using the syringe driver for flow control is demonstrated in Figure 2-5. The control software was configured to deliver target flow rates integrated with a flow sensor (Elveflow MFS2) to monitor the flow rates achieved. It is believed that the quality of the syringe driver contributed to the noisy behaviour.

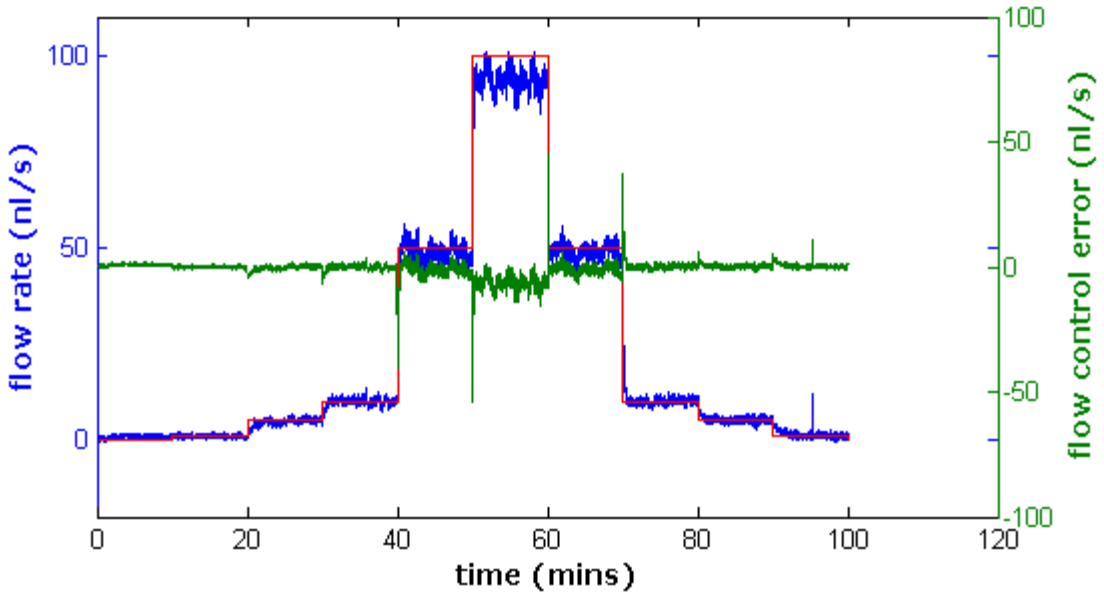

Figure 2-5: Flow inconsistency using a Cole-Parmer syringe driver for fluid control
The syringe driver was automated with software written in LabVIEW to target flow rates (red line) while logging the measured flow rate (blue line). The error between them is also displayed on the chart (green line).

The setpoints were modified to simulate an fast flow switching operationg with target flow changing every one second interval. The result of the latency tests shown in Figure 2-6 confirms that the syringe driver is unsuitable for fast flow switching operations that are necessary to deliver neuromodulator drugs to neuronal cultures on target relevant timescales of 1 second. As such a pnenumatic pressure control system was developed to achieve rapid drug signalling flow control capabilities.

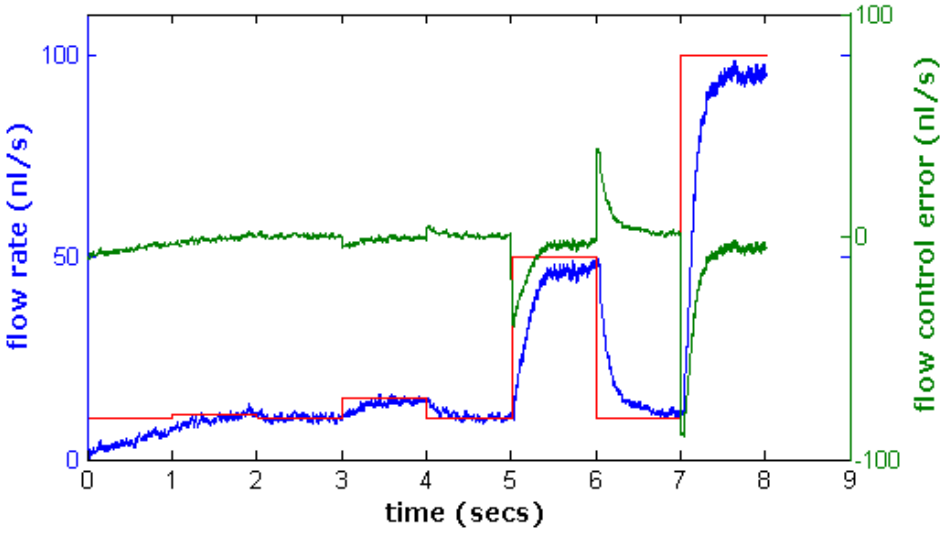

Figure 2-6: Fast flow rate switching with the syringe driver
The target flow rate (red) delivered to the syringe driver cannot be realised within one second confirmed by the measured flow rates (blue). The low latency of the syringe driver makes it unsuitable for rapid drug delivery which requires flow rate change within 1 second of target command.

2.3.2 Pneumatic Pressure Control

The syringe driver was incapable of realising high latency flow control prompting the development of pneumatic pressure-driven control. A pressure regulation system was designed to provide real-time pressure control in a liquid reservoir. This is illustrated in Figure 2-7. Pressure from a cylinder was regulated using step-down regulators and pressure controllers to a useful pressure for realising fluid flow control in microfluidic devices between 1 – 100 $nL.s^{-1}$.

2.3.1 Pressure Source

An air compressor (Thorlabs PTA513) fitted with a regulator was used to provide gas pressure (up to 8 bar) for development work. A gas cylinder with 5% CO2 / 95% room air (BOC Gases Ltd product 225742) was used for pneumatic pressure-driven flow control applications where cells where involved. CO_2 is driven into solution via pressurisation ensuring its delivery CO_2 to the cells that require it for survival. Non-electronic hardware previously exposed to air from the air compressor were soaked

overnight in non-corrosive detergent like hand-wash to remove potentially damaging contaminants that may have escaped the filter used. This was done before using the hardware on applications involving cell cultures. A 1 bar air pressure supply was also supplied through a standard laboratory air supply tap.

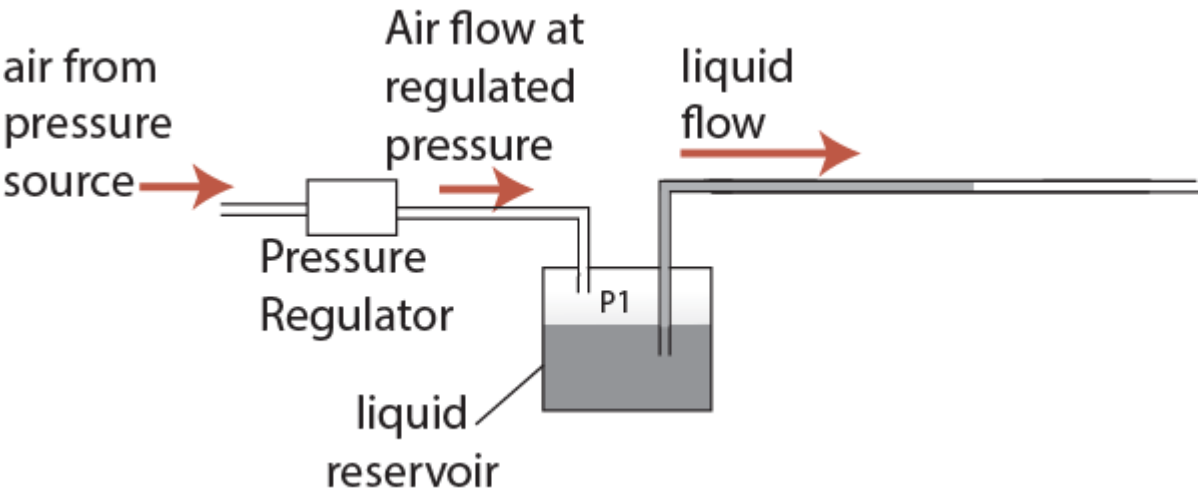

Figure 2-7: Pressure driven flow control
The pneumatic pressure-driven flow control system was developed using a pressure source, regulator(s), a liquid reservoir and tubing connections.

2.3.2 Step Down Regulators and Filters

The supplied gas was always passed through a filter (IMI Norgren Ltd product F72G-2GD-QT1) that had used an adapter fitting for 6mm and 4mm pneumatic tubes (IMI Norgren Ltd products C02250628 and C02250428). The filter is designed to dehydrate the air and to prevent large particulates from getting into the components used.

The filtered air is then passed through any of two step down regulators (IMI Norgren Ltd products RM1L-NND-NCV and 11-818-100) for finer static control of air pressure from the main source. This enables one high pressure source to provide regulated gas pressure for several applications without crosstalk. Manual adjustments can be

made to the pressure using the tap on these regulators while reading the pressure value with a sensor (GE Druck product, PMP 5074).

2.3.3 On/Off Pressure Valves

Applications requiring on/off pressure application were pressurised with on/off solenoid valves (SMC SY100 series). These valves are arranged on a manifold base with up to 6 valves per manifold. Each valve requires 12V actuation that can be provided through a power supply unit or a relay circuit. They can pass and stop 0 to 0.7 MPa pressure with 10 ms response time. The operation of these valves is illustrated in Figure 2-8.

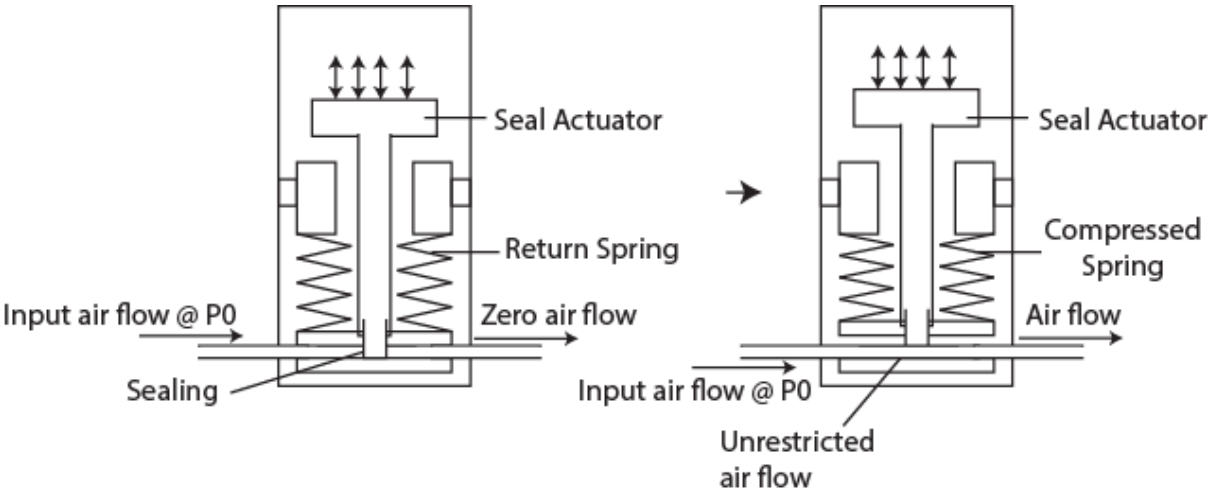

Figure 2-8: On/Off solenoid valves
These on/off valves (left) have a seal that blocks air flow from the input orifice (left). These seals can be actuated, usually with the aid of an electromagnetic coil, to pull the seal away from the air flow path (right). This allows the unrestricted air flow through the output orifice.

2.3.4 Pressure Controllers

Proportion air regulators were obtained from Proportion Air but they quickly developed faults and were difficult to tune as the control algorithms were hardware based requiring special knowledge. A custom pressure control system was therefore designed and developed by a collaborator, Sorka Abanu, comprising 2 proportional

air valves, pressure sensing equipment, relief valves and a manifold housing. The designed system is shown in Figure 2-9.

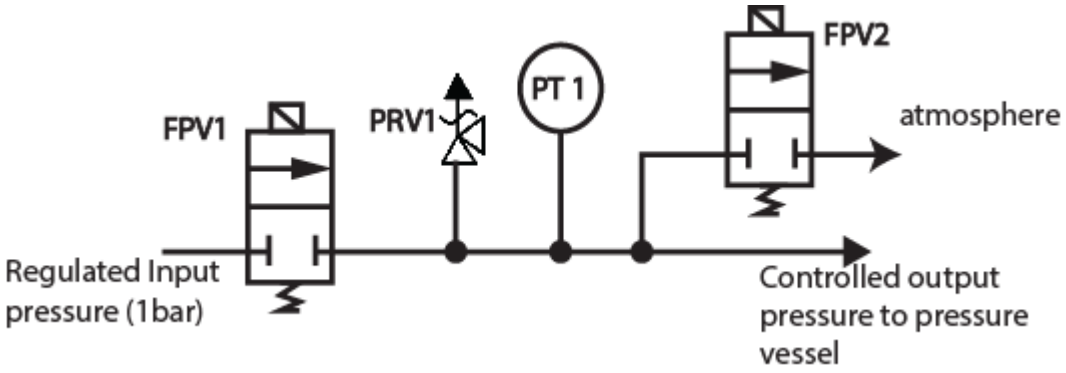

Figure 2-9: Control diagram for a two valve pressure controller
The two valve pneumatic pressure controller was used to manipulate pressure output by controlling the flow rate of air going into the system using the input Flatprop valve (FPV1) and the flow rate of air vented to atmosphere by the vent Flatprop valve (FPV2) valve. It is also comprised of a pressure relief valve (PRV1) to vent excess pressure (> 260 mbar). The pressure transducer (PT1) provides system pressure feedback for closed loop pressure control.

2.3.5 Pressure Sensing

Pressure sensors (GE, Druck-DPI104) were used for quick pressure checks and valve configuration. These sensors did not provide fast response times and were not used for time sensitive applications like the pressure controller. Pressure transducers (GE PMP-5074) with 3.5 kHz frequency response were used for these applications. These transducers output 0 – 5 V in response to 0 – 250 mbar pressure and have ±0.04% Full scale (0.1 mbar) accuracy specification.

2.3.6 Relief Valves

The pressure transducer used had a maximum pressure tolerance of 500 mbar and required a relief valve (Norgren, 1002/BM000) to vent air from the system when the pressure exceeded 300 mbar.

2.3.7 Proportional Valves

Proportional valves (Norgren FAS FLATPROP) were used as pressurisation and depressurisation valves. These high-resolution miniature valves were specified to provide high air flow rates 186 L/min with 2 bar input air pressure and quick response times (10ms). An electromagnetic coil in the valve responds to applied current which then opens the orifice for air flow in proportion to the applied current. The operation is very similar to the operation of an on/off solenoid valve in Figure 2-8 but the electromagnetic force of the coil is directly proportional to the current passing through it.

High resolution current control was required for proportional valve operation and a PWM signal was used to improve the dynamic response of the currents delivered to the valves. PWM signals generated from available data acquisition (DAQ) systems (National Instruments, Multifunction DAQ) could not provide sufficient current (200 mA) and voltage (12V) to drive the valves and an amplification circuit was used. This circuit was designed to modulate a current source using the digital signal (0 – 5 volts) provided from the DAQ digital outputs

The integration of these components allowed deterministic pressure control described in the Performance and Optimisation section. They were then integrated with a liquid reservoir (sealed Duran bottle) and flow sensor for liquid flow control by the collaborators Soka Abanu and Fu Bo.

2.3.8 Liquid Flow Sensors

Liquid flow sensors (sensirion) were used to monitor flow rates of the integrated system. Flow sensors (Elveflow MFS2) with sensing range of ±7 µL/min were used to provide an analog output voltage of 0 – 5 volts corresponding to the measurable range for feedback in the liquid flow control system.

2.3.9 Duran bottle sealing

Liquid reservoirs were made using duran bottles with customised lids. Two holes were drilled into the caps for gas and liquid transfer in and out of the bottle respectively. Fluid bulkhead connectors (Thames Restek, VIZBU.5FPK) were used to pass liquid. BSP bulkhead connector (ACC, C4-10/8) and male adapter (ACC PC0628) was used to provide gas connection to the duran bottle.

The system was able to achieve flow control but did not do so on the desirable 1 second timescales. This prompted the further investigation into the system design and control algorithms required in order to realise rapid flow switching.

2.4 Liquid Injection

Liquid injection was realised using a refurbished commercial autoloader (Jasco AS-950).

2.4.1 Autoloader operation

This system used a high pressure (HP) two-position injection valve illustrated in Figure 2-10. The valve is fitted with 6 ports labelled 1-6 in Figure 2-10(a). The normal operation mode is shown in Figure 2-10(b) where a flush and sample loading sequence can also be performed without affecting the main flow between the pump to the microfluidic device aided by the internal fluidic connections in the valve. The HP switching valve performs fast high pressure switching between ports to avoid fluid loss and contamination.

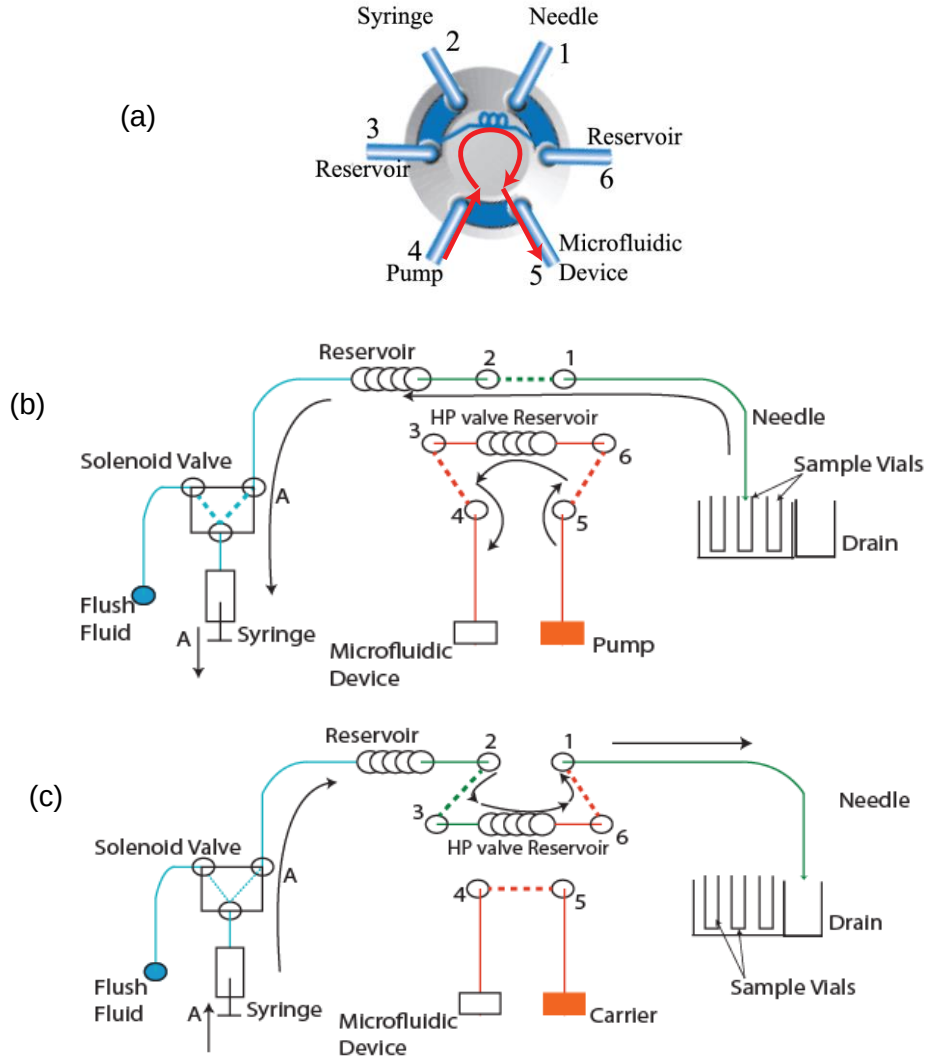

Figure 2-10: Schematic of injector switch and operation of Jasco AS-950 autoloader
The inector switch (a) has six ports that connect to the syringe, pump, microfluidic device, reservoir and needle that is moved using an XY-translation stage to any sample position or the drain position. The injector position in (b) allows the syringe driver A to take up samples into the reservoir and then through the internal fluidic connection between port 1 and 2. This injector position is the default position and the pump maintains the flow of the carrier liquid through the internal fluidic connections and the reservoir at the high pressure (HP) valve. The HP valve switches position (c) creating an direct fluidic connection between 4 and 5 and the syringe infuses the loaded sample from the reservoir through port to and 3 to the HP valve reservoir. The injector valve returns to normal operation (b) to allow the pump continue the fluid transport of the loaded sample from the HP valve reservoir.

The autoloader inserts a volume of sample into the flow line after a sequence of operations involving motion control, timing and signalling. During sample uptake, the solenoid valve is switched such that port 2 leads to the syringe. The sequence of operations required to insert a volume of sample into a flow line is:

1. With the HP valve in normal position, stepper motors and an XY translation stage move the needle to the position of the sample vial.
2. Motors controlling the syringe plunger move to aspirate the sample into the flow line. It continues to do so until the sample is in the reservoir between the syringe and port 2.
3. The HP valve switches to insertion position redirecting the internal channels of port 1 to 6 and port 2 to 3.
4. The syringe then pushes the programmed volume into the reservoir.
5. The HP valve switches to the normal position and the normal flow from the pump line combines with the inserted fluid and transports the fluid to the microfluidic device.

The autoloader required an interface chip (Masco, 6540-M553A) to enable RS232 communication access over a 25-way D-Sub socket. A 25-way to 9-way D-sub adapter was then connected to an RS232 to USB adapter. This allowed PC to interface with the internal chip and send high level load sequence commands using RS232 protocols.

The autoloader was first cleaned before initial use and cleaned intermittently after periods of inactivity to remove residual chemicals in the machine tubes.

2.4.2 Autoloader cleaning protocol

A protocol was used to clean the autoloader to remove residual chemicals in the tubes:

1. Wash with 4% Decon 90 detergent for 10 minutes.
2. Rinse with distilled water for 30 minutes.
3. Wash with weak Hydrochloric acid. 1%. 10 minutes.
4. Rinse with distilled water for 30 minutes.

5. Wash with methanol for 10 minutes.
6. Wash with Isopropanol (IPA) for 10 minutes
7. Wash with Distilled water for 2 hours.

This protocol was realised with the following steps.

1. The wash reagent was pumped with an external syringe through the pump port to the output port. This was done while using another syringe to pump the reagent through the flush tubes to the needle for the specified time.
2. The machine was turned on and set to flush. This actuated the solenoid valve to a position that allowed the syringe direct connection to the flush liquid reservoir. The machine was turned off during the flush initialisation to maintain the solenoid valve position and a syringe with reagent was used to flush the fluidic path.
3. The device was then turned on and set to flush. When the flush was complete the reagent filed syringe was used to flush the flush path through the needle.
4. The system was primed by loading the autoloader syringe with distilled water outside of the autoloader mechanism and then causing the syringe to flush the system manually while throughout an automated flush sequence. This ensured that no bubbles were left trapped in the system before operation.
5. Vials with the reagents were loaded with the reagents and a load sequences were performed while using the syringe driver as the pump mechanism.

2.5 Integrated Liquid Handling

This integration of a commercial autoloader and a pneumatic pressure-driven flow control system was carried out as a starting point to apply liquid handling techniques of flow control and liquid injection to a microfluidic device. Figure 2-11 shows an overview of the integrated handling system which is comprised of a pump system,

agonist loader, flow rate sensor, microfluidic device, fluid sampler and a back pressure system.

The commercial pressure controller (Proportion Air) was used as a pump and the signal terminals were connected to a data acquisition system (NI USB-6009) which generated an analog voltage (0 – 10V) that controlled the output pressure. 1 bar pressure was supplied to the pressure controller input.

Deterministic flow control was not realised due to restrictions in accessing the flow rate data on the flow sensor. Flow could only be monitored on the proprietary software supplied. A set of calibration experiments was done to identify pressures settings for target flow rates.

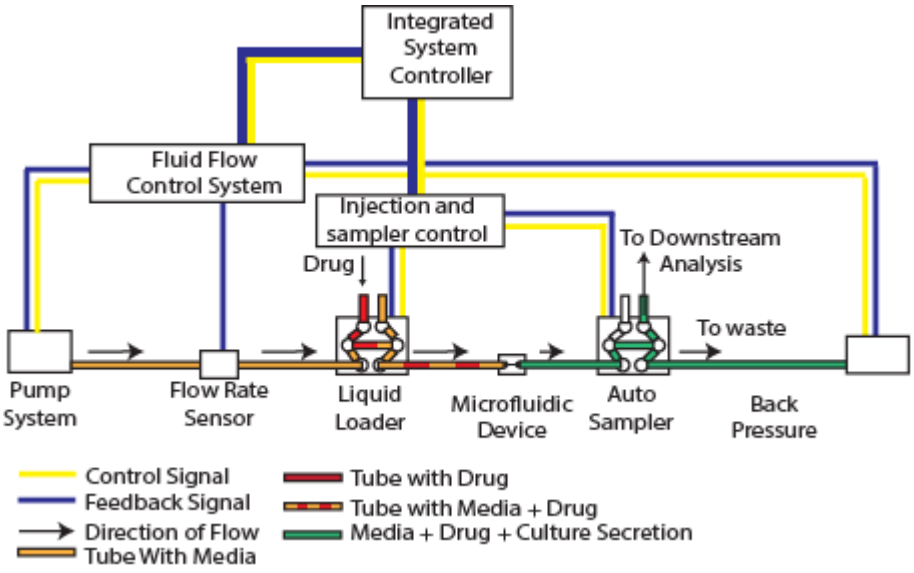

Figure 2-11: Schematic for integrated liquid handling

Ultimately, the replacement of the sensors with analog output sensors enabled the realisation of a real-time flow rate control system to achieve the desired integration.

The back pressure was required to apply compressive force on any bubbles trapped in the system. This back-pressure, typically 70 mbar was applied to a liquid reservoir which was connected to the fluid line from the microfluidic device.

Downstream sampling was required to enable sampling of used media from cultures in the microfluidic device for off-chip analysis. This requirement could not be achieved using the autoloader since it was primarily built for loading reagents from sample vials. Low level control of the injection valve was not possible to independently activate the switching mechanism that would have enabled downstream sampling. This limitation prompted the development of a liquid manipulation system that could replace the autoloader for loading operations and enable liquid sampling downstream of the microfluidic device.

However, a full implementation and charactersation of the autoloader as a liquid injection system was required to identify the pros and cons of this macro liquid manipulation system that further provided a suitable set of design constraints which informed the design process for a suitable alternative for fabrication.

One of the capabilities of the autoloader that was verified was its accuracy and precision in loading required volumes. Other characteristics considered included operational range, determinism in loading times, form factor, sampling capabilities and flow disruption.

2.5.1 Autoloader Accuracy and Precision

The accuracy and precision of volumes loaded by the autoloader was tested to quantify how reliable and repeatable the autoloader is at sampling programmed volumes. It was aimed to determine the errors to expect in the sampled volumes in other to compensate for them.

Using air as the carrier liquid, the autoloader was manually configured to dispense 10µl, 20ul, 30µl, 40µl, 80µl and 100µl of distilled water into an empty pre-weighed sample vial. The vial was then sealed to reduce evaporation. The liquid was weighed

and density of 1g/mm^3 was used to calculate sampled volume. This was repeated for n=6. The volumes delivered are compared to programmed volumes in Figure 2-12.

The fluid sampled by the machine had a mean loss of 4.2µl at the output of the HP valve with a standard deviation of 0.94µl. This shows the device is fairly precise but inaccurate. Since the fluid was sampled into a dry tube, it was possible these losses occurred on the channel walls but was not confirmed. By compensating for the mean loss in the autoloader control system, the autoloader could be made to sample more accurately. The results also show that if the device is programmed to compensate for the mean deficit in the final system, the sampled fluids will have a maximum error of 0.94µl. This is ~19% error in 5µl dispensed or 0.94% in 100µl.

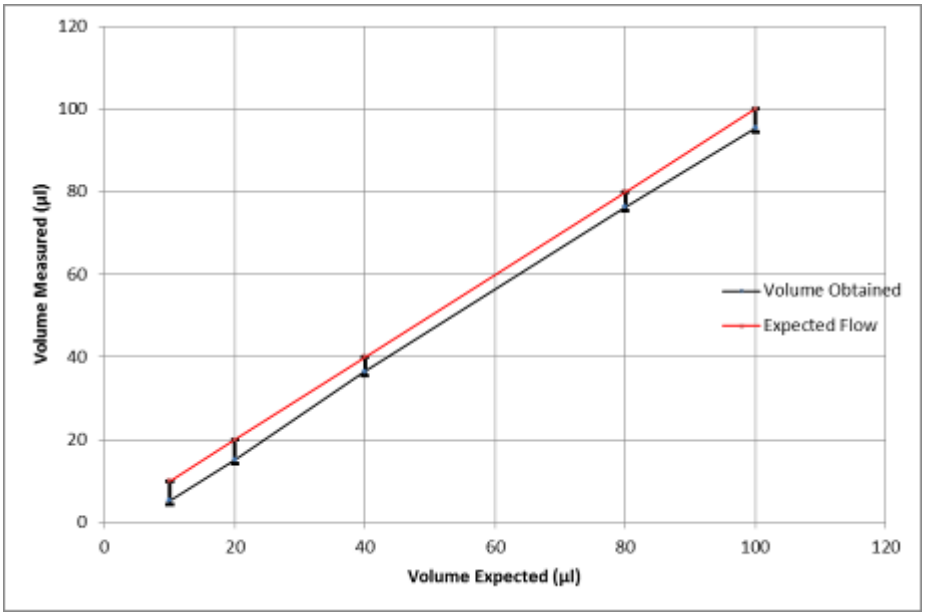

Figure 2-12: Comparison of target volume and volume injected.
The autoloader was manually configured at its terminal to load different drug volumes using air as the carrier fluid. The loaded volumes were collected in a pre-weighed sample vial container and weighed. The mass of water loaded and density 1g.mm^3 was used to calculate the volume loaded. This was done for n=6 and the mean difference of 4.2 µL with 0.94 standard deviation was obtained.

The performance of this integrated system with a carrier liquid needed to be assessed to show Taylor dispersion effects that will occur during the application of the system to reagents loading experiments. An optical detection methods was required to characterise these effects.

2.5.2 Operational range

The autoloader was capable of loading volumes between 1μL and 100μL. The operational range limits were imposed by the syringe size, HPLC tubing and size of the reservoir (100μL) fitted in the HP valve. Improving the range of the autoloader would allow the ability to load anything from sub-microlitre volumes to arbitrarily large volumes.

2.5.3 Autoloader Size

The size of the autoloader (200 x 400 x 600 mm) imposed constraints on its proximity to the microfluidic device which would be positioned on the microscope. Dead volumes and load times increase with longer distances. This was mitigated using a shelf which allowed the use of a tubing of length (400 mm). A loading system with an improved form factor that allowed it to be mounted on the microscope would improve the reagent delivery times.

2.5.4 Sampling Capabilities

As identified, one of the requirements may be to remove media downstream of the cells. The autoloader available does not meet the requirements. A customised fluid handling system (see later chapters) was designed and fabricated to meet this need. A set of protocols were implemented to characterise the autoloader and liquid flow control system as a starting point to identify key advantages for the developed system.

The characterisation process of the integrated autoloader and liquid flow control system required an optical detection method to characterise the concentration profile inside the fluidic components. Fluorescent dyes have been used in combination with

optical detection systems to characterise the accuracy and precision of fluid handling systems (Harris and Mutz 2006).

2.6 Optical Detection

A custom fluorescence detection system was setup to measure and characterise the fluorescence in a tube flowing varying fluorescein concentrations and volume. A microscope was also used for imaging this process as well as the results of an immunocytochemistry protocol on cell cultures in a microfluidic device.

2.6.1 Fluorescence detection setup

A fluorescence detection system was assembled to measure or quantify fluorescence in a microfluidic tube comprised of an LED of excitation wavelength, pinhole, tube alignment, filters, lens system, photo detector, current to voltage amplifier, DAQ and a PC for logging the measurements. This system illustrated in Figure 2-13 was used to characterise dispersion effects in the cross section of a tube carrying an injected fluorescent liquid. The setup was aligned using optical cage plates (Thorlabs) and the LED (thorlabs, M470D2) with 470 nm wavelength emission was used in the assembly.

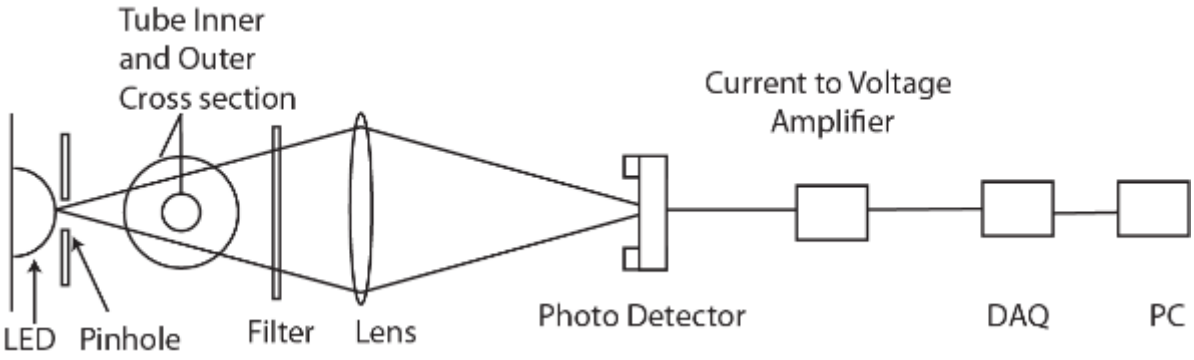

Figure 2-13: Fluorescence detection system
An LED emitting light at 470 nm wavelength was used for excitation and the pinhole with an orifice dimension (d = 0.7 mm) was used to allow light through to the centre of transparent microfluidic tube with internal diameter (ID = 0.7). The emission from the fluorescence of liquid flowing in the tube was

captured by a lens (f=25 mm) that focused the emitted light on a photodetector. A dichroic bandpass filter (Edmund optics) was used to allow light at the emitted wavelength 520 nm.

The photodetector (Thorlabs, PDA 100A-EC) with controllable gain and inbuilt amplifier produced a 0 – 10 volts response to light intensity incident on the dye. The gain was set to 50 dB for the experiment. The tube alignment tool was fabricated by creating a groove across the diameter of an aluminium disc of diameter and thickness (d = 20 mm, t = 3 mm). A hole (diameter = 0.7 mm) in the centre was drilled with a laboratory work press to allow incident light on the transparent FEP HPLC tube (Kinesis).

2.6.2 Microscope System

Cameras (point grey Grasshopper 2, Hammamatsu Orca C11440-22CU and Photometrics QuantEM camera) were mounted on inverted microscopes (Brunel SP99F and Nikon Eclispse Ti-U) to capture bright field and fluorescent images using 1x, 4x, 10x, 20x and 40x magnification objective lens (Olympus, Nikon). Fluorescence microscopy was done using standard filter sets (Olympus, Nikon and Brunel) that band pass excitation frequencies at one plane and band passes the emission spectra at another. The standard filter sets used are FITC, TRITC and DAPI which allow excitation excite with 480, 550 and 390 nm spectra and allows 520, 600 and 470 nm emissions to the cameras respectively. The filter sets used are illustrated in

Table 2-1: Typical summary of excitation and emission spectra for filter cube sets

Target Fluorophore	Excitation wavelength	Emission wavelength
FITC	480 nm	520 nm
TRITC	550 nm	600 nm
DAPI	390 nm	470 nm

The brunel microscopes were illuminated using warm LED light source (Thorlabs MWWHL3), LED driver (Thorlabs LEDD1B) and 15 volts power supply (Thorlabs TPS001).

These optical detection systems were used to demonstrate the suitability of the liquid manipulation system for automated drug injection; characterise the dispersive effects on injected volumes and image results of immunocytochemistry protocols on neuronal cultures in microfluidic devices. These demonstrations required chemicals reagents like fluorescein and phosphate-buffered saline as well as other reagents.

2.7 Chemicals, Reagents and Usage

This section describes chemicals and reagents used for the demonstration of the liquid handling system and the applications. Fluorescein solution was used to characterise the functionality of the liquid handling system. It was prepared by dissolving fluorescein powder in phosphate buffered solution. The phosphate buffered solution was also used in the immunocytochemistry protocol as well as other reagents described.

2.7.1 Chemical Preparation

2.7.2 PBS (Phosphate Buffered Saline) Solution

PBS solution was made by dissolving PBS tablets (Sigma Aldrich) in distilled water in proportions that are stated on the product label. A stirrer was used to speed up the process.

2.7.3 Fluorescein Concentrations

100mg of fluorescein powder (Sigma Aldrich product F-6377) with formula weight (FW = 375.3) was dissolved in 1L of Phosphate Buffered Saline (PBS) solution for a final concentration of 2.65 x 10^{-4} mol.L^{-1}. The solution was used where non-critical fluorescein concentrations were required and kept in a dark place to avoid bleaching over time. It has been shown that dark storage of fluorescein would maintain its integrity over long periods (Harris and Mutz 2006, C, N et al. 2013). Fluorescein calculations were done using the equations in Equation 2.2 and Equation 2.3. Another stock of fluorescein was made for experiments where specific concentrations were required. 500mg of the fluorescein powder was dissolved in 50ml distilled water for a final concentration of 0.02mol.L^{-1}. The stock solution was then dissolved in more distilled water to obtain lower concentrations when required.

Table 2-2 shows the fluorescein concentrations obtained from further dilution of the 0.02mol.L^{-1} stock solution.

$$C = \frac{m}{v} \; x \; \frac{1}{MW}$$ Equation 2.2

Where
- C = final solution concentration in (mol.L^{-1})
- m = the mass of solute dissolved (g)
- v = volume of the final solution (L)
- mw = molecular weight of the solute

$$C_1 V_1 = C_2 V_2$$ Equation 2.3

Where
- C_1 = stock solution concentration (mol.L^{-1})
- V_1 = aliquoted volume of the stock solution (L)
- C_2 = final solution concentration (mol.L^{-1})
- V_2 = final volume of dilution.

Table 2-2: Fluorescein concentrations obtained from dissolving 0.02mol.L^{-1} fluorescein stock solution

Vol of stock solution 0.02 mol.L^{-1}	Total diluted volume	New concentration g/L	New Concentration µM
1ul	20ml	0.0005	1.33
2ul	20ml	0.001	2.66
5ul	20ml	0.0025	6.6
10ul	20ml	0.005	13.3
20ul	20ml	0.01	26.6
50ul	20ml	0.025	66.5
100ul	20ml	0.05	132.9
200	20ml	0.1	266
500	20ml	0.25	665
1000	20ml	0.5	1330

2.7.4 Immunocytochemistry Reagents

Reagents used for the immunocytochemistry protocol were obtained for fixation, permeabilisation and blocking, antibody incubation and washing. Phosphate-buffered saline (PBS) was used to wash off reagents after each incubation step.

4% paraformaldehyde (Sigma Aldrich) was used as a fixation agent to keep the cells intact throughout the process. 0.1% Triton-X (Sigma Aldrich) diluted in PBS was used for permeabilisation which breaks the bilipid membrane of the cells to allow the antibodies reach target enzymes within the cells for staining. 0.5% BSA (Bovine Serum Albumen) was used to block non-specific sites from binding to antibodies.

Glial specific GFAP (Anti-Glial Fibrillary Acidic Protein) and neuron specific beta-tubilin (ABCAM ab78078) were diluted (1:200) in 0.5% BSA as primary antibodies to target glial and neurons in the culture. The GFAP is synthesized from goat polyclonal and the beta-tubulin is synthesized from mouse monoclonal. Monoclonal refers to

Anti-GFAP (ABCAM ab53554) and anti-rabbit (ABCAM ab18207) were diluted (1:400) in 0.5% BSA as secondary antibodies to target the GFAP and beta-tubulin. The nuclei of the cells were stained using Hoechst (Sigma Aldrich) diluted (1:20) in PBS.

2.7.5 Immunocytochemistry Protocol

Immunocytochemistry protocol was performed on cells in a microfluidic device by loading reagents into cell culture devices. An immunocytochemistry assay was manually performed on cells in a single input microfluidic channel by a collaborator (Katharina Reusch). This was done to first establish a standard protocol for the assay in microfluidic devices. Cells were seeded in a single-input microfluidic device and the protocol was performed at 7 DIV (days in vitro).

Each reagent was manually loaded into the device through one inlet port using a 1ml syringe and left for incubation times defined in Table 2-3.

Figure 2-14 shows the post processing of images obtained from the assay. Fluorescence imaging was performed using an inverted fluorescence microscope (Nikon) and images were obtained for each of the target spectra (FITC, TRITC and DAPI) using a camera (Photometrics QuantEM 512SC). Artificial colouring and image overlay was done using an image processing and analysis software (ImageJ version 1.4v). Figure 2-14 shows a brightfield and fluorescence image for the immune protocol used. Further development of the liquid control system was required to realise fast liquid flow control. The software and hardware integration of the flow control system with a liquid loading and sampling system would be demonstrated using with immunocytochemistry and calcium imaging experiments. The ability to rapidly switch various agonists will be demonstrated using various fluorescein concentrations as the separate agonists.

This integrated automation exercise required instrumentation for signal acquisition and generation; control interface that provides user friendly controls and desired functionalities to the experimenters.

Table 2-3: Manual Immuno Staining Protocol

Step	Incubation time
Wash with Phosphate buffered solution (PBS)	2 minutes
4% paraformaldehyde in PBS	20 minutes
3x wash with PBS	10 minutes
0.5% BSA with 0.1% Triton-X (blocking solution in - BS)	30 minutes
Primary antibodies in BS (1:200)	150 minutes
3x wash with PBS	10 minutes
Secondary antibodies in BS (1:400)	60 minutes
Wash with PBS	5 minutes
Wash with Hoechst in PBS (1:20)	5 minutes
Wash with PBS	5 minutes

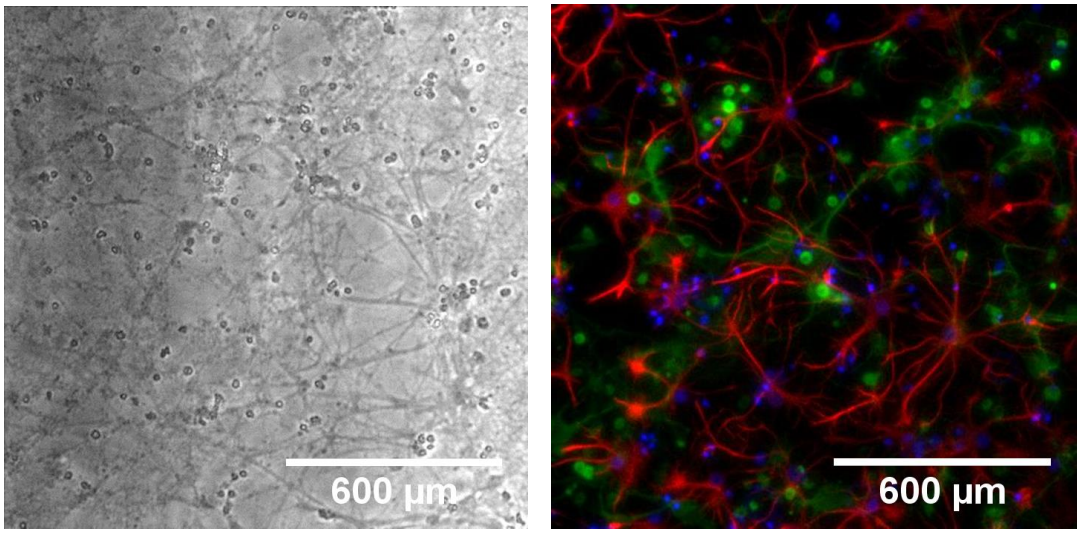

Figure 2-14: BF and overlaid fluorescence images from Immunocytochemistry protocol
This immunocytochemistry protocol was used as a trial run to establish incubation times that will be used subsequently for automated immunocytochemistry. The brightfield image (left) show the layout of one section of the microfluidic device with the cells present. The fluorescence image (right) shows that the cell culture is comprised of neurons (green) and glial (red). The blue stains show the presence of a cell nucleus that was also stained for.

2.8 Automation and Control

2.8.1 Signal Generation and Acquisition

Signals were generated using function generators and oscilloscopes and used to monitor signals for brief periods where data logging or synchronous activity was not required. Other experiments that required logging and/or synchronous signal triggers were performed using Data Acquisition Devices (National Instruments (NI) products USB-6009, USB-6259, PCI 6259).

A programming language (NI LabVIEW) was used to write programs to enable signal acquisition and generation with the data acquisition devices when logging and more synchronous triggers were required like real-time camera triggering. The programming style adopted for the larger applications is discussed in the Software Development chapter.

Equipment in the laboratory were also controlled using LabVIEW where possible. LabVIEW communication over RS232 interface was used to automatically control the syringe driver and the autoloader. An adapter (FTDI Chip product US232R-100-BLK) was used to link the exposed RS232 interface to USB ports on the PC.

An arduino board was investigated as an alternative to the DAQs to improve the capabilities the flow control system. This was done in an attempt to decouple the low level valve actuation functions from the high-level integrated LabVIEW program to improve response times of the flow controller.

2.9 Computational Fluid Dynamics (CFD)

Rapid onset of agonists in a microfluidic channel was characterised using a CFD application (COMSOL muliphysics environment version 4.0). This has been used to characterise drug delivery in simple and complex microfluidic channels (Berthier,

Renaudot et al. 2010, Hashim, Diyana et al. 2012). It has also been used to determine the limits in realising chemical switching in microfluidic devices (Bae, Beta et al. 2009).

The dimensions of a Y-shaped (dual input) microfluidic device designed with a CAD package manager (Autodesk Inventor Student) are shown in Figure 2-15. The CAD model was imported to COMSOL multiphysics environment for fluid dynamics computations. The boundary conditions were set up in the model with every part acting as a wall except for the faces that were setup as flow inputs and outputs. The fluid properties were set to water as initial condition and the simulated inputs had water or drug at specified concentrations. The CAD geometry was divided into finite elements in a meshing step and a choice of “coarser” mesh was selected to reduce the number of calculations performed and memory utilisation when compared with finer meshes possible. This mesh type was shown to provide similar results when compared to finer mesh sizes in a mesh independent study performed. Figure 2-16 shows some COMSOL simulations with different mesh selected. Important variables like peak and the full-width-half-maximum of the concentration of the mesh results were analysed and it was found that the coarser mesh and the normal mesh were different by 0.02% which was acceptable for drug distribution within the microfluidic device.

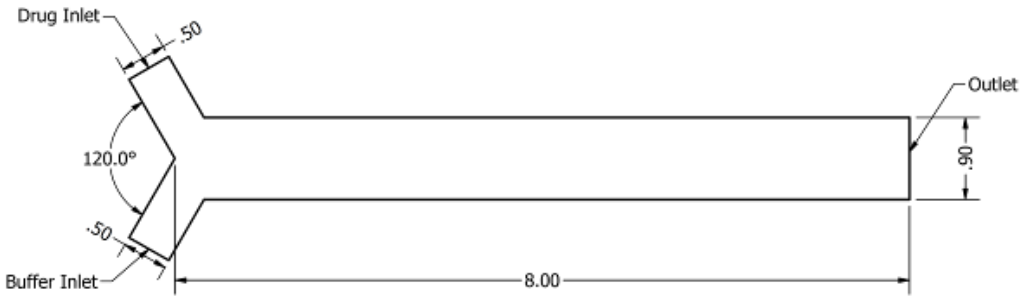

Figure 2-15: Y-shaped channel
(a) A Y-Shaped channel fabricated with a 50 µm double sided silicon tape (3M) was modelled in COMSOL to visualise concentration profile and the characteristic interface shift that will occur with different flow regimes. The buffer flowrate F_b and drug flowrate F_d were changed such that the total output flow rate was varied for the various ratios (F_b/F_d). (b) Results of the concentration at the different regions (channel entry, centre and outlet) are plot against time compared to the applied switching signal.

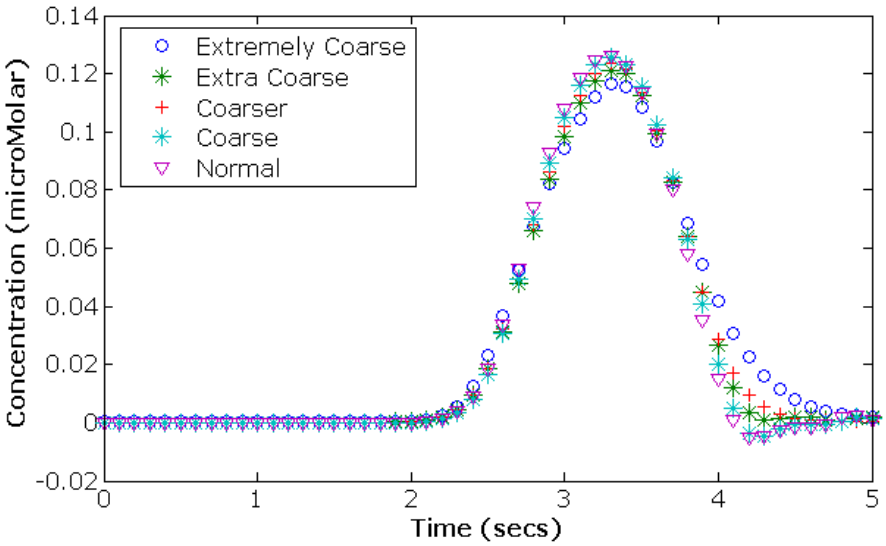

Figure 2-16: COMSOL Mesh Independence
The mesh was altered and the same simulation was run to determine acceptable mesh sizes to be used when using COMSOL results.

In order to obtain a solution quickly, the relative tolerance was modified to 0.1. This produced slightly less accurate results, like negative concentrations but, it enabled advantage of faster modelling computations. Tighter tolerance of 0.001 took too long to compute and sometimes failed to find a solution but more importantly, did not provide a better result.

COMSOL modelling was performed on a PC with relatively lower specifications (Intel i7 CPU, 2.8GHz, 16GB RAM) than High Performance Computers (HPC) used to obtain accurate models. COMSOL has been used to demonstrate the ability of a low-flow rate (1 - 100nL.s^{-1}) controller to apply rapid drug signalling, steady interface shifting for controlled drug exposure and concentration gradients with spatial resolution in a microfluidic device. These ability of the integrated physical system to realise all these applications will provide new tools for researchers to perform complex signalling patterns on cultures in a microfluidic device.

2.10 Ethics

All experiments were performed in accordance with the guidelines set out in the code of practice for humane killing under Schedule 1 of the UK Home Office Animals (Scientific Procedures) Act 1986, and were approved by the University of Nottingham Animal Welfare and Ethical Review Body.

2.11 Cell culture

All cell work involving sterilisation, harvesting, plating, and feeding was carried out by technicians and researcher who were specialised in these fields such as Mr Tim Smith, Mrs Dhruma Thakker and Nitzan Herzog.

The materials and systems available are to be utilised in the development process for a liquid handling system that can perform off-chip liquid manipulation for cell cultures in microfluidic devices. The development process must cater to the requirement of precision, accuracy, modularity, ease of use, ease of assembly/replication of the solution. The development process must also cater to the requirements of lab users such as sterility and cell survival within the microfluidic device. Surface treatment to promote these requirements may deteriorate during fabrication and this prevents the use of integrated microfluidic systems.

The design process for a novel off-chip liquid controller must first identify limits in the use of a commercial liquid loader and use this as a basis for the design of the novel alternative. Liquid transport system developed must be optimised and Software considerations made towards development of the integrated system.

The research will seek to provide alternatives that could be pursued towards realising the integrated liquid handling system for microfluidic applications.

3. Liquid Handling Requirements and System

This study is focused on the development of an integrated off-chip microfluidic liquid handling system that is expected to allow:

- Upstream stable flow control system for long term perfusion,
- Fast flow rate changes for rapid interface switching,
- Volume loading system for agonist delivery; and
- Volume sampling downstream of the microfluidic device.

An integrated system illustrated in Figure 3-1 shows a liquid transport system – comprised of a forward pressure and back pressure system; a liquid loading and sampling system and the microfluidic device connected inline. This system is designed to integrate the drug injection capabilities of a loading system together with the possible applications from a liquid transport system, thus allowing and improving on applications like interface shifting, rapid drug signalling, sequential loading and a combination of these applications.

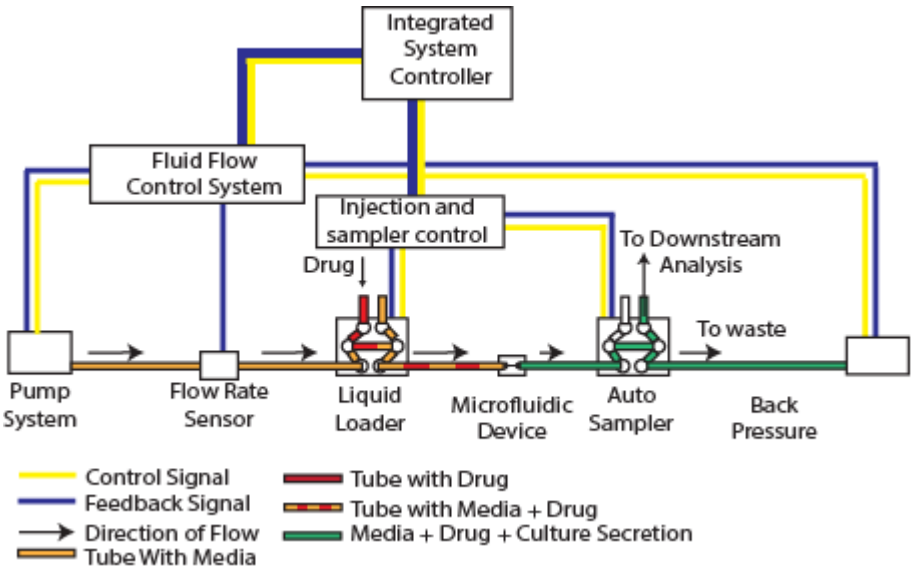

Figure 3-1: Proposed Liquid handling solution for microfluidic devices
The liquid handling system was designed to implement fast chemical triggers using various agonists as well as sampling used media from cell cultures to quantify the chemicals used up and ejected into the media. The back pressure and forward pressure provide positive pressure difference for flow control which is maintained by the fluid flow controller with feedback from flow sensors. This system shows one implementation with single input microfluidic device.

A custom built liquid transport system was capable of steady and precise flow control but lacked appropriate control logic to perform rapid interface switching. A 10 second flow switching time which was achievable with the system was unsuitable for use with the intended applications. A systematic re-assessment of the control system design and implementation was proposed to improve this switching time scale to the order of 1 second duration. This was to keep in line with the rapid interface switching duration for neuronal activity reward experiments.

A used commercial autoloader was also identified as a good starting point for developing the sequential injection aspect of the integrated system. This autoloader is characterised to show its advantages and limits. The use and application of the autoloader would inform on the design constraints for the need and/or development of a novel liquid loading system.

This Chapter will look at the applications for the integrated system, establish some constraints that will be considered in the design process for the liquid transport and injection system. It will then discuss the optimisation efforts for the liquid transport system and the characterisation of the commercial autoloader. Constraints with the integrated system which will include lack of downstream sampling will be discussed as part of the development process for a highly modular and integrated liquid handling system.

3.1 Applications for Integrated Liquid Handling

The ability to rapidly change the interface for rapid drug-signalling applications has been demonstrated using flow control, valve induced switching, light induced switching (Bae, Beta et al. 2009). The integrated liquid manipulation system was designed and developed to enable the experimenter to:

- Load various agonists into single input and dual-input microfluidic devices;

- Shift the buffer/drug interface for spatial resolution of chemical signals in a Y-shaped microfluidic device;
- Perform temporally precise agonist loading of these chemical signals in the dual inlet microfluidic device; and
- Apply the spatio-temporal chemical signalling capabilities with various agonists in the dual inlet microfluidic device.

3.1.1 Interface Shifting

The Y-shaped microfluidic device gives experimenters the ability to deliver drugs with spatially resolution across the width of the device. This can be realised by changing the flow rates of the respective agonists flowing into the device. The buffer/drug interface in the microfluidic device closely follows the ratio of buffer flow rate to drug flow rate (f_{buffer}/f_{drug}).

This has been illustrated using a COMSOL simulation for different ratios (99:1, 50:50, 1:99) while maintaining constant flow at different flow rates (10, 50 and 100 $nL.s^{-1}$). Figure 3-2 shows surface plots of the microfluidic device for these varying settings.

Dispersion effects limit spatial resolution of the buffer/drug interface and this increases with lower flow rates demonstrated with the results of the computation. While this is usually non-ideal, this mixing effect was exploited to provide drug concentration gradients to cultures in a Y-shaped microfluidic device(Marques and Fernandes 2011). The same technique will be applied to delivery concentration patterns to HEK cells and Astrocytes.

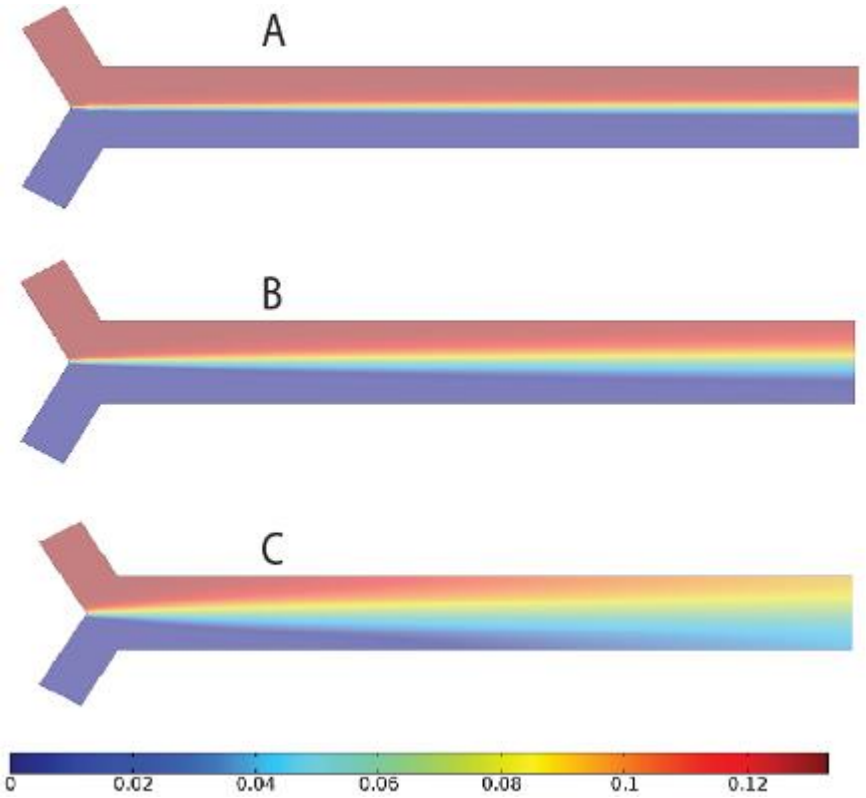

Figure 3-2: 50:50 drug/buffer interface for spatial resolution of chemical signals
The mixing in the channel is dependent on the total flow rate and the flow ratios. A sharper interface is seen with total flow rate of 100nL.s^{-1} (A) and mixing occurs more readily down the channel. (B) has total flow rate of 10nL.s^{-1} and (C) is at 2nL.s^{-1}. In these simulations, the ratio is an actual ratio of the total flow rate in the system. All concentrations in microMolar (μM).

3.1.2 Rapid Drug Signalling

Rapid drug signalling can be achieved by quick interface shifts and a switching time of 0.1 s has been demonstrated using a syringe driven system with flow rates at order of 1 μL.s^{-1} (Kuczenski, LeDuc et al. 2007). This system applied to drug signalling for cells would be detrimental due to the very high flow velocities setup in the channel (u = 2 x 10^2 mm/s).

COMSOL was used to characterise the drug-signalling capabilities for the Y-shaped channel for different switching ratios (f_{buffer}/f_{drug} = 100:1, 100:10, 10:1 nL.s^{-1}). The simulation was run for 0.1 second increment over 10 seconds. The concentration of the drug at the input was set as 132 μmol.L^{-3}. The concentration profile at different sections of the device was extracted from the solutions. Figure 3-3 shows the

graphical results of surface during the drug pulse and 2 seconds after the drug pulse for flow rate ratios (f_{buffer}/f_{drug} = 100:1 $nL.s^{-1}$).

Figure 3-4 shows concentration profile at points indicated in the Figure 2-15; and the concentration profile along the width of the channel at the inlet ports for the different flow ratios in a 50 μm high channel. This model assumes that the flow rate change occurs within 100 ms which is critical to realising rapid on-off drug signalling. In the efforts to realise this flow rate transition speed, it may be more practical to use longer time scales at which point a more realistic model may be computed using the physical limits of the realised flow control system.

These results also pose constraints on the location of cells in the microfluidic device. The fast signalling system requires the cells positioned closer to the inputs of the y-shaped microfluidic where these rapid signalling patterns are expected to occur within the relevant time scales. Optimisation of the cell culture environment microfluidic device to address these constraints were outside the scope of work and were not attempted.

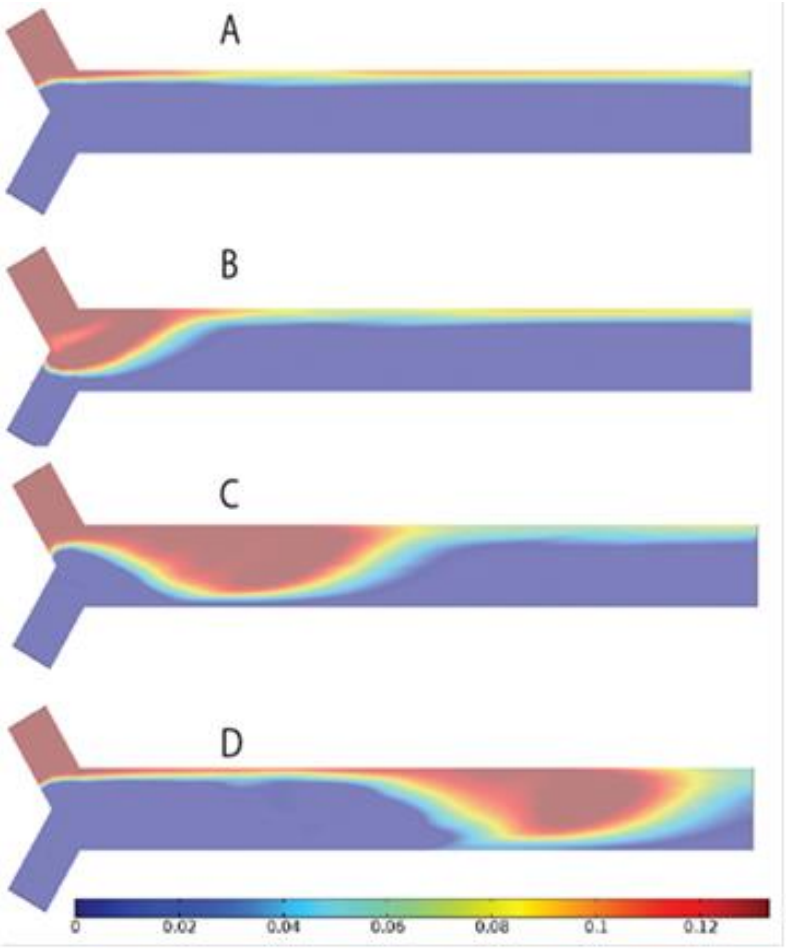

Figure 3-3: COMSOL surface results for rapid interface switching

The model is done on a Y-shaped microfluidic device with 50 µm height. A drug-pulse is applied for 1 second at 2 seconds into the simulation. (A) shows concentration distribution in the microfluidic device 0.1s before the start of the rapid flow switching. At 0.5 seconds after the switch initialisation (B), the centre of the device close to the inputs is ¾ full of drug. At the end of the drug switch (C), the travelling drug wave is yet to just reaching the centre of the device. (D) 2 seconds after the drug switching has ended, the effect is not yet experienced at the output of the channel. The scale bars are in (x10 $^{-3}$ mol.L^{-3} = mol.m^{-3}).

(a)

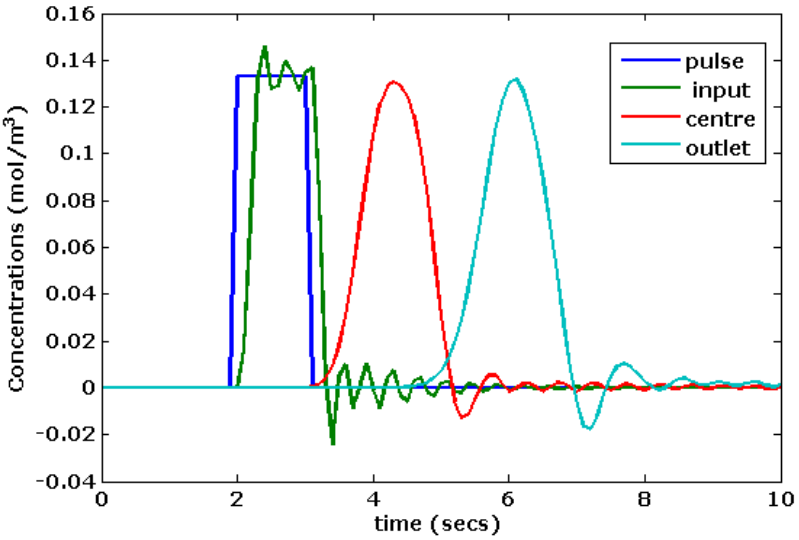
pulse
input
centre
outlet
Concentrations (mol/m3)
time (secs)
0.16
0.14
0.12
0.1
0.08
0.06
0.04
0.02
0
-0.02
-0.04
0
2
4
6
8
10

(b)

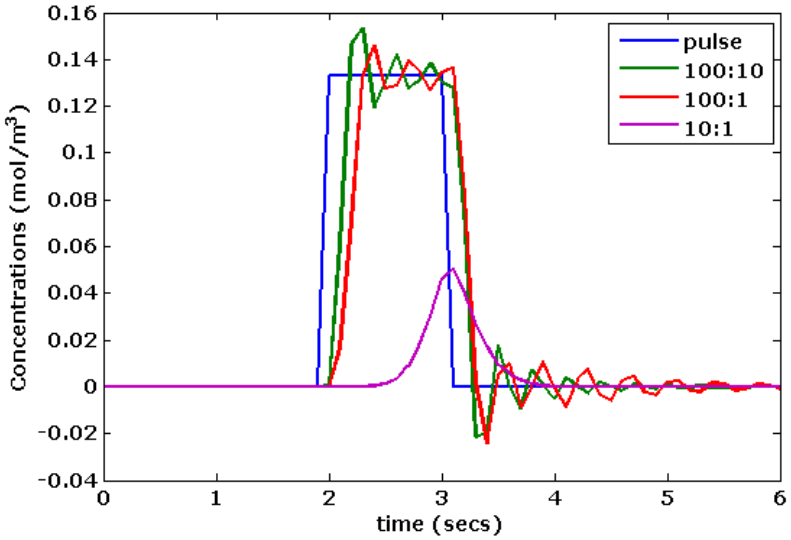
pulse
100:10
100:1
10:1
Concentrations (mol/m3)
time (secs)
0.16
0.14
0.12
0.1
0.08
0.06
0.04
0.02
0
-0.02
-0.04
0
1
2
3
4
5
6

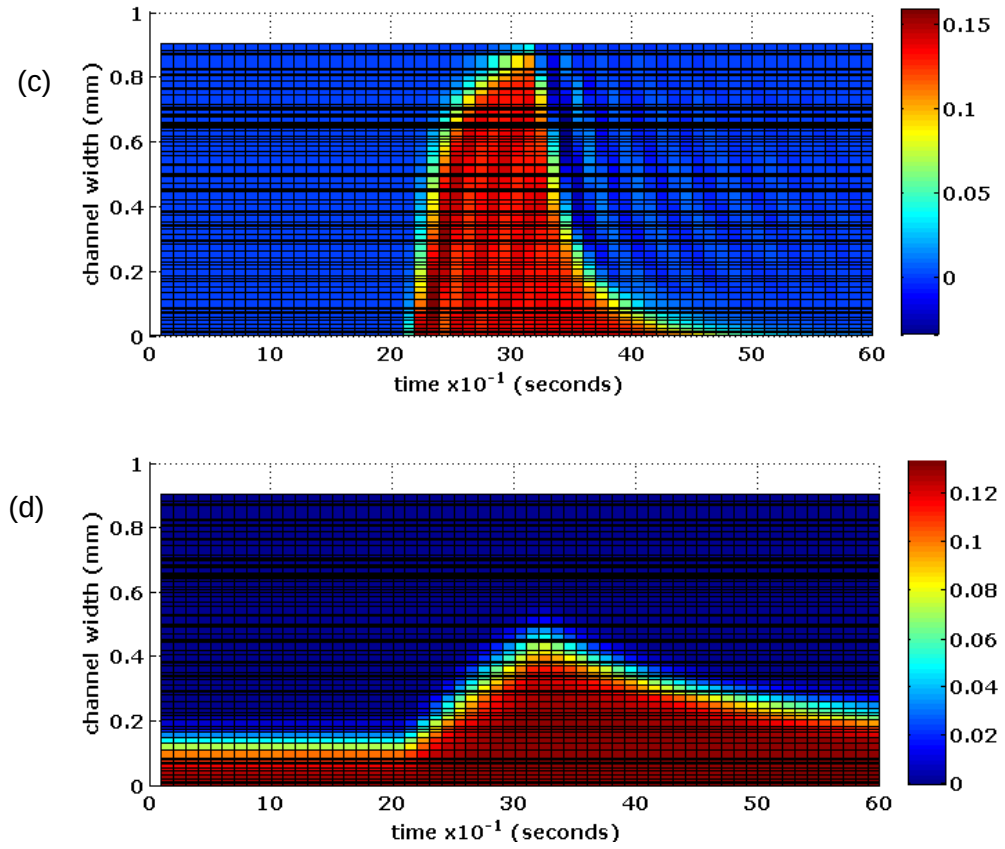

Figure 3-4: Concentration profile at centre of the channel width

*1D plots of points at the middle of the channel width along its length are provided (a). The concentration at the **inlet**, the **centre** of the channel length and the **outlet** of the channel are shown to experience different temporal drug switching patterns. The concentration at the start of the channel is shown for different flow rate patterns (b).The low peak-concentration for the flow ratio (f_{buffer}/f_{drug} = 10:1) is explained (c) and (d) which shows variation of the concentration profile along the width of the channel at that same position over time. The drug pulse is applied at 2 seconds but drug does not completely fill the channel. This is due to lower velocities in the channel at the low flow rates. It should be noted that the flow ratios refers to actual flow rates in nL.s^{-1}. Cells positioned along the channel length will experience different temporal chemical patterns from a drug switching pulse applied. The **pulse** is set to change from low (zero) to high (132 μM/L^{-3}) but the flow rate transition (100 - 1 nL.s^{-1}) is assumed to occur within 100 ms which is the technological challenge. Note that high tolerance (0.001) was used to get more accurate results but the mesh coarseness still allowed inaccuracies in the results like the negative concentrations (<0) on the chart.*

3.1.3 Loaded Drug Signalling Patterns

The ability to perform signalling patterns for different agonists will be of immense benefit to experimenters to enable characterisation of cultures in microfluidic devices while making to the drugs used and applying. A train of agonists can be delivered in series while applying drug signalling patterns when the drugs arrive at the device. The ability to perform this task will depend on knowledge of the drug arrival in the device as well as knowledge of effective concentrations. The ability to perform real-

time sample operations for offline analysis will further provide experimenters more information on cell response to these chemical signals provided. The novel liquid manipulation system is expected to enable:

1. Deterministic liquid loading operations
2. Reduced drug delivery distances to limit dispersion effects
3. Injection of arbitrarily large drug volumes for long term operations

3.2 Fluorescein for Flow Visualisation

The change in intensity due to loaded fluorescein concentrations was analysed in order to confirm the use of fluorescein for flow visualisation similar to a previous study (Harris and Mutz 2006). Different fluorescein concentrations (C = 266, 133, 66.5, 26.6, 13.3 and 6.6 μM) were placed in the liquid reservoir for flow through a microfluidic device that was setup on an inverted fluorescence microscope. The different concentration volumes were subjected different flow rates (Q = 0, 10, 20, 40, 60, 80, and 100 $nL.s^{-1}$) and the mean intensity of a region of interest (ROI) at the detector was observed for 30 seconds to identify changes in intensity at these different flow rates. There was an observed dependence of fluorescein intensity on flow rates which but the dependence was negligible when compared to the intensity for other concentrations shown with error bars in Figure 3-5.

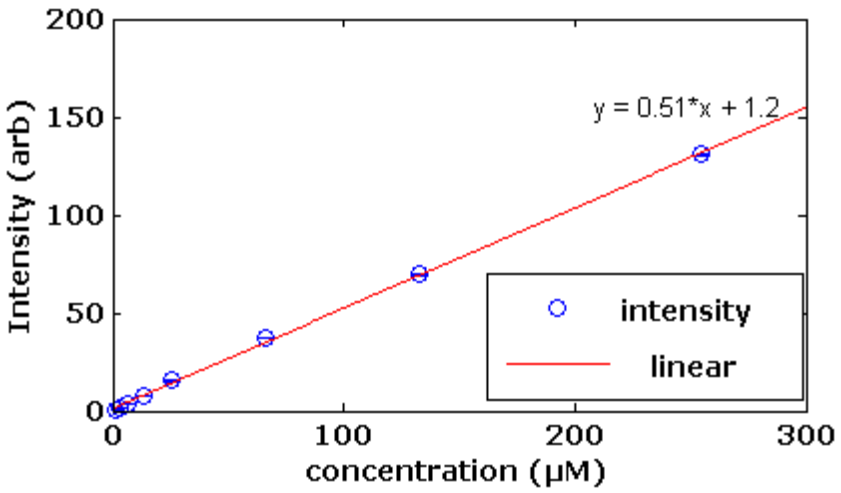

Figure 3-5: Linearity of Fluorescein Signal
The mean intensity of an ROI in a microfluidic device was obtained for different fluorescein concentrations. The mean intensity per concentration (blue) is shown with error bars that are standard deviation over the different flow rates. The linearity confirms the suitability of fluorescein in performing concentration characterisation experiments.

3.3 Liquid Transport for Perfusion

The need for continuous delivery of nutrients to cells in a microfluidic channel has been established. This media transport as well as agonists delivery for experimental analysis of the culture must occur using steady liquid transport systems with high precision and accuracy. Pulses are undesirable as they may produce unwanted physical stimulation to the cells so high fluidic resistance must be applied to counter the pulses due to capacitive behaviour of compliant tubes. The main system requirements for the flow control system are:

- 1 – 100 $nL.s^{-1}$ flow rate range
- 500 millisecond flow switching response time
- Low noise and pulseless flow eliminating the use of peristaltic pumps
- Modular design and easy to integrate with laboratory equipment
- Fully programmable with control of low-level functions

This restricted the use of commercial systems like the Elveflow and the Proportion air pneumatic pressure controllers. These systems had the advantage of high-level

control of the pressure but tuning was not possible to improve the pressure switching speeds on these systems since the pressure control interface was locked from user manipulation. These commercial systems were not flexible enough to the needs of the liquid transport system prompting the development of a custom system. The custom liquid flow control system was realised with two configurations and the images are shown in Figure 3-7. The “TYPE A” configuration was developed as a pressure controller that was connected to a liquid reservoir. The “TYPE B” controller had the pressure control implemented directly over a liquid reservoir (Duran bottle).

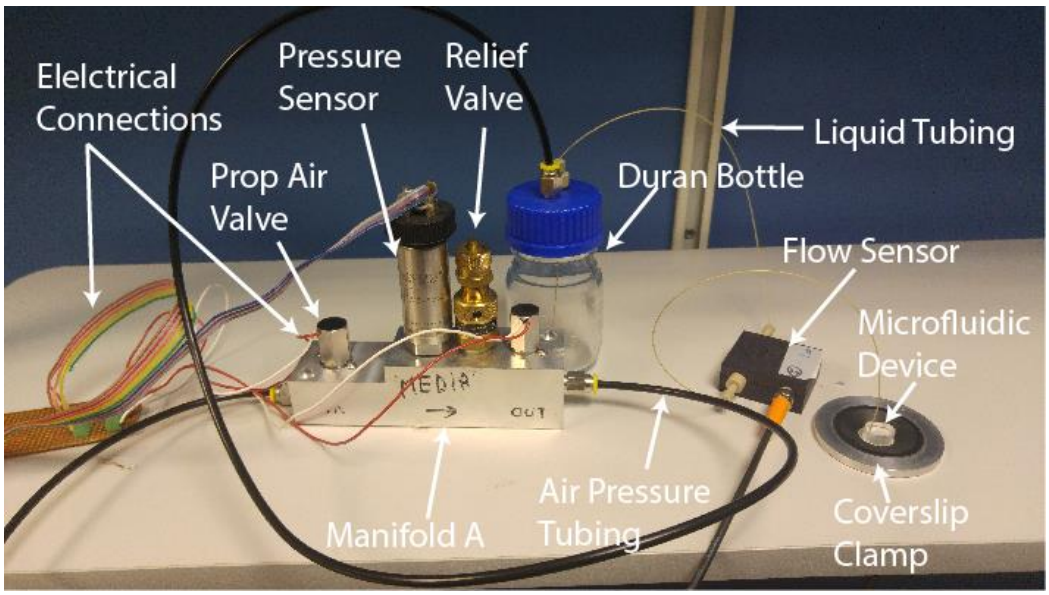

Figure 3-6: Type A liquid manifold for liquid flow control
This was assembled as a pressure controller connected with tubing to a liquid reservoir to pressurise the space over the liquid reservoir.

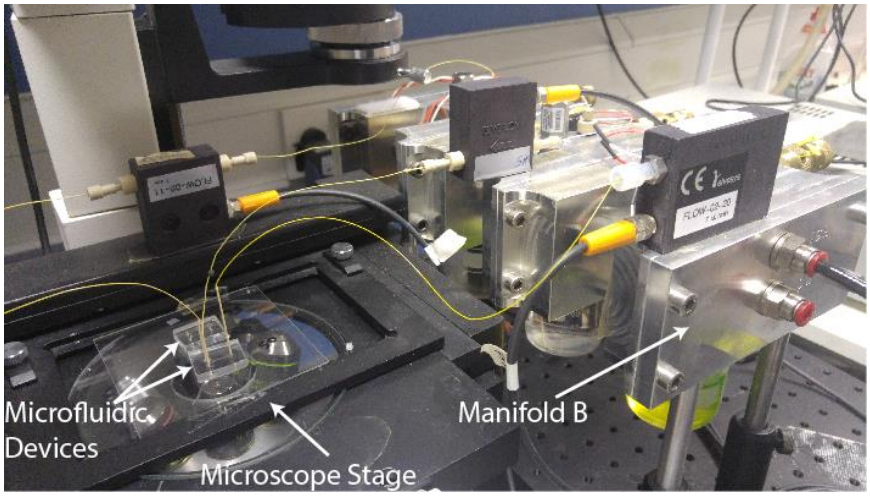

Figure 3-7: Type B liquid flow control option for liquid transport
Type B" manifold allowed the reservoir to be directly connected to the pressure source as an integrated flow control solution.

3.4 Custom Pressure and Flow control

The disadvantages to using the commercial pneumatic controllers warranted hardware and control system design and build of custom pressure controller. The hardware design and build was undertaken by the collaborators Sorka Abanu for "type A" and Alexander Johnstone for "type B". The lack flexibility of available pneumatic-pressure driven control systems were among reasons for the custom builds. The build and design aimed to limit the point of failure for the system using modular parts that could be easily replaced and at considerably lower costs to the lab than whole pressure controllers. The control design and development aimed to provide suitable control system design for the actuation of the valves to produce target range of pressures as well as use feedback system to correct for errors in the pressure and flow when the system is coupled as a liquid flow rate controller.

3.4.1 Pressure Controller System Overview and Design

The control diagram in Figure 3-8 shows the general control schematic of the custom built systems comprised of two proportional valves, one pressure transducer and one

relief valve. These components are contained in a manifold with machined air flow paths. The proportional valve at the input regulates the air flow input to the system and the second regulates the air flow out to atmosphere. The pressure transducer converts the sensed pressure to voltage that can be measured. The transducer outputs an analog voltage (0 – 5V) in response to the measured pressure range (0 – 250 mbar). Its maximum tolerable pressure (500 mbar) was avoided by setting a relief valve to vent when pressure in the system exceeds a limit (300 mbar).

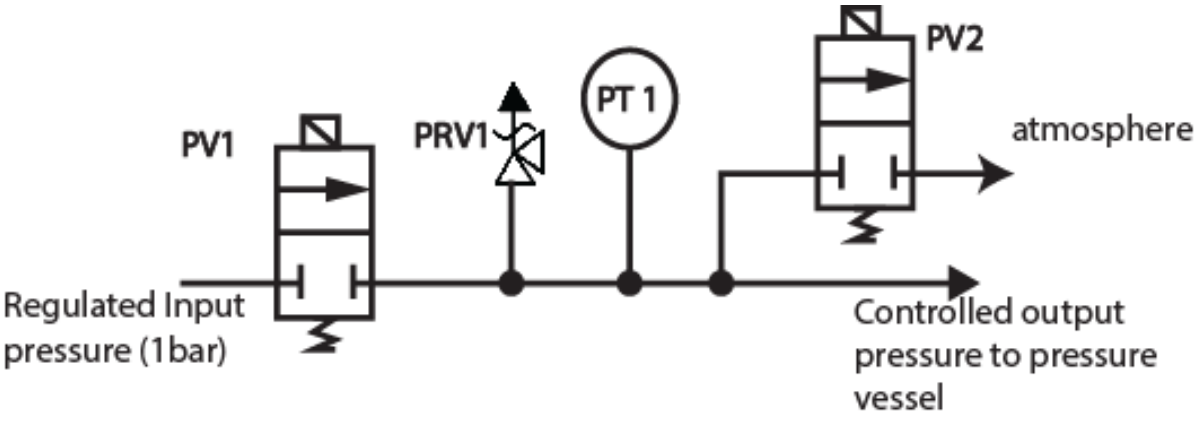

Figure 3-8: Control diagram for a two valve pressure controller
The two valve pneumatic pressure controller was used to manipulate pressure output by controlling the flow rate of air going into the system using the input Flatprop valve (FPV1) and the flow rate of air vented to atmosphere by the vent Flatprop valve (FPV2) valve. It is also comprised of a pressure relief valve (PRV1) to vent excess pressure (> 260 mbar). The pressure transducer (PT1) provides system pressure feedback for closed loop pressure control.

This pressure controller control system pressurises a fluid reservoir in either of two configurations as seen in Figure 3-9 and Figure 3-11. Figure 3-9 shows the “TYPE A” controller system akin to the proportion air controllers that provides pressure through an orifice and a tube connects the pressure source to the liquid reservoir. The advantage is that the system is strictly a pressure source that can be used in other applications.. Three pressure regulators were connected liquid reservoirs connected to a Y-shaped microfluidic device. Two of these were used as inputs for media and drug while the third was used as the output back pressure. Three flow sensors were connected to the lines and target flow rate was applied to the forward flow controllers such that they reached target flow rate ratios (f_{media}/f_{drug}) of (1:3>>3:1>>1:3) while

maintaining the total flow rate at 40 $nL.s^{-1}$. Figure 3-10 shows that the system is not able to realise the required 1 second rapid flow switching times since it takes 10 seconds to realise the full interface switching operation.

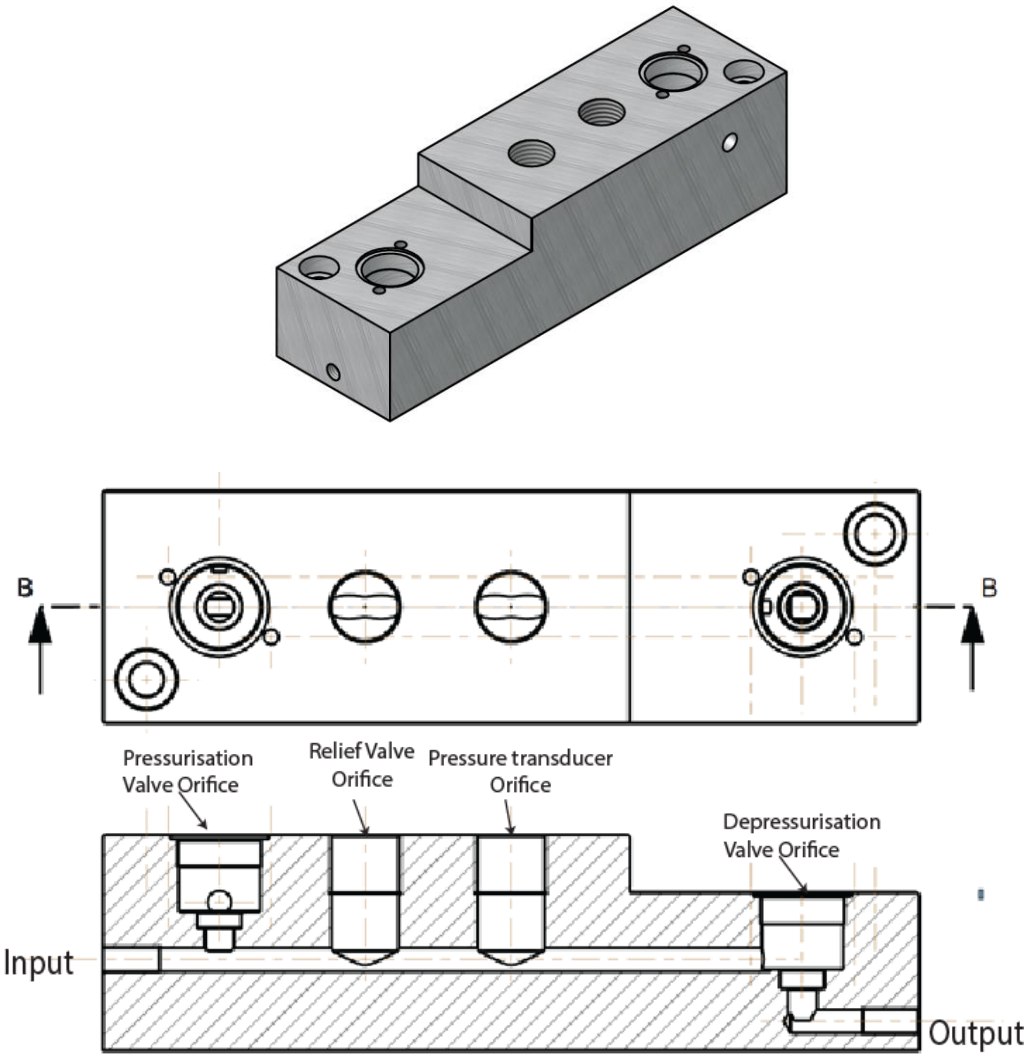

Figure 3-9: Manifold configuration “type A”
Image courtesy of Sorka Abanu, designed in ProCAD. (a) orthorgonal view of the manifold with the holes for the proportional valves, relief valve and pressure transducer. The output of this controller is connected to a sealed Duran bottle using pressure pipes.

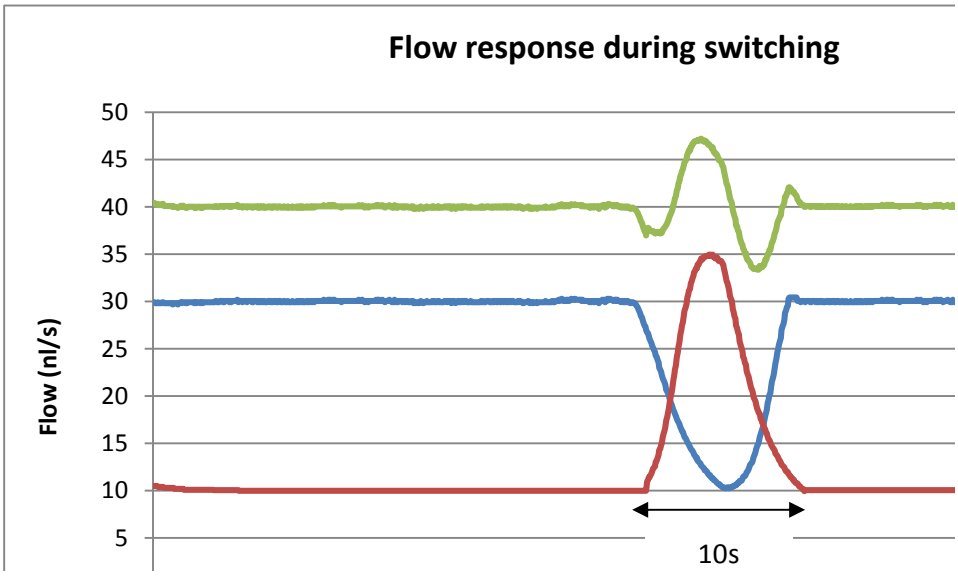

Figure 3-10: Flow switching using “type A” manifold after initial development process
The flow was switched in a Y-shaped microfluidic device using the previously developed flow control system. Flow switching was slow and it took 10 seconds to perform the pulse operation.

A system redesign by a collaborator, Alexander Johnstone, aimed at improving the system performance resulted in the “TYPE B” controller in Figure 3-11. This new controller pressurised the reservoir directly without the interconnecting tubing which aimed to reduce the response time of the pressure controller to ~100ms. This increased air volume buffer above the liquid was also added to minimise noise. However, this new design did not improve the system performance, which prompted a re-investigation into the control system architecture used and an optimisation process to improve the system performance.

The delay in the switching time is clearly due to the slow response of the flow controller as it takes about 5 seconds to get to the first target and then another 5 seconds to return to the original position. In order to reduce the switching times, the flow controller response must be optimised. Success of the control system optimisation efforts would be applied to the “type A” controllers to realise fast interface shifting applications.

The research then proceeded to develop an improved control and instrumentation system towards achieving fast, precise and stable pressure and flow control for microfluidic applications. Experimental characterisation of the system has been performed instead of numerical modelling approaches.

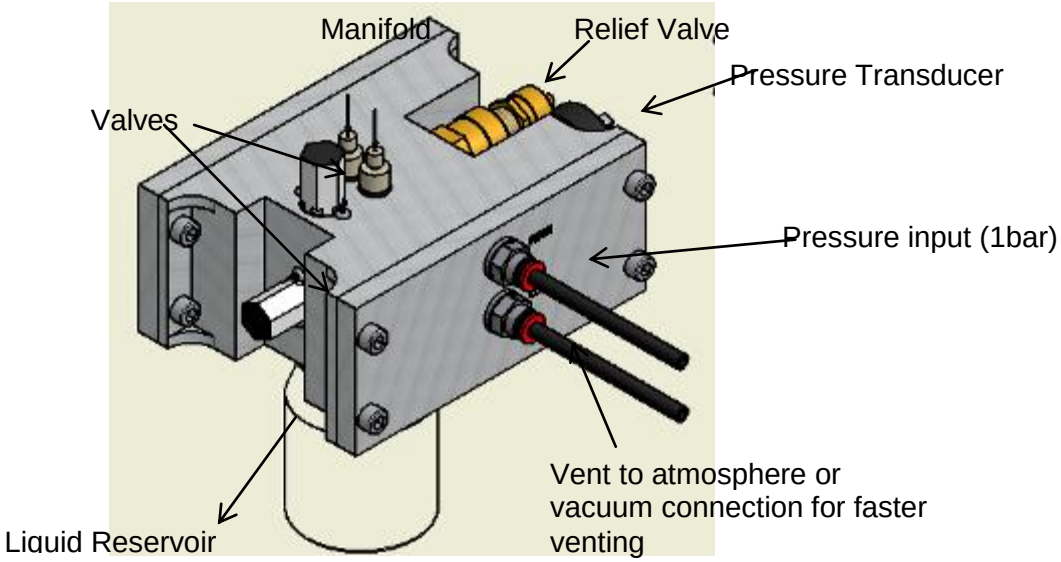

Figure 3-11: Manifold configuration type B
Type-B was developed with an increased buffer to improve stability when there is noise at the main pressure source by providing a buffer air supply in the manifold. (a) Top view of the manifold shows some orifice for the pressurisation valve, fluid connectors and the large buffer air inflow orifice. (b) Shows the bottom part of the manifold where the Duran bottle screws into and the orifice for relief valve and depressurisation valve

3.5 Pressure Control System Optimisation

The connections that make up the control system of valves and sensors for pressurisation will be identified. A low level system identification process is also undertaken to understand the system response to set input impulses. This will provide information on the speed at which the controllers can reliably switch pressure. The interactions between the valves for pressure control will be investigated and alternative methods attempted towards the optimised control objectives. Other control system modifications implemented towards this objective will include:

- PID system controller tuning
- Model Predictive Controller Options
- Implementation of alternative system hardware controllers like real-time FPGA and Arduino controllers for faster system responses.

Solutions obtained using the “type A” controller will be applied to the “type B” controller for similar improvement.

3.5.1 System Connections

Schematics of control and instrumentation connections for the liquid transport system are illustrated in Figure 3-12. A PC with LabVIEW software and a multifunction data acquisition (DAQ) system from National instruments were used to generate the control signals that were input to the switching module. The valves require current (up to 200mA to fully open) for control which is higher than the available output from the DAQ. Precise control of the current to the valves was achieved by a PWM control of a current source using an amplifying circuit that used the PWM output from the DAQ to modulate a 200mA supply. The amplifying circuit is shown in Figure 3-13 as a voltage follower circuit comprised of two transistors with one acting as a trigger to allow current through the second when it is triggered by the signal from the DAQ.

A pulse width modulation (PWM) signal train with pulse width (w = 1 ms) and frequency (f = 1 KHz) was configured for generation from the DAQ with high resolution pulse for precise current control. The signal pulse was configured to have 5000 samples and a buffer was configured to update the DAQ with new duty cycle values. The update rate of 50 ms was set due to the limits of the computing system and data acquisition system which could not provide a real time 1 ms duty cycle update.

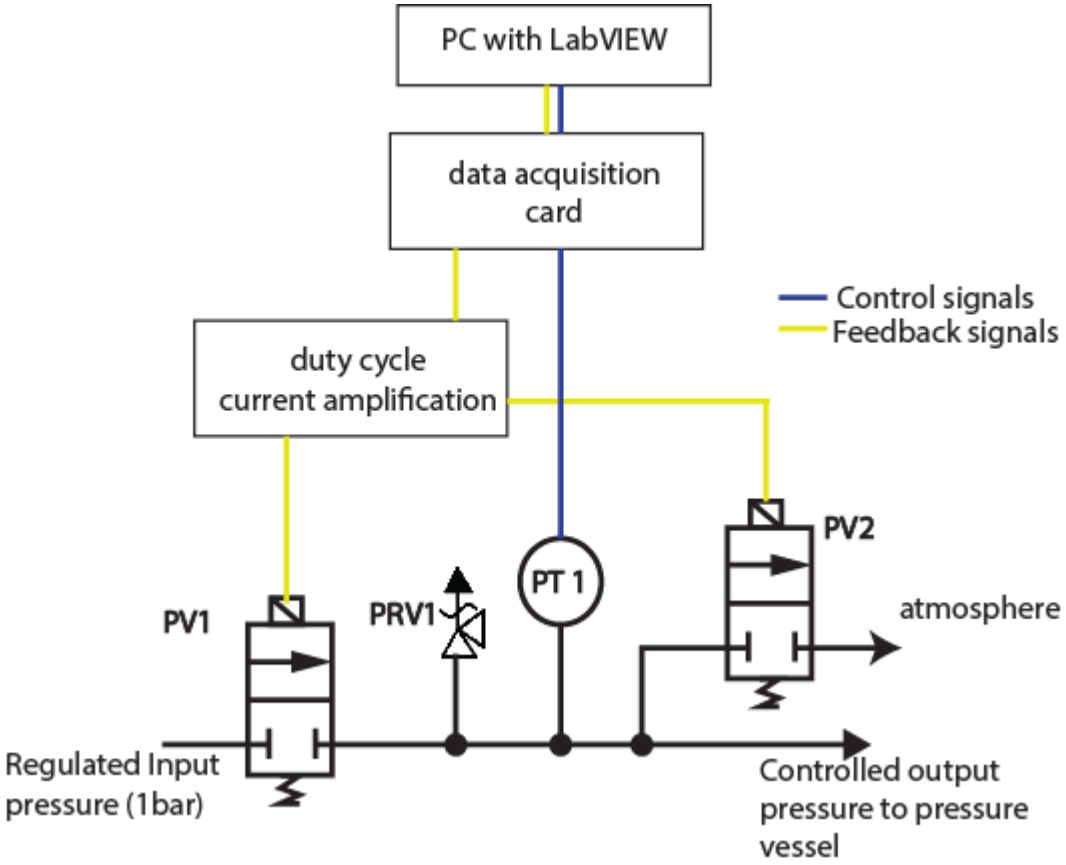

Figure 3-12: Control and instrumentation schematic of custom pressure control systems
The custom pressure controller has two valves that are connected to an amplification circuit that amplifies the current in the duty cycle supplied by the data acquisition card. This duty cycle setting is supplied by a PID control algorithm in LabVIEW program in PC that monitors the system pressure that is provided by the pressure transducer.

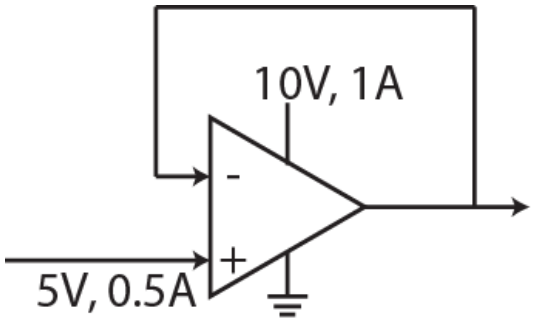

Figure 3-13: Voltage Follower Circuit
The DAQ cannot produce a high enough current to drive the valves so the circuit is used to increase the current available.

The pulse width is 1ms long and is comprised of 5000 samples to produce a high resolution pulse. This high resolution pulse is first transmitted to the DAQ that generates it but the transmission can be hindered by small ram size and data

transmission medium. In practice, USB DAQs required higher RAM (≥ 8 GB) to achieve this transmission in quick succession while the PCI DAQs could perform this with 4 GB of RAM.

The pressure transducer converts the pressure (P_s) to a voltage and the in-line flow sensor generates a voltage proportional to the liquid flow rate (Q_i). These signals are read by the DAQ at frequency of 1 KHz and the averaging of 50 samples resulted in a 20 Hz data update.

3.5.2 Valve operation

The inlet valve (V_{in}) allows air flow into the system at a flow rate $Q_{air.in}$. When air flow into the system is larger than the flow out $Q_{air.out}$, the pressure in the system increases until pressure inside the manifold is equal to the pressure at the inlet. The air in the system is only able to vent out when the exhaust valve is opened, which decreases the pressure in the system (P_s).

An open loop characterisation test was done by sealing the output of the manifold "type A" and actuating the input valve. A duty-cycle setting was applied for one cycle (t = 50 ms) and disconnected with the venting valve closed so that $Q_{air.in} >> Q_{air.out}$ but the sealed output meant that eventually the maximum pressure would be reached. The test was done to determine the time required to reach the maximum pressure and the maximum pressure reached for the impulse signal for this small air volume within the manifold. The input pressure of 300 mBar was set at the input since the maximum measurable pressure was 250 mBar.

This open loop characterisation test was repeated in a configuration where the output was unsealed and connected to a liquid reservoir (Duran bottle with volume, v = 100 mL). this increased air volume reflects real operating scenario for the pressure controller and will inform on how fast the air volume can be filled and pressurised.

The test was repeated with different actuation duty-cycles (d = 0.1, 0.2, 0.3, 0.4, 0.5, 0.6, 0.7, 0.8, 0.9, 1.0).

An experiment was conducted to assess the time taken to fully pressurise the liquid reservoirs. A constant duty cycle setting was applied for 1 second to actuate the input valve and the pressure was monitored throughout the period. The peak pressure and the time to reach the peak pressure was extracted from the logged pressure

The action of the two valves required to set one pressure target on the pressure controller system defines the controller as a multiple input single output (MISO) system since the pressure is obtained by the interplay of the input and exhaust valves. It was therefore necessary to investigate the options available for implementing this strategy.

3.5.3 MISO to SISO

The MISO pressure control system can be further reduced to a single-input single-output (SISO) system by inclusion of a duty-cycle calculator that converts a PID output variable, u, into the two duty cycle settings for the input and exhaust valves. The control loop illustrated in Figure 3-14 shows the control design when the duty-cycle calculator is integrated for precise pressure control. The options for the duty-cycle calculator are illustrated in Figure 3-15 based on work by (vanVarseveld and Bone 1997).

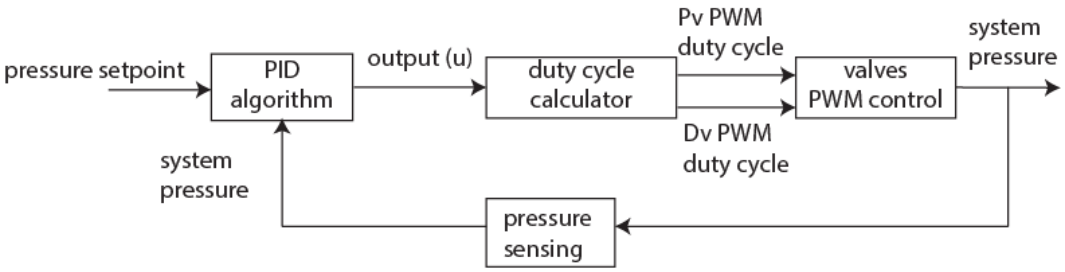

Figure 3-14: Control loop for SISO pressure control system

The MIMO system would have required more rigorous control design approach but this is solved by adopting a SISO system where the single input to the controller is the output from the PID and the single output is the pressure in the system. This use of a duty cycle calculator converts the PID output, u to a pair of duty cycles for pressurisation and depressurisation valves (Pv and Dv). The pressure in the system is monitored using the pressure sensor.

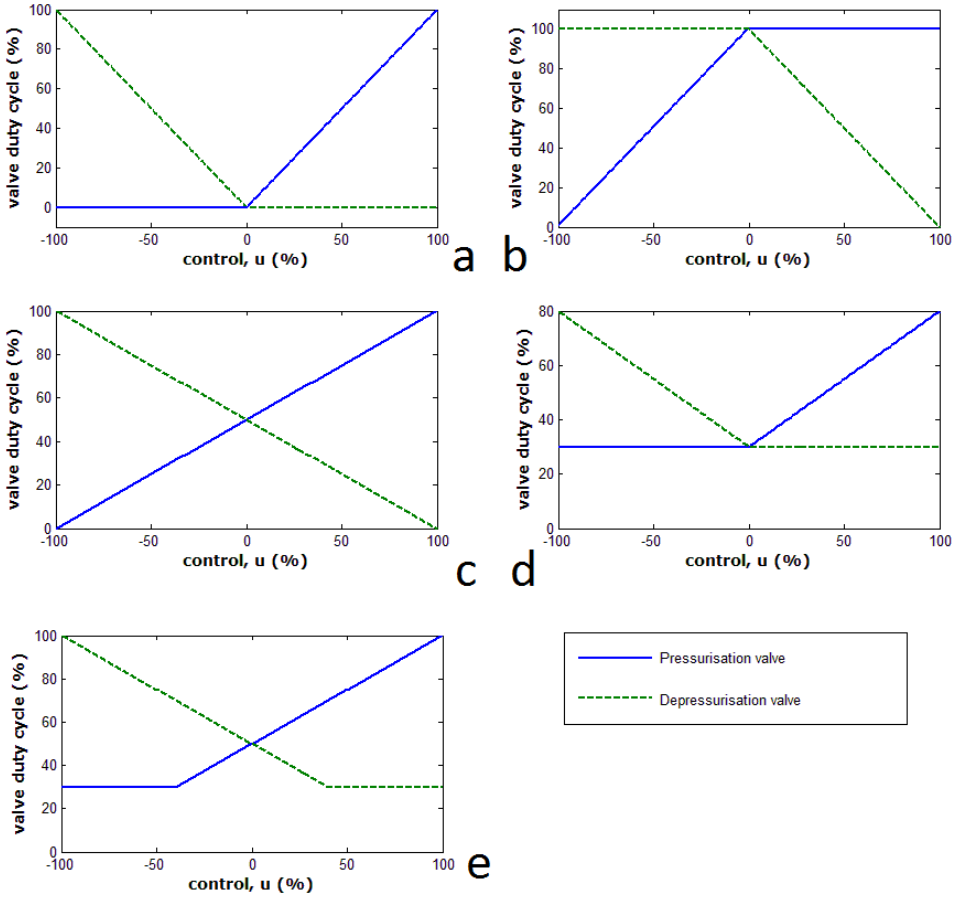

Figure 3-15. Options for controlling valve inputs due to pressure controller output

The choice for valve interplay is based on (vanVarseveld and Bone 1997) and they are: a) non pressurised mode – where the pressurisation and depressurisation valve are set to zero when there is zero error but only one valve is actuated to control the pressure when error is not zero; b) pressurised mode – both valves are set to maximum when error is zero and the only one valve value is decreased to increase or decrease the pressure; c) half-pressurised mode – both valves are at the mid-point when error is zero and they are actuated simultaneously during the control ; d) limited minimum pressure mode – an improvement on the non-pressurised mode where the non-actuated valve is at some level higher than zero to reduce dead band in the control; and e) half-pressurised with limited minimum pressure mode – an improvement to the half-pressurised mode where the reducing valve cannot get lower than a set limit but the increasing valve can get to the maximum..

The practical options described were implemented and the output was monitored to determine which output provided optimum balance between the rise time and fall time when a single sinusoidal signal is applied to control the two valves.

Option A sets the valves to zero when the control signal is zero which indicates a zero error. When the error is non-zero, only one valve is activated with increasing inputs, depending on the sign of the error. This option was not ideal as a dead band of ±35% was recorded when this scheme was used in a pneumatically controlled actuator (vanVarseveld and Bone 1997). This method was not explored further.

Option B is sets the valves to the maximum when the error is zero and reduces only one valve when the error is non-zero. This will mean the input valve will be fully open even when the pressure change required is small causing waste to pressurisation gas which is not ideal. This option is impractical and was not explored further.

Option C controls the valves simultaneously. When error is zero, the valves are set at the midpoint of their minimum and maximum duty cycle values. This system was further investigated for use with the pneumatic pressure control system.

Option D is a modification of A where both valves are open by a small signal when the error is zero. This option is expected eliminated the deadband that exists around input signal of zero (vanVarseveld and Bone 1997). This was further investigated for use in the pneumatic pressure control system.

Option E is a modification of C where the control signal to the valves is set to never go below a point. This was to ensure that the valves were always responsive.

Option D was implemented and used to demonstrate the multiple-input-single-output conversion to single-input single-output system. This was then compared to the results from using option C and option E. The result of implementation will inform on the range of duty-cycle settings that are appropriate for use with the pneumatic pressure control system.

3.5.4 PID Control

The PID controller design is a fast controller implementation that requires little knowledge of the plant model (Marlin and Marlin 1995). The single PID loop illustrated in Figure 3-16 provides a plant input, u, based on the error between the target and current pressures shown in Equation 3.1 and Equation 3.2. The output of the PID controller is the sum of the proportional, integral and derivative functions of the error.

$$error, e = P_{target} - P_{current} \quad \text{Equation 3.1}$$

$$-100 < u < 100 \quad \text{Equation 3.2}$$

An automatic PID tuning algorithm library in LabVIEW was used to find the gain settings for the controller. The auto tuner uses the Ziegler-Nichols tuning method with a relay to step through target process variables. The gains obtained were then applied to the system controller. An experiment was done to assess the performance of the PID gains obtained. Set pressure targets were compared to the measured pressure and the performance of the controller was obtained by visually inspecting the plots of the target and measured pressure.

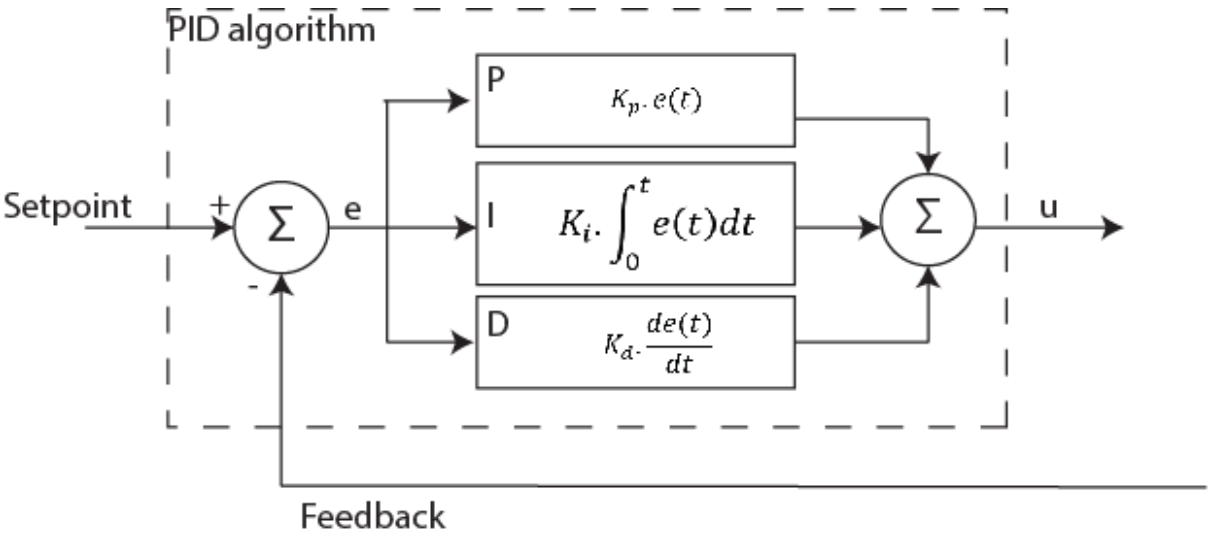

Figure 3-16: Control algorithm schematic for pressure and flow control
The PID algorithm computes an output based on the proportional, integral and derivative of the error. Typically, the PID algorithm implemented in code will take the system output as a feedback and deduct the difference from the set point to obtain the system error.

The work towards optimisation of the pressure controller showed an inconsistent performance of the PID algorithm in controlling the pressure across the pressure ranges. The following were further investigated towards achieving a consistently fast response from the pressure controller:

- Development of alternative controller like model predictive control (Åkesson and Toivonen 2006). See the Appendices for details on its implementation. This was attempted simultaneously with other approaches and not implemented when an alternative solution was achieved.
- Improve the loop rate of the controller to enable frequency PID system control. This was investigated and a high level design was implemented to incorporate an external hardware that could provide the rapid low level pressure control. An arduino was investigated to solve this problem and code was developed to implement the control system in the microcontroller system.

3.5.5 Arduino Development

It was believed that the data acquisition system limited the implementation of rapid pressure change requirements for rapid liquid flow control due to large loop interval (Δt = 50 ms) which limited the reaction time of the PID algorithm to errors in the system. The approach to develop the pressure controller outside of LabVIEW was conceived to reduce this loop time to 1 ms in an attempt to improve PID performance.

An Arduino has been investigated as a faster alternative to improve the reaction time. The addition of a micro controller was expected to enable lower level control logic to be performed by the microcontroller at faster intervals (1 ms) while receiving control updates from and updating the PC with sensor values at the slower interval (50 ms).

shows important characteristics of some Arduino boards that were considered in choosing an ideal controller. The Due CPU clock rate was a distinct advantage at 84 MHz but the limitation of this was the maximum voltage input of 3.3 volts. The Arduino UNO is limited in clock rate but is able to read 5 volts at its analog inputs. The UNO was used to eliminate the need for an additional voltage divider circuitry. The Arduino was also connected to an external DC power supply (10v, 1A max) to provide enough power for PWM generation.

Table 3-1: Arduino controllers for acquisition and control

Property	Uno	Due	MEGA	UNO32
CPU clock rate (MHz)	16	84	16	80
Analog Input Range	+5V	3.3	5	3.3
Digital Output	+5V	+5V	+5V	+5V

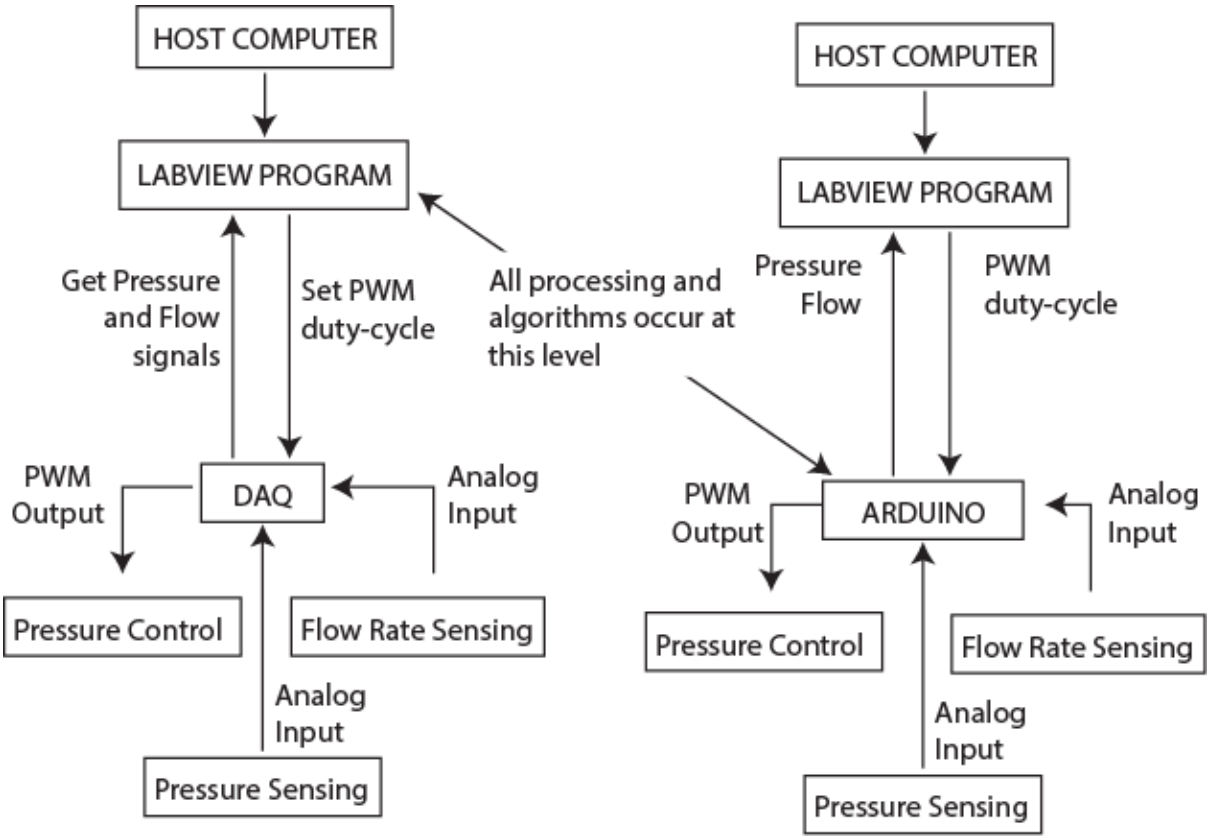

Figure 3-17: Control schematic for DAQ and Arduino implementations
An Arduino as a replacement for the DAQ required a different control schematic. All the pressure sensing, flow sensing and control processing would occur on the microcontroller allowing the LabVIEW program to set high level tasks like pressure and flow targets.

An Arduino program was developed to implement a low level pressure and flow control while a LabVIEW program was written to allow communication with the Arduino over RS232 to update parameters for the perfusion control system. High level commands such as target pressure, target flow and active PID were sent from the LabVIEW program while the microcontroller handled the smaller tasks such as data acquisition, PID computation and PWM generation.

The Arduino program was designed to cycle through the data acquisition, PID computation, PWM generation, PC communication, and timer functions every loop interval (Δt = 1 ms). The data acquisition process was set to read the signals from the pressure and flow sensors at the analog inputs.

The PID computation was achieved using the available PID libraries available and the conversion of the PID output to PWM duty-cycle values was preconfigured as two options (A and B) that can be selected during run time. The operational range of the valves could also be set by the user of the program.

PWM generation was more difficult to achieve in the Arduino. A hardware change was implemented to allow higher frequencies on the PWM outputs. The default frequency for PWM output on the digital lines is 490Hz on the pins 3,9,10 and 11; and 976Hz on the pins 5 and 6. This was altered by changing the timer prescalers (Krauss 2014, Muller, Mohammed et al. 2015). This allowed all the pins to have PWM 1 kHz frequency. The limit of the Arduino UNO is the low resolution of the PWM signal with two channels at 10-bit and four digital output channels at 8-bit. The Arduino Due however has 12-bit on all the PWM output channels.

The communication with the PC over the serial interface was setup to allow the LabVIEW program update the Arduino with new targets and changes to the system parameters using ASCII strings. The ASCII string to update a single parameter took the format of “<”KK”><XXX><YYYY>” where KK was the initialisation string to state the start of an update parameter, “XXX” is the parameter to be updated which could be any of the keys shown in Figure 3-18. “YYYY” is the new value of the updated parameter. The format used to simultaneously update several parameters was “<”KK”><AAA_1><$BBBB_1$>,<AAA_2><$BBBB_2$>, <AAA_2><$BBBB_2$>,\n”. “AAA_1” and “AAA_2” are the first and second parameters to be updated respectively with $BBBB_1$ signifying the value of the first parameter and so on.

KK	–	starting string.
P1Kp	–	PID Kp term for pressurisation of manifold 1 (0 – 1)
p1Kd	–	PID Kd term for pressurisation of manifold 1 (0 – 1)
p1Ki	–	PID Ki term for pressurisation of manifold 1 (0 – 1)
Tp1	–	Target pressure for manifold 1 (0 – 250 mbar)
Tf1	–	Target flow for manifold 1 (0 – 120 nl/s)
f1Kp	–	PID Kp term for flow control of manifold 1 (0 – 1)
f1Kd	–	PID Kp term for flow control of manifold 1 (0 – 1)
f1Ki	–	PID Kp term for flow control of manifold 1 (0 – 1)
p1pDCh	–	maximum duty cycle value for pressurisation valve of manifold 1
p1pDCl	–	minimum duty cycle value for pressurisation valve of manifold 1
p1dDCh	–	maximum duty cycle value for depressurisation valve of manifold 1
p1dDCl	–	minimum duty cycle value for depressurisation valve of manifold 1
PIDp1	–	PID on/off for pressurisation of manifold 1 (on if value > 0.4)
PIDf1	–	PID on/off for flow control of manifold 1 (on if value > 0.4)

Figure 3-18: Set of parameters that can be changed from the LabVIEW program

An example ASCII string to update the target pressure on the Arduino system is “KKTp130” which sets the target pressure to 30mBar. The speed of serial write could reduce the overall speed of the system so read operations were minimised. The code to set all parameters was used once at initialisation of communication with the LabVIEW program and the individual updates were done when the user changes a parameter in code.

3.5.6 FPGA Development

The high-speed advantages of field-programmable gate array FPGA systems was also leveraged in the optimisation process This was demonstrated using a high-end programmable automation controller (PAC) based on FPGA technology (National Instruments CompactRIO - cRIO). The real-time FPGA system implementation required minimal changes to the original program used to develop the pneumatic pressure controller using the simple data acquisition system. Preliminary test showed that the system was able to achieve sub-millisecond loop rates (Δt = 0.5 ms). New PID gains were obtained using simple manual tuning methods and implemented for optimised system control.

3.6 Results of Pressure Control System Optimisation

3.6.1 Impulse Response

The open loop characteristics of the sealed output system showed that the peak pressure of 250 mBar was achieved one cycle (50 ms) after the trigger signal. This was achieved when a duty-cycle of 0.4 was applied to the input valve. However, only a peak pressure of 100 mBar could be achieved when the output was connected to the liquid reservoir (100 mL Duran bottle). Figure 3-19 shows open loop characterisation results for the duran bottle experiment with different actuation duty-cycles to the valves.

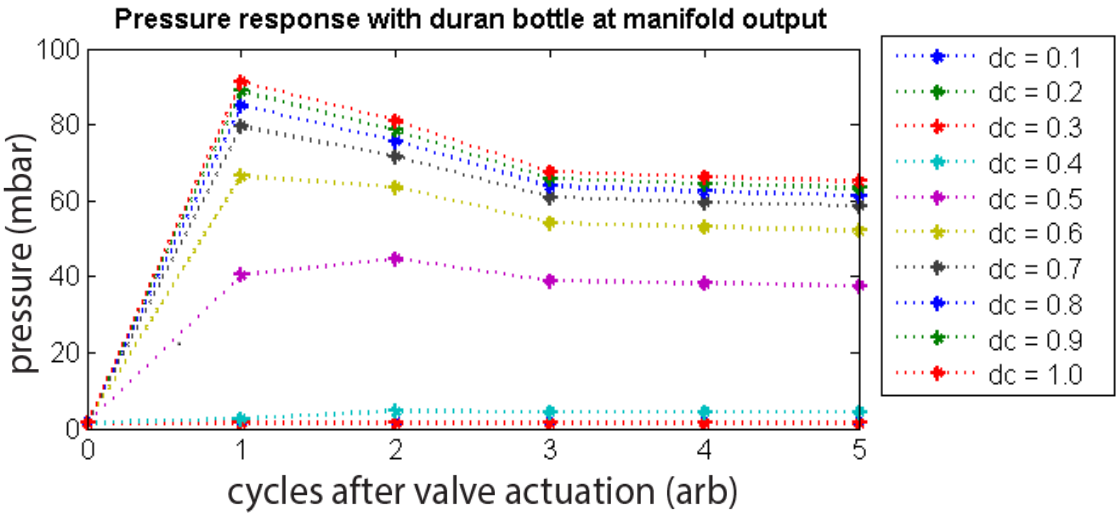

Figure 3-19: Open loop valve characterisation for type A manifold
The pressurisation valve for the "Type A" manifold system is actuated at a duty cycle (dc1= 0.1) for 1 cycle of operation (Δt = 50ms) and the pressure in the system is logged from that valve actuation cycle till 5 cycles after to determine the maximum response to the actuation duty cycle. The actuation is repeated for n= 6 and the mean of the pressure obtained for each duty cycle is shown for the different cycles after the actuation. The output of the manifold is closed off in image (a) but was connected to a Duran bottle in image (b)

The maximum pressure (250 mBar) is not reached when the output is connected to the reservoir because the reservoir was not completely filled by the air that passed through the orifice during the valve actuation period. The pressure in the reservoir would only have increase if the valve was actuated for a longer period allowing more air into the sealed reservoir. The pressurisation valve was found to be responsive with duty cycle range (0.4 – 1.0) in both the "type a" and "type b" manifolds very

limited changes were observed in the higher duty cycle range (0.7 – 1.0). As such the operational ranges for the pressurisation and depressurisation valves were set to (0.4 – 0.7) which was seen to be the more responsive range of duty cycles for the pressurisation valve. The leakage in the systems makes it impossible to characterise the performance of the depressurisation valves but it is expected that they perform the same as the pressurisation valves since they are the same product.

Figure 3-20 shows the effect of changing the input pressure to the pressure controller. The peak pressure in the system increases to 200 mBar. It indicates that a faster pressurisation can be achieved by increasing the input pressure to the system. The time taken to reach peak pressure (250 mBar) is shown in Figure 3-21.

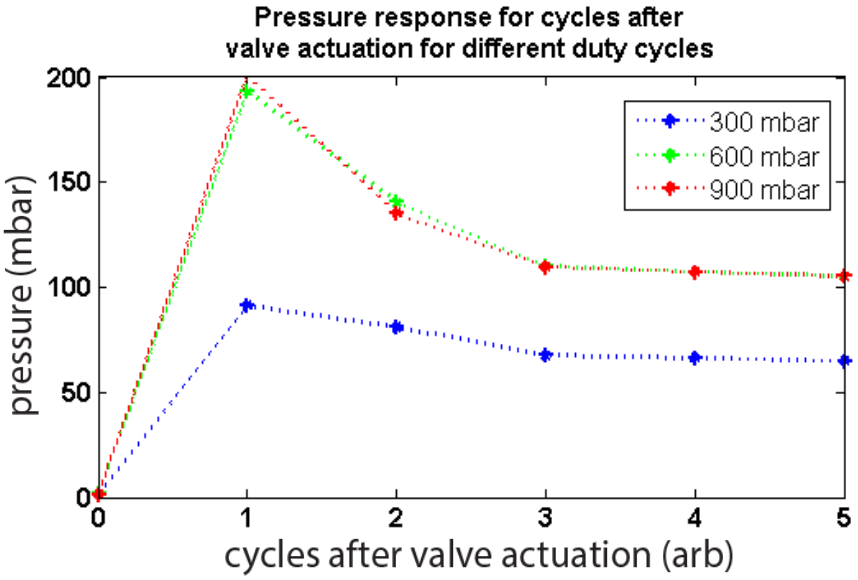

Figure 3-20: Open loop characterisation for different input pressures

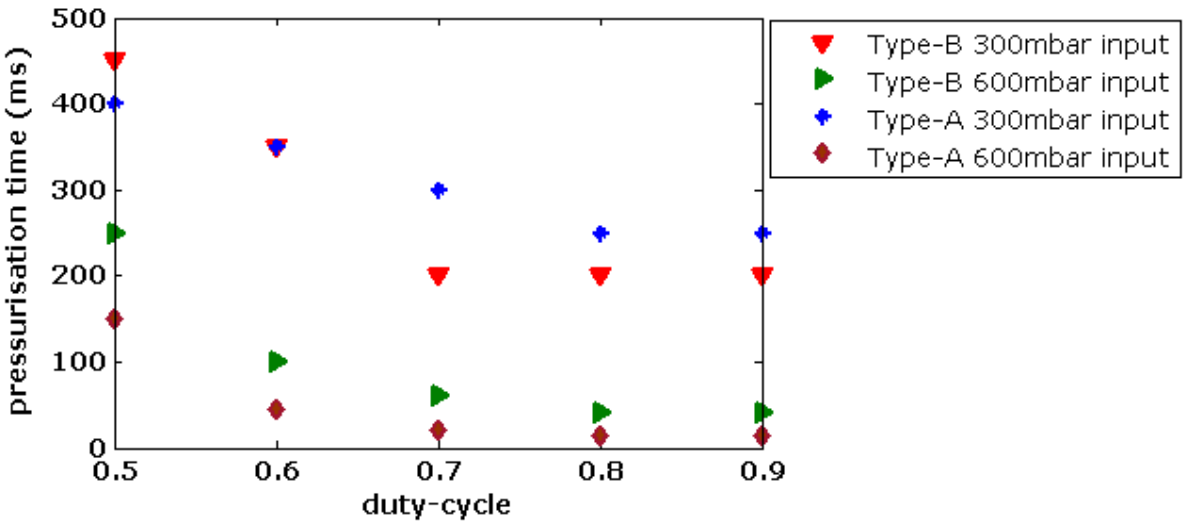

Figure 3-21: Time taken to reach peak pressure for manifold types A and B

It is observed that higher pressure input to the system will provide faster response times as expected. However the “type a” manifold showed faster response times than the “type b” at this high pressure. One reason for this may be due to the speed at which high pressures may be achieved within the manifold type-A which requires a connection to the liquid reservoir. Another reason may be the total air volume of the setup in the manifold which is more in the type-B than type-A. Both systems reach peak pressure of 250 mBar within 150 ms of continuous actuation when an input pressure of 600 mBar and duty-cycle of 0.6 was applied.

3.6.2 MISO Control Approaches

Figure 3-22 shows results from the implementation of Option D for the pneumatic pressure control system where a sinusoidal system input, u was used to control the two valves resulting in a varying pressure change in the system. It can be seen here that the peak pressure here is about 200mBar with 1 Hz signal which change the duty-cycle to the two valves between the range (0.4 -0.7). Increasing the high limit of the range would result in higher peak pressures and higher frequency result in faster responses of the pressure controller in open loop control.

The use of Option C produced similar responses but had a disadvantage of excessive waste of the supplied gas especially when the control signal was close to zero. Here, the pressurisation valve is mostly open and the depressurisation valve will have to also mostly open. The same effect was observed in **Option E** and the methods were not further explored due to this disadvantage.

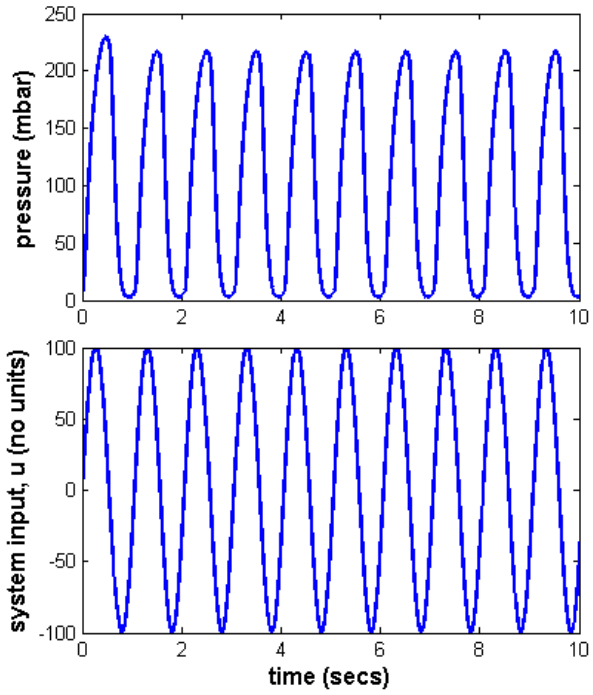

Figure 3-22: Pressure response to applied sinusoidal control signal
The sinusoidal control signal (A = 100) is applied to the duty cycle calculator that activates the pressurisation and depressurisation valves accordingly. The chart shows the signal applied between -100 and 100 and the corresponding pressure oscillations setup in the system. The operating range of the valves were set to 0.4 -0.7.

3.6.3 PID Tuning

It was found that the PID gains obtained from tuning did not give the same system performance over the pressure output range of the controller. However, it did give a mean overshoot of 12% from the target. Visual inspection of the performance in

Figure 3-23 also shows variable settling time and response time of the controller for the different targets.

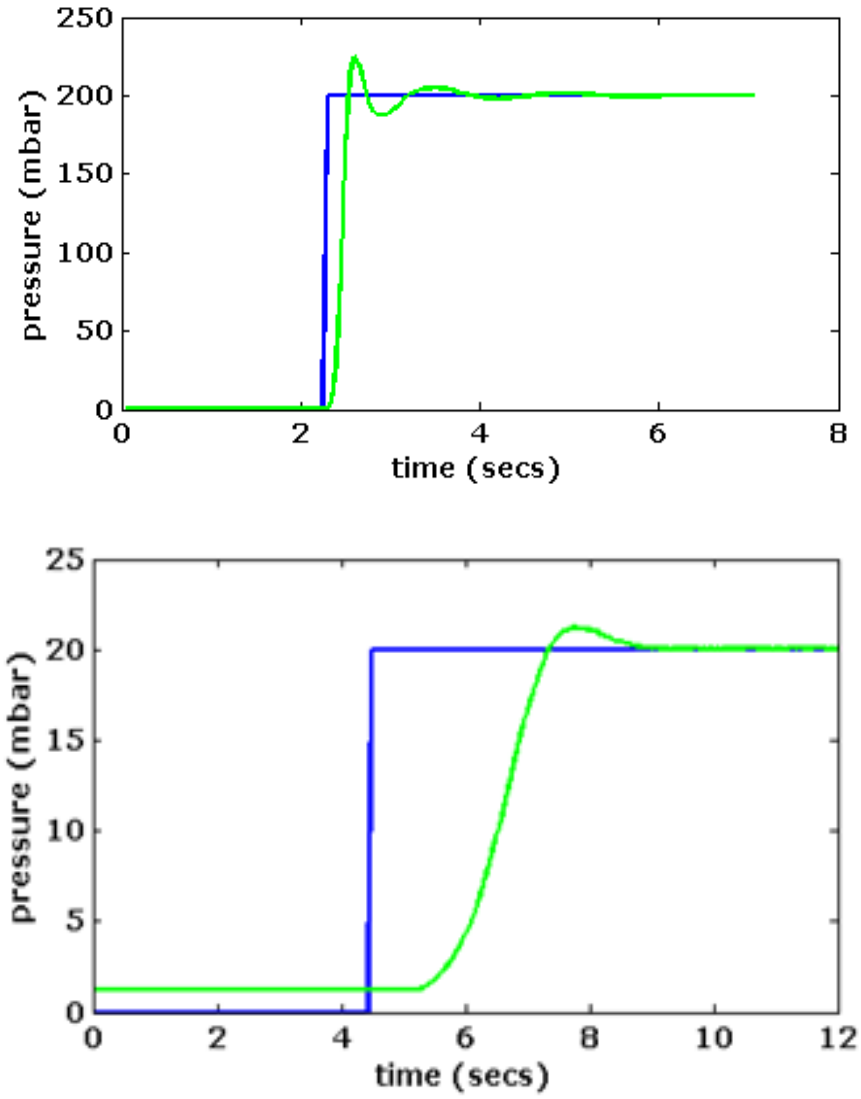

Figure 3-23: Differences in performance for different pressure targets using PID control
The performance of the system after auto-tuning was able to achieve 12% overshoot but the settling time and rise time varied with target pressures. This was not ideal for the flow control where deterministic performance is required.

The use of optimum PID parameters was not sufficient to realise stable, and rapid pressure changes with the pneumatic pressure control system using the available data acquisition and control system. An Arduino system was also investigated to improve the system as well as a high speed FPGA hardware system.

3.6.4 Arduino Implementation

The system developed with Arduino was found to have a loop rate of 10 ms which was 10 times the target loop rate of 1 ms.

The limit of the Arduino UNO was the resolution of the PWM signal which was limited to 8 bits. Only 256 discrete duty cycles could be provided and the resolution of duty cycle control is 0.004 (1/256). Another limitation was the hardware changes required to change the default frequency for PWM generation on the digital pins. This hardware change could cause serious damage to the board if done incorrectly.

A 12-bit PWM module available from Adafruit can solve the resolution problem and programming complexity problem by using the digital pins from the Arduino to configure the PWM output on the module. The libraries to effect this are available further reducing development time. These module have duty cycle resolution of 0.0002 (1/4096).

The timing interval (Δt = 9 ms) was better than the 50 ms achieved using a deterministic DAQ configuration but less than the 1 ms target. However, this timing was only realised on configuration of one pressure controller and would increase with added flow control and additional controllers. This is due to the block coding approach in the Arduino that executes code serial regardless of the dependencies.

The lack of multi-core functionality on the Arduino makes it impossible to run parallel threads (Buonocunto, Biondi et al. 2014) for the different manifolds which causes the addition of more manifolds to increase the interval time for the entire application. This can be solved by applying a distributed system architecture where each Arduino manages one task such as pressure control and another Arduino manages the communication between these Arduinos and the PC. This is illustrated in . This approach, was however, not developed further, with an alternative approach taken of implementing a more robust system with parallel processing capabilities. It was

realised that a processor with ability to implement parallel threading would run parallel processes simultaneously to reduce the loop rate. A field-programmable gate array (FPGA) system was implemented as a controller to show the impact of an improved loop response time on the pressure controller performance.

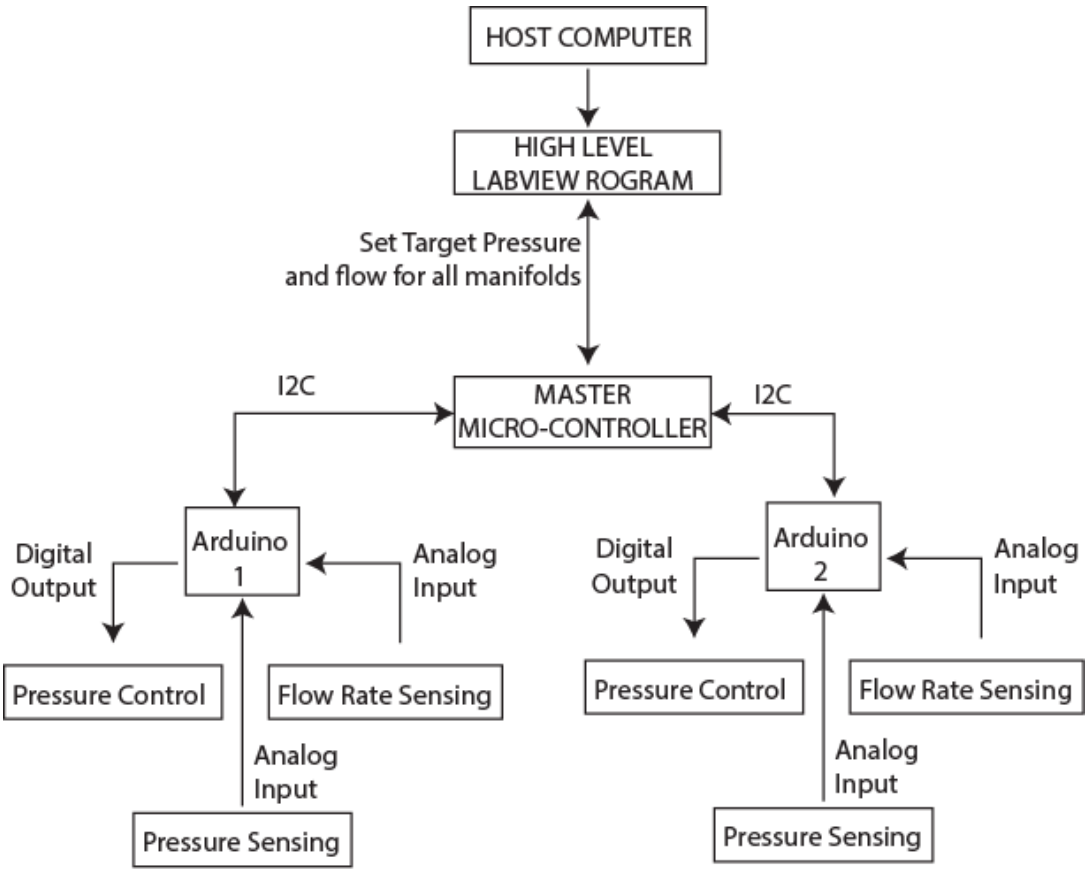

Figure 3-24: Distributed system control for multiple pressure control systems
Distributed system control using multiple microcontrollers for specific tasks and a single microcontroller to manage communication between these systems and the PC. The master microcontroller will receive targets from the PC and relay these to the target Arduino for that task. It will also relay system state information back to the PC.

Further development with the arduino to improve control of the pneumatic pressure controller by collaborators Mr. Ahmed Abdalla was unable to improve the timing characteristics. Another route is currently ongoing to develop advanced control

strategies such as Fuzzy control or Model Predictive Control (MPC) on the arduino.by a collaborator, Yuezhao Li

3.6.5 Real-time FPGA Control

PID manual tuning was done to obtain the performance shown in Figure 3-25 shows the performance of the system with a simple PID manual tuning applied to an FPGA-based controller. The pressure control was very stable with a 0.05 standard deviation. The system suffered slightly at higher pressure targets but was able to reach these targets within 300 ms. This data shows that the system is capable of reaching a higher performance metric with little emphasis given to optimising the PID control algorithm.

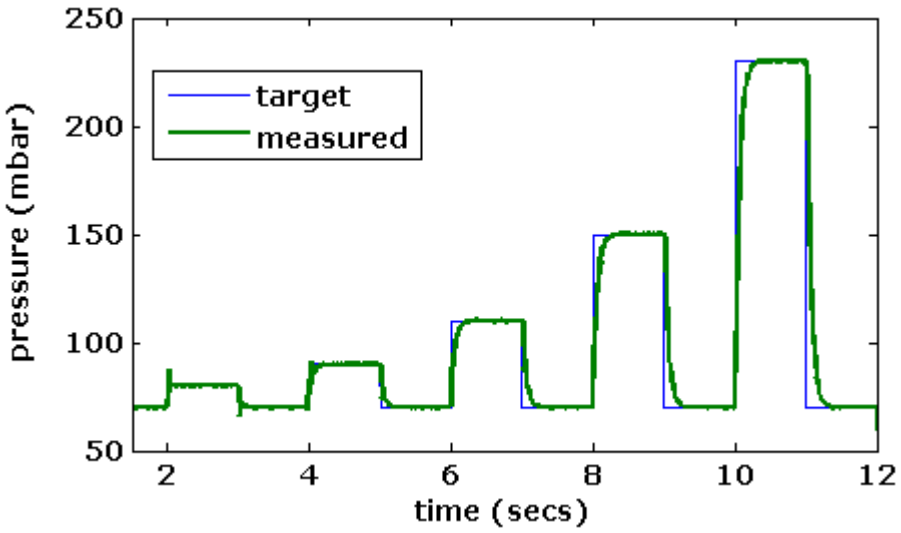

Figure 3-25: Pressure control performance with real time FPGA controller
Pressure targets (blue) were given to the control software implemented on a real-time controller. The measured pressure is seen to closely follow the target pressures and a maximum overshoot of 8% was measured across the range of targets. Response time was well within 1 second for f the target pressures. PID gain settings of P = 10; I = 0.001; and D=0 were used.

The drawback of the FPGA system is the high cost of implementation and the slightly higher technical competency required to achieve the solution. The cost of implementing this real time system long term may be justifiable if the rest of the processing power can be applied to the control of other systems in the laboratory.

Cheaper FPGA alternatives can increase the possibility of widespread usage of FPGA solutions for liquid handling, however, the boards required deeper knowledge of FPGA programming to implement. An recommended alternative is the Mojo board with 84 digital IO pins and 8 analog inputs. This board has the added advantages of allowing programming with an Arduino style syntax and provision to handle up to 5V input. The speed of this board may enable one board to control the pressure and flow requirements with the 1 ms targets. This route is recommended for developing high end open source controllers for liquid handling systems.

3.6.1 Optimised PC DAQ Control

Further work has been done on the LabVIEW program to optimise the processes involved and reduce the loop time. It was found that non-essential communication with the data acquisition device were previously implemented to ensure determinism but these had the added disadvantage of increased loop rate (Δt = 50 ms). These non-essential DAQ communications queried task completion to enable a consistent system operation. A reduced deterministic time interval (Δt = 5 ms) was the result of removing these tasks with USB connected multifunction DAQ devices while PCI connected DAQ devices could reach much lower intervals (Δt = 1 ms). A default interval (Δt = 5 ms) was set to ensure uniform performance across all devices and computers used.

A downside with the high speed implementation was the rare occurrence of a failed acquisition caused by insufficient time given to read data from the DAQ. These failed acquisition attempt caused the program to view all sensors at zero resulting in a noisy PID response condition. A code was implemented to track the number of failed acquisition attempts per hour. It was found that these occurred up to 200 times at initialisation when 1 ms interval was implemented with the PCI DAQ system.

The frequency then changed to 1 every 4 minutes during system operation. However, they did not occur over 1 hour of recordings when the loop rate was set at 5 ms with this particular PCI DAQ. A frequency of 1 every 4 minutes was also observed for the USB DAQs when running at 5 ms. This failure was cancelled out by repeating the previous sensor values when the failure occurred. The result was a zero occurrence in both DAQ implementations with over 10 hours of operation.

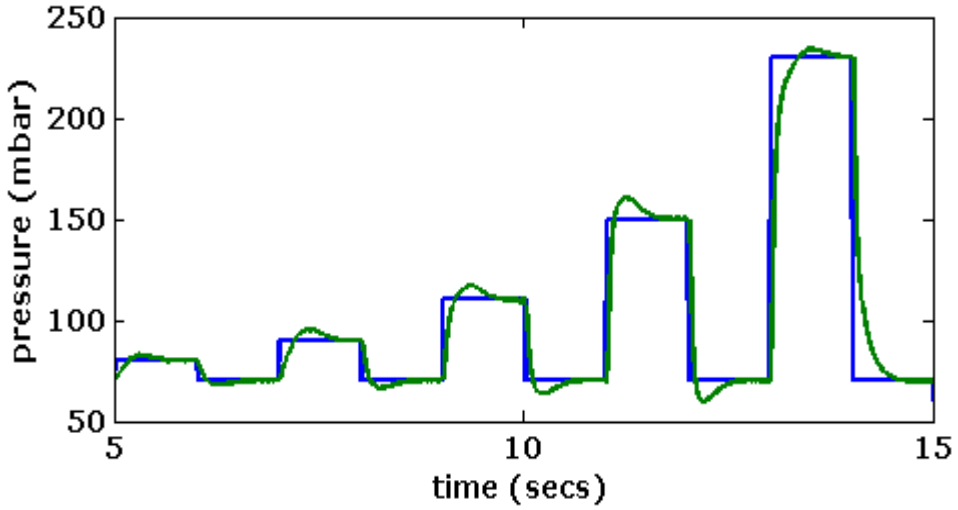

Figure 3-26: Pressure Control and Flow Control with 5 ms interval rate
pressure is seen to closely follow the target pressures and a maximum overshoot of 6% was measured across the range of targets. Resonse time was well within 1 second for f the target pressures. PID gain settings of P = 1; I = 0.003; and D=0 were used.

3.7 Flow Control Applications

The fast response of the pressure control was achieved after optimisation efforts aimed at improving the performance of the overall flow control system. This was then used to pressurise a liquid reservoir and a nested PID loop which incorporated an external flow PID loop with the pressure PID loop as illustrated in the Figure 3-27. The flow PID loop sets a target pressure to the pressure PID loop that sets a plant input, u, which then translates to a pair of duty cycle settings that drive the valves.

The tuning parameters were quickly found using manual search method and the system was incorporated for rapid flow switching as well as long term flow to assess the system performance.

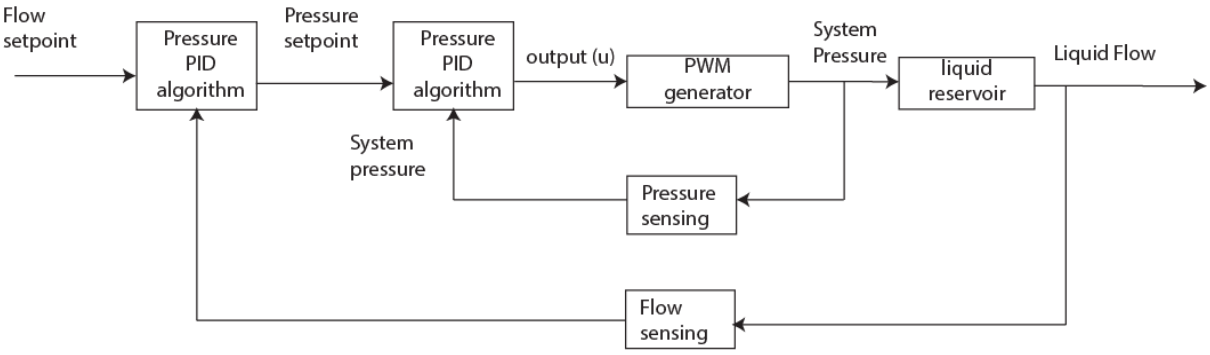

Figure 3-27: Schematic of nested PID loop for flow control
The nested PID loop for flow control allows the flow PID controller to set target pressures for the pressure PID controller in response to the flow rate target and measured values.

3.7.1 Rapid Drug Switching

A Y-shaped microfluidic device was connected to the flow outputs of three custom flow control systems. The optimisation of the control system enabled a fast response time for flow rate change (~0.5 ms) to realise rapid drug switching in the dual-input microfluidic device.

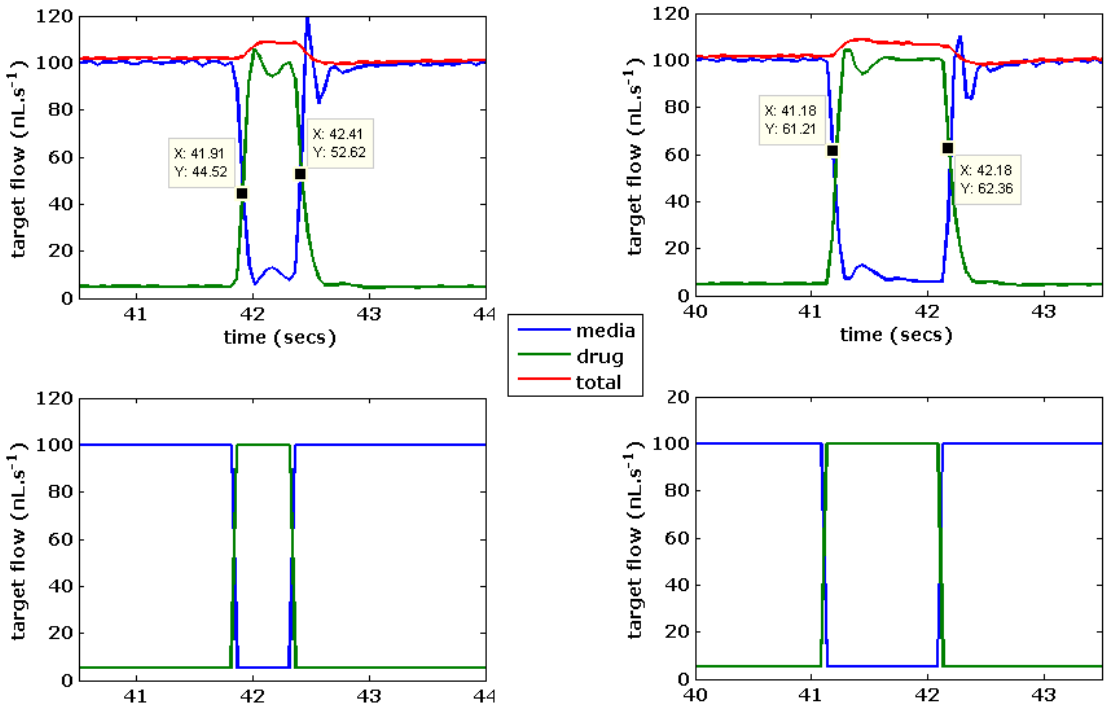

Figure 3-28: Rapid flow switching for rapid interface sweeping with agonists
Successful implementation of a rapid flow controller with rapid switching times. 0.5 s interface switching (left) was achieved as well as 1 second interface switching (right). The measured flow rate data for media, drug and output flow rate is shown (top) as well as the target flow (bottom).

Figure 3-28 shows the rapid response to flow rate changes at some time point during a switching sequence. This was then used to rapidly switch between fluorescein and water in the same dual-input device while recording the detected grey-scale intensity of captured images at 10x magnification during the switching operation.

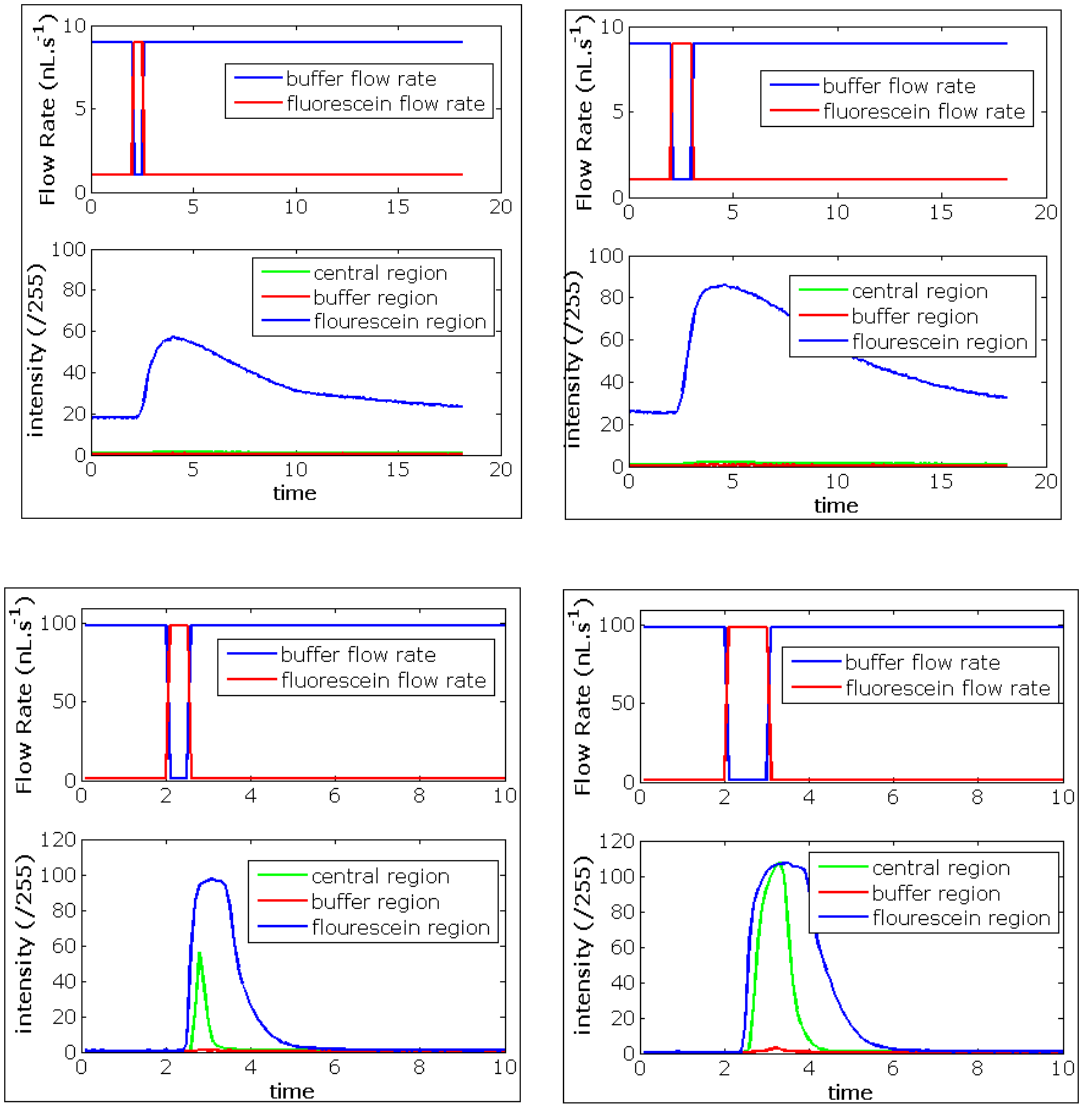

Figure 3-29: Actual Drug switching Response in a Microfluidic Device
A dual-input device with channel height and width (h = 125 µm, w = 0.5 mm) was used connected to the lab developed flow control system using fluorescein and water to simulate drug/buffer conditions. The data shows results for 0.5 second (Left) and 1 second (Right) switching time. It also shows flow switching for 9-1 nL.s^{-1} (Top) and 99-1 nL.s^{-1} (Bottom). The chart shows mean of intensities at regions of interest along the width of the channel at a point along the length very close to input of the device. The

drug is able to reach peak intensity at the centre of the channel with high flow rates only and is a practical demonstration of the limitation to the use of the low flow rates for rapid drug switching.

3.7.2 Gradient Generation and Interface Shifting

The concentration gradient in a Y-shaped microfluidic device was changed by altering the flow rates of the two inputs (F_1 and $F_{2)}$) to the device. This is illustrated in Figure 3-30.

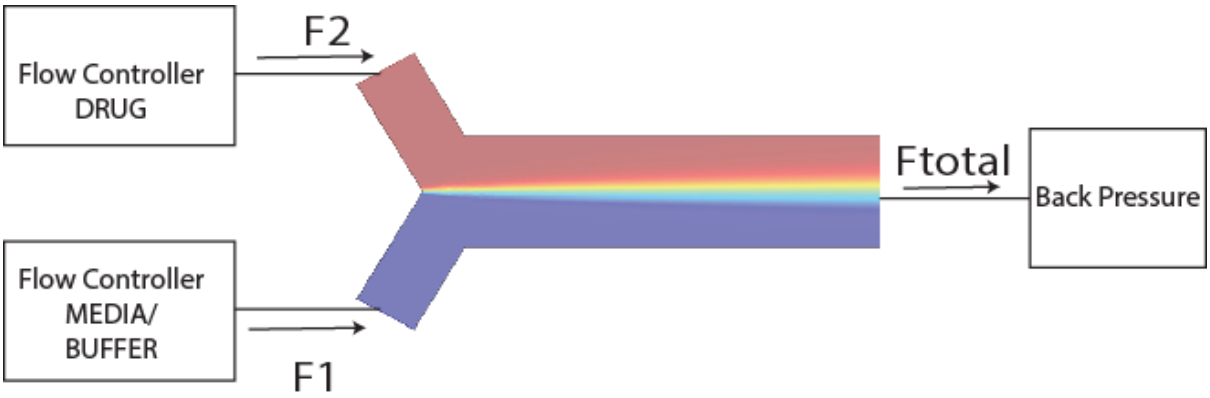

Figure 3-30: Connections for interface shifting in a Y-shaped microfluidic device.
The Y-shaped microfluidic device has been connected to three liquid reservoirs with pressure controllers that regulate the flow in the drug and media reservoirs but only provides a back pressure in the reservoir connected to the output. The interface is shifted by controlling the flow rates at the inputs such that their ratio is equal to the spatial ratio of the interface in the device.

The relationship between the input flow rates and the total output flow rate (F_{total}) is maintained by using Equation 3.3 and Equation 3.4.

$$F_{total} = F_1 + F_2 \qquad \text{Equation 3.3}$$

$$F1 = x \,.F_{total} \qquad \text{Equation 3.4}$$

where x = a fraction of the channel width to be covered by buffer/media

An experiment was setup to demonstrate the effect of changing the flow rates in the device on the concentration profile along the device width. Distilled water was placed in the reservoirs for the media flow controller and the back pressure controller. Fluorescein solution was placed in the second input reservoir (drug). The back

pressure was set (P_{back} = 10 mBar) and the pressure to the liquid at the two inputs was set such that the pressure difference along the flow line for either input ($\Delta P = P_1 - P_{back} = P_2 - P_{back}$) was equal to 10, 20, 40, 80, 100, 160 and 190 mBar). The microfluidic device was placed in microscope for fluorescence imaging and grey scale intensity of the images captured with the camera at 1 second trigger intervals. Timeouts were employed to prevent camera acquisition delays and ensure the expected acquisition rates. Failure in camera acquisition were set to produce errors to stop the acquisition. The intensity of a linear region of interest of 718 pixels was analysed and the intensity observed is shown in Figure 3-31. The larger pressure difference (higher flow) produced a sharper gradient across the channel due to increased flow rate that reduced the diffusion time of the liquid. This confirms a COMSOL model that shows a sharper gradient along the channel with higher flow rates. Flow sensors were not used in this experiment but they could be integrated to show the same results.

The pressures in the reservoirs leading into the two input lines were varied to move the boundary across the width of the channel with a back pressure (P_{back} = 100 mBar). The graph in Figure 3-32 shows that the boundary moves in the direction of the increased pressure. Diffusion plays a role in the concentration of the drug observed at either side of the boundary.

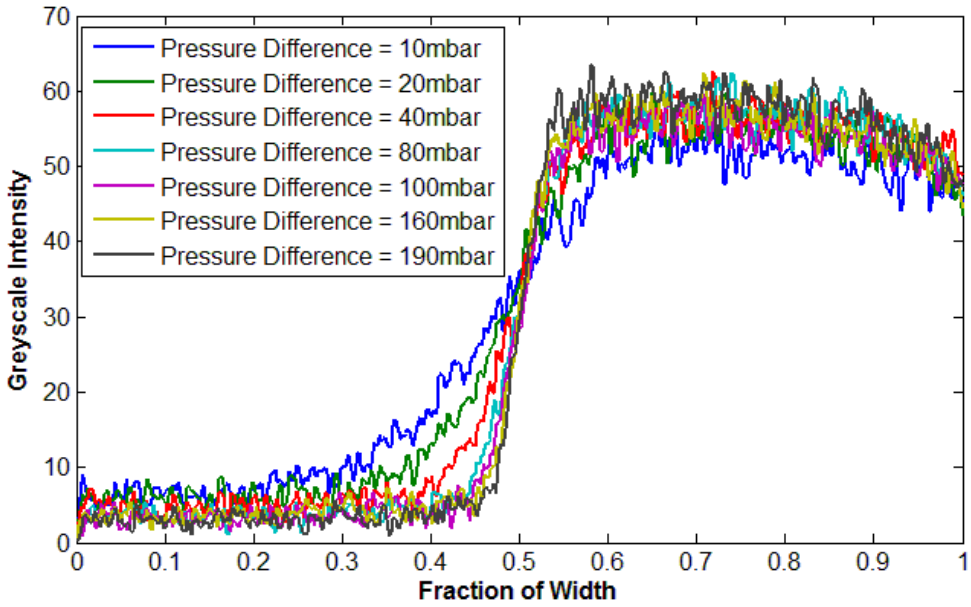

Figure 3-31: Concentration slope with different pressure difference (flow rates)

Higher flow rates provided a steeper gradient across the channel geometry. The flow rate changes were obtained by increasing the pressure difference between the input pressures and the back pressure. A flow rate was not incorporated in this experiment.

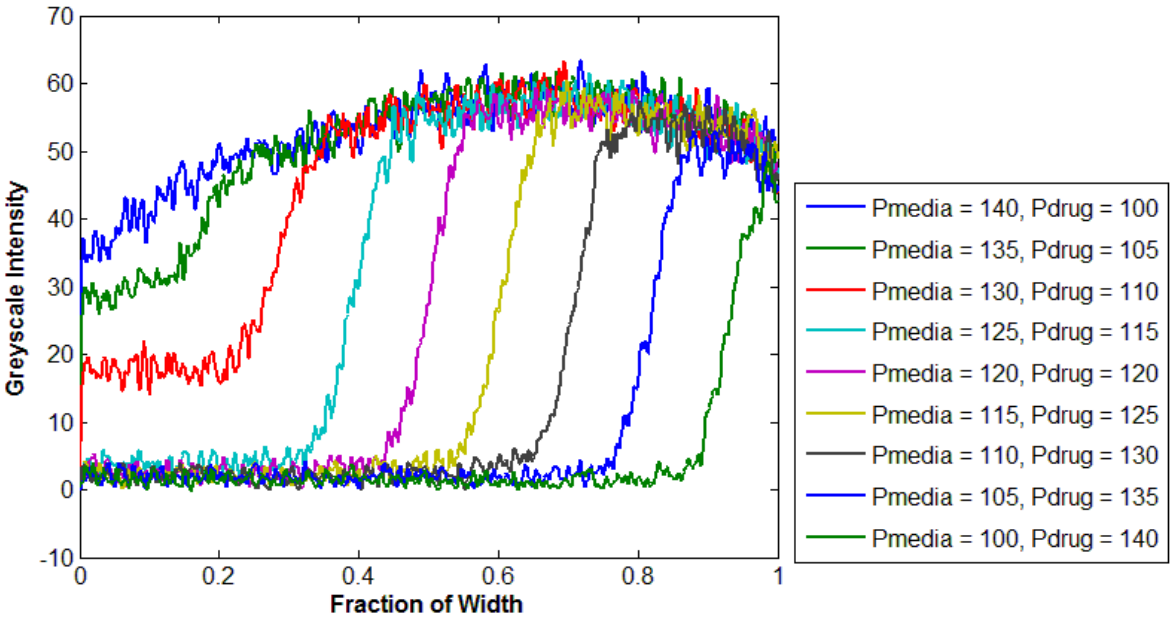

Figure 3-32: Constant back pressure while moving the boundary position

The change to input flow rate ratios was obtained by changing the pressure in the media reservoir and the drug reservoir while keeping the back pressure constant. The interface can be seen to sweep across the channel but the diffusion of the drug zero concentrations when the drug is closer to the wall of the channel.

3.8 Liquid Injection with Commercial Autoloader

The development of the liquid flow control system was simultaneously carried out with an integration of a flow controller with a commercial autoloader to:

- Demonstrate the stability of the flow rate during autoloader switching behaviour.
- Demonstrate the minimum requirements for liquid injection in a microfluidic device that which the autoloader could provide which set the standard for a novel liquid handling system to be developed.

First, fluorescein the use of fluorescein for flow visualisation was confirmed, then the precision of the autoloader loaded volumes was also demonstrated and then the effects of different tube lengths were shown as well as different concentrations loaded. These experiments were performed using the pinhole detector and a single input microfluidic device mounted on an inverted microscope. Figure 3-33 shows the setup for liquid injection with the autoloader.

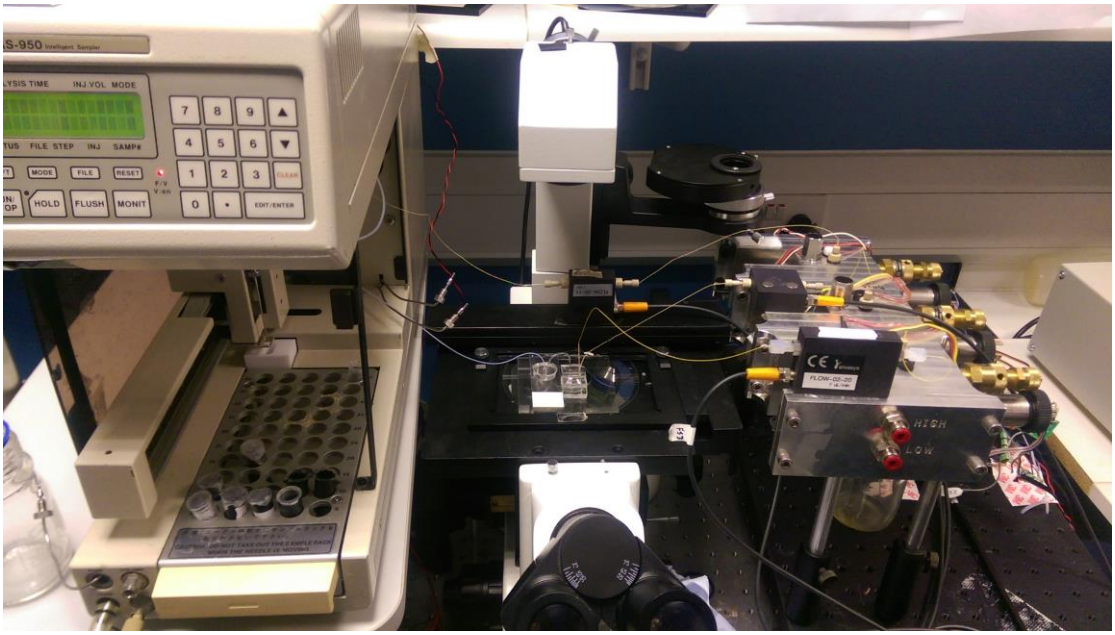

Figure 3-33: Setup of integrated system
The autoloader on the left has 50 vial positions that can be loaded. The flow control system on the right allows liquid flow transport control. Some connections on the autoloader have been removed to give immediate access the autoloader injector directly. The microscope is used to for fluorescence detection.

3.9 Autoloader Performance Characterisation

The use of the autoloader to demonstrate an integrated liquid handling system will hinge on the level of precision obtained during its operation and the effect of the loading system on the concentration of the loaded volume. The relationship between fluorescein concentration and the detected fluorescent light intensity relationship has already been demonstrated in the previous section as linear and will, therefore, be appropriate to quantify the performance of the autoloader for drug delivery.

The characterisation experiments were performed by loading different fluorescein concentrations using the autoloader while detecting the fluorescent light intensity at a microfluidic device. The experiments were setup to determine the precision of the loader, the effect of the tube length on the drug concentration at the microfluidic device and the effect of flow rates on that concentration. Advantages and limits to the use of the autoloader were also identified in the process and are presented subsequently.

3.9.1 Autoloader Precision

An experiment was performed to assess the autoloader precision during loading operation for different volumes. Volumes of fluorescein (v = 5, 10, 20, 40, 80, 100 µL) with concentration (C = 26.6 µM) were loaded six times using the autoloader with a flow rate 100 $nL.s^{-1}$. PEEK tubing of diameter (d = 0.15 mm) and length (l = 150mm) was used to connect the autoloader to the microfluidic device.

The mean intensity of the region of interest was logged over time and the signal was filtered using a MATLAB smooth function to average filter the profile over 20 samples. The peak concentration obtained over the entire experiment was used to normalise the entire data set after deducting the offset at zero concentration from the data. The full width half maximum of the concentration profile was used as a

measure of the effective duration of the drug. A MATLAB script was written to get the full width half maximum (FWHM) of the normalised smoothed intensity profile.

Figure 3-34(a) shows that the result of the filtering algorithm does not adversely affect the data by comparing the unsmoothed and smoothed data. Figure 3-34(b) shows the peak intensity obtained for the loaded concentrations while (c) and (d) show the FWHM obtained for the loaded volumes as a time and as volume respectively. This has been defined as the effective drug exposure time and volume of drug present in the channel respectively.

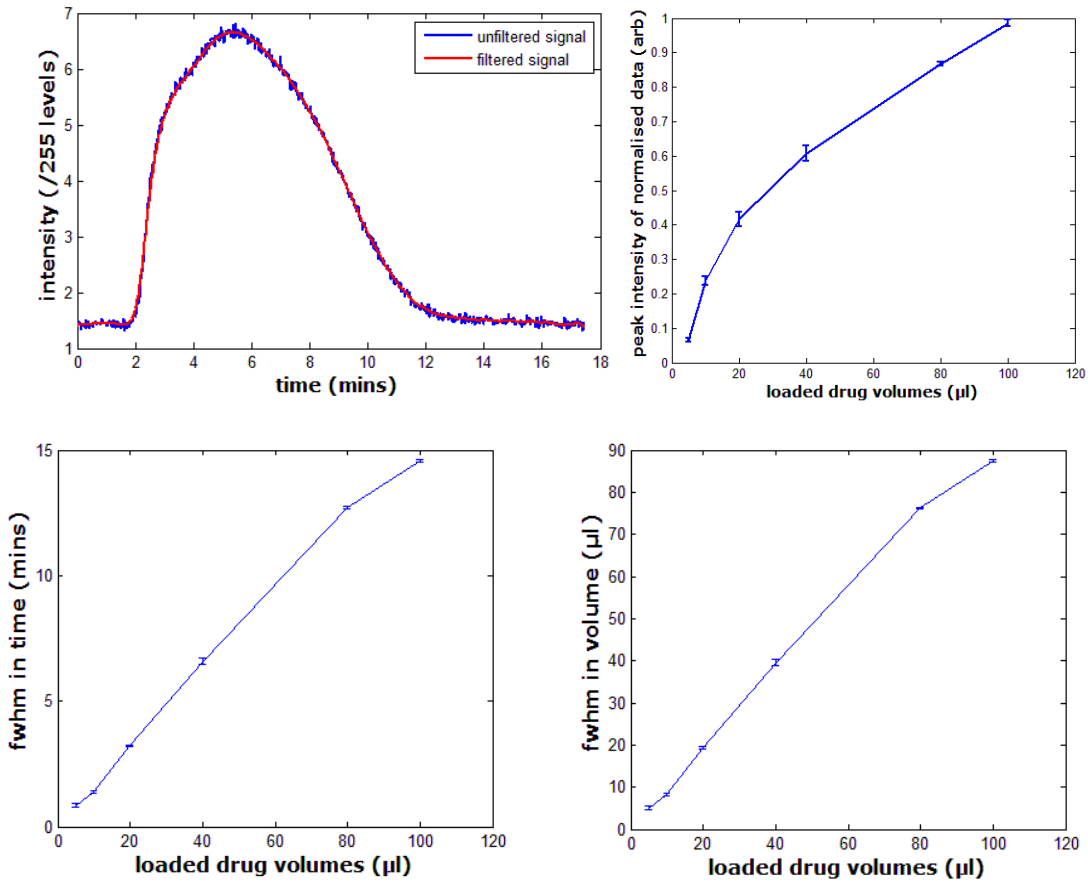

Figure 3-34: Autoloader precision
Analysis of fluorescent signals obtained from loading different drug volumes at same concentration and flow rate (Q = 100 nl/s)

The autoloader precision (error bars) shows fairly consistent behaviour for the different volumes loaded but the peak intensity detected varies with the volume

loaded. This showed that Taylor dispersion effects were dominant with the system and would be detrimental to the implementation of concentration dependent studies. These results were normalised over the peak intensity detected throughout the experiment and did not compare the detected intensity with saturation level where no autoloader is used. A more detailed experiment was designed to determine the extent to which this concentration obtained at the detector is diminished which could affect the use of the system for drug dependent studies which may rely on repeatable dose concentration delivery.

3.9.2 Effect of tubing length on Peak Concentration at Microfluidic Device

The validation of the use of fluorescein to visualise concentration changes in a microfluidic device agreed with past studies (Harris and Mutz 2006). This was then applied to show the precision and accuracy of using the autoloader with results showing drug exposure times that are similar to theoretical expectations of the volume presence.

Taylor dispersion has been attributed as a potential feature of microfluidic drug delivery which may be detrimental to the effective drug concentrations at the microfluidic devices. This in turn is mostly affected by the tube dimension, as well as the flow rate. The autoloader used has fixed internal tubing and an operating mechanism that cannot be altered while the external tubing connecting to the microfluidic device could be chosen to minimise these dispersion effects. However, the extent of the effect of this external tube change is unknown and there is a practical limit to the tubing dimension selected. The size of the loader requires a minimum of 300mm length tubing. We have investigated the peak concentration vs

injected volumes for three different tubing lengths (l=300, 600, 800mm) to evaluate the effect of the tubing size on the Taylor-dispersion effects.

This approach allows us to collect more information about the system to ascertain the possibility of empirical prediction of drug concentration delivered at the device. The peak concentration was obtained from the peak intensity detected and normalised over the intensity expected at saturation of the fluorescein concentration. Figure 3-35 shows the normalised intensity plot against the loaded volumes for the different tube lengths used. Blue – 300mm; Magenta – 600mm; Red – 800mm tube lengths used. Figure 3-36 shows the mean of the data with standard deviation. The linear and the logarithmic curve fits are shown. Both figures show that there is no major influence of the tube length on the behaviour of the loaded drug. This means that in our configuration, Taylor-dispersion effects are negligible. This result may be due to the limit in sensitivity of the detection system.

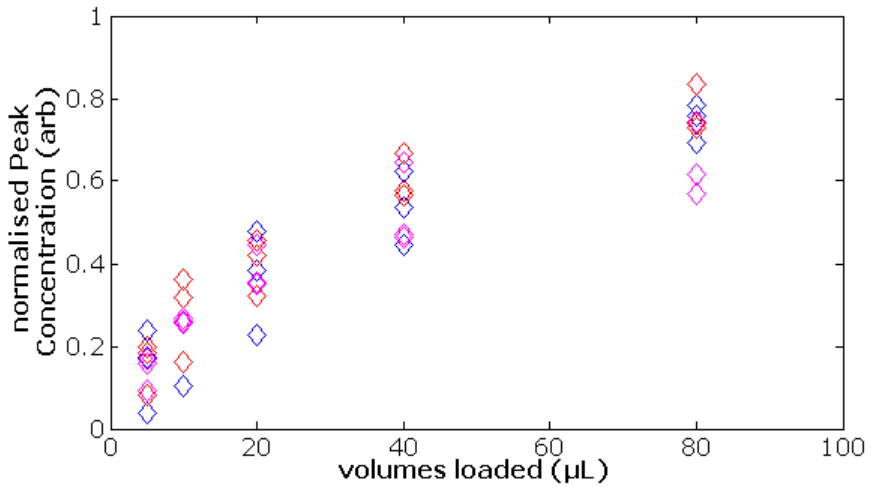

Figure 3-35: Peak concentration with varied microfluidic device distances from the autoloader
5, 10, 20, 40, and 80 µL of fluorescein concentration were loaded through a microfluidic tube with length (l = 300, 600, 800 mm) to a microfluidic device where the intensity was detected with a fluorescence microscope. The normalised intensity was obtained using the intensity that is expected for the loaded concentration. This provided information on the drop in concentration due to the autoloader and the tubing used. The peak intensity at the detector are shown for the different volumes and different lengths used (blue – 300mm; magenta – 600mm; Red – 800mm).A proportional relationship appears to exist between the loaded volumes and the peak concentration of the drug which arrives at the device which is a percentage of the original drug concentration loaded. The limit to the reservoir size prevents the observation of loaded volumes greater than 100 µL and as such the exact relationship between the volumes loaded and the drop in concentration cannot be defined explicitly as logarithmic or linear. The variation between the tube lengths and the drop in concentration cannot be ascertained from the information in the chart. This shows that the effects of Taylor dispersion that occurs due the tube length may be far less important than mixing effects that happen during the autoloader operation.

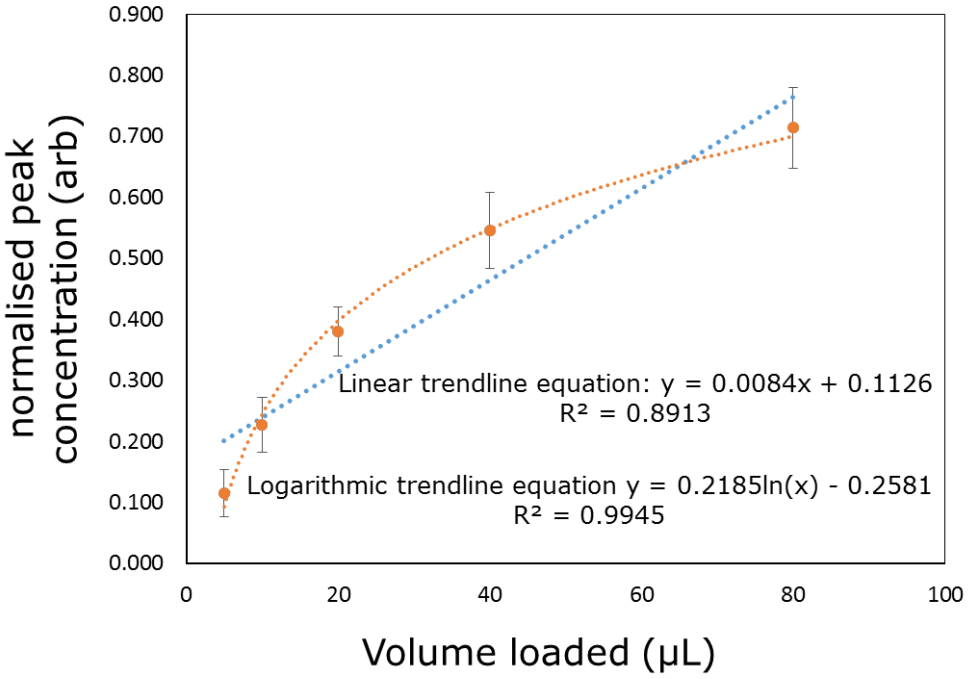

Figure 3-36: Mean Peak Concentration with varied Microfluidic tube lengths
The mean of the data sets from Figure 3-35 is presented with two of the most likely curve fits attached. The r-squared measure shows that the logarithmic trend line fits the data better and agrees more with the expectation of saturation level (1.0) when a large volume is loaded such that the effects of Taylor dispersion at the boundary of the loaded volumes does not affect the peak concentration at the microfluidic device. This could not be tested due to the upper limit on the range of volumes that can be loaded autoloader. The standard deviation, shown as error bars depicts a wide range of concentrations per volume which also shows the margin of error when using this data subsequently.

If we consider that the volume/concentration dependence is linear, then saturation would occur with 121 µL. On the other hand, if we assume that the relationship is logarithmic, then saturation would occur with a loaded volume of 311 µL. The logarithmic behaviour explains the data better and reflects more the fact that the maximum concentration will be reached if an arbitrarily infinite volume was injected such as when flowing the volume from a large reservoir.

The logarithmic curve fit equation will be used subsequently to adjust the minimum volume for desired concentration at the microfluidic device.

3.9.3 Effect of Flow Rate on Concentration at Microfluidic Device

One set of experiments to determine the overall effect of the autoloader was performed while varying flow rates (Q = 20, 40, 80 $nL.s^{-1}$). This was performed using tubing length (l= 600mm).

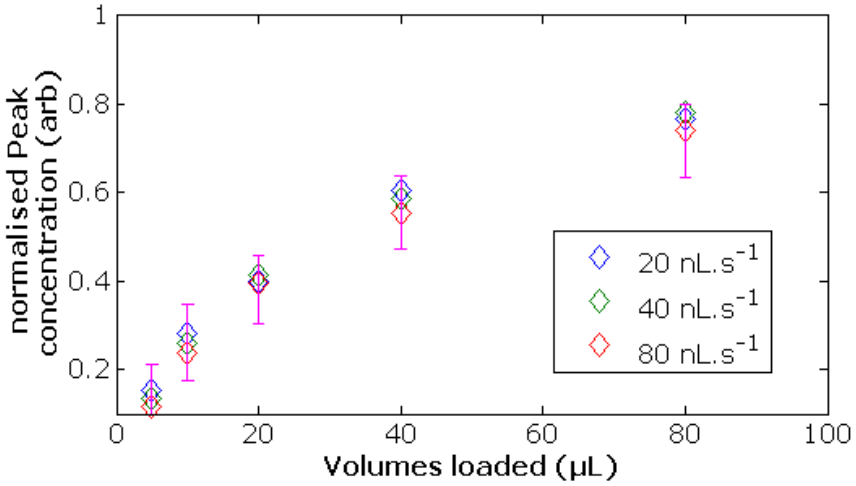

Figure 3-37: Effect of flow rate on the concentration peaks detected.
Different volumes were loaded at different flow rates. The mean peak intensity from the comparison with different tube lengths is also overlaid (magenta) to show that we cannot fully establish that an ideal flow rate exists that will prevent the drop in peak concentrations when loading the volumes.

Figure 3-37 shows the results overlaid with results of the mean peak concentrations. Here, the difference is not large enough to warrant specific preference of one flow rate over another. This also shows the greater dependence of the peak concentration on the autoloader operations.

3.9.4 Advantages and Limits to Autoloader Use

The autoloader was a good starting point to realise volume injection capabilities into microfluidic channels. The advantages that were identified were:

i. Automation capability. The automation of the injection sequences was done on PC.

ii. Fair operating range. The autoloader was able to load volumes over two orders of magnitude (1 – 100 μL). A microfluidic device with surface area of 10 mm^2 will have 0.5 μL volume per 50 μm height.

iii. Only high level programming is required for interfacing. HPLC applications that typically use the autoloader only require a load sequence and very little low-level control of these sequences. As such the ability to control the high level operations of the autoloader will be beneficial for these applications.

For the system being developed, there is need to inject wide range of volumes similar \aSDASto the autoloader but able to exceed the higher limit of 100 μL. This will enable long term switching applications to continue without the need for repeated injections to fill the volume.

The reward system requires low level signalling to track progress and help to synchronise other tasks that depend on the liquid injection system. This ability to signal task completion was problematic on the autoloader since:

i. The only signal automatically sent by the autoloader was an “injection complete”. This was useful to track the time to get the drug to the microfluidic device. However the serial line had to be kept open to wait for these signals and querying the sampler process sometimes stopped the “injection complete” signal.

ii. It was also common for the “injection complete” signal to fail due to errors in the communication line. These communication system failures occurred at least once each day requiring the autoloader to be restarted.

iii. The communication protocols over the RS232 interface was probed without a solution found.

An alternative method of signalling was adopted by connecting a 5V source in series with the autoloader injection marker and a DAQ. A data acquisition task was setup to

read the voltage at the DAQ input which read 5V during normal operation but temporarily changed to 0V at injection completion.

Flow inconsistencies were problematic during autoloader operation. These inconsistencies were due to the switching of the injection valve as well as the bubbles that formed in the system. An example is illustrated in Figure 3-38 where the flow rate is altered during the injection operation by the autoloader. A low level signalling process could warn the integrated software of the pending injection in order to mitigate the effects. One way to do this might be to depressurise the liquid in that line which will drop flow to zero if there is no back pressure.

The issue of bubbles severely hampered the data collection process. Efforts to mitigate this by application of high back pressure and extensive cleaning procedures were largely unsuccessful. This bubble nucleation issue was mitigated by the use of tubing with larger tubing diameter (d = 0.3 mm). It is believed that this dimension allows the bubbles to stay stationary on the tube walls while allowing liquid to flow past it. The smaller diameter tubes (d = 0.15 mm) forced the bubbles to flow with the liquid causing massive spikes and drops to concentration at the water/fluorescein interface from the lack of dispersive effects.

Doing this may prevent this switching operation from interfering with the interface setup in the microfluidic device.

Flow injection systems that use contact sampling can result in cross-contamination from the use of the same sampling needle for various agonists (Dunn and Feygin 2000, Doktycz, Johnson et al. 2004, Halldorsson, Lucumi et al. 2015). This is especially problematic where the experimental process is highly sensitivity (Cunningham 2001).Undesirable dilutions may occur during sample uptake that affect the desired results. This cross-contamination will obviously increase over time for lengthy experiments. Finally, it may be desirable to load multiple agonists in quick

succession but this option is limited by the autoloader's rigid operational sequence. It is not possible to load multiple agonists serially into the reservoir before injection.

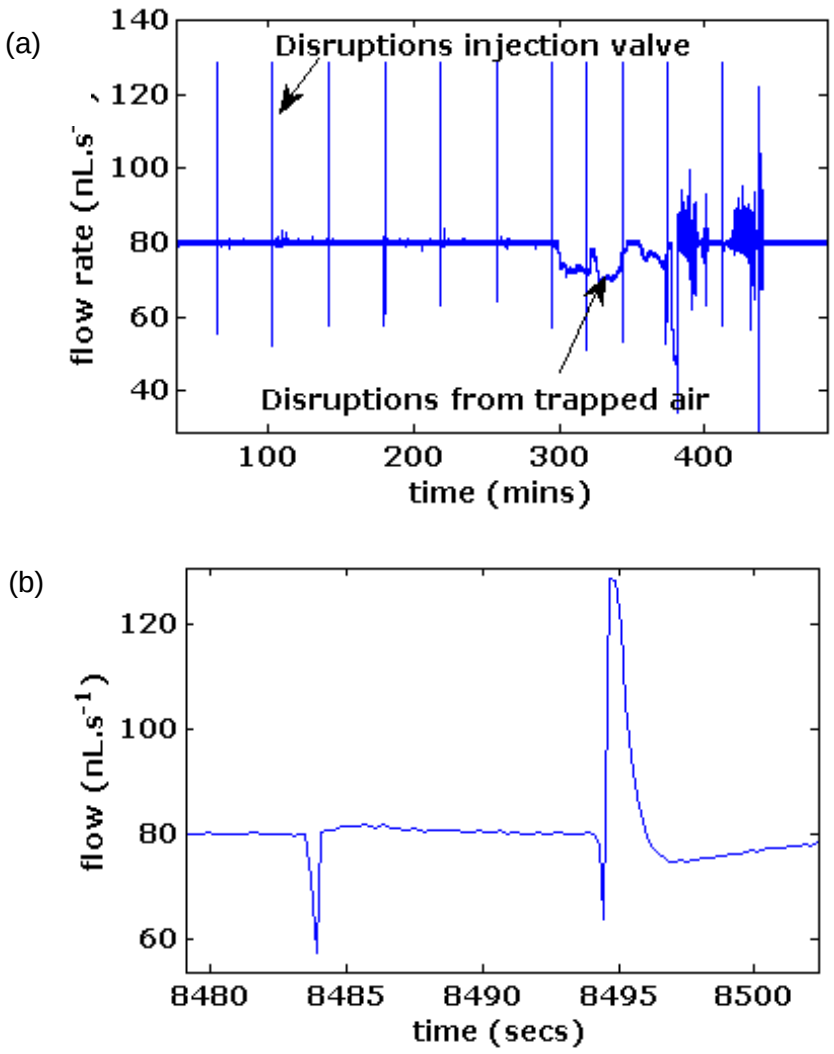

Figure 3-38: Flow disruptions from injection and bubbles
(a) The trapped bubbles in the system are typical of microfluidic liquid handling but more so prevalent with the injection valve. Some air volume may become trapped in the system after injection and continues to cause flow variations since the pressure increases to compensate for the fluid capacitance in the flow line. The injection process (b) is twofold: the first occurs when the autoloader syringe has loaded the volume into the primary reservoir. The second occurs after the volume has been loaded into the HP valve reservoir. These variations are caused by temporary lack of opposing pressures across the flow line.

3.10 Discussion

The liquid handling requirements have been established for liquid transport and liquid loading applications. A stable liquid transport controller is required to allow consistent performance in microfluidic applications like long-term delivery of media and drugs to cultures within microfluidic environments. This in addition with rapid control system would allow applications like interface shifting, rapid drug signalling and could be combined with an external liquid loading system to allow these applications with varied drug inputs. The limits to the existing liquid transport system were assessed and an optimisation process was undertaken. Preliminary checks on the low level performance of the established pneumatic pressure controller and the control operation revealed expected performance expectations. PID control algorithm optimisation only improved the performance but did not offer consistent performance across the desirable pressure target range of 0 to 250 mBar. It was discovered that a faster response time from the data acquisition and control system was required to achieve the desired system performance. A sub-second switching time was achieved by increasing the data acquisition and control rate. The increased ability of the control system to quickly respond to changes in the system while comparing it to the target changes improved the performance of the flow control system.

This result presents an opportunity for the developed liquid handling system to be applicable to the target applications for media and drug transport and rapid signalling. This is beneficial to the wider microfluidics community that seek similar solutions that allow rapid control. Example applications such as rapid drug switching, concentration gradient generation and interface shifting were demonstrated with the improved liquid transport system. The application of the gradient shifting was demonstrated in an application with collaborators and is described further in the Applications Demonstration section of this thesis.

An autoloader was also characterised to enable liquid loading system for microfluidic applications. The device accuracy and precision were characterised and the effect of Taylor Dispersion on peak concentration of drug loaded was demonstrated using Fluorescein concentrations. This effect was characterised for varying tube lengths and flow rates which did not significantly affect the peak concentrations obtained. The biggest influence to peak concentration obtained was found to be the volume of the drug loaded. This will influence the operation of the liquid loading system as more drug volume will need to be loaded to achieve a target drug concentration at the microfluidic device. An expected outcome that the autoloader did not integrate well with the liquid transport system was described the limits to the autoloader use. The recorded limits and benefits from its use will inform on requirements for a suitable liquid loading system that can be applied to developing microfluidic applications for cell cultures in Life Science reseach.

4. Gatling-styled Sequential Injection System - GSIS

The development of an automated liquid handling system for microfluidic applications aimed to develop flow control and liquid injection systems that could be integrated to realise liquid handling applications within microfluidic devices. A commercial autoloader (Jasco) was investigated as a macro sized liquid handling system solution for the liquid loading requirements. The commercial autoloader used is limited in volume range allowing 1 – 100 uL volume injection. It does not allow volume sampling from the microfluidic device since this requires deterministic operations that are facilitated by low level sensing and control of the autoloader equipment which is unavailable. Flow and pressure inconsistencies during column switching operations are undesirable since they have the potential of disrupting the cell environment during the switching operation. Sample carry over from use of the same needle for multiple sample uptakes is also a challenge. It also does not allow for automated control of multiple serial liquid loading operations within the same drug plug to be delivered to the microfluidic device.

A design process was carried out towards the development of an alternative liquid manipulation system that could improve on the short comings of the commercial system by allowing deterministic control of the liquid injection operations as well as allow volume sampling downstream of the microfluidic device. This chapter discusses the design and development process for a macro-sized off-chip sequential fluid loader with an operation that is characteristic of the Gatling gun developed by Richaed Gatling (Gatling 1862), hence, the name. It was expected that the Gatling-styled Sequential injection system (G-SIS) could be designed and fabricated as a simple device that would mitigate the problems with the loader and be capable of liquid sampling downstream of the microfluidic device.

The G-SIS is developed as a modular add-on to liquid flow control system to facilitate answers to questions about information processing in the brain using simple

microfluidic technology. Device operation transparency was a requirement to ensure that the cells do not respond to physical changes in the flow pattern brought about by abrupt pressure changes as experienced with the commercial autoloader. This design constraint also informed the design process which included problem definition, solution design, prototype fabrication, prototype analysis and improvement, and finally product development. It was expected that a successful design process would result in a product of high research interest and commercial value due to its potential for high impact within the immediate research laboratory and the wider field of microfluidic liquid handling systems.

4.1 Design Process

The problem defined was the requirement of a modular liquid handling system that was capable of sequential injection and sampling in and from a microfluidic device. A sequential flow injection system was proposed to solve this aspect of the liquid manipulation problem as the liquid transport system was fully functional. The sequential loading/injection system, illustrated in Figure 4-1, was designed to:

- allow loading/sampling from the microfluidic device
- improve the dynamic range of the volumes that could be loaded to the microfluidic device
- mitigate flow inconsistencies
- allow tighter controls and signalling of the low-level functions and commands

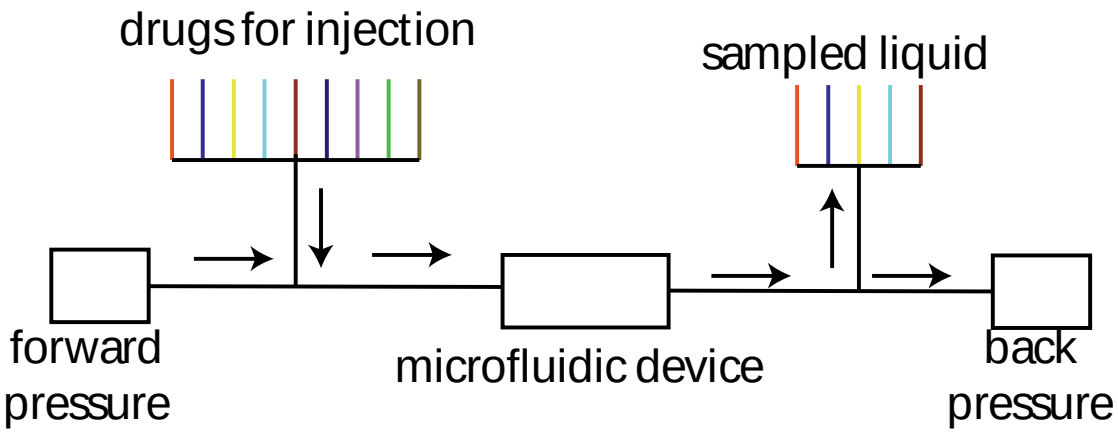

Figure 4-1: High level System Architecture for Sequential Injection and Sampling
The forward pressure and back pressure systems form the liquid transport mechanism to enable forward flow. The sequential delivery system will allow drugs be injected into the flow line to the microfluidic device while the sampling system will allow the content of the flow line to be sampled for collection and off-site analysis or sampled into a connected analytical system.

The system design in Figure 4-1 illustrates the upstream volume introduction system and downstream volume sampling system. The volume introduction system comprises volume sampling and liquid injection. The sampling process loads the drug samples from containers into a temporary reservoir while the injection system allows the temporary reservoir to become in line with the primary flow path to allow the primary liquid flow transport the contents of the reservoir to the microfluidic device. The downstream sampling operation is slightly different with a switching and collection operation. The switch diverts the flow path of the target volumes from the microfluidic device towards a collection vessel. This would then be manually picked up by the user. The possibility of replacing the manual sample pickup process with an analytical station has been adopted.

The proposed system is an interchangeable device that could perform either injection or sampling depending on where it was placed in the integrated system architecture. The concept of the designed system sections is illustrated in Figure 4-2. Liquid reservoirs are loaded with volumes from the sample introduction system when they are aligned with the loading orifice. These reservoirs are then mechanically shifted to a position where the stored liquid can be ejected from the reservoir by the carrier liquid. The continuous operation will allow arbitrarily large volumes to be loaded,

satisfying the requirement of enabling large volume injections. The lower limit of the range of volume sampling is determined by the volume of the reservoir and is discussed in the Volume Injection section.

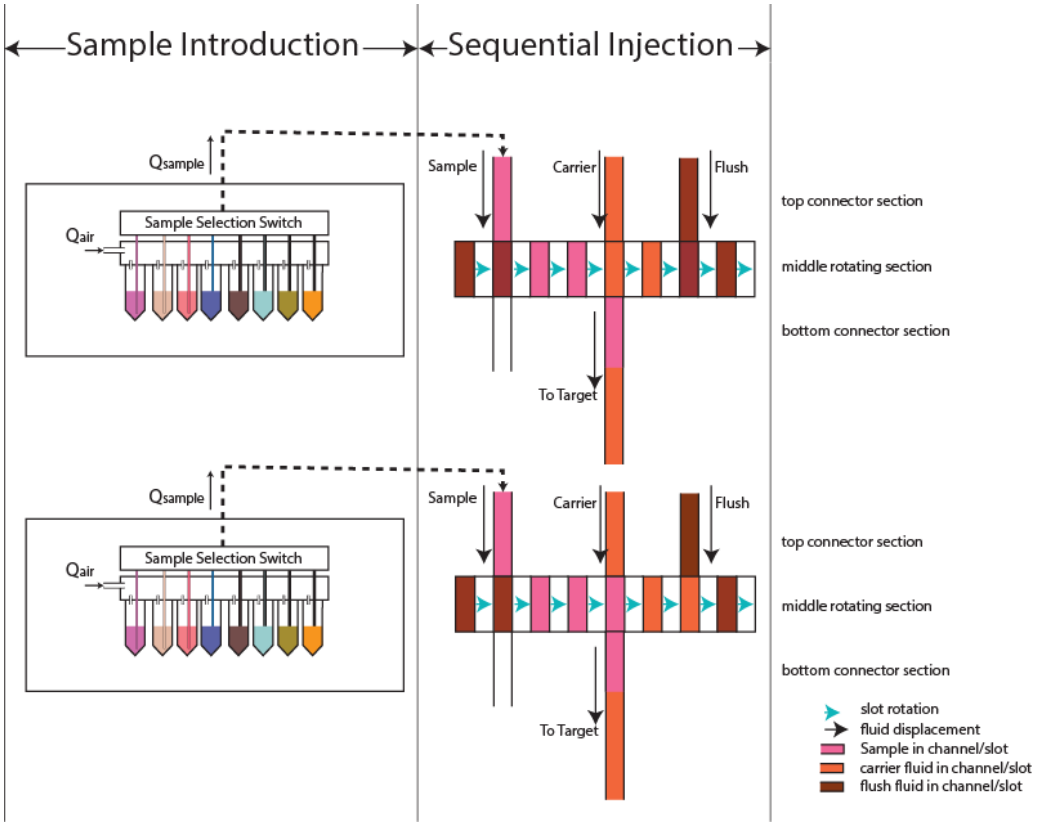

Figure 4-2: Figure of operational schematic of G-SIS system
The sequential injection system is split into the sample introduction and the sequential injection sections. This design uses compressed air to pressurise sample containers that force the liquid in the activated sample container to flow into the sequential injection section.

4.2 Volume Sampling

The design process resulted in the volume manipulation system operation split into volume sampling and injection mechanisms. Precise volume loading, minimal dead volume and operation simplicity are key requirements of the volume sampling system. One is the use of an array of syringe drivers all containing the different drugs to be loaded. This solution does not scale well since every drug must be loaded in a separate syringe driven with a separate driver. Another potential solution is the use of

pressurised air to displace the liquid. The compressibility of air makes this a non-linear solution and a feedback system incorporating flow sensors will be required to achieve higher precision. The addition of flow sensors for each drug that can be loaded (Yaxin, Chen et al. 2009) is not a scalable solution and simpler solutions are required.

Figure 4-3 illustrates a simple method to realise volume sampling where a pressurised fluid such as air is used to pressurise selected sample containers. Microvials are used as volume containers to hold samples that will be loaded into the injection system. The ease of access to microvials makes them ideal liquid containers for volume sampling. A syringe driver can be placed at the sample sampling system output to further achieve accuracy and precision in the sampled volumes. Syringe drivers or nano-dispensers are options that can be implemented to realise this simple solution and are investigated further.

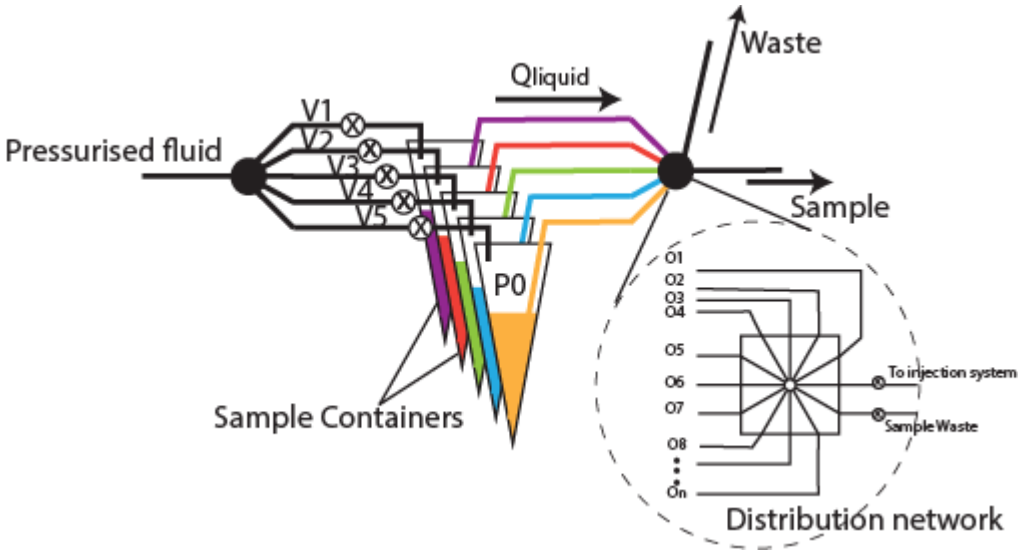

Figure 4-3: Volume sampling with pressurised liquid
The pressurised fluid (air or oil) could be transported into the sample containers to pressurise the containers and allow the liquid to be sampled through a distribution valve to the injection reservoir. Valves (V1 – V5) can be used to allow or stop flow in any target flow path.

4.2.1 Syringe Dispensing

The syringe driver direct volume displacement method directly displaces the volumes in the sample container using an immiscible liquid like oil as the displacing fluid as illustrated in Figure 4-4. Sample vials of volume (500 μL) are fitted with a PDMS cap punched out of a bulk piece of cured PDMS with thickness (2 mm). The conformal nature of PDMS allows them to fit tightly as microvial caps for liquid displacement.

One consideration for the use of oil for fluid displacement is the risk of oil contaminating the sampled liquid transported to the cell culture. Another consideration is the increased complexity imposed on the user due to oil handling requirements. Experiments to determine the toxicity of the oil used to neuronal cell cultures have been performed to better assess the suitability of this syringe driving method for sample introduction.

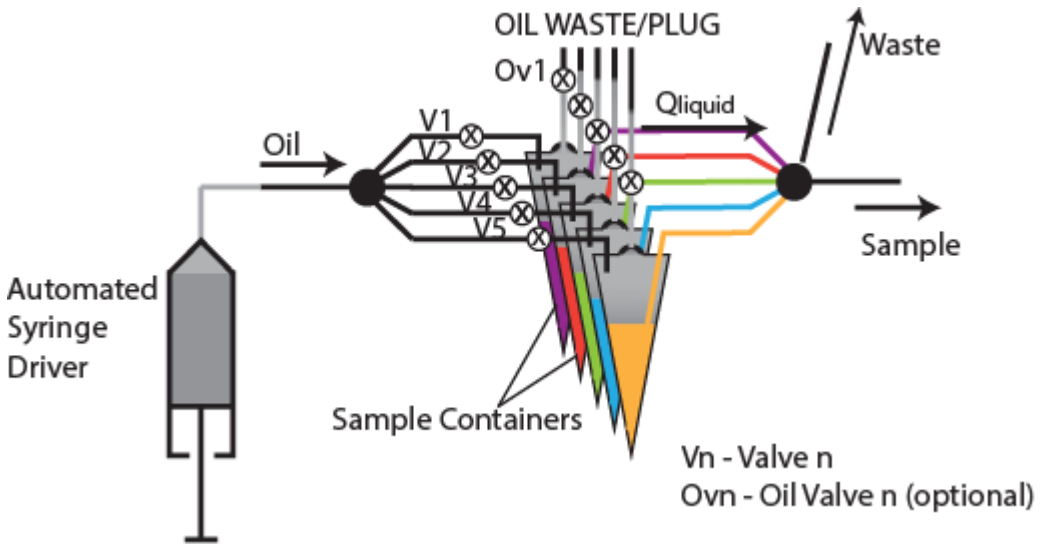

Figure 4-4: Syringe driven oil displacement for sample introduction
The syringe driven oil displacement for sample introduction was designed as a liquid sampling part of the novel liquid injection system. This would employ lab grade micro vials as sample containers for agonist loading into the flow path for injection.

4.2.1 Nano-Volume Dispensing

Nano-volume dispensing was also investigated as an option to achieve sample introduction for liquid handling. This concept has been applied in a system for nano dispensing (Haber, Boillat et al. 2004) where the volumes were checked using a custom built flow sensor while dispensing the specific liquid. The overall architecture illustrated in Figure 4-6 adopts the technique used. Compressed air of known pressure is used to pressurise the sample containers. These are then connected inline to a inject dispenser (Lee) that is capable of dispensing very small volumes (~50nL) per pulse when actuated. This valve in combination with a flow rate sensor would enable precise volume loading since the control can automatically stop the valve actuation in response to the delivered volumes recorded by the flow rate sensor. However, it may be impractical to have one flow sensor per drug loaded and the flow rate sensors can be placed at the sample output since every sampled volume will go through that output. This will ensure precision and accuracy in volume sampling but will increase the volume between the sampling system and the volume injection system. An open loop control must be established to allow liquid loading operations in cases where the flow sensor is not an option. Experiments have been performed to show the variability of the Lee valves when in open loop pulse control.

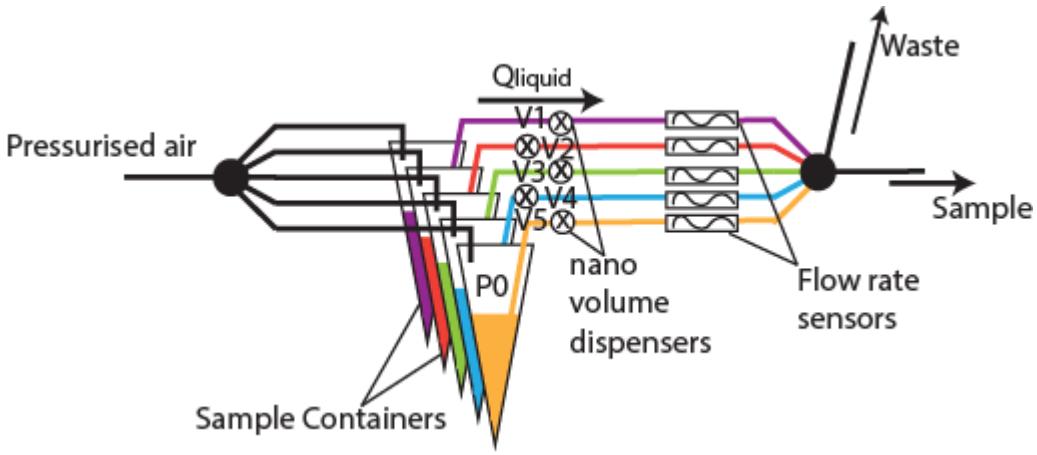

Figure 4-5: Flow confirmed nano-volume dispensers
The use of nano-volume dispensers for volume dispensing has been demonstrated (Haber, Boillat et al. 2004) with the implementation of flow sensors. Here these flow sensors will detect the loaded volumes and pass that information to the software for liquid injection. This will perform volume tracking operations to ensure that exact volumes are dispensed for injection.

4.2.2 Volume Sampling Tests

4.2.2.1 Oil Toxicity Tests

The use of oil as a transport fluid of desired nutrients, drugs or reagents was presented for use in volume sampling operations in the Gatling liquid loading system. It was critical that the oil does not contaminate the volumes loaded leading to detrimental effects in the cells. As such an experiment was carried out to assess the effects, if any, that such oil operation would have on cells.

Sterile mineral oil (sigma Aldrich, M-5310), sterile olive oil (sigma Aldrich, O1514), Media and cortical cells were used in these experiments. A preliminary check was done to identify the worst case scenario when users handle a vessel with oil-over-media liquid contained. It was found that vibration from dropping or mishandling of an oil/media 2-phase liquid solution was possible. Mineral oil was sonicated with media in one centrifuge tube while another centrifuge tube was tilted on a tilt machine. The liquids were well mixed in the sonicated version and remained cloudy and was not used but the liquids remained as two-phase liquids in the tube that was tilted. However, these conditions did not represent real life cell biology prep conditions where physical handling is performed with caution.

The experiment carried out to quantify the number of cells in the well plates at 1DIV, 5DIV and 9DIV was performed by plating twelve well plates with cells and using media with different realistic contact conditions with mineral and sterile oil.

Four well plates were plated with the same cells and exposed to media that had previously been in contact with mineral oil in a centrifuge tube vessel. The tube was kept stable during the contact period and the media was extracted through a hole made at the bottom of the tube.

Another four plated well plates were exposed to regular media and then topped with oil to completely seal the media layer over the cells. This was to simulate conditions closer to that expected during the operation of the Gatling liquid loader.

A final set of well plates were exposed to plain media without any oil interaction and used as control.

Figure 4-6 shows example images of cells at 1 DIV and 5 DIV that do not visibly show detrimental effects from oil contact with the media used.

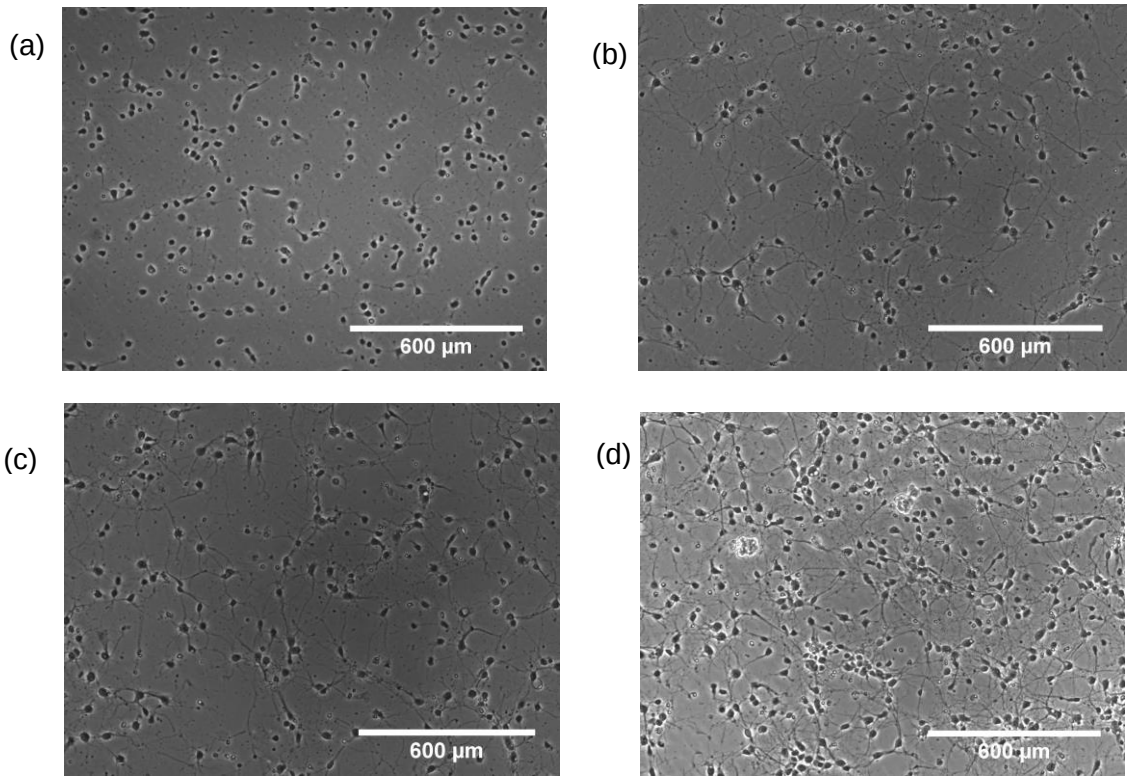

Figure 4-6 oil toxicity results
Media used to plate cells in polystyrene well plates were exposed to oil at different conditions. (a) and (b) shows x10 images for 1DIV and 5DIV respectively for the control experiment where no oil was added. (c) and (d) shows x10 images for 5DIV when the cells are plated with media previously exposed to mineral oil and olive oil respectively.

Bright field images were captured with a point-grey grasshopper2 camera on a Nikon microscope with magnification 10x. Three images were captured per well and six

regions of interest (ROIs) with size (l x w = 0.72 x 0.72 mm; a =) were defined per image for image analysis in Fiji image processing software to detect the cells in each ROI.

An image threshold was set to subtract parts of the image below a set greyscale value limit. This retains the nucleus in the image as black spots over a white background. Particles are analysed to count the number of cells by defining the cell size range as (0.0002 - 0.0004 mm^2). A macro was written to automate to process of threshold, ROI and particle analysis definitions for 48 images. Figure 4-7 shows an example image in (a) with the threshold applied in (b) and the macros written to automate cell counting process for images. Additional lines, not shown were added to cycle through the images stored in a specified directory.

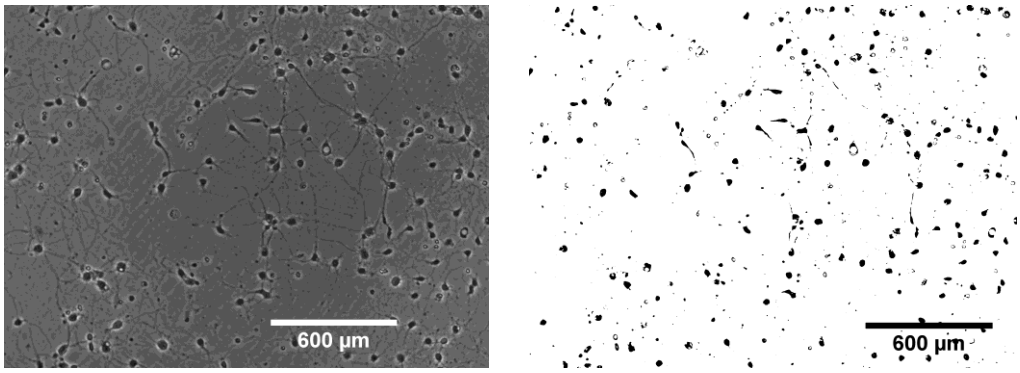

(a) (b)

```
setAutoThreshold("Default");
//run("Threshold...");
setThreshold(0, 50);
setOption("BlackBackground", false);
run("Convert to Mask");
//run("Close");
makeRectangle(18, 10, 600, 600);
run("Analyze Particles...", "size=100-300 circularity=0.00-1.00 show=Nothing clear summarize");
makeRectangle(654, 10, 600, 600);
run("Analyze Particles...", "size=100-300 circularity=0.00-1.00 show=Nothing clear summarize");
makeRectangle(1286, 10, 600, 600);
run("Analyze Particles...", "size=100-300 circularity=0.00-1.00 show=Nothing clear summarize");
makeRectangle(18, 778, 600, 600);
run("Analyze Particles...", "size=100-300 circularity=0.00-1.00 show=Nothing clear summarize");
makeRectangle(654, 778, 600, 600);
run("Analyze Particles...", "size=100-300 circularity=0.00-1.00 show=Nothing clear summarize");
makeRectangle(1286, 778, 600, 600);
run("Analyze Particles...", "size=100-300 circularity=0.00-1.00 show=Nothing clear summarize");
close();
```

(c)

Figure 4-7: Cell counting image analysis in Fiji
An example image for analysis is shown in (a) and the result of the threshold adjustment for the image is shown in (b). The macros for automating the process is shown in (c). The script defines the values that successfully extracts the background from the cell nuclei resulting in (b). The "analyse particle" plugin then detects the number of particles of defined size (0.0002 - 0.0004 mm^2) and saves the results in a summary chart that can be exported.

4.2.2.2 Nano-Volume Dispenser Characterisation

The LEE valves nano-dispenser was used to dispense distilled water from a pressurised liquid vessel (Duran 100 mL). The liquid vessel was pressurised with an operating pressure (P0 = 200mBar) and the setup is illustrated in Figure 4-8.

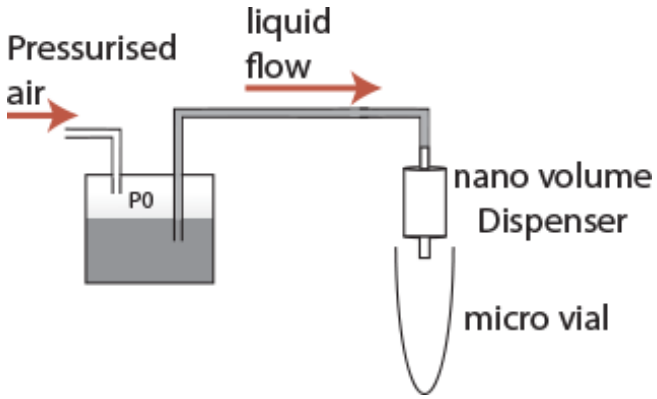

Figure 4-8: Experimental setup to validate dispense volumes under different conditions
The nano-volume dispenser uses a LEE valve that dispenses as low as 50 nL volumes per actuation. This dispensed volume depends on the pressure in the reservoir as well as the fluidic resistance in the flow path. Pre-calibration can be done to identify volumes per pulse for a given system condition and then used to deliver the volumes without a flow sensor. This experiment actuates the valves with different pulses and then records the volumes after ten seconds to obtain the volume per pulse delivered.

The valve was positioned to dispense directly into a pre-weighed micro vial without additional tubing. PWM signals with duty-cycle (d = 2%) and frequency (f = 100 Hz) were delivered to the Spike and hold circuit for a duration (t = 10 secs) using a function generator.

The volume of distilled water dispensed by the valve for the period was weighed and the volume was calculated by assuming density of water (ρ = 1mg/ml). The process

was repeated to obtain a sample size (n = 10) to quantify accuracy and precision. The experiment was performed for different duty cycle settings (d = 2.5%, 5%, 7.5%, 10%, 12.5%, 15%). The experiment was then performed for different input pressures (P_{in} = 200, 400, 500, 600 mBar).

In another experiment, a flow rate sensor was connected in-line with the dispensing valve and the control signal to the dispensing valve was regulated by a control logic written in LabVIEW programming interface. This control logic was set to integrate the measured flow rate over time and stop actuating the dispensing valve when the target flow rate was reached. This was done over a range of volume dispensing targets from 10 µL – 100 µL.

4.3 Volume Injection

The concept for a system capable of continuous liquid injection and sampling in Figure 4-2 is comprised of the sample introduction and the injection aspects where the top connection layer serves as the liquid introduction and the middle layer acts as the injection into the flow line. This sequential system schematic designed for the G-SIS and the operation concept of the injection operation is illustrated in Figure 4-9.

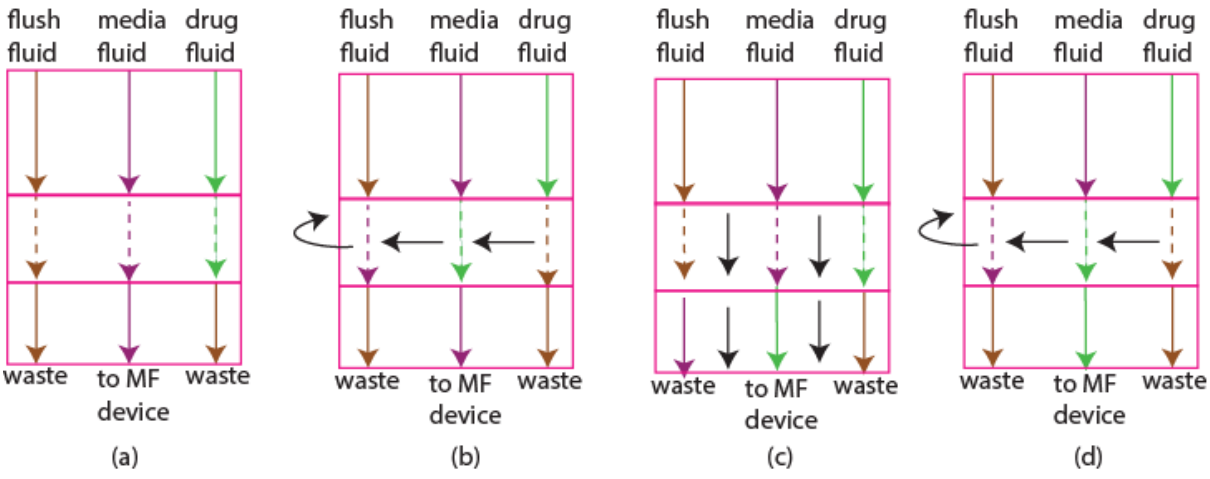

Figure 4-9: Operational schematic of sequential injection
The reservoir is moved to displace the direct of the loaded volumes into a microfluidic (MF) device. A rotating disc housing these reservoirs will ensure continued alignment of the reservoirs with interfacing connections.

A switching mechanism was required to enable the rotation of the reservoir. The choice of a switching mechanism was in tandem with the choice for an appropriate reservoir design that will allow a wide dynamic range of loaded volumes as well as high accuracy in loading. Flow consistency was also factored in the decision process and commercially available liquid switching mechanisms (Rheodyne) were briefly investigated for use in the G-SIS.

Figure 4-10 shows two options for loading with one reservoir and two reservoirs. If one reservoir is used, it must be capable of holding the range of volumes specified in the design criteria which in this case is arbitrarily large. The second option of two (or more) low volume reservoirs can be used to provide high resolution of injected volumes. The alternating switch between the two reservoirs will also make for the possibility of loading much larger volumes as long as one reservoir is refilled while the other is being emptied. A make-before-break switching mechanism was also adopted to isolate the switching process and maintain flow consistency. Both operations are illustrated in Figure 4-11. One flow connection is made before the previous connection is broken. The

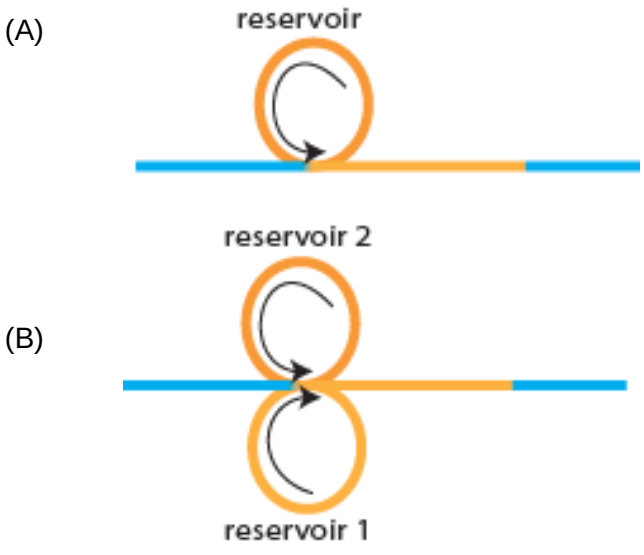

Figure 4-10: Single and dual reservoir switching.
(a) A single reservoir is loaded with the sample before inserting the contents to the flow line
(b) Two reservoirs are loaded in sequence and a switch alternates between them to insert the contents into the flow line.

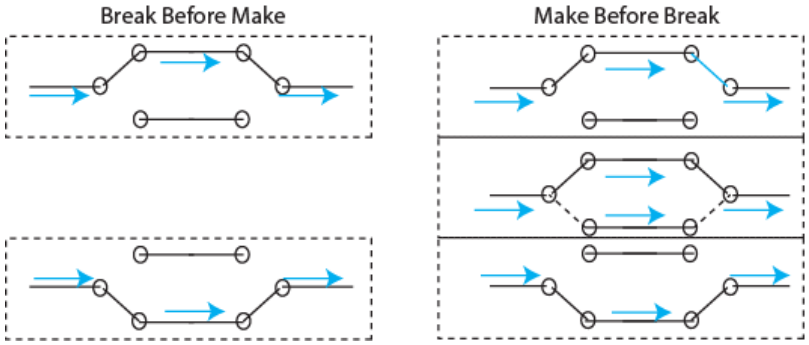

Figure 4-11: Break-before-make and make-before-break switching options
The make-before-break switching system prevents flow disruptions during switching since another flow connection is made before the previous one is broken (right). This offers the advantage of steady flow over the break-before-make system (left)

The Rheodyne make-before-break injection valve was identified as a good fit for the GSIS system in terms of its flow consistency during switching but were limited to an alternating switching motion. This was not adequate for the designed system since volumes will could only be loaded in one position. It also meant that the output only one single reservoir could be used which would further delay the loading operations. This prompted the design of a custom switching mechanism that would enable the use of multiple reservoirs.

The design process then proceeded with development of operational and design schematics with extensive review of the required components which resulted in a version 1 of the G-SIS switching system and subsequent iterations.

4.3.1 Operational and Design Schematics

Extensive design schematics were made in CAD before each iteration of the G-SIS system to ensure that the system met the design constraints. Operational schematics were made as illustrations where necessary to illustrate the operation of that design

iteration. Two versions were developed, designed and fabricated for testing – a through-hole switching system and a surface mount reservoir switching system.

4.3.2 Through-Hole Injection System (Version 1)

A through-hole rotor version of the injection section of the G-SIS has two stationary connector blocks (stators) which allow for connections and a rotating disc (rotor) in the middle of the blocks with holes which act as reservoirs. This design is illustrated in Figure 4-12. The lateral view of the G-SIS switching component in Figure 4-12a shows the side view of the component parts and connections. Figure 4-12b shows the top view of the rotating disc with the sample introduction viewed as from the side. The disc size, port dimensions and angle between the holes shown in Figure 4-12c are based on initial design constraints

a

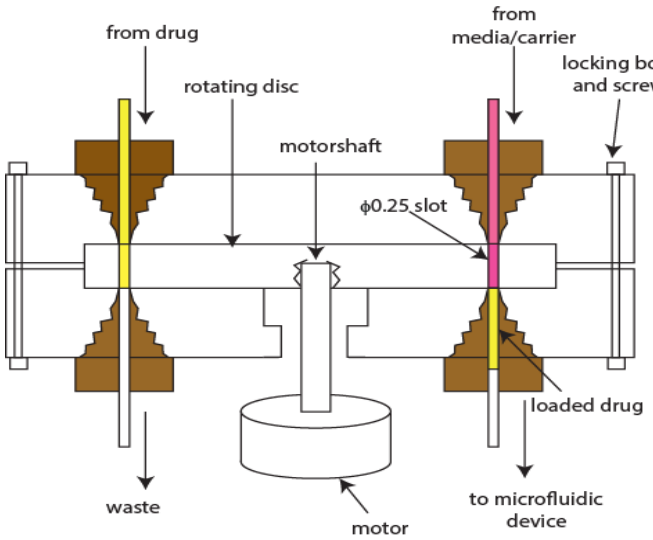

b

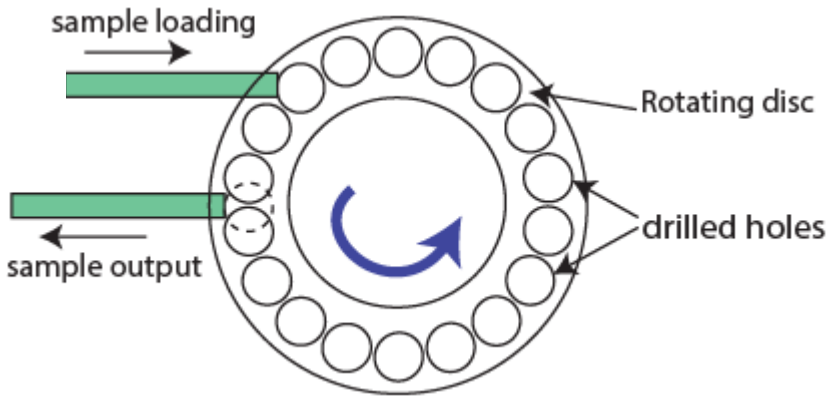

c

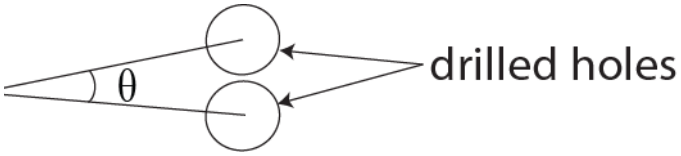

Figure 4-12: Rotating slotted disc for switching mechanism
a) Lateral view of G-SIS switching part with primary and sampling connections
b) Cross section of rotating disc with inlet and outlet
c) Angle θ between the holes in the rotating disc.

During a loading operation, each hole will be filled with the sample when the reservoir is at the filling position. The disc then rotates to enable another reservoir be filled by the same sample. This continues until the total volume loaded is equal to the target volume required while, at the same time, the volumes are ejected from the reservoirs when they arrive at the output connection.

The system operation was designed such that the reservoir would be filled when directly aligned with the connection orifice but the ejection would occur continuously while the disc rotates the reservoir into the connection orifice and out of the orifice.

A reservoir diameter (d= 0.5mm) was selected to provide small reservoir volume (~200 uL) per mm disc height for scalable reservoir volume while a small reservoir height was desirable for high resolution volume injections ~1 μL per 5 mm ($v= \pi d^2 h/4$). The disc height of 5 mm was more realistic to enable a good articulation with the rotating motor shaft.

Figure 4-13 shows a computer-aided design (CAD) for a prototype of the G-SIS switching component. The top part has connectors for the flush liquid drug loading and carrier fluid inputs. The middle section has several holes drilled in a rotating disc that align with the top three connections. The bottom piece has the connections to the microfluidic device. The next step in the design process established a good starting point as a prototype to establish viability in the initial concept.

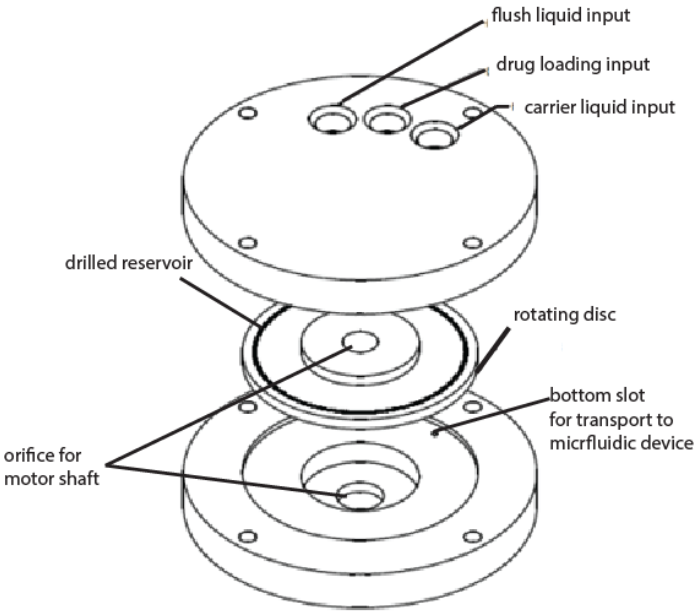

Figure 4-13: CAD schematic of version 1 G-SIS switching component without connections
The designed prototype presented machining issues and risk of damage to the rotating disc from the combined effect of compression of the disc to prevent leaks and rotation of the disc for reservoir switching.

The prototype for through-hole version of the G-SIS was designed to quickly identify ideal material, and potential issues with machining and risk of damage to the rotating disc. Leakage in the prototype was expected to inform future decisions. The prototype was built with similar through-hole dimensions (d = 500 μm, l = 1 mm) for a 196 nL volume in the reservoir.

Materials shortlisted for use in the design were based on expert recommendations from machining and process technicians and engineers. PEEK (Polyether Ether Ketone) plastic, Stainless Steel, and UHMWPE (Ultra-high-molecular-weight polyethylene) plastic were recommended for use. These recommendations were based on properties like material's availability, cost, strength, chemical resistance, and thermal expansion of the materials while machining; and thermal response during operation. These materials are highly resistant to most chemicals hence the use of Stainless Steel and PEEK for tubing in commercial autoloader devices used in analytical chemistry. UHMWPE has been used for medical devices due to its high

strength and is especially good for applications with rotating surfaces due to its self-lubricating properties (Liu, Wu et al. 2006, Sui, Zhong et al. 2009). Stainless steel is more expensive than aluminium but is stronger. Its strength was deemed more critical to ensure long term operating lifespan. Even force distribution across the disc is guaranteed with stainless steel since it is less likely to deform compared to aluminium.

The machining process may cause undesirable effects causing some materials to burr, soften, deform, and even melt. High pressure between the connection blocks on the rotor was required for leak free operation and the deformation of the material used as a rotor was considered. The expert advice available from the machining technicians was invaluable since these properties could not be quantified within the research environment. Teflon was more susceptible to burring during machining

Figure 4-14 (a) shows a CAD design of the prototype that was fabricated in stainless steel, Ultra-high-molecular-weight polyethylene (UHMWPE) and PEEK to assess the machinability of these materials and the possibility of liquid flow in the small reservoir. Figure 4-14 (b) shows the result of the prototype fabrication in PEEK material.

(a)

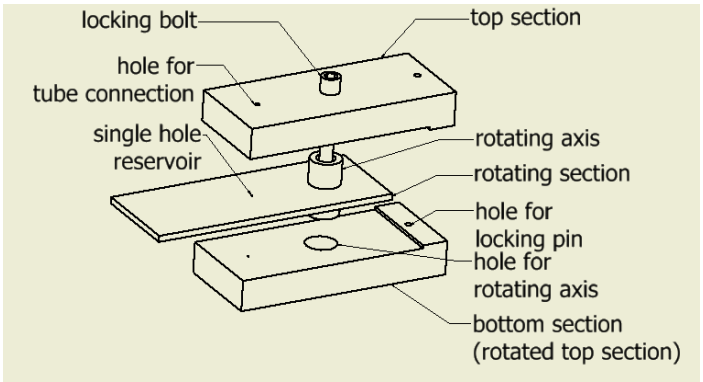

(b)

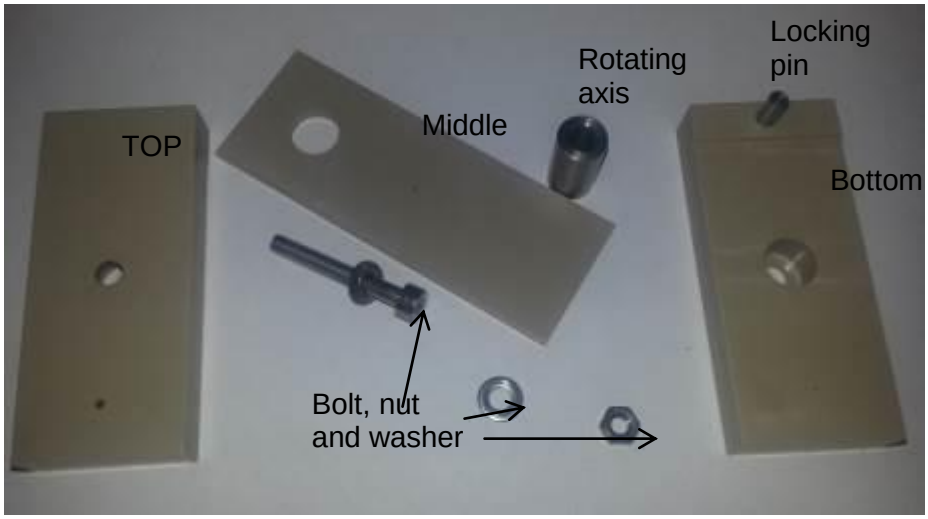

(d)

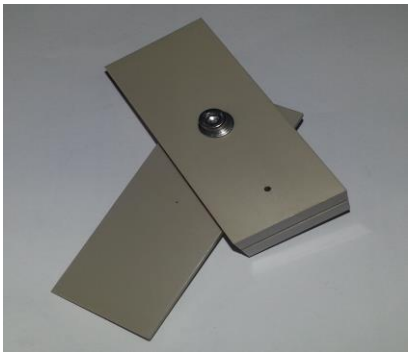

(c)

Figure 4-14: Prototype of G-SIS version 1
The prototype was designed to test the fluid flow capabilities in the small hole drilled in the precision workshop. The top, middle and bottom parts in (a) were machined in three materials to test the machinability of these materials and the quality of the finished product (b). (c) and (d) the rotating axis allows the centre section to rotate out of the way.

4.3.1 Surface Mount Injection System (Version 2)

The through-hole system design was seen from the prototype to be incapable of realising liquid injection goals. A rethink of the injection system design was undertaken subsequently. The through-hole reservoir design was replaced with a surface-grooved reservoir design. CAD designs and illustrations of three versions of the surface-grooved reservoir are shown in Figure 4-15 as type 1, type 2 and type 3. A larger reservoir size was designed as a prototype to mitigate the capillary effects. This increased the reservoir volume (V = 3 μL) also reduced the resolution possible.

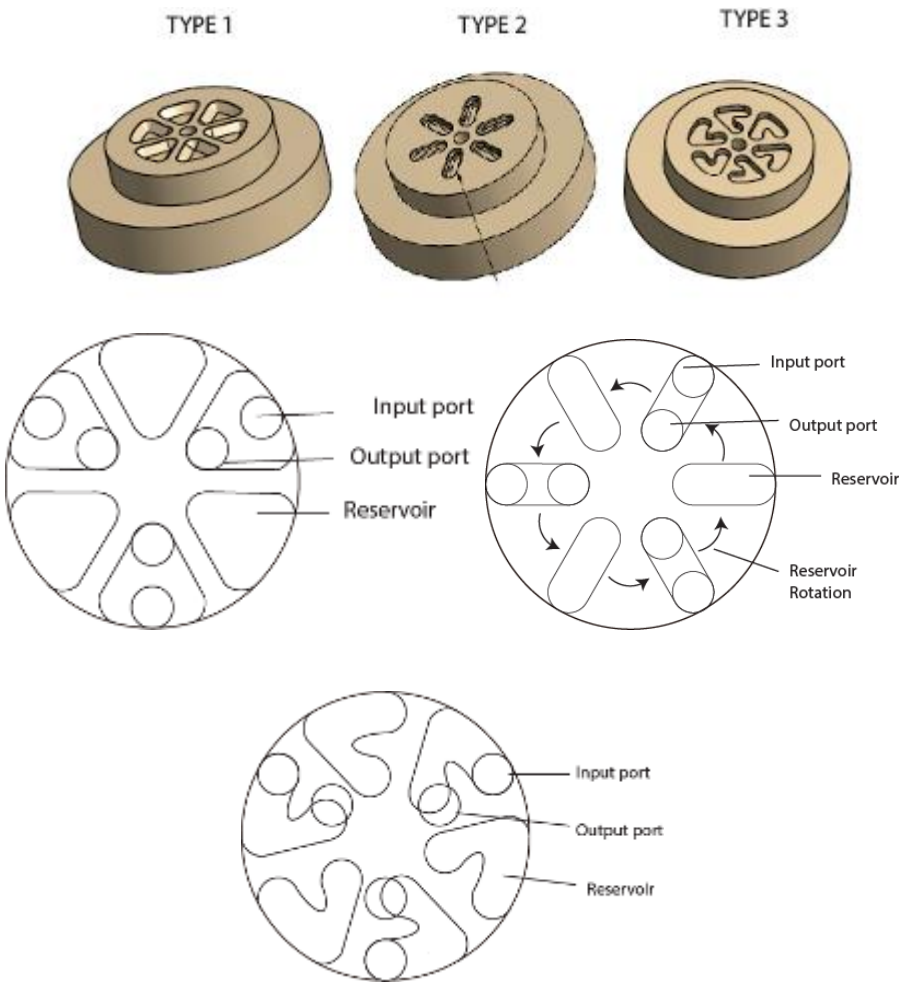

Figure 4-15: CAD designs and illustrations of the 3 rotors for development of G-SIS version 2
The new designs were developed to enable liquid injection with some emphasis on non-disruptive flow. Two of the rotors (type 1 and type 2) allow non-disruptive flow since the reservoir makes a new connection with the next input and output ports before disconnecting from the previous one during rotation. Type 2 is more similar to a Rheodyne injection rotor and was added to the design.

The designs for type-1 and type-3 were expected to enable make-before-break connection while type-2 was designed with a break-before-make connection. These surface-reservoir designs are similar to rotors present in the Rheodyne systems but are distinct in the number of reservoirs which allows continuous loading operations.

Rapid prototyping of the prototype was restricted by the precision machining requirements for the rotors. The University precision workshop was contracted to produce the PEEK rotors while the general engineering workshop was contracted to produce the steel stator, stator mount and bearing clamp. The face of the PEEK rotors and steel stator were passed through a grinding process for additional flatness

(<1 um). Burring in the PEEK reduced the ability to get very smooth feature size. The large physical size and the surface features prevented precise measurements of the flatness of the rotors and smoothed stator faces using optical methods like profilometry and AFM.

The fabricated pieces for the prototype was assembled and used to perform tests to characterise the leakage during static motion and rotation of the rotor while applying different torques to the screws for mounting.

The motor selection process was carried out by calculating the torque required to move a commercial Rheodyne injector valve. A factor of 4 was applied to that value and a motor was sourced (Nanotec) with that torque specification (T = 0.4 N.m).

An orthogonal view is shown in Figure 4-16 and a CAD cut-out of the assembled device is shown in Figure 4-17. A more detailed schematic is contained in the Appendices. Holes for “press-fit” tube connections were made in the stator. The holes connect to the reservoirs created in the rotor and are cut off when the rotor is rotated.

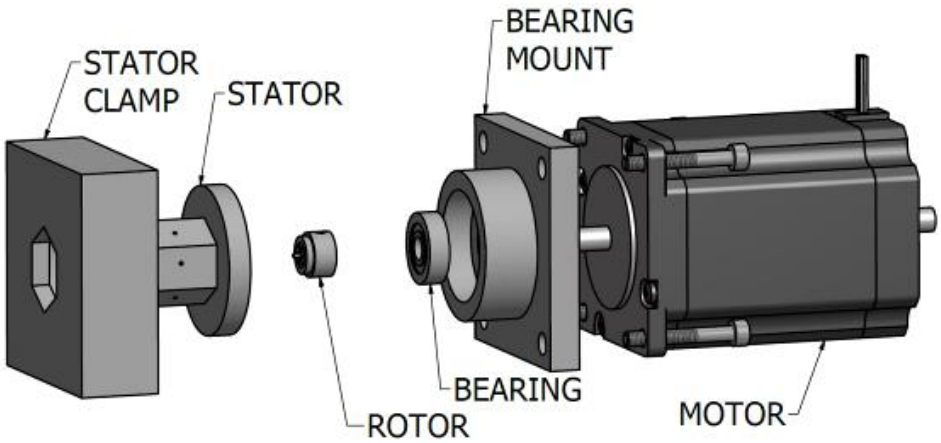

Figure 4-16: Orthogonal view of G-SIS with illustrated components.
The G-SIS was designed to act as a switching system to allow make-before-break connections or break-before-make connections using interchangeable rotors. This prototype reduces the space constraints required with the autoloader and, with modifications, allow an arbitrarily large volume to be loaded into the microfluidic device. The details on the parts are contained in the appendices.

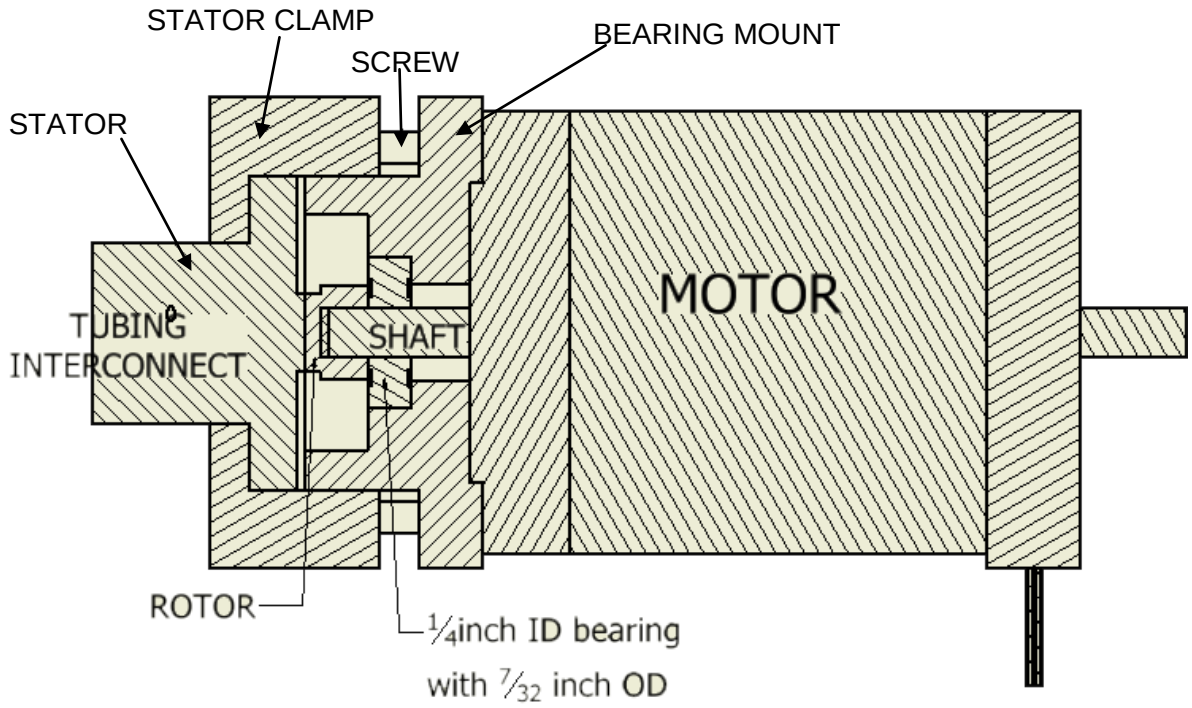

Figure 4-17: Final G-SIS design
The final design incorporated a stator, rotor, bearing and a motor stator. Precision manufacturing was required to fabricate the rotors. Details of the parts are contained in the Appendices.

4.3.2 Volume Injection System Tests

Characterisation of the liquid flow through the assembled prototypes was performed to check that liquid could flow through from input to output and to check and assess leaks in the system. Each prototype was connected with external hardware as described in Figure 4-18. A pressure regulator was connected to pressurise the liquid reservoir carrying liquid that will flow through a flow sensor to the prototype device. The output of the prototype device is connected through another flow sensor to a back pressure system. The leakage will be determined by the difference between the flow rate experienced at the output of the prototype and the input of the prototype.

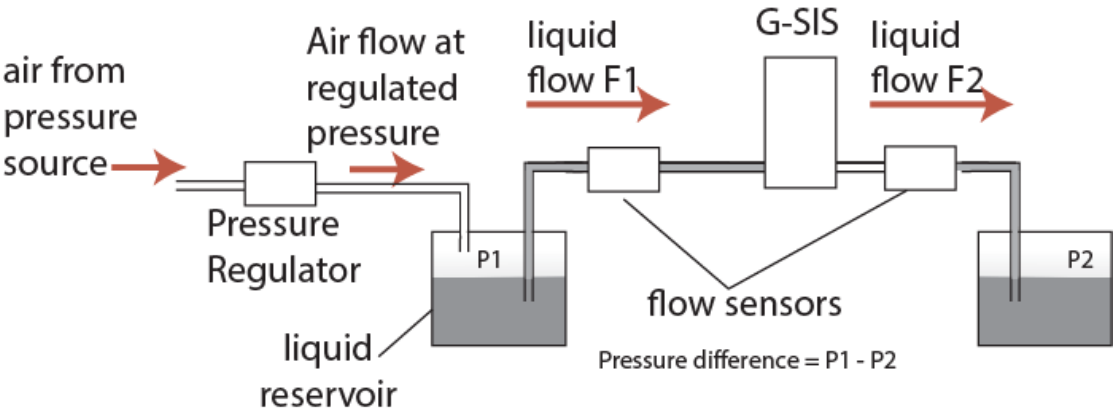

Figure 4-18: Illustration of connections to test liquid flow through orifice and leakage
The flow sensors measured flow to and from the device (F1 and F2 respectively). The leak is defined as the difference of these two flow rates and is found for different torque settings applied on the bolts on the system.

The through-hole prototype was assembled as in Figure 4-14 (c and d) and a tube carrying water was press-fit into the orifice in the top connection block. Another was connected in the bottom connection block. Both flow paths were connected through inline flow sensors with one of them terminating at a pressure vessel where a forward pressure (P_1) was applied to initiate liquid flow. The flow at the output was monitored for different pressure differences ($\Delta P = P_1 - P_2$) while keeping the back pressure constant (P_2 = 70 mBar).

The rotor for the surface mount prototype was positioned to align the device reservoir with the liquid entry and exit ports to allow liquid flow through the reservoir. This was done before assembly and the motor position was noted since it was not possible to view the reservoir once the system was assembled. The prototype screws were tightened to a set torque (T = 5, 10, 15 cN.m) while and a positive liquid flow was applied by pressurising the liquid in a Duran bottle. Liquid was pumped into the G-SIS with rotor type 2 configuration and flow sensors were connected to the input and output of the G-SIS connections as illustrated in. the flow was measured for varied pressure differences ($\Delta P = P_1 - P_2$) where the back pressure was kept constant (P_2 = 70mBar).

4.4 Results

4.4.1 Volume Sampling Results

4.4.1.1 Oil Toxicity Results

Toxicity tests were carried out to assess the suitability of sterile mineral oil or olive oil when brought in contact with media used to maintain neuronal cultures. Mean statistics of the data set of analysed images is shown in . The three conditions of the media are represented on the chart as control – fresh media with no contact with either oils; MOW – mineral oil over media; MMO – media extracted from mineral oil; and MOO – media extracted from olive oil. The horizontal axis show the days in vitro and the vertical shows the mean number of cells per 0.5 mm^2 area per condition.

The cells counted per 0.5 mm^2 area for the control were 17, 13 and 26 cells with standard deviation of 7, 7, and 10 for 1DIV, 5DIV and 9DIV respectively. This initial drop and then rise in mean number was also observed the MOW and MOO cell conditions with mean: standard deviation as (28, 18, 61: 10, 7, 17) for MOW and (31, 19, 32: 8, 8, 11) for MOO. The MMO condition did not change by much after 5DIV with mean: standard deviation as (13, 21, 25: 5, 10, 10).

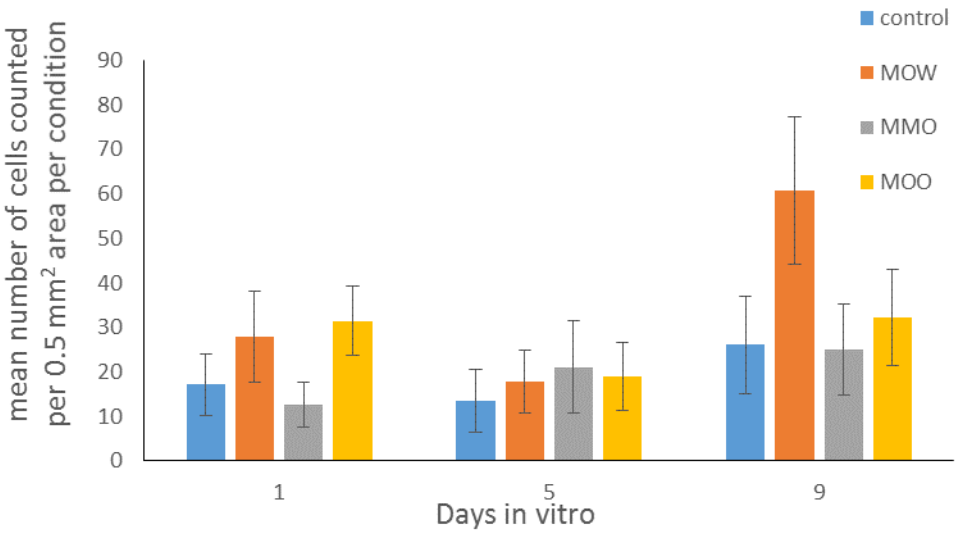

Figure 4-19. Mean Statistics of Automated Cell Count

The cell count data was analysed to obtain mean of the number of cells for the ROIs in the images. The mean number of cells for six ROIs per image was first obtained to get the number of cells per 0.5mm^2. These mean values per image were then averaged over all the images obtained (3) over the number of well plates per condition (12), to get the mean number of cells per 0.5mm^2 for the condition. This is presented in the histogram plot for all the conditions used (control – fresh media with no contact with either oils; MOW – mineral oil over media; MMO – media extracted from mineral oil; and MOO – media extracted from olive oil). A reduction in the number of cells counted between 1DIV and 5DIV is evident in the control, MOW and MOO cultures. However, these numbers improve at 9DIV but with the MOW culture recovering faster than all others. This similarity in behaviour shows that the cells behaved identically regardless of the media condition but the MOW culture may require further looking into if this method is applied to the liquid handling system.

It appears that the similarity in behaviour is consistent in all culture conditions except MOW. However, these results do not show a disproportionately adverse effect of using either sterile oil as carrier liquids in the system. This put to rest the concern that the transport mechanism for liquid sampling would produce toxic effects in the cells.

4.4.1.2 Oil Handling

The ease of use and setup time is a constraint to the adoption of liquid handling techniques. This method using oil would have introduced additional issues to the user such as maintaining sterility, difficulty of handling oil as well as slow or cumbersome system setup. When compared to the commercial autoloader system, this was too difficult to implement and was discarded as an option for sampling in the Gatling liquid handling system.

4.4.1.3 Nano-Volume Dispenser Results

Figure 4-20 shows the level of precision in volumes per pulse for different valve actuation signals under open loop control. The lack of linearity in the relationship between volume per pulse and duty cycle applied makes this open loop solution imprecise as expected. However the level of precision with higher duty cycles means that we can get really close to the target volumes when using higher duty cycles to

actuate the dispensing valves. It is recommended that duty cycle above 15% be used to achieve more precise results.

Figure 4-21 shows the results for the experiment performed at different input pressures (P_{in} = 200, 400, 500, 600 mBar). We can further use this information in the open loop liquid sampling control system.

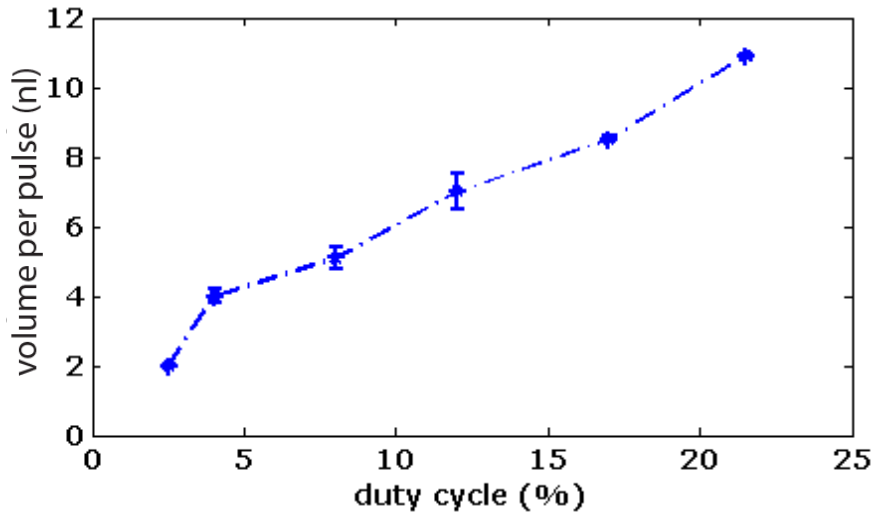

Figure 4-20: Dispensed volume per pulse with 200mBar pressure
The volume per pulse shown was calculated from a mass of volume of water dispensed into a vial after 10 second actuation period of the LEE valves. Since they follow a trend, the remaining experiments were performed with n =1 measurements.

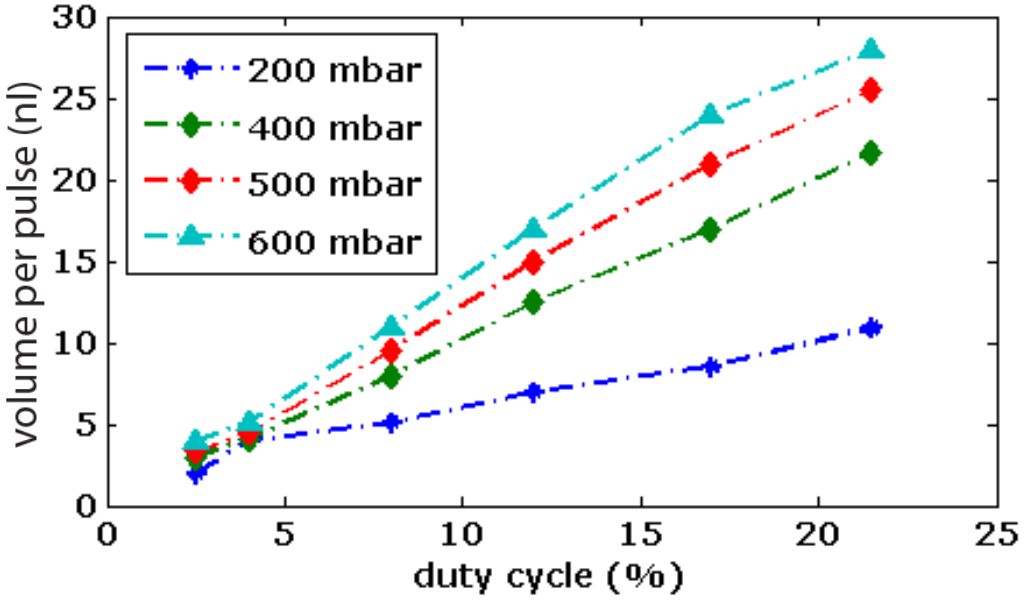

Figure 4-21: Dispensed volume with different input pressure
This results were obtained from repeating the experiment with different reservoir pressures. A linear trend can be seen between the duty cycle used and the volume dispensed. This relationship could be exploited to achieve high precision dispensing.

Figure 4-22 shows the result of the closed loop control system where high accuracy in dispensed volume target is achieved via feedback of liquid flow rate. This system of control is very precise and will provide the best option for volume sampling.

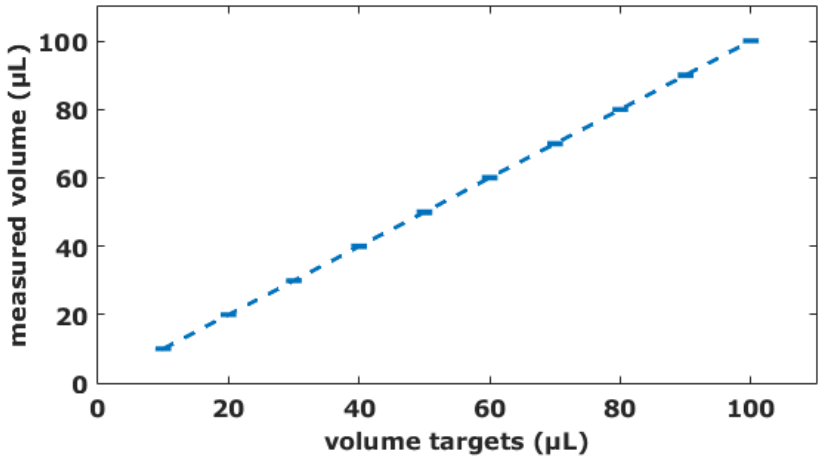

Figure 4-22: Measured volume vs target volume in closed loop controlled liquid sampling

The experiments conducted for liquid sampling showed that very precise volume dispensing can be achieved using the LEE valves coupled with flow sensing feedback control logic. Dead volume constraints may make this feedback control method unsuitable and an open loop control may be used instead. This is particularly true when considering the low volumes that may be required to be dispensed (<10 µL). The liquid transport through tubes and flow sensing interconnections may add to the mixing affects that between the drug and the carrier liquid (Sabourin, Skafte-Pedersen et al. 2013). The syringe driven liquid dispensing system is suitable where the dispensing valves are not available but oil handling may prove too challenging. This volume sampling system will then transport the sampled volume to the volume injection system.

4.4.2 Volume Injection System Results

4.4.2.1 Through-hole Prototype Results

Flow was observed in the flow sensor at the end closer to the pressurised vessel while flow was not present in the other end. Two major reasons impacting the behaviour of the flow are misalignment between the connection blocks and the reservoir; and capillary forces acting between the connection block and the reservoir which restricts liquid from flowing through. The influence of misalignment is negligible since the pieces were aligned at the start and unchanged throughout the process.

The effects of capillary forces are dependent on the applied pressure regime, geometry of the system and the materials used. We haven't been able to overcome this capillary effect even when applying the maximum pressure allowed by our pressure control system. The same zero through-flow result was experienced with different combinations of the fabricated PEEK, stainless and UHMWPE pieces. The device was disassembled after air was pushed through to clear the orifice and it was observed that the interface of the layers were wetted.

The results obtained with this prototype showed that the designed through-hole liquid injection system was not operational and could not be used to achieve the desired goals. In addition, during the design process, the expected number of reservoirs and their close proximity were considered as a potential issue as this configuration increases the risk of the rotor breaking during operation. In conclusion, this system design should is not a viable solution for liquid loading.

4.4.2.2 Surface Mount Prototype Leakage Result

Flow was present at the output flow sensor for this prototype. Figure 4-23 shows the difference in measured flow rates between the two flow sensors for varied pressure differences and over the range of Torques used to tighten the assembly.

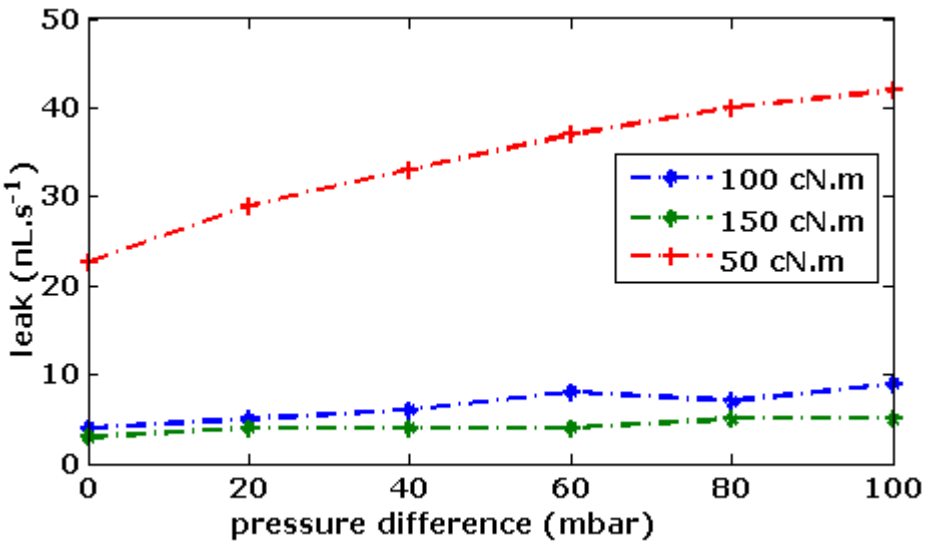

Figure 4-23: Chart of difference between input flow and output flow for the G-SIS system
The leak rate is defined as the difference between the forward flow rate and the back flow rate. High torque settings (150 cN.m) on the screws were able to reduce leaks to less than 10 nL.s^{-1}. However the torque settings that would allow the motor rotate the rotor was 20 cN.m.

The results show that high assembly torque is required to reduce leaks in the system and we did not obtain 0 nL.s^{-1} leakage for the measurable Torque which was limited by the available Torque driver range. The unexpected high leakage may be the result of the surface roughness of the PEEK rotor or Steel stator and the surface features prevented roughness measurements with high resolution systems. The result of this leakage at high torque meant that the selected motor was unsuitable to drive the system. The motor could not rotate when the torque on the assembly was set above 20 cN.m.

One possible solution to this is to perform torque characterisation and obtain actual motor torque requirements at this point before acquiring a motor and as such motor selection should be the last stage. The assumption that the industry injector valve could be compared to the novel system was flawed and a critical design error in hindsight.

It was also observed that the PEEK rotors became deformed after rotation. This deformation happens when the assembly screw torques are set high (10 - 20 cN.m).

it is, therefore, critical that we do not select higher motor power to overcome the lack of rotation encountered at 20 cN.m torque set on the assembly screws.

It may be possible to apply a low frictional coating to the stator and rotor that will also increase the contact area of the featureless surfaces and further reduce leaks. The application of such a coating will add more complexity to the development of a novel macro-scale liquid handling system for microfluidic systems. This system does not appear to be a simple system to develop and will not be further investigated.

4.5 Discussion

The development of a macro-scale liquid handling system for liquid manipulation in microfluidic devices was investigated to provide a highly modular and integrable system that could be beneficial to research environments. Previous systems have been developed and implemented using over the shelf tools (Sabourin, Skafte-Pedersen et al. 2013) but some of these systems do not scale well and are typically able to perform singlular functions. This was demonstrated with a commercial autosampler which showed high precision but low modularity and limited ability to control lower level functions. The G-SIS system was developed as a replacement that would allow these features and also be capable of sampling downstream of the device. It was also designed to have reduced sized for closer proximity to the target microfluidic device.

Design constraints were reviewed during the development process and the volume sampling aspect and the sample injection section of the system were investigated. Toxicity tests were performed on neuronal cell cultures to validate the use of sterile mineral oil or olive oil in transporting the samples from the sample reservoir to the device reservoir. This was done as part of investigation into syringe driven volume sampling using immiscible liquid as the carrier liquid. It showed that sterile mineral oil

would not adversely affect the cell development when in contact with liquid being transported to the cells. This agrees with microbiological practices where oils have been used to form microdroplets to carry volumes for biological analysis or cell encapsulation (Piccin, Ferraro et al. 2014). The limitation to this method is the more involved nature of the oil handling process. The mechanism required to degass the system to ensure that the displaced oil at the syringe equals the displaced sample volume. Another challenge to this method is the high pressures setup in the system. Flow obstruction in the system may result in a rupture as the syringe driver will constantly build up pressure. The Lee micro dispensing valves provides an opportunity for precise liquid volume sampling when combined with a flow sensor inline for flow rate feedback to the volume dispensing logic controller. This can be further applied to liquid transport technologies that require precise volume displacement (Liu, Chen et al. 2009). The connection of the volume samples into one single sample output presents an opportunity to utilise one flow sensor for multiple sample volumes.

The prototypes for volume injection were developed as through-hole and surface mount reservoir configurations. They were assembled and tested to confirm liquid flow and leaks in the system. The through hole failed to allow liquid flow through and this is not recommended for future development. The surface mount prototype allowed liquid flow through the reservoir from the input to output ports but leaks were observed. The system assembly torque required to prevent leaks was found to be too high to allow the motor rotate the rotor component in the prototype. That is, the reservoir could not be moved to change the input/output port position at the high screw torque required. Furthermore, the rotor was deformed when rotating at the motor limits. The surface roughness is the most likely reason for the leaks and may be solved by the application of a low friction coating to the rotor and stator surfaces that would provide adequate sealing and reduce friction between the surfaces.

The challenge to the development of a macro scale system for microfluidic liquid handling is not trivial as it includes requirement for high precision machining, and extensive design process comprised of design, prototyping, fabrication and testing steps. These challenges were not realised at the outset and utilised resources could be best put towards an alternative strategy. The adoption of existing injectors (Rheodyne) into custom integrated designs may best serve future research for automated macro-size liquid handling system. It is recommended that further attempts at such macro scale system first start with the challenge of leaks and sealing between the surfaces to ensure liquid flow through the system prototypes.

5. Fabrication of On-Chip Liquid Handling System

The project objectives to develop, build and integrate a custom liquid handling solution was undertaken to provide a system that was modular, highly customisable, and easy to reproduce for widespread adoption.

The requirement for a parallel collaborative research into surface modification of micro devices used as cell culture environments limit the implementation of a fully integrated liquid handling chip. This prompted the development of modular liquid handling strategies for off-chip volume manipulation. One strategy to use macro-scale liquid handling systems to address this requirement was investigated in the "Gatling-styled Sequential Injection System - GSIS" Section. The other approach is the focus of this chapter where on-chip liquid handling components are used. There is a gap between microfluidic technology production and end users (Langelier, Livak-Dahl et al. 2011). Cost and expertise seem to be a big contribution to the lack of adoption of microfluidic technology by researchers (Whitesides 2006). Simpler fabrication methods have been proposed to obviate the need for clean-room lithography (Liu, He et al. 2005)like replacing the photomask with high-resolution transparencies (Duffy, McDonald et al. 1998) or direct mold printing (Tan, Rodgers et al. 2001, Grimes, Breslauer et al. 2008). Modular designs have also been developed using fluidic breadboards to assemble components (Shaikh, Ryu et al. 2005). However, these breadboards limit the system flexibility. The requirement of SU-8 master molds in the development of a microfluidic assembly block platform (Langelier, Livak-Dahl et al. 2011) contradict their original claim that clean-room lithography poses cost and technical challenge to the wider adoption of microfluidics. It is advantageous to produce a prototype chip that could be easily replicated in-house and externally to increase the potential for wide spread adoption and extend the possibilities for high level applications to be built around the chip. A rapid-

prototyping and fabrication approach can be taken to realise these objectives. It will also be beneficial to take advantage of emerging trends like chip modularity to ensure interconnection between the developed on-chip liquid handling solutions.

Some of the rapid prototyping techniques discussed in the Literature are further investigated here. The investigation presented here will not focus on SU-8 molds for feature transfer, milling, laser ablation, injection molding and other fabrication techniques that may increase the design and fabrication steps as well as technical expertise and equipment needed to fabricate the devices. An ideal fabrication technique is presented that is new in its application to research laboratories especially for those with limited resources. This fabrication technique can truly be defined as a “rapid-prototyping” fabrication method for multi-layered microfluidic devices. This new method is alluded to in research but has never been demonstrated or has been applied using other techniques that may be outside the reach or regular non-microfluidic laboratories. The advantage of this method will be minimal requirement for specialised equipment, facilities, and expertise and is expected to draw more attention to the suitability of microfluidic technology as the primary workstation of biomedical research in the future. This will potentially create more opportunity for investments into microfluidic technology to produce workable tools that can be integrated to form larger components.

Some of the rapid-prototyping methods for multi-layered devices are highlighted and methods are presented for their characterisation. The proposed modular chip designs are then proposed for implementation as well as their operation.

5.1 Rapid prototyping Techniques

Some rapid prototyping techniques have been identified to be characterised to identify an optimum method that could be adopted for the development of modular on-chip liquid handling solutions. These include:

- PMMA-clamp-assisted tape adhesion (Lamberti, Sacco et al. 2011, Chen, Li et al. 2013, Temiz, Lovchik et al. 2015)
- Chemically-assisted bonding techniques from Tang's group (Tang and Lee 2010), Aran's group (Aran, Sasso et al. 2010) and Wu (Wu and Lee 2014)
- PDMS to PDMS bonding techniques

The device fabrication protocols used are presented along with tests and results that demonstrate the suitability of the protocols for development of durable multi-layered microfluidic devices.

5.1.1 PMMA Clamped Devices

A PMMA-clamp assisted device was developed and assembled using PMMA sheets with height (h=2mm). A tape-bonded microfluidic device with normally-open on-chip valves was assembled using tape as the liquid channel and actuation layers. An uncut PET film with height (h = 0.1 mm) was used as the substrate.

Through-holes were machined into one piece of PMMA plastic for screws and tubing connections to the PDMS bulk layer. The machined PMMA layer and another unaltered PMMA layer with similar dimensions were used to sandwich the assembled tape-bonded microfluidic device. Screws were then used to pressure clamp the assembly. Figure 5-1 shows an image of the PMMA clamped device. It is crucial to first test the tape bond durability and assess the benefits of the clamps. Further to this a test was conducted to see the effect of the screw clamps on liquid flow and how this was affected by the PDMS stiffness. Finally, the assembled device shown in

Figure 5-1 was characterised to identify the pressures required to stop and allow liquid flow within the liquid channel.

The use of a torque driver to apply compressive force has been utilised previously for clamped PDMS devices where the compressive force was quantified using a spring with known and verified Young's modulus constant. The same was not done here and all figures obtained using the torque driver quote the torque setting applied to the screws. The justification is that it is more relevant to know what torque was set than the compressive force for future work as a double conversion (from torque to force and then back to torque) is impractical when developing PMMA clamped devices.

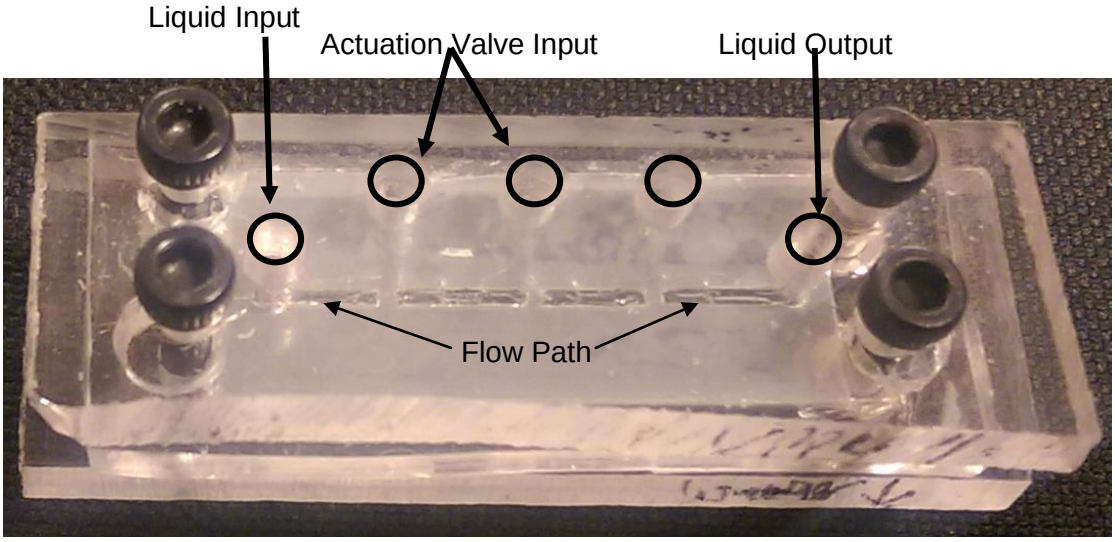

Figure 5-1: PMMA layer added to clamp a multi-layered tape-bonded assembly.
Image was taken in the lab of a PMMA clamped device. The device shown has one input, one output and three pneumatic inputs for valving. The PMMA is machined in the lab with a drill press and handsaw.

5.1.1.1 Bond Durability in PMMA Clamped Devices

An experiment was designed to identify the permissible pressures with the PMMA clamped device. Two tape bonded devices were fabricated to have a single actuation layer sandwiched between the thin PET layer and a PDMS layer for tube connections. One of the devices was clamped using two sheets of PMMA of

thickness (t = 4.6mm). The tape layer was cut into patterns shown in the Figure 5-2. Each feature width (w = 1mm) represented the minimum proximity between features in the device. Holes were punched in the PDMS to act as push fit connections for tubing carrying gas pressure. The tape was placed between a thick PDMS layer and thin PET film. The PMMA Gas pressure was applied through the PDMS holes into the features for time (t = 17 hours) that is greater than the expected average usage time (t = 8 hours) based on past experience automating the immunocytochemistry procedure. The time taken for the gas to leak from the feature was taken as burst pressure for the different torque settings (T = 4, 5, 6 cN.m) with 5 repeats per torque setting. The time taken to burst was also recorded for the specific torque.

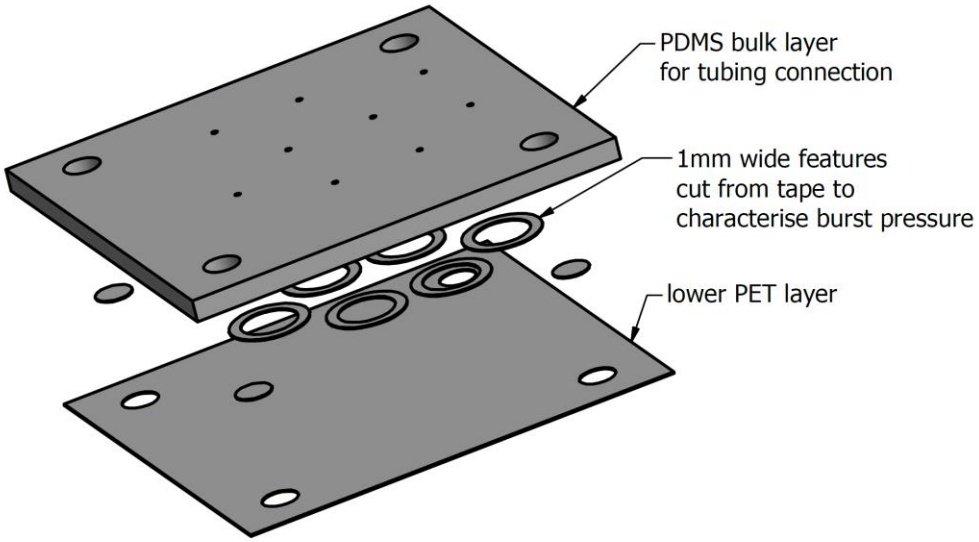

Figure 5-2: Layers used to test burst pressure of tape bonded devices
The burst pressure was tested using features of size (w = 1mm) as actuation layer. The burst pressure was defined as the air pressure that will cause air to leak through that feature under 17 hours of pressurisation. Typically, the target applications will run for 8 hours.

5.1.1.2 Effects of Increased Torque on Liquid Flow

An experiment was performed to determine the characteristic effect of compression on liquid flow. A flow path of width w = 1mm was excised from a silicone tape with thickness h = 125 um and sandwiched between a bulk PDMS slab (50 x 50 x 2 mm)

and a PET plastic (50 x 50 x 0.125 mm). Two PMMA plates (50 x 50 x 2 mm) are used to apply compressive force with screws at the corners of the plates. The screws were tightened using a torque driver (Torqueleader QSN40) and liquid was then transported through the flow path using the manifold flow control system. The back pressure was set (P_b = 70 mBar) and the forward pressure (P_f) as well to give a pressure difference ($P_f - P_b$ = 20 mBar) until maximum pressure of the pressure controller was reached (P_{max} = 250 mBar) giving 9 repeats per torque settings used. The flow through the device is monitored over the range of set torque (T = 5, 6, 7, 8, 9, 10 cN.m).

5.1.1.3 Effect of PDMS Properties on Liquid Flow

The PDMS cure time and temperature was altered to change the PDMS stiffness. A secondary PDMS device with single flow channel layer and no actuation layer was fabricated with a different curing time. The PET/tape/PDMS assembly was cured for 8 hours at 80 degrees Celcius on a hot plate. The effect of this cure time change on the liquid flow rates in the channel was quantified in the same way as the previous test where the PDMS used was cured for 2 hours at same temperatures.

5.1.1.4 Effect of Channel Dimensions on Liquid Flow

The channel dimensions were also altered to change the proportion of the liquid channel that was filled by the PDMS creep under compressive forces. A PDMS device with a single flow channel layer was made with channel width (w = 0.75 mm) and flow rates were compared to those from the previous device with channel width (w = 1 mm).

5.1.2 Chemically bonded microfluidic devices

The use plastic for rapid-prototyping microfluidic device fabrication process was further investigated with chemically bonded microfluidic devices. The protocols were

first confirmed experimentally and the devices produced using these protocols were then characterised.

5.1.2.1 Chemical Bonding Protocol 1

The Tang and Lee protocol (Tang and Lee 2010) was performed in the laboratory. Oxygen plasma was used to treat PDMS and plastic surfaces at 50 – 60 watts power for 1 minute. The treated PDMS surface was exposed to 1% (v/v) APTES solution for 20 minutes while the PET film was exposed to 1% (v/v) GPTES solution for 20 minutes. They were then rinsed thoroughly in distilled water and left to dry. The surfaces were then brought into contact and kept in contact for 1 hour at 80 degrees Celsius.

5.1.2.2 Chemical Bonding Protocol 2

Another chemical bonding method implemented required a single surface APTES treatment (Aran, Sasso et al. 2010). A 5% APTES solution in a glass petri dish was heated on a hot plate for at 80 degrees Celcius. The plastic was then plasma activated and immersed in the heating APTES solution for 20 minutes and then left out to dry. The PDMS slab was then plasma activated and immediately brought in contact with the functionalised PET sheet and kept on a hot plate at 80 degrees Celsius for 2 minutes.

5.1.2.3 Chemical Bonding Protocol 3

The “one-step” bonding method was also performed but with slight variation using a plasma generator in place of the corona discharge to functionalise the sheet. A plastic pipette was used to drop 0.5 mL of amine-PDMS linker solution on the PET

sheet which was then placed on a hot plate at 37 degrees for 20 minutes. The sheets were then sonicated in IPA solvent for 1 minute and then plasma activated along with the PDMS slabs.

5.1.2.4 Strength Testing Chemically Bonded Devices

A simple device design illustrated in Figure 5-3 was used to confirm these protocols. The devices were designed equally as a square PDMS slab (20 x 20 mm x 5 mm) cut from the same PDMS that was previously cast in a plain featureless 80 mm diameter petri-dish. The square slabs were punched in the centre with a biopsy punch (diameter = 1.5 mm). PET film with dimensions (l x w x t = 25 x 25 x 0.1 mm) used for the bonding protocols. Five devices were fabricated for each of the three chemical bonding method selected.

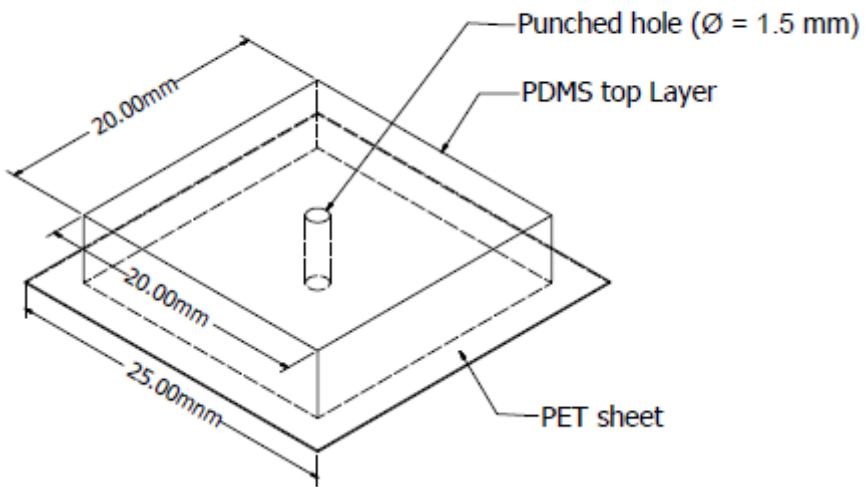

Figure 5-3 –Device fabricated to confirm chemical bonding protocols

Pressure was applied to each bonded device through the orifice in the PDMS layer in increments of 0.5 Bar. Preliminary findings showed that rupture was faster (t ≤ 1 minute) with these devices in comparison with the slow progression of Taylor-fingers

experienced with tape bonded devices. Therefore, the test was only required to show what pressure was sustainable and which ones were not.

5.1.3 PDMS-to-PDMS bonding

The PDMS to PDMS bonding technique shows the most promise from the Literature section. The added constraint for rapid-prototyping development limits the use of SU-8 molds. Therefore, there was need to develop molds to characterise PDMS-to-PDMS bonding methods using Xurography techniques. The effect of spin-coating speed on the outcome of devices made with stamp-and-stick method is characterised. Tests have also been carried to verify the bond strength obtainable from devices developed with both stamp-and-stick and partial curing PDMS bonding protocols.

5.1.3.1 Mold Fabrication using Xurography Technique

The molds used to transfer features were developed using Xurography methods (Martínez-López, Betancourt et al. 2017). The features are designed in CAD and imported into software used to control a desktop craft cutter (Silhouette Cameo).

A tape/PET combination is made by sticking a layer of tape (thickness 50 µm) to a layer of PET Plastic film (50 µm). The combination is loaded into the craft cutter and the designed features are excised from the combination. The backing layer on the tape is then removed and the exposed tape surface is stamped onto a petri dish. This forms the mold with features that will be transferred to the PDMS. PDMS mixture at 10:1 base to curing agent ratio is poured over the mold and the Petri dish is set on a hot plate to cure at 80 degrees Celsius for 30 minutes. The method adopted for stamp-and-stick (Satyanarayana, Karnik et al. 2005) was then characterised to investigate the effect of spin speed on the bonded device.

A significant amount of physical handling is required to develop molds with Xurography methods and this affects the realisable mold dimensions. In practice, it was found that larger mold dimensions (>1 mm) were more feasible to obtain and retained their shape in spite of the manual handling in this step. As a rule of thumb, the design used minimum of 1mm width when with rectangular features where length was at least 3 mm and a minimum width of 2mm when with square features. Circular features were realised with minimum of 2mm diameter.

5.1.3.2 Spin Coating Speed for Stamp-and-Stick

The stamp-and-stick method requires PDMS to be spun in a spin coater machine to obtain very thin PDMS films. It was required to obtain suitable spin speeds for this method that will allow minimal creep of the uncured PDMS into the features during assembly. The effect of spin speed on the microfluidic device features was demonstrated in an experiment. Molds were made to have features with dimensions (l x w = 4 by 4 mm) and used to create PDMS slabs with these features. Drops of uncured PDMS were applied to a glass cover slip that was loaded on a spin coater. This was then spun at different spin speeds (s = 600, 1100, 1400, 1700 and 2100 rpm). The PDMS slab was then placed in contact with the spun PDMS and then transferred to another featureless PDMS slab. The resulting PDMS assemblies were placed under a microscope to image the effect of the spin speed on the features.

Further characterisation of the PDMS-to-PDMS bonding techniques requires verification of the bond strength obtained using these methods. The verification was done for devices assembled using the stamp-and-stick method as well as the partial curing method (Eddings and Gale 2006).

5.1.3.3 Bond Strength Verification

Devices were assembled with the same dimensions as in Figure 5-3 using the stamp and stick PDMS glue bonding and PDMS partial curing methods. Air pressure was then introduced into the 1.5 mm diameter orifice created with the bio-punch at different pressure until the device burst or delaminated. The pressure was recorded for burst pressure for the devices.

5.1.4 Effect of Device Geometry on Bond Strength

Previous tests were carried out to verify the bond strength of the devices for chemically bonded and PDMS to PDMS bonding strategies. It was then necessary to assess the effect of device geometry on the bond strength and device performance. This test has been carried out to show the durability of multi-layered devices which is critical to the long term usage and it was desirable to confirm the limits for the different bonding techniques.

It was assumed that the force applied was critical to the performance of the bond than the bond surface contact area. The relationship, $F = PxA$, implies that larger actuation area would generate larger downward force against the base of the bonded device. Also, it was expected that wider bond contact surface would give greater strength to the bond.

Molds were made with patterns and dimensions illustrated in Figure 5-4 The patterns in (a) produced a PDMS slab with fixed square actuation area (w = l = 4 mm) and varied bond contact surface width (w = 1, 2, 3, 4 mm); while (b) produced rectangular actuation area with fixed actuation area (w = 1mm, l = 20 mm) with same bond contact area as (a). This was to characterise the effect of the bond contact area on the bond strength. A bonded device is shown in Figure 5-5 with a piece of PET plastic sheet bonded to PDMS that was cast on an example pattern.

The patterns were altered to provide various actuation area dimensions (w = l = 1, 2, 3, 4 mm) while maintaining a fixed bond contact surface (w = 4 mm) for the square pattern. This was also applied to the rectangular pattern by varying the actuation area dimension (l = 20 mm, w = 0.5, 1, 2, 3, 4 mm) with the same fixed bond contact surface (w = 4 mm).

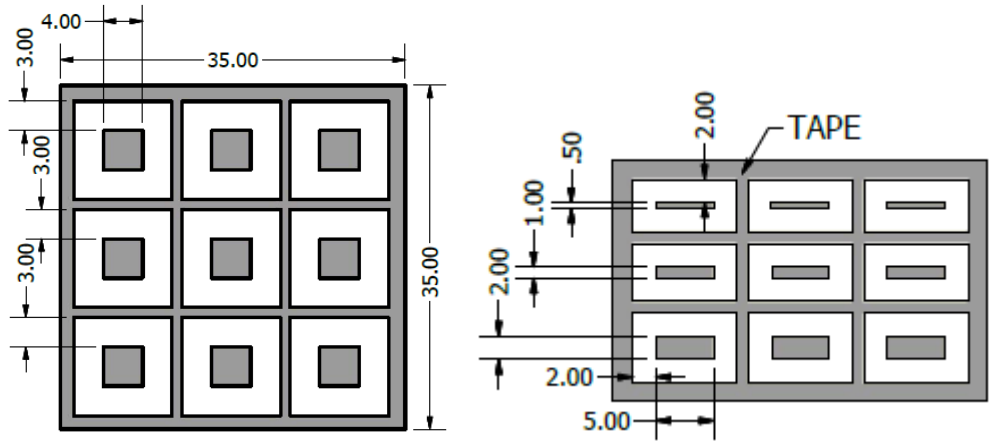

Figure 5-4: Patterns excised from Tape for Actuation Layer PDMS moulds
The patterns (grey) used as moulds were excised from a tape/plastic combination using a silhouette craft cutter. The backing layer of the tape was meticulously removed while scotch tape was used to maintain the excised patterns in place before placing the moulds on a Petri dish for PDMS casting. The patterns were used to test maximum permissible actuation pressure with varied feature separation distances on the same PDMS cast shown in (a) and varied width on different PDMS casts shown in (b) with a feature separation of (w=3 mm). The valve chamber dimension used was (w x h = 4 x 4 mm).

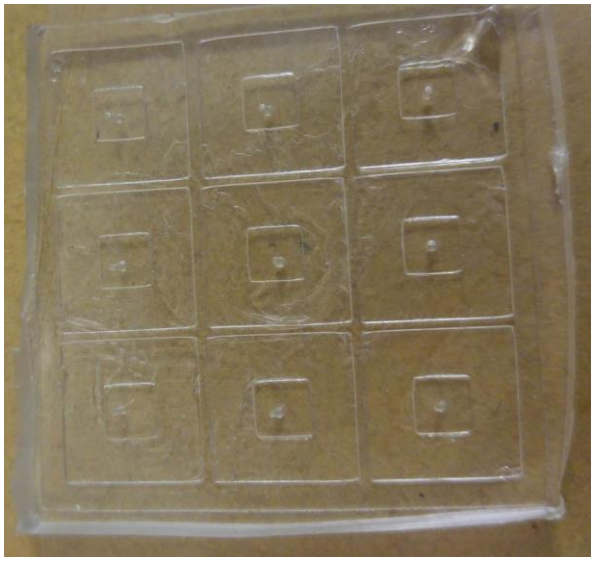

Figure 5-5: Fabricated Device with Patterns to Test Bond Strength

The bonding methods tested were PDMS partial curing, PDMS glue bonding, chemical methods proposed by (Wu and Lee 2014) as well as that presented by (Aran, Sasso et al. 2010). These methods are designated as PC (partial curing), PG (PDMS glue), AL (Amine-linker chemical bonding) and AC (APTES chemical bonding) respectively.

Air at set pressure (P = 1 – 8 Bar) with integer increment was introduced into each of the bonded devices for 10 minutes and then triggered in an on/off cycle for 20 actuation at 1Hz till to find out the last integer pressure value that was tolerated. The last integer pressure where the device survived the actuation test was recorded as the recorded tolerable bond strength. Peel tests (DIN 1990), previously performed (Tang and Lee 2010, Gu, Liu et al. 2011) would not provide any additional information as they do not characterise the forces that the devices undergo in actual microfluidic applications.

5.2 Results

The results from tests carried out on promising rapid-prototyping techniques are presented.

5.2.1 PMMA Devices

5.2.1.1 Bond Durability from PMMA clamping

Figure 5-6 shows the results of the quick test with error bars from standard deviation of the 5 repeats. The device failed at 3 bar of gas pressure when the torque was set to 5 cN.m and at 4 bar gas pressure for 4 and 5 cN.m. This showed that the PMMA clamped device will be able to withstand up to 2 Bar air pressure for actuation without failing for up to 17 hours continuous operation with the torque setting at 4, 5, 6 cN.m.

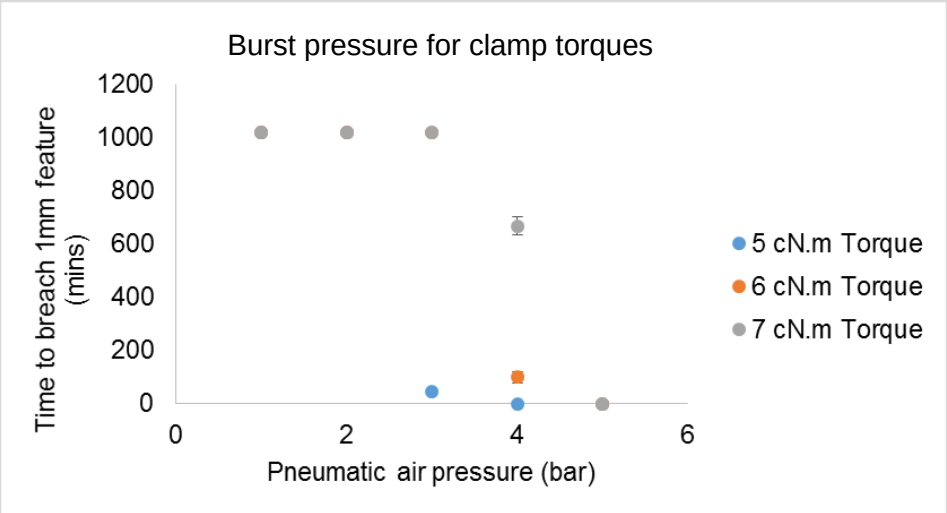

Figure 5-6: Burst pressure for different clamping torques.
An actuation layer is formed from a 1mm wide tape feature with thickness (125 µm) and is bonded between a bulk piece of PDMS with thickness (2 mm) and a piece of PET plastic with thickness (125 µm). The layers are then sandwiched between two PMMA plates with dimension (50 x 50 x 2 mm) and screws are tightened to a known torque. A pressure is applied to the layer of tape through an input orifice to determine where the conditions that will maintain the bond features for up to 17 hours (1020 mins). It is assumed that the bond will perform less well at pressures higher than the burst pressure for a given torque and the burst time is assumed as 0.

5.2.1.2 Screw Torque Effects on Liquid Flow

The result of this test is shown in Figure 5-7. The mean flow change (Δflow) and standard deviation for flow change per 20 mBar pressure change is presented. There is a reduction in the flow response to pressure when the screws are tightened to a torque (T ≥ 7 cN.m). This is caused by a constriction of the channel geometry by the compressed PDMS bulk which increases the fluidic resistance in the flow path. The compression force applied reduces the channel dimensions available for fluid flow. This effect has been previously quantified using optical profilometry techniques (Konda, Taylor et al. 2015). Their analysis shows that application of compressive forces reduces the width and height of the fluid channel. The compression of the PDMS due to externally applied force is a function of its Young's Modulus constant. It was seen that the composite was able to withstand up to 3 bar when the screws were set to the applied torque (T= 7 cN.m) and it is desirable that this torque setting has minimal effect on the liquid flow.

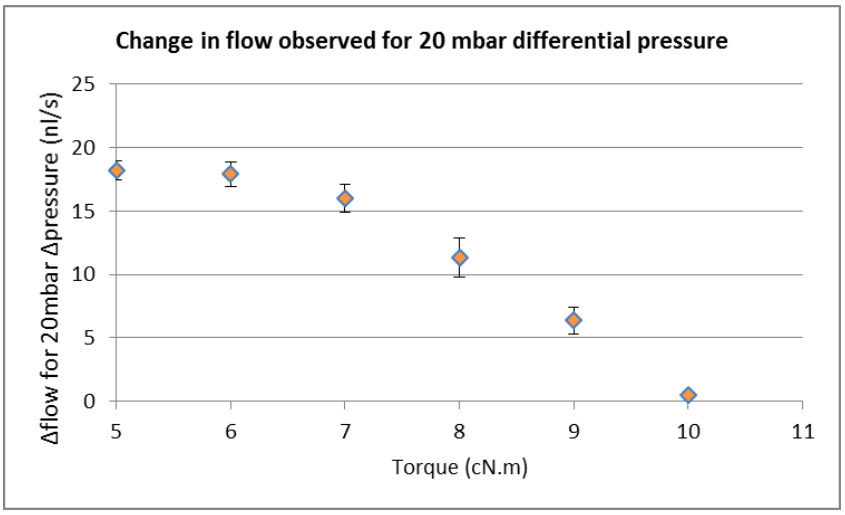

Figure 5-7: Restriction to fluid flow from various torque with 1mm channel geometry
A fluid flow path is cut from tape of thickness (125 µm). The flow path has cross section width (w = 1.0 mm). The tape is sandwiched between a bulk piece of PDMS with thickness (2 mm) and a piece of PET plastic with thickness (125 µm). The layers are then sandwiched between two PMMA plates with dimension (50 x 50 x 2 mm) and screws are tightened to a known torque. Liquid is transported through the flow path using the flow system with a differential positive pressure (ΔP) for forward flow. The

forward pressure is altered at 20 mBar increments while recording the old and new flow rates. The change to flow (Δf) due to pressure change (Δp) is logged for forward pressure (70 ≤ P ≤ 190 mBar).

5.2.1.3 PDMS Cure Time Effect on Liquid Flow

The comparison in Figure 5-8 shows a large difference in the flow characteristics between 2 hours bake time and 8 hours bake time. The device with the 8 hours bake time started to limit flow at a higher torque setting (T= 12 cN.m) with the same Pressure difference settings for 9 repeats. This is due to the increased crosslinking that occurs in PDMS which affects the stiffness of PDMS after long bake times (Fuard, Tzvetkova-Chevolleau et al. 2008). It has been shown that cure temperature affects the Young's modulus constant of PDMS (Liu, Sun et al. 2009). Higher cure temperatures or longer cure times will increase the crosslinking, thereby reducing the Young's modulus constant and reducing the compressibility of PDMS.

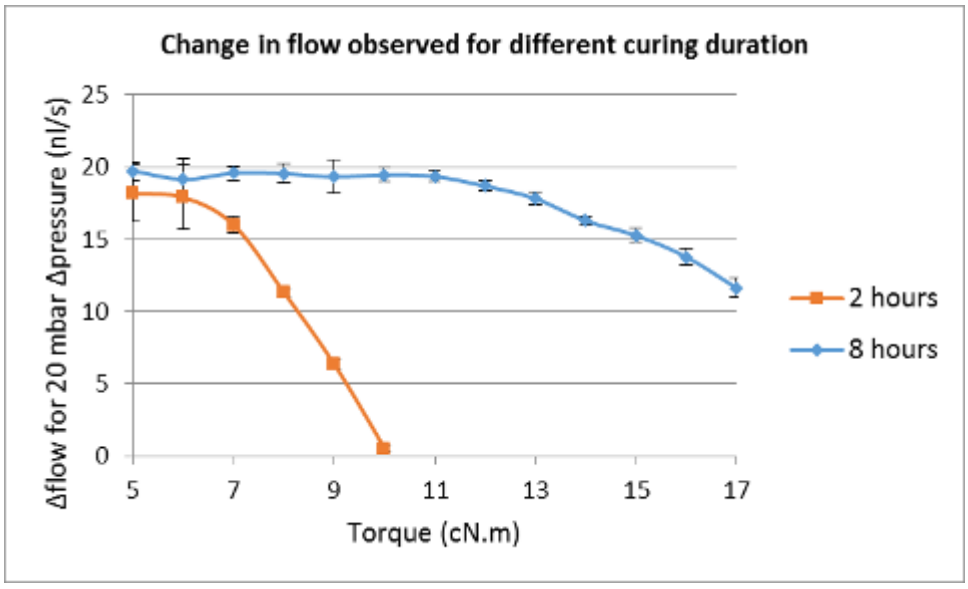

Figure 5-8: Effect of bake time on PDMS compressibility as a function of flow restriction
Two bulk PDMS pieces with different bake times are used separately to fabricate a PMMA clamped PDMS liquid channel. The effect on cure times on young modulus of PDMS have previously been characterised (Fuard, Tzvetkova-Chevolleau et al. 2008) where it was shown that longer bake times results in a PDMS material with low compressibility. The graph here agrees with literature and thus increases the extent to which we can compress our clamped devices to improve longevity of the device.

5.2.1.4 Effect of Channel Dimension Width on Liquid Flow

Figure 5-9 shows the results from this experiment and compares the results with results when using the previous channel width (w = 1.0mm). In both cases, the fluid flow is not noticeably marred for torque (t ≤ 10 cN.m). It is believed that PDMS does not deform sufficiently in this clamp-force regime. Increased compressive forces continue to constrict the liquid path until zero flow for the smaller channel. The most likely reason for the reduction in flow rate is the increase in fluidic resistance from the reduction in channel dimensions (Kim, Toh et al. 2007).

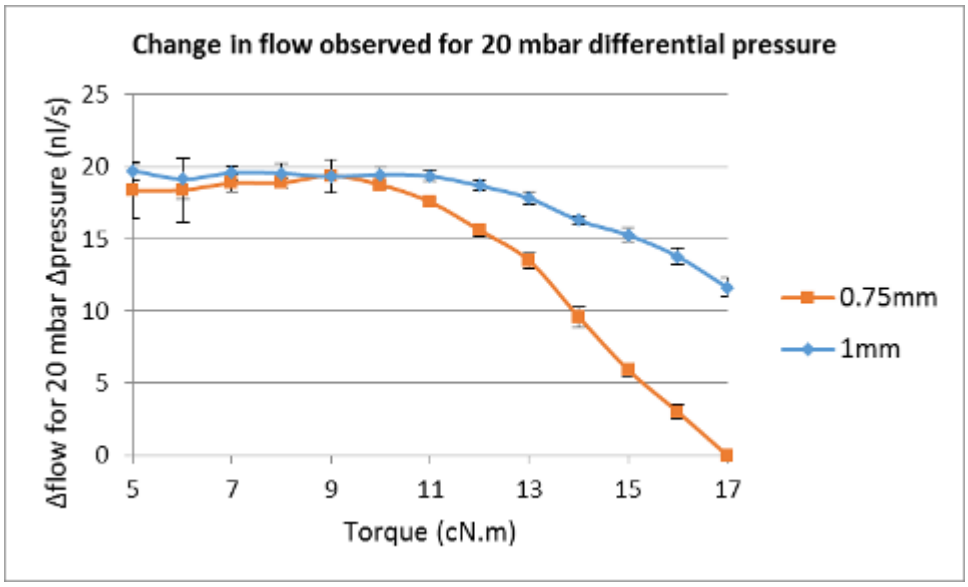

Figure 5-9: Liquid flow restriction for various compressive forces with different Young's modulus

5.2.1.5 Assembled PMMA Clamped Device

The ability to withstand high pressure makes for the possibility of tape bonded microfluidic valves. This was implemented in the laboratory with thin PDMS membrane (t = 50, 80, 100µm) in both normally open and normally-closed

configurations. However, liquid flow could not be achieved with the thin PDMS valving membrane. Food dye was added to provide quick visual inspection and it was discovered that the liquid did not get through the liquid channel inputs for some channels or did not flow through the entire channel in others. The blockage at the input was found to be due to residual parts of the membrane left behind during the punching process. These small pieces would adhere to the tape and become partly dislodged with liquid input and block off the inputs causing zero flow into the device. The blockage in the channel was found to be due to the membrane pinching that occurs when the torque is applied to the screws.

Attempts were also made to achieve liquid flow with different liquid channel widths (w = 0.5, 0.75, 1.0 and 1.25 mm). The liquid was established only in the channel with width (w = 0.5 mm) in some instances but was not repeatable. The partial success with that channel width could be attributed to the width-to-height ratio ($^{width}/_{height}$) being smaller than the configurations with larger width and the membrane is unable to completely seal it. This width-to-height ratio plays a significant role in the design of multi-layered microfluidic devices that perform on-chip valving (Fordyce, Diaz-Botia et al. 2012). A larger channel width will cause the valve membrane to sag, sealing off the channel even when it is not actuated. Thinner channels will only allow the membrane seal the channel when it has been actuated. These two challenges proved impossible to ameliorate and a repeatable fabrication procedure could not be achieved that would allow liquid flow for multi-layered designs using PMMA clamping method. This method was, therefore, discontinued for fast prototyping on-chip liquid handling. It will still be beneficial to research seeking to develop highly durable bonded devices using tape-bonding method (Chen, Li et al. 2013).

5.2.2 Chemical Bonding Techniques

5.2.2.1 Confirmation of Chemical Bonding Techniques

It was found that the 5 devices made using the Chemical bonding protocol 1 with APTES/GPTES could only withstand 2.5 Bar of air pressure consistently and started to delaminate at 3 Bar pressure. It was assumed that the epoxy rings of the epoxy silane (GPTES) were opened in the aqueous solution and hexane was proposed as a substitute solvent. The result of using the hexane solution was a bond that delaminated instantly at application of 1 Bar pressure.

This repeat of this experiment in the laboratory showed that the bonds on all five samples were maintained at 4 Bar pressure with two failing at 4.5 and complete failure of the remaining three failure at 5 Bar pressure for a mean of 4.3 Bar pressure tolerance. This limit was a considerable improvement over the previous one and showed greater promise for highly durable devices.

This protocol was repeated in the lab as far as was practical with the exception of the hydroxylation process which was induced using a plasma generator instead of a corona discharge lamp. The reaction of the amine-PDMS linker was done at 37 degrees on a hot plate for an hour instead as experience showed inconsistent results when it was kept at the recommended room temperature for 20 minutes. The resulting bond was able to withstand 7 bar air pressure without any signs of wear.

There was no apparent onset of Taylor fingers when the bonded piece was examined under the microscope at the pressure (7 Bar). It is uncertain if the higher pressures obtained were due to the plasma activation used in place of corona discharge or the temperature used during the plastic functionalisation step. This bonding technique was preferred over the others for further development of on-chip liquid handling solution. However, the complete device fabrication procedure would need to be addressed to provide a good balance between rapid prototyping and time taken to

completely assemble the device. This is subsequently treated in the “Device assembly using PDMS-to-PDMS Bonding Techniques” section.

5.2.3 PDMS to PDMS Bonding

5.2.3.1 Uncured PDMS glue bonding

Figure 5-10 shows the results of glue bonding feature cast PDMS to a plain PDMS base. The higher spin speeds of 1700 rpm and 2100 rpm were produced better bond that did not affect the features. Spin speed of 3500 rpm for 30 seconds was used with 2g by weight of uncured PDMS with base to curing agent mix ratio of 10:1 for further experiments requiring PDMS glue bonding method.

(a) 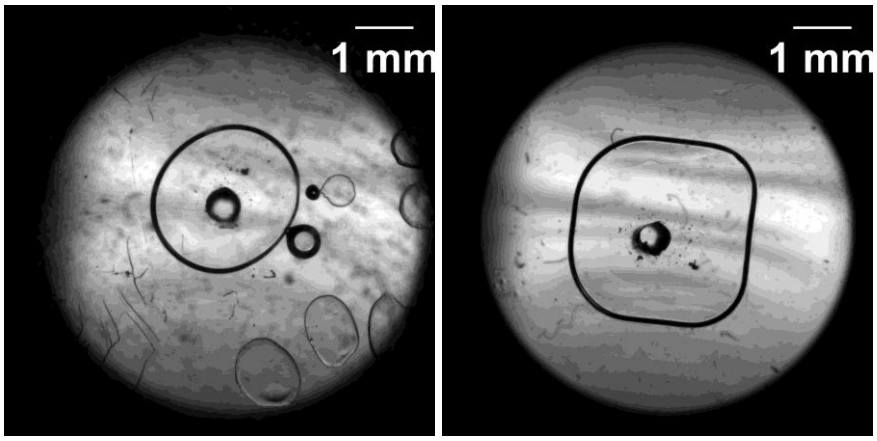

(b)

(c) 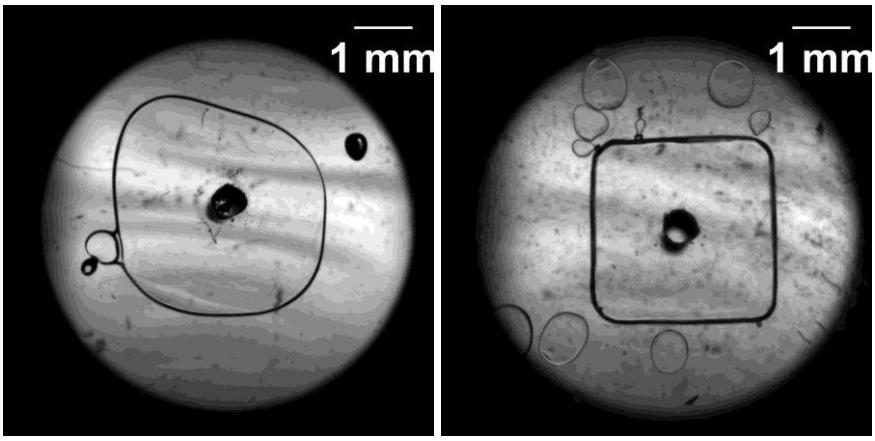

(d)

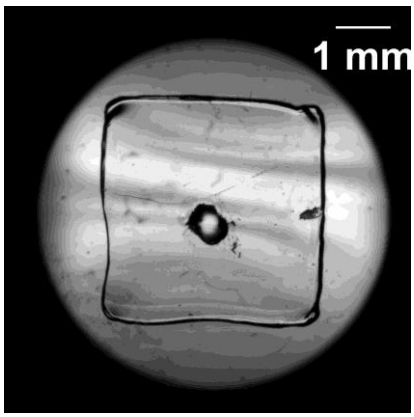

(e)

Figure 5-10: Effect of PDMS Glue Creep into Feature at Different Glue Spin Speeds
The different spin speeds (a) 600 RPM, (b) 1100 RPM, (c) 1400 RPM (d) 1700 RPM and (e) 2100 RPM were used to spin a 10:1 PDMS mixture for 30 seconds after an initial 500RPM for 10 seconds. The thickness of the layer of PDMS glue left after the spin cycle affects the amount of creep into the feature that occurs. Thicker layers allow more creep and the1700RPM and 2100 RPM spin speeds produced cleaner features than the others. In practice, a 3500 RPM was used.

5.2.3.2 Confirmation of Bond Strength

The PDMS-to-PDMS bonding methods were replicated in the lab and the stamp-and-stick method outperformed the partial-cure method. The former could withstand 7 bar air pressure consistently while the later could only take 4 bar air pressure. The mold fabrication process and the PDMS glue bond spin settings are also important considerations while proceeding with PDMS-to-PDMS bonding protocol characterisation. These tests will show how these techniques would hold up with different geometries that will be typically used in the actuation layer.

5.2.4 Effect of Device Geometry on Device Performance

Tests were done to show the effect of larger device geometry on devices made using rapid prototyping techniques such as PDMS partial curing (PC), glue bonding (PG) chemical bonding using Amine-linker (AL) and Chemical boinding using APTES (AC).

It was found that the variation to the bond area did not affect the bond strength of the device for all the permanent bond methods used with the devices PC, PG, AL, AC surviving 3, 5, 3 and 3 Bar air pressure respectively for the various bond contact area tested. This is shown in and Figure 5-11. The test, however, showed that slight effect of actuation area dimensions on the maximum air pressure that could be tolerated by the devices. This is shown in the figure below. This is shown in and Figure 5-11.

Table 5-1: Tolerable Air Pressure with varying bond surface contact width

	16mm^2 Square bond contact width				60mm^2 rectangle bond contact width			
Bond contact area	1	2	3	4	1	2	3	4
PC burst pressure (bar)	3	3	3	3	2	2	2	2
PG burst pressure (bar)	4	4	4	4	4	4	4	4
AL burst pressure (bar)	3	3	3	3	3	3	3	3
AC burst pressure (bar)	3	3	3	3	2	2	2	2

Table 5-2: Tolerable Air Pressure with varying actuation area

	Square actuation area (mm^2)				Rectangle actuation area (mm^2)			
Actuation area (mm^2)	1	4	9	16	10	20	40	60
PC burst pressure (bar)	4	4	3	3	3	3	3	3
PG burst pressure (bar)	6	6	5	4	5	5	5	4
AL burst pressure (bar)	4	4	4	3	4	4	3	3
AC burst pressure (bar)	4	4	4	4	4	4	3	3

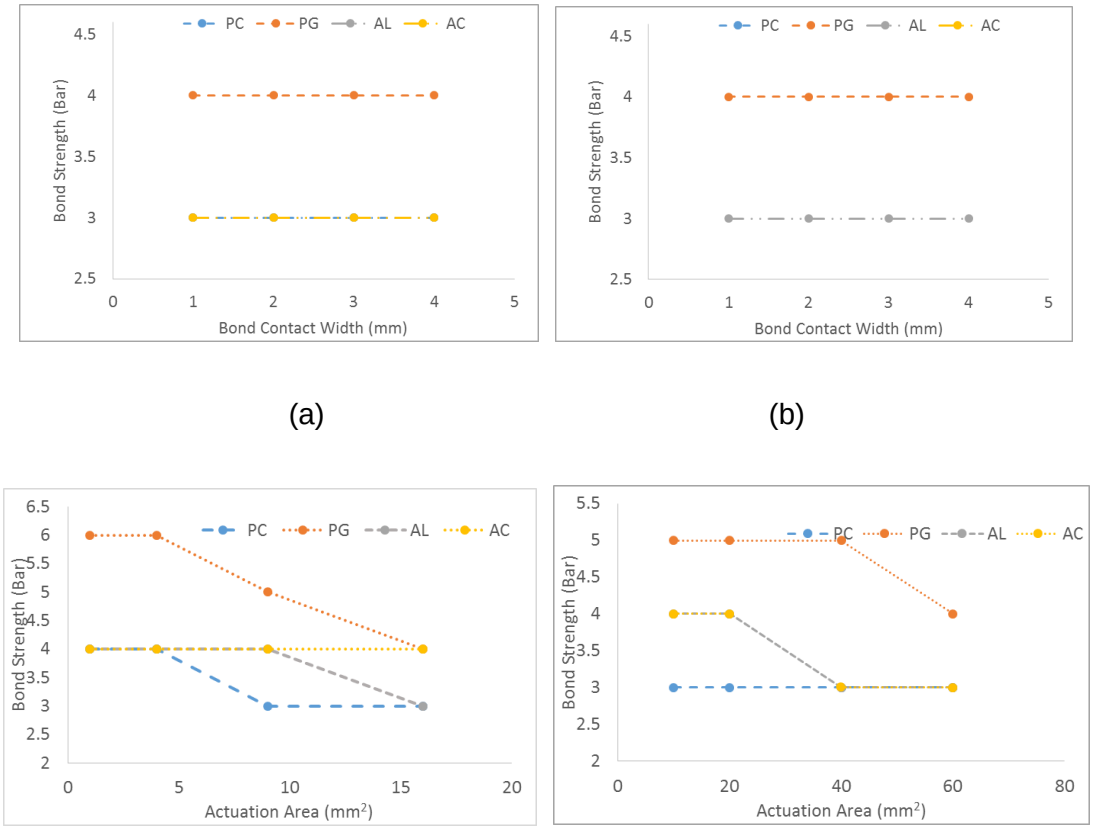

Figure 5-11: Device Geometry Effect on Bond Strength
The devices were fabricated using patterns illustrated in in square and rectangular dimensions. (a) shows tolerable air pressure of bonds using square dimensions with varied bond contact width and constant actuation area (A = 16mm^2); (b) shows the same as (a) in rectangular geometry with actuation area (A=60mm^2). (c) shows results for square geometries while (d) shows results for rectangular geometries.

The devices with larger actuation area in (b) were able to withstand 2 Bar pressure, which was a target constraint for the design of multilayed microfluidic devices that can withstand the air pressure present during repeated actuation cycles. However, some of these devices failed at 3 Bar especially under continuous and repeated actuation cycles. Changes to the surface contact width did not have any added benefit as the devices failed in similar manner and relative time. None of the devices lasted up to 7 Bar as was initially found since they had significantly smaller actuation and larger bond contact area geometries. These results showed that smaller actuation area geometries are preferred for multi-layered microfluidic device

fabrication when implementing features over 0.5 mm dimensions. An inconsistency in bonding success was observed when implementing the partial curing method in comparison with the glue bonding technique. The glue bonding technique performed better and produced consistent bonding results and is recommended for future applications requiring PDMS-to-PDMS bonding.

5.3 Proposed Modular Chip Design

Chip design can be done in a monolithic style assembly where the layers are irreversibly bonded together but an alternative method has been proposed where the actuation layer assembly is reversibly bonded to the liquid layer assembly to reduce the steps taken to make a secondary chip for the same application (Huang, He et al. 2012). While this solution improves the turnaround time for chip development, it does not account for the changes during development of microfluidic cell culture environments. Changes to the cell culture environment could render the entire liquid handling chip obsolete.

A modular chip design is proposed for liquid handling in the Neurophotonics lab. This improves flexibility in usage for different applications requiring drug delivery. It is common place to have a set standard for fabricating biological cell compartments in the lab since the chemistry required in some applications may not be compatible with some fabrication techniques. This modular liquid loading chip decouples the functions available in an on-chip liquid handling system. Sample loading, volume distribution, cell environment, flow merging are made as independent parts and are connected together in hardware and software.

The component parts of the system are illustrated in Figure 5-12 and typical configurations are illustrated in Figure 5-13. The main advantage of the system is the simplicity of the design and practicality for extended use. It is expected that 90% of

the liquid handling requirements in the lab could be achieved with this simple setup. This system heavily depends on software and timing to provide effective volume transport and loading. The software is discussed later.

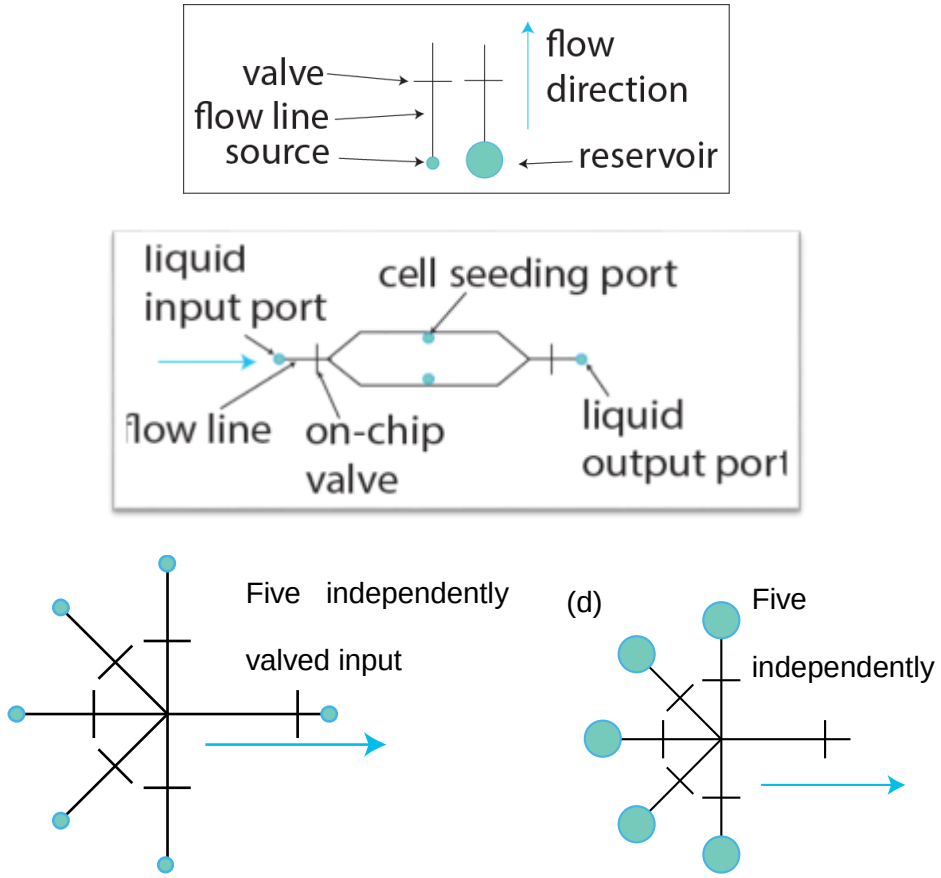

Figure 5-12: Decoupled components for a Liquid Loading microfluidic chip without the cell environment. *These decoupled components will make it easier to decouple the liquid manipulation systems and allow multiple fabrication techniques to be deployed towards realising these integrated systems. (a) shows the description of the patterns in the microfluidic subcomponents. (b) shows a standalone microfluidic device for culturing cells with entry ports and on-chip valves to enable incubation. (c) shows the design for a five-input device with independent on-chip valves and a valve at the output (d) shows the use of on-chip reservoirs as the sources of the liquid.*

(a)

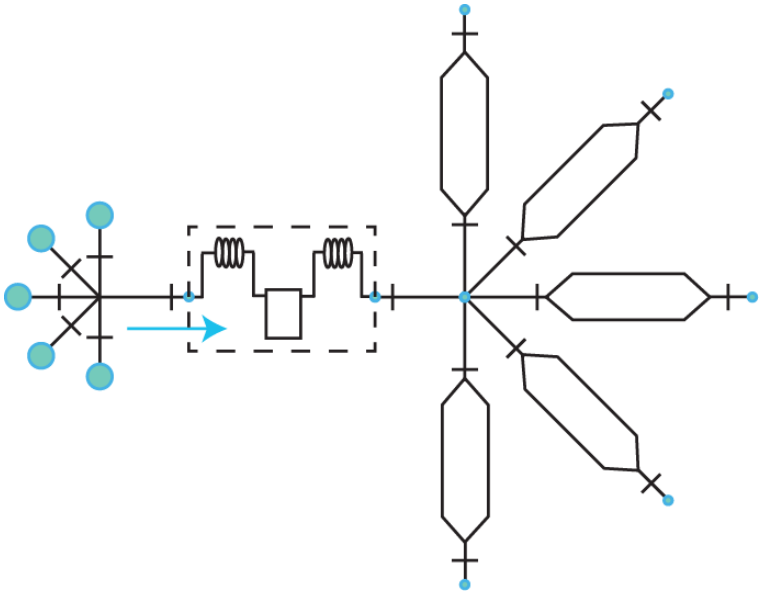

(b)

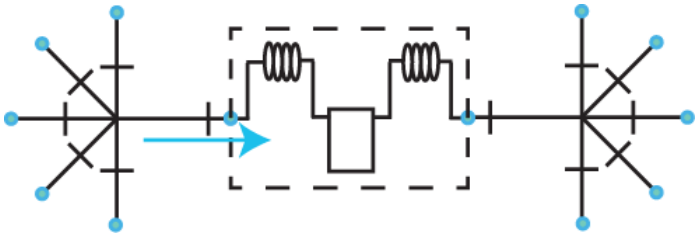

Figure 5-13: Integrated microfluidic chip designs with cell environment and liquid actuation valves
These examples of combined liquid manipulation components demonstrate the integration of these systems without implicit dependence on combined fabrication. (a) shows the use of the on-chip reservoir connected to a flow sensor which connects to a five way culture chamber. (b) shows the use of input sources instead with the flow sensor.

The integration of a flow sensor allows accurate metered control of volumes loaded into the system. A fully functional microfluidic auto-sampling chip has been designed with these modular components in mind. The chip has been designed to allow up to 5 reagents to be introduced to the system, as well as sample products from the microfluidic devices. This autosampler chip is illustrated in Figure 5-14 as (a) a fully integrated system; and (b) as a liquid handling component that can be connected to the microfluidic device.

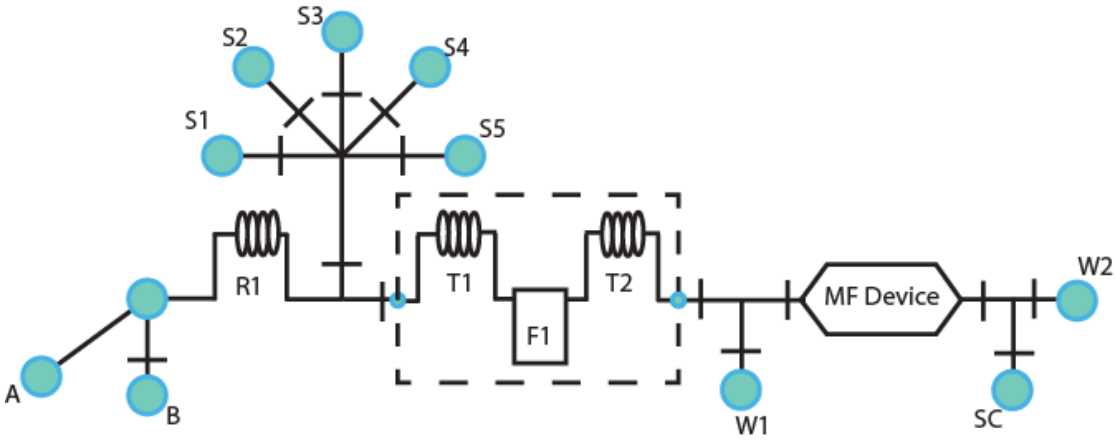

Figure 5-14: Microfluidic Auto-sampler Chip Designed as a Fully Integrated Chip

The design has a microfluidic device (MF Device) integrated with the auto-sampler chip. The Port A is expected to have connection from a liquid pump and B, from a syringe driver for bi-directional flow. The syringe driver will be primarily used for aspirating liquid volumes from any of the samples located at connections S1 – S5 as well as other back directional flow required in the rest of the circuit. The reservoir R1 will hold the loaded samples during the sample loading step. The flow sensor measures flow rate and is connected through Tube 1 (T1) and Tube 2 (T2). The split at this point takes the liquid to the waste container or to the microfluidic device. The microfluidic device is connected via MFD1 and MFD2. On return to the modular chip a splitter leads the liquid to a sample collection (SC) or waste (W2)

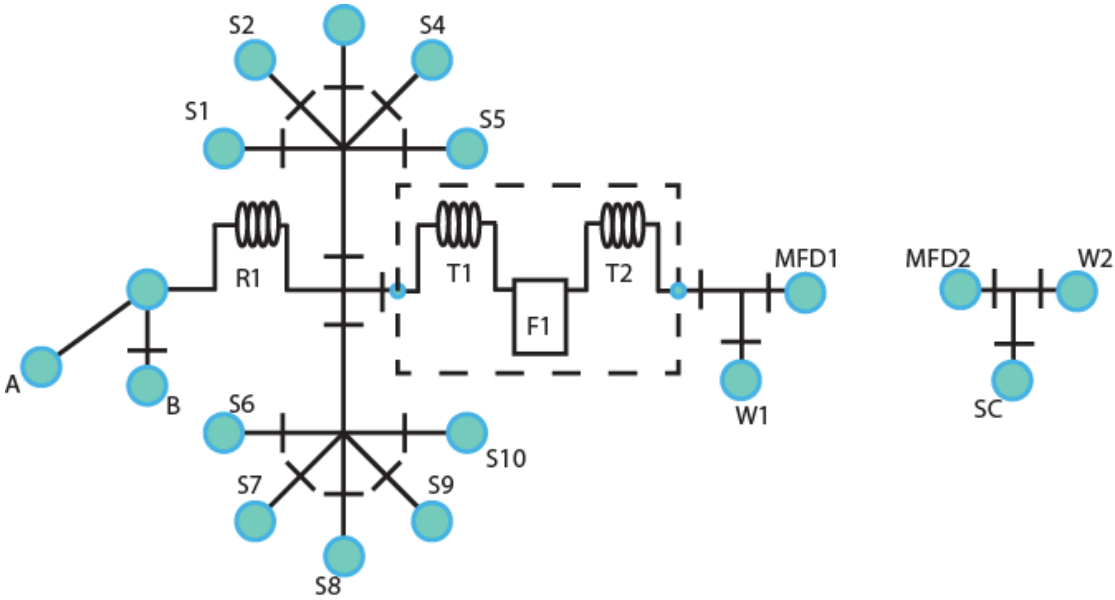

Figure 5-15: Microfluidic Auto-sampler Chip Designed as a Module

The alternative design design allows a microfluidic device to be used external to the auto-sampler chip connected across MFD1 and MFD2. The Port A is expected to have connection from a liquid pump and B, from a syringe driver for bi-directional flow as well as increases the number of sample introduction points. The syringe driver will be primarily used for aspirating liquid volumes from any of the samples located at connections S1 – S10 as well as other back directional flow required in the rest of the circuit. The reservoir R1 will hold the loaded samples during the sample loading step. The flow sensor measures flow rate and is connected through Tube 1 (T1) and Tube 2 (T2). The split at this point takes the liquid to the waste container or to the microfluidic device. The microfluidic device is connected via MFD1 and MFD2. On return to the modular chip a splitter leads the liquid to a sample collection (SC) or waste (W2)

5.3.1 Operation of Proposed Chip

The operation of the designed modular chip will account for sample storage, sample introduction, sample injection, flow control, and volume sampling. In practice, each design step affects the other and a good balance must be reached to ensure all pieces fit together in the most efficient way possible.

5.3.1.1 Sample Storage

The vast majority of applications requiring small volume injections will use pre-loaded pipette tips with typical volume size (v = 100μL, 1000 μL). The design can be used in one configuration using 5 different sample storage points but this can be extended to 10 by modifying the design slightly as seen in and Figure 5-15. Physical dimensions of the pipette tips may limit the possible number placed on a device. The use of pipette tips has the added advantage of being very familiar territory with most life science researchers and technical staff.

The pipettes are loaded with the volumes and plugged into the PDMS top layer at the sample entry point (S1- S5) or (S1 – S10).

Other applications where considerably larger volumes are required may take utilise off-chip volume reservoirs with a tube leading into the sample entry point.

5.3.1.2 Sample Introduction

Each of the sample reservoirs connected are expected to be zero flow connections discounting gravity induced flow which is almost unavoidable. The connections at A, B and W2 in Figure 5-14 and Figure 5-15 will have tubing from a syringe driven flow, pneumatic pressure driven flow controller, and second pneumatic pressure driven

flow controller respectively. The syringe will aspirate samples from either of the sample storage units through the chip into the reservoir.

The specific sample aspirated can be controlled by disabling the corresponding on-chip valves during the aspiration sequence. High precision sample introduction can be achieved by adding a flow sensor before the syringe driver and adding an integration algorithm that indicates the volumes loaded.

Care must be taken to account for the dead volume in the device during the sample intake which is driven by the dimensions of the device. A width by height dimension of 0.5 x 0.08 mm will mean 40 nL dead volume per milimeter of sample introduction channel length. Experience showed that the use of pipette tips required minimum of 20 mm which results in 0.8 μL dead volume. This is equal to a 0.8% dead volume in a 100 μL pre-loaded pipette tip. An extreme case of spacing means that 1.6 μL may be dead volume with 40 mm spacing. This equates to 1.6% dead volume in a 100 μL pre-loaded pipette tip.

The sample introduction step loads the sample into the reservoir R1 which is an external tubing plugged into the chip circuit. The use of external tubing reduces the amount of real estate required to provide on-chip channel reservoirs.

5.3.1.3 Flow Control

The syringe connected to A in the Figure 5-14 and Figure 5-15 will be used to realise bi-directional flow in the device. The pneumatic pressure connections to position B and W2 will also allow bi-directional liquid flow control as well, while using the flow sensor (F1) for realtime feedback.

On-chip valves are required at several positions in the device to ensure that flow only occurs in the intended path defined by the system user.

5.3.1.4 Volume Sampling

Volume sampling downstream of the device will be possible in either configuration presented in Figure 5-14 and Figure 5-15 at the SC position. A pipette can be placed there to collect the ejected volume when the on-chip valve in the area are actuated to allow liquid flow through to the SC position. The operation of the proposed chip includes the aspects of volume handling as desired by the project requirements. Fabrication of the multi-layered devices must be investigate to achieve a development method that furthers the research within the scope of the constraints for modular, easily realisable devices with quick turn-around time despite design changes.

5.4 Fabricating Multi-layered devices

Previous tests verified the bonding techniques that would be suitable for developing multi-layered devices. Proposal for the modular chip design has been presented along with its operation. This section will present the complete assembly process for multi-layered devices using the preferred bonding strategies and show modifications to the process that can be undertaken to optimise the fabrication processes. The section will also compare the fabrication methods with other methods used for fabricating multi-layered devices.

A possible technical to all multi-layered device fabrication techniques presented here is the need for a spin-coater to produce the thin PDMS film for actuation layer which may affect its implementation in poorly equipped research laboratories. Possible DIY alternatives have been proposed previously (Bianchi, Panssiera et al. 2006, Fardousi, Hossain et al. 2013) but have not been assessed thoroughly. Another

solution to this challenge is commercial availability of thin PDMS films but these are made to order and may prove to be more challenging in the long term.

This technical limit cannot be avoided when using the PDMS glue bonding technique for PDMS-to-PDMS fabrication technique but the partial curing method has been demonstrated as a suitable method if performed carefully.

5.4.1 Device Assembly using Chemical Bonding Techniques

The preferred method for chemical bonding required each layer to be treated and then surface activated for strong bonds between the plastic sheets and the PDMS layer. However, this method presents a time costly option for device fabrication if a plasma generator is used. The first step is bonding the bulk PDMS layer to the actuation layer which is followed by bonding the assembly to a thin PDMS membrane. This assembly is then chemically bonded to a liquid layer and finally, the whole assembly is bonded to a substrate, preferably PDMS. Each of these four bonding stages will require 30 minutes for preparation and plastic functionalisation; 20 minute for Plasma activation procedure, 2-5 minutes for general assembly, hole punching. This brings the total assembly time to ~ 4 hours which in practice can be longer due to actual laboratory conditions and logistics. The longer time for plasma activation is due to the preparatory steps for plasma generation described in the Methodology section. A corona discharge lamp/pen would significantly reduce that time to about 2 mins since vacuum pressure is not required.

Reducing these steps would benefit the fabrication process and an opportunity to do so is presented in the low pressure requirements for the liquid layer (typically $P < 200$ mbar) (Huang, He et al. 2012). The fully chemically bonded liquid layer (Thin PDMS-Plastic-PDMS or Thin PDMS-Plastic-Glass) can be replaced with tape bonded liquid

layer (Thin PDMS-tape-PDMS or Thin PDMS-tape-glass) as illustrated in Figure 5-16.

A further reduction in the number of steps can be achieved by plasma activating the plastic sheet along with the bulk PDMS layer and thin PDMS membrane by placing the plastic sheet in an upright position in the plasma generator as described in Figure 5-17. However, actuation holes must be pre-punched and the challenge of alignment must be addressed to successfully realise this option. Another important consideration is the maximum permissible time gap after plasma before the layers are brought into contact.

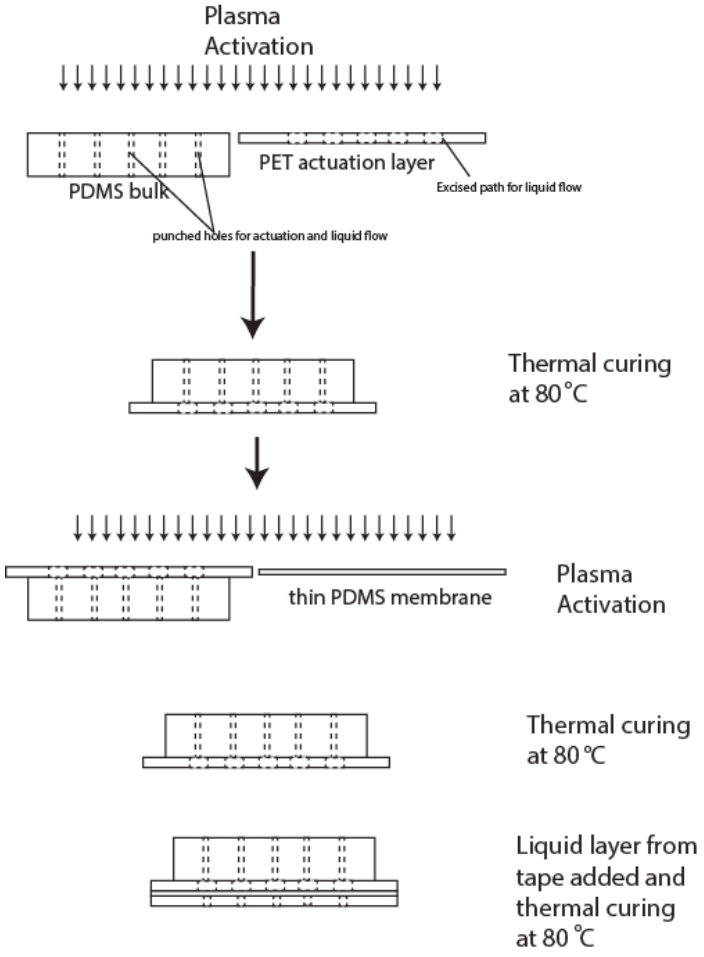

Figure 5-16: Bonding steps for valve actuation section
The steps for chemically bonded devices described. The functionalised PET sheet is plasma bonded to the bulk PDMS layer and the thermally cured at 80 ^{o}C for 30 minutes. The reverse side of the plastic is plasma bonded to the thin PDMS membrane and again cured at 80 ^{o}C for 30 minutes. The liquid layer can then be added as a tape layer.

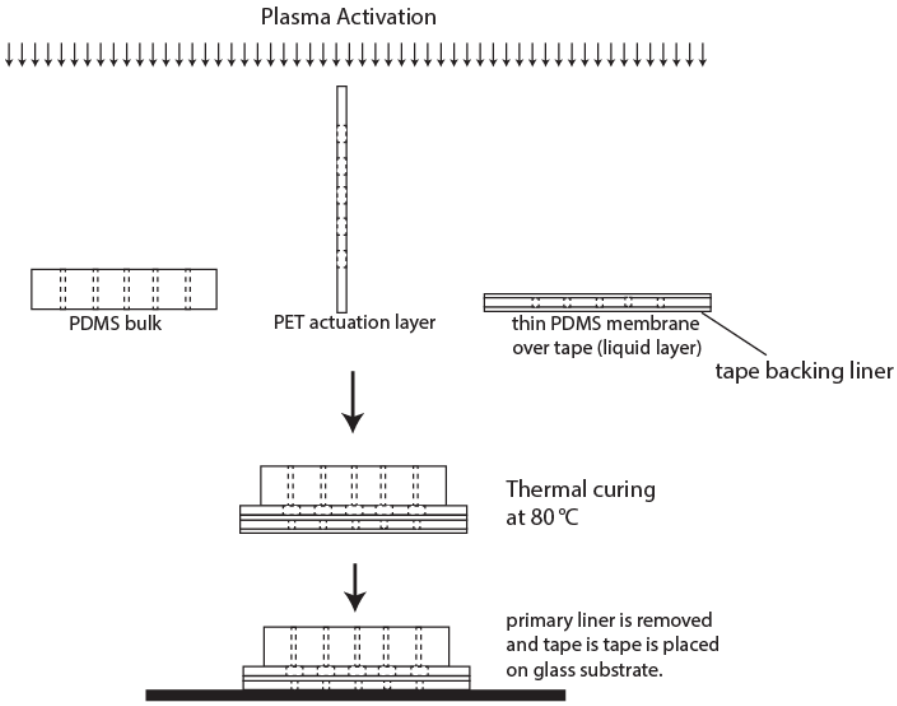

Figure 5-17: One step alignment procedure for hybrid microfluidic chip
A one—step alignment can be achieved by pre-punching the holes for the actuation layer through the bulk PDMS and plasma bonding the bulk PDMS, functionalised PET and thin PDMS membrane in one go. Alignment is not be very difficult to achieve since low resolution features are being used.

5.4.2 Device assembly using PDMS-to-PDMS Bonding Techniques

The assembly process for devices using the PDMS-to-PDMS bonding techniques includes a mold fabrication, PDMS feature casting stage and layered assembly process. The top bulk PDMS layer is bonded to the thin actuation layer. The assembly is allowed to cure first to allow the thin PDMS completely come off the glass layer where it was spun

5.4.3 Fabrication Technique Comparison

It will be beneficial to compare the fabrication techniques with other methods that have been highlighted and are available for developing multi-layered devices. A scale has been adopted to relate these methods in terms of resolution of device features, ease of fabrication, technical expertise required, equipment limitations, practical limitations, res.

5.5 Considerations for Valve Designs

On-chip valve designs were generally considered as NO or NC valves. The doormat style valve as a normally open valves was proposed for larger dimensions since the larger dimension in the actuation layer allows the liquid to flex the membrane sitting on the wall in the liquid layer (Samuel, Thacker et al. 2014). The doormat valve was only applicable when considering PDMS-to-PDMS bonding methods and would present technical constraints if applied with chemical bonding methods. A mask would need to be applied to prevent the membrane from permanently sealing to the wall during bonding process. As such, a normally open valve is more applicable for chemically bonded devices.

A recent study (Samuel, Thacker et al. 2014) proposed a “simple and cost-effective fabrication” of on-chip valves with PDMS material, yet used a laser cutter that removes the cost-effectiveness. The study, however, extends the study to geometry dimensions that are achievable with low resolution craft-cutters. It recommends a range of geometry areas that are suitable based on a theoretical analysis of stiffness and practical experiments checking for valve failures.

It was found that a capsule designs outperform, over the circle and square designs, as they are smaller in one direction. This performance is related to the actual tear to the membrane. Usable area dimension ranges of 1.1 – 4 mm^2, 1.1 – 5.5 mm^2 and 2.5 – 7.2 mm^2 was recommended for valve designs using circle, square and capsule styles respectively. These recommended ranges tightly constrain the usable range in the proposed design since we already established that the mold fabrication with low resolution craft cutters as well as extensive handling limited the minimum feature size possible as seen in the Mold Fabrication Section.

The use of chemical bonding techniques meant that smaller dimensions could be developed in plastic sheets without losing the features during the limited physical handling required with chemical bonding methods and features as small as 0.5 mm could be obtained.

There is a lack of empirical data for on-chip valves in this larger resolution domain which will be beneficial to optimising the on-chip valve designs previously proposed. The use of the low resolution craft cutter may be able to reduce the technology gap faced by researchers who are interested in implementing microfluidic systems.

A matrix (4 x 4) of liquid and actuation geometries was designed in CAD and excised from PET of thickness (t = 80 µm) for actuation layer and double sided tape with thickness (t =80 µm) for the liquid layer as illustrated in Figure 5-18.

The layers for a chemically bonded on-chip valve matrix are shown in Figure 5-19.

Four sets of 16 x on-chip valves were made using different PDMS membrane thicknesses (t = 40 µm, 80 µm, 100 µm, 120 µm) formed by spin-coating PDMS on a glass slab.

The designed experiments would have been able to characterise for the first time, the possibility of liquid handling using low resolution features. However, it was not possible to complete characterisation tests on these alternatives due to limited resources that were originally invested in the macro liquid manipulation system.

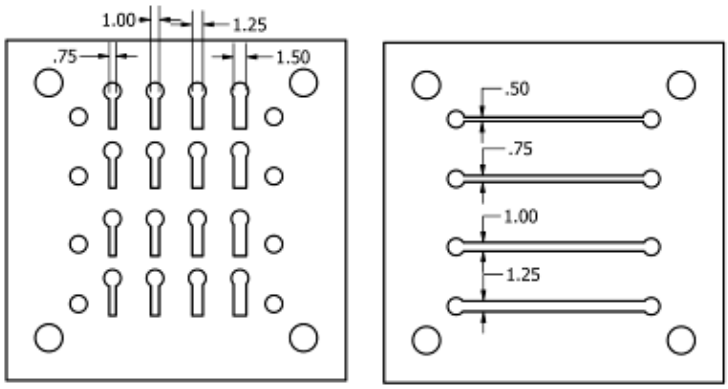

Figure 5-18: CAD sketches of 4 x 4 matrix of liquid and actuation layer

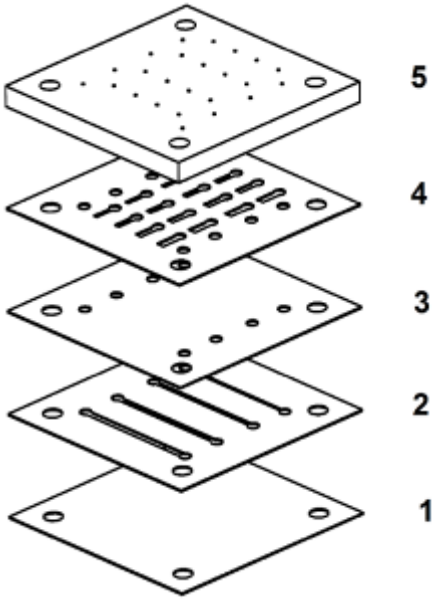

1. Base PMMA or glass substrate
2. Liquid layer made from tape
3. Thin flexible PDMS membrane for actuation
4. Actuation layer made from tape
5. Buik PDMS layer with small orifice to allow tight tube

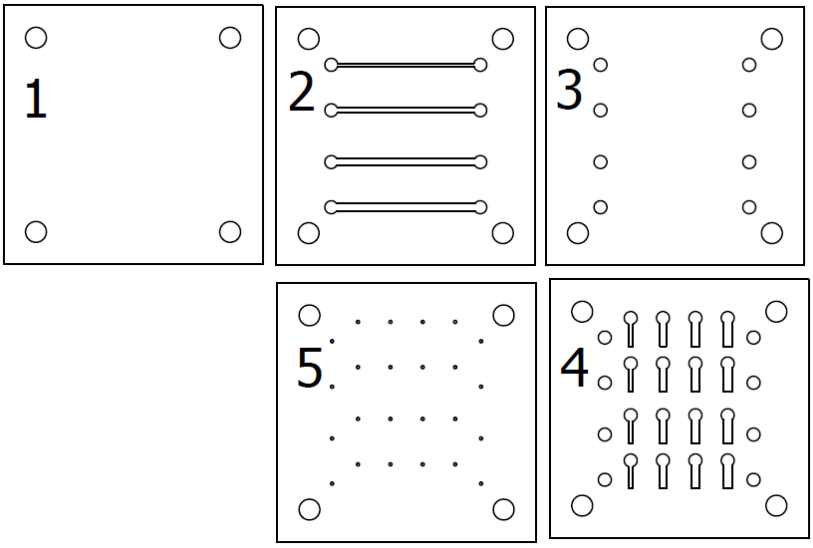

Figure 5-19: Layers for a chemically bonded on-chip valve matrix
The device assembly can use tape adhesion and Xurography to form the fluid layer and bond the device to the substrate.

5.6 Discussion

Microfluidics technology is a useful tool for answering questions involving living cells because it enables the culture of such cells in a controlled microenvironment and the delivery of precise agonist volumes (Streets and Huang 2013). Microfluidics development has recently evolved towards modular interfacing and this section has investigated the feasibility of implementing modular designs with rapid-prototyping fabrication procedures (Liou, Hsieh et al. 2010, Langelier, Livak-Dahl et al. 2011). This modular design view was adopted towards developing on-chip liquid handling components that could be interfaced with a simple microfluidic device to achieve sophisticated fluidic manipulations. Rapid prototyping fabrication techniques were implemented and characterised to determine methods that provided the best device bonding characteristics. The challenge to some laboratories in terms of lack of technical expertise, clean room facility and equipment requirements necessitated the development using these rapid prototyping techniques that did not include SU-8 mold development. An objective was to establish a relatively simple and durable multi-layered microfluidic device that would perform fluidic operations. The available technical tools available were a low resolution craft cutter (Silhouette Cameo), Spin Coater, and Plasma generator. It was assumed that these were fundamental tools required for laboratories venturing into microfluidics.

The use of PMMA slabs to clamp PDMS to tape can improve tape-bond longevity for high pressure applications as seen in the data provided and it has been demonstrated that this is also applicable in non-tape bonded devices (Chen, Li et al. 2013). The challenge with this method, however, is the obstruction to liquid flow when a multi-layer device was assembled. This made it unsuitable rapid prototyping method but could still be a useful tool in research requiring high pressure capabilities (Chen, Li et al. 2013). Chemically bonded devices have been shown to have high

bond strength and can be simple to develop with resources like a plasma generator and spin coater. A clean room facility was not required and non-technical expertise is required. Liquid flow in the channels remained the same as they would in single-layered configuration since compression was not applied to the device surface. The PDMS-to-PDMS method however outperformed the other bonding techniques in terms of ease of fabrication. The major technical requirement is a spin-coater machine and this method is highly advantageous due to the limited requirements.

A liquid handling chip was proposed and an operational procedure was established. This chip is comprised of subcomponents that act as modules that could be fitted together with interconnecting tubing. The simple microfluidic device intended for the cell culture can be connected to these modules for fluidic operations upstream to carry media and agonists to the device as well as perform sophisticated agonist signalling operations. It is expected that the addition of this design and the relatively easy fabrication methods is beneficial to modularity in microfluidics (Yuen 2008, Sin, Gao et al. 2011) and adds to the number of tools available to researchers for developing sophisticated applications using microfluidic systems.

The project objectives to develop an in-house microfluidic technology that could address gaps between the technology development and adoption phases produced a design that had the potential to allow versatile simple development of microfluidic subcomponents as well as integrate these systems. Further research will need to be done to fully develop and characterise these reproducible cheap and relatively easy rapid-prototyping devices to provide information on the actuation pressures for these low resolution solutions such as has been done with higher resolution solutions (Fordyce, Diaz-Botia et al. 2012). This presents the future direction of research for this technology for a more pervasive microfluidic technology adoption.

The results of this research will benefit the wider community of non-microfluidic experts who will only incrementally invest in microfluidics utilising quick fabrication

procedures when available. It will also change the dynamics in the microfluidic community in the following ways:

1. Companies who are invested in delivering microfluidic tools are likely to be able to reduce the costs of these tools if they are widely adopted.
2. Further applications are likely because this system comprises basic microfluidic elements that can be rapidly developed and scaled into much larger systems for more complex tasks.

6. System Integration, Example Applications and Software Development

The project aims to develop, integrate and apply modular liquid handling tools for microfluidic systems required the hardware development as well as software control of component systems which could be integrated. Applications using the developed system was expected to be performed by laboratory users in the primary laboratory as well as third party users with similar demands for liquid handling. This restricted the use of typical liquid handling system development strategies where minimal software development considerations are made. The integrated system is required to be easy to assemble and use in terms of hardware with a user friendly user interface. Concern was given towards the core modularity and ease of integration requirements of the system as well as consideration for future development of these systems. This prompted an investigation into software design methodologies that could be applied towards robust implementation.

Some applications during the research required some of these systems to be functional as singular operational systems to realise specific handling operations like basic flow control, liquid injection and drug gradient moderation. This chapter highlights the Software development efforts carried out to achieve these standalone objectives. It was expected that some aspects of the software design process could be applied towards integrating the hardware components for the designed chip in the "on-chip liquid handling system" section. As such, software implementations towards the integration of hardware components for microfluidic chips were also reviewed.

The schematic for the proposed integrated Liquid handling solution is captured again in Figure 6-1 as a quick reference. It is crucial that the integrated liquid handling system development undertake software design process that will:

- Give users simple, yet adequate control of liquid transport systems such as the custom built pressure control system.
- Enable interface switching using a pre-loaded script or user triggered switching
- Enable single and sequential loading operations using the autoloader
- Integrate the loading system with the interface sweeping operations
- Allow flexibility for interchangeable devices and components (hardware abstraction) which could help increase the usability across a wide range of applications
- Enable easy integration with other laboratory equipment

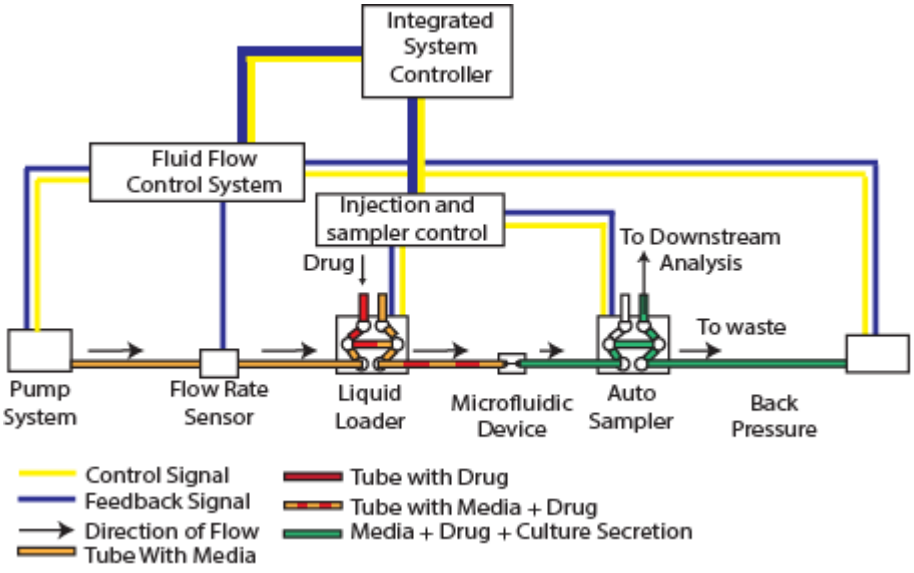

Figure 6-1: Proposed Integrated Liquid Handling System

The ever constant demand for a working system and prototype thwarted efforts at a high level system design from the outset. Initial considerations to develop high level system architecture that allowed for high modularity and flexibility could only be achieved by extensive design process like a waterfall approach often undertaken by software design teams with considerable resources. It was crucial to adopt a more realistic design process that could realise short term goals of independent system control while incrementally advancing the control objectives to include integration.

6.1 Liquid Control System

The final software developed for liquid control allowed basic users to perform simple tasks such as change flow rates, switch the interface for a two inlet microfluidic device manually or with a preloaded script. The user interface was designed to hide advanced controls that could be used to optimise the system performance. Changes to the system performance was observed when the system was deployed with different manifolds. While this is a design issue and could be rectified with better fabrication precision of the manifolds, the ability to use the advanced settings allowed tuning operations to be performed before final deployment.

The front panel of the designed liquid flow control system is shown in Figure 6-2 – Figure 6-4. The system was designed to minimise the controls available to end users and allow further controls as well for advanced users. Typically, the user can modify the behaviour of the system to have more stable response as well as faster responses. The system software operation is implemented using a producer-consumer architecture where one loop logs front panel events (producer) to determine the operation that will be executed by the second loop (consumer). An abstracted state diagram of the process is illustrated in Figure 6-5.

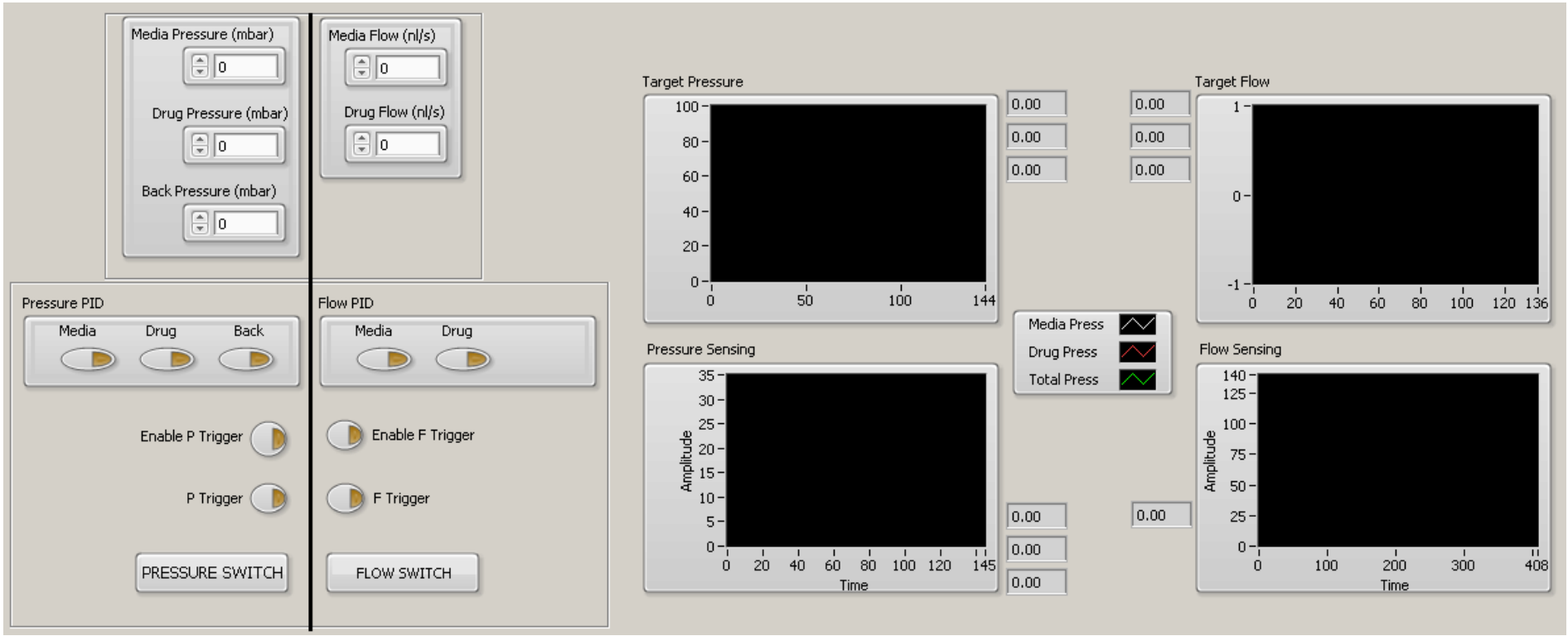

Figure 6-2: Simple view for Flow and pressure control interface

The front panel for the pressure and flow control is designed to give the user a simple interface for controlling pressure in the liquid reservoir or flow rate. This is the primary function of the system and does not need any further abstraction of the settings. It is also important for the user to define the back pressure and enable the automatic PID controller here to allow any other operation requiring automatic control.

Figure 6-3: Advanced view for modification of control system settings

It was expected that most users will not use this view and as such is not engaged by default when the program starts. The option of locking this section has been considered to avoid unnecessary tampering by other basic users of the system and will be implemented during deployment to basic user rigs. The graph displaying current values of flow and pressure is shown (centre) The PID settings here can be modified for flow and pressure (left). The minimum and maximum operating points of the valves in the manifold can also be set (right bottom). The output duty cycles to the valves are also shown to the user (right top).

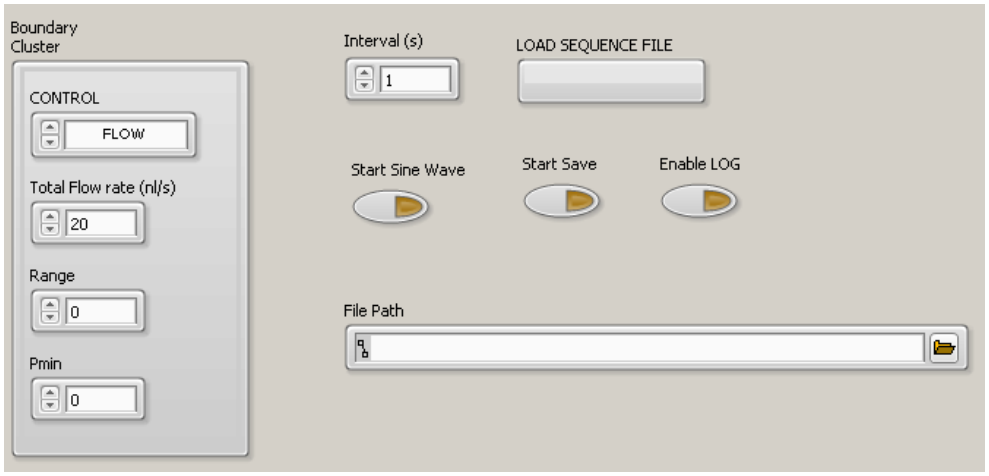

Figure 6-4: Boundary switching operation view

Users are able to load a boundary position file which is comprised of ratios (0 – 1) which controls the boundary position by changing the flow rates at the inputs of the microfluidic device such that they sum up to the Total Flow rate also defined in this view. The range and minimum pressure is used to define the boundary position with pressure control when flow sensors are not connected for feedback control. This later system assumes that the two inputs to the microfluidic device are always identical, a condition which is difficult to realise due to the differences which may exist in dimensions and connections used for tubing. Users are also able to log the flow and pressure data.

+

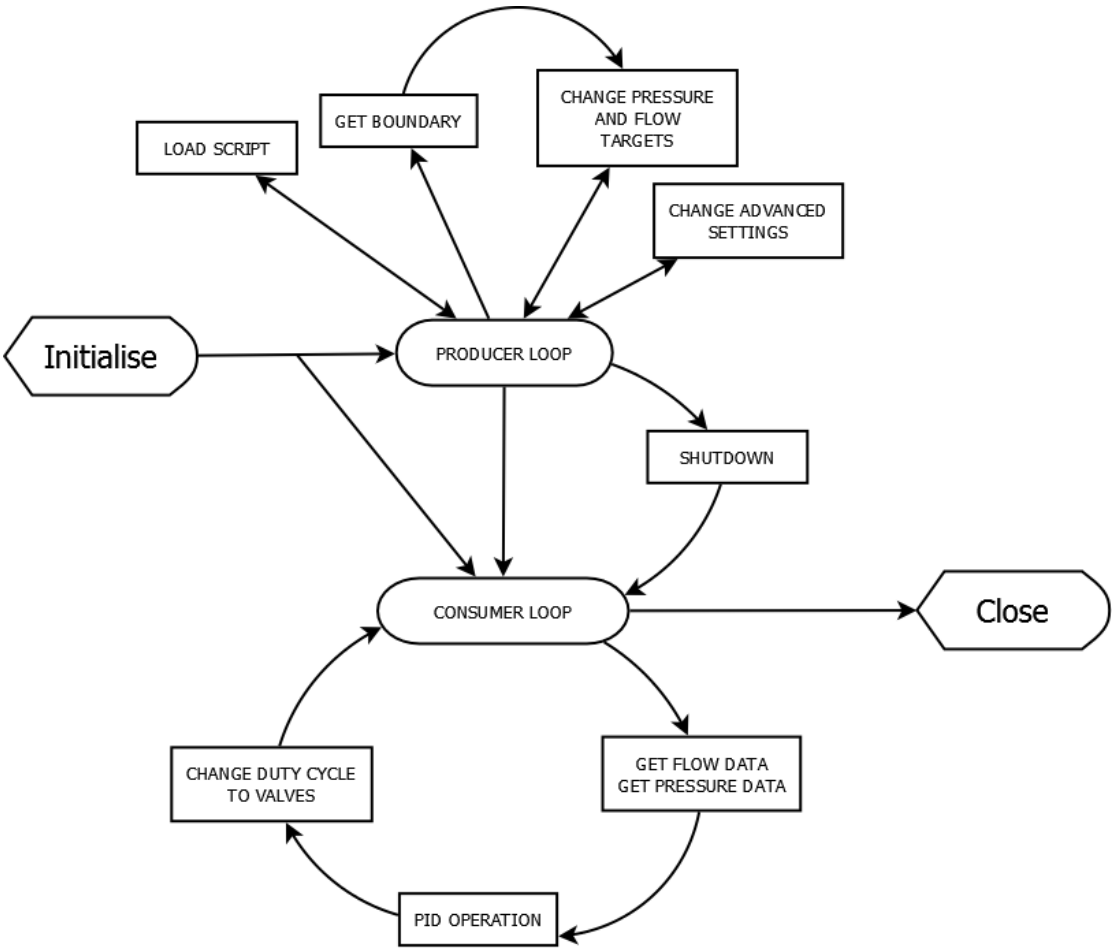

Figure 6-5: State diagram for liquid transport system

The states show the possible transitions between the operations. The actions that cause the transitions are not shown. The load script is activated when the user selects the load script command and the action returns the producer state to the default. The start of the boundary sequence causes the system to first transition to the state where it gets the next specified boundary position that was loaded from the script and then transitions to change the pressure and flow targets. This state always transitions back to the producer loop and the producer loop checks to see if there are more boundary position entries. It also waits the time interval before transitioning to the get boundary state. Under normal flow/pressure control mode, the user can change the front panel flow and pressure targets that will cause the system to transition into the state of changing the targets and then transition back to the producer loop. The advanced settings tab allows the program to transition to the advanced settings state. The producer constantly updates the consumer loop with pressure/flow targets. The consumer loop is a looped sequence of operations that transitions between sensor data acquisition, PID operation and actuator control. The shutdown state is shared by the producer and consumer but is first initiated at the producer loop then transitions the consumer loop to a shutdown which closes the program.

6.2 Liquid Loading System

The autoloader PC program was designed to enable configuration and start of single and sequential drug loading. The software was also designed to inform the user on

the status of the system by reading the status information provided by the autoloader hardware over the RS232 interface.

The front panels for the autoloader hardware and software program is shown in Figure 6-6 and Figure 6-7 respecitvely. The software program has buttons for run, stop, flush, hold, reset and quit. The VISA In allows the user to select the communication port used for the communication. The file number is the default load sequence file that will be loaded when the sequence load button is pressed. Figure 6-8 shows the dialog box for the sequence load settings that pops up when the user selects the sequence load button. This allows the user to define an infinite sequence of load operations and delays between the load operations. Typically, the set delay should be enough to allow the loaded volume leave the autoloader injector at the flow rates used in the experiment. The formula in Equation 6.1and Equation 6.2 were used to determine the minimum delay time, T_d, for a load volume, V, and a flow rate, Q. The added time (10 mins or 20 mins) was expected to compensate for longer volume plug length in the tubing which occurs due to dispersion. The system operation is executed by a finite state machine described in the state diagram in Figure 6-9.

$$T_d = \frac{V}{Q} + 10\ mins\ when\ Q < 50\ nl/s \qquad \text{Equation 6.1}$$

$$T_d = \frac{V}{Q} + 20\ mins\ when\ Q > 50\ nl/s \qquad \text{Equation 6.2}$$

The program can collect the loading sequence from a file containing “comma separated values” (*.csv) which defines the vials to load from, the volumes to load, the delays between the steps and the number of times to flush the system after the step. The program currently supports loading 1 file but can be quickly modified to support up to 10,000 loading sequences.

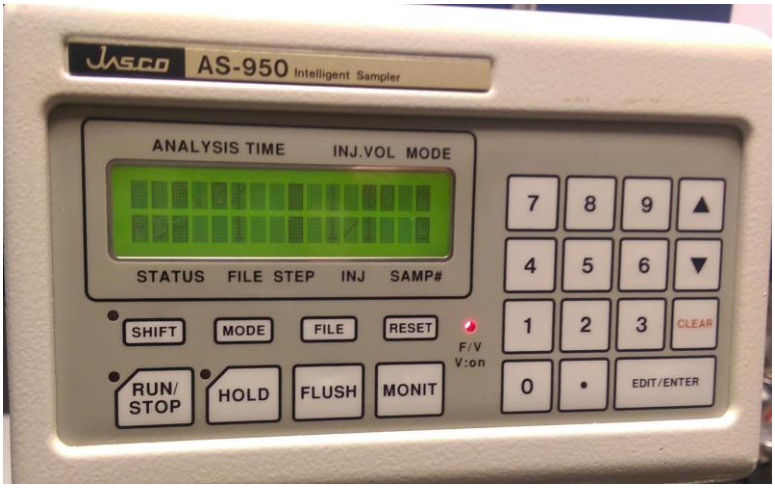

Figure 6-6: Autoloader Hardware front panel
The user interface of the autoloader allows the user configure the operations of the loading system and can be used to define long term processes.

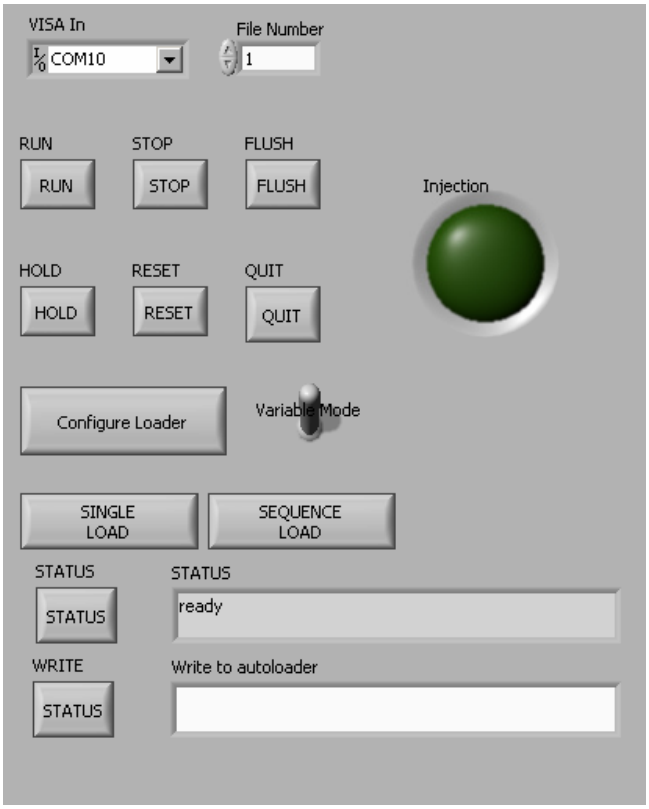

Figure 6-7: Autoloader program front panel

The communication port for interfacing with the autoloader device is defined in the software front panel which also contains some of the common commands found on the autoloader front panel. Advanced settings can be configured on the dialog box that pops out when the Configure loader button is pressed. The sequence load button allows the user to load up a sequence file that defines the vial to be sampled, volume to be sampled, the number of flush operations after the load, and the time delay before the next load operation.

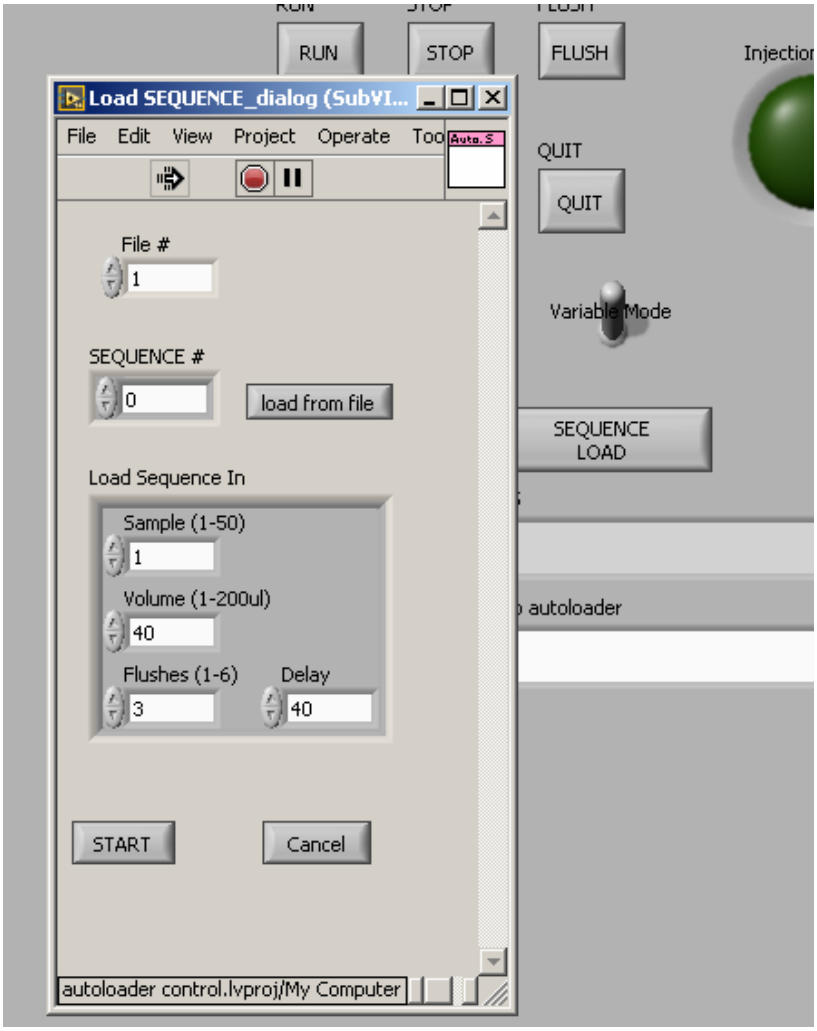

Figure 6-8: Dialog box for sequence load settings

The sequence load button loads this dialog box to enable the user define the loading operations to be carried out. The user can also load the sequence from a text file which contains tab separated values. The software currently allows the user to define 4 files but can be extended to have an infinite list.

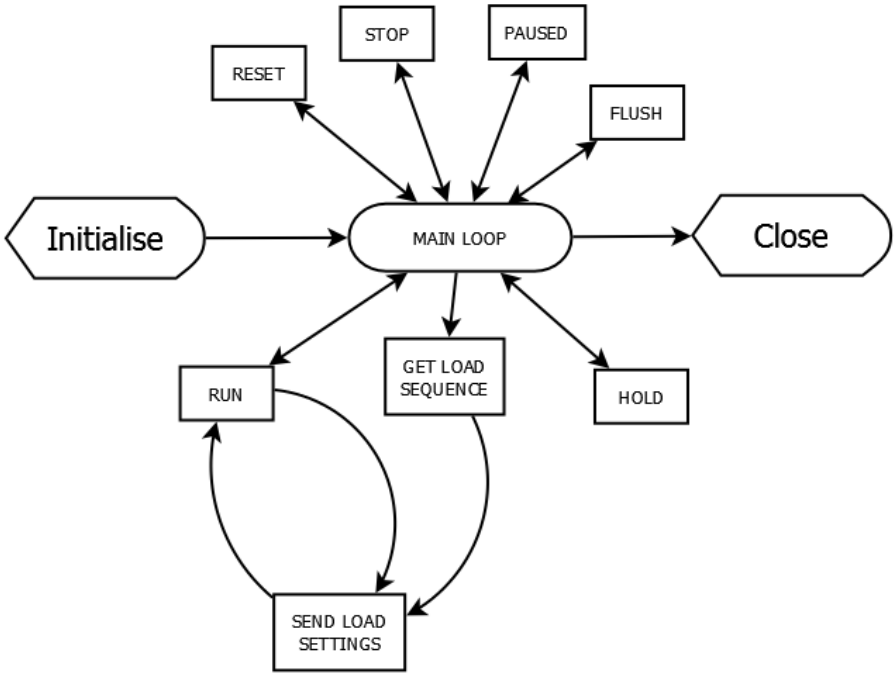

Figure 6-9: Abstracted state diagram for Autoloader program

The abstracted states in the finite state machine that runs the autoloader are usually triggered for an instant by a button press and returns to the main loop. The "get load sequence" state transitions to the "send load settings" which then transitions to the "run". The run executes and loops back to the send load settings as long as there are more steps to be executed.

6.3 Integrated Liquid Transport and Loading (ILTL) Software

The design of the integrated system has been done to allow coupling of the loading operation and the interface switching capabilities of the flow control system. Typically, the user has control of either interface responsible for the operation but this prevents the user from performing long term tasks that may require high level of synchronous activity. A script will be used to define a load operation step and the boundary position at times intervals after the load step. In the first iteration, the user must have constant knowledge of the expected concentration profile when a drug volume is loaded into the device at a flow rate. The user will set the time at which the system will shift the interface of the two input liquid as seen in an example script in Figure 6-10. The state diagram showing the operation of this system is shown in Figure 6-11 respectively.

Initial flow	initial b.pressure	initial boundary position			
60	70	0.1			
operation	Wait	boundary position	total flow rate	back pressure	delay
operation	wait	vial	volume	flush	delay
vol	0s	1	5	2	10 m
int	0s	0.1	60	70	1 s
int	0s	0.9	60	70	1 s
int	0s	0.1	60	70	1 s
int	0s	0.9	60	70	1 s
int	0s	0.1	60	70	1 s
int	0s	0.9	60	70	1 s
vol	0s	1	10	2	10 m
int	0s	0.1	60	70	1 s
int	0s	0.9	60	70	1 s
int	0s	0.1	60	70	1 s
int	0s	0.9	60	70	1 s
int	0s	0.1	60	70	1 s
int	0s	0.9	60	70	1 s

Figure 6-10: Example script for integrated transport and loading operations

The first two rows define the initial flow control system state but an option is available to the user to ignore this initial state and use the state active before the script was loaded. The next two rows show the format/syntax for populating the script. The rows after these descriptive rows set the operation as volume loading, wait time before executing the step, autoloader vial to load, volume to load, number of flush steps and delay after loading before moving to next operation respectively for the "vol" operation. The row starting with "int" sets the operation as interface switching, the wait time before the switching step, the boundary position (ratio between drug to media presence along channel width), the total flow rate, the back pressure and delay before moving to the next step respectively.

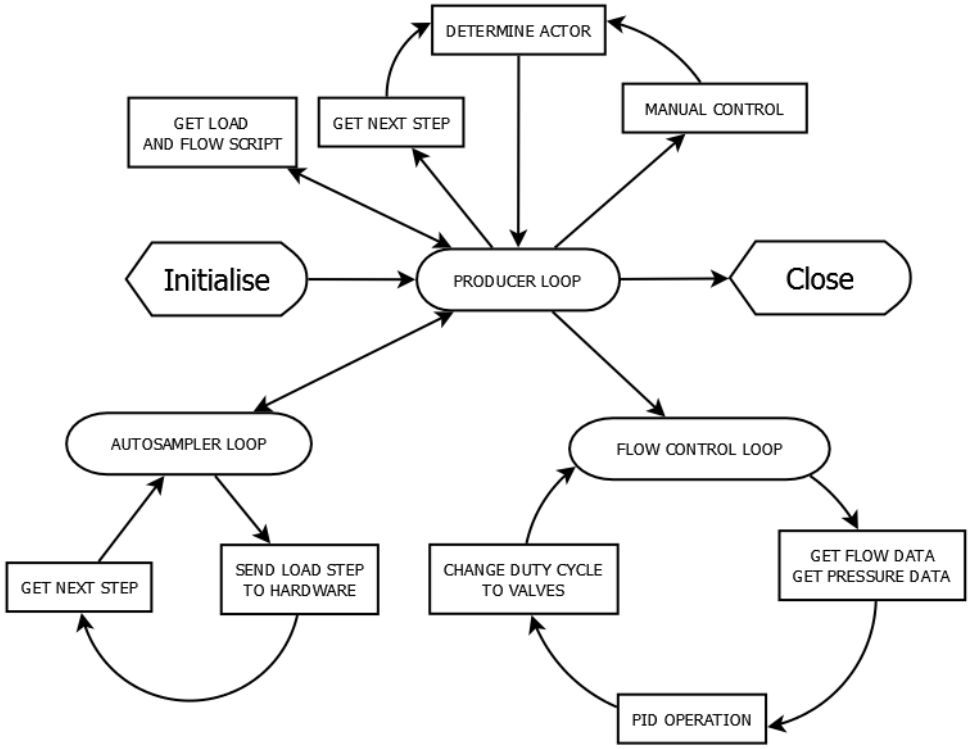

Figure 6-11: Abstracted state diagram for operation of integrated liquid transport and loading
The system applies the desired operations by effecting the operation on the required actor. The actor term refers to the components that perform the actual operation. This level of design is closer to the actor framework which relies heavily on the interface available from the autoloader and the flow control system.

The second iteration, is expected to track the volume of the drug and the concentration profile and allow the user perform interface sweeping operations with minimal knowledge of the concentration profiles. This second iteration requires long term characterisation of different fluorescein concentrations under different conditions such as tube dimensions. An interpolation of the data will allow the program predict the expected concentration profile and allow the user define the sweep operation over the concentration profile expected.

The integration of these systems in software represents the immediate future direction of this research in addition to the completion of a more suitable off-chip liquid transport system. The system will require analytical knowledge of the system under several characterising properties like tube length, diameter, volume loaded, and concentration. Figure 6-12 shows the intensity of the volume detected

normalised over the expected intensity. In this case, different volumes of a 1330 μM fluorescein concentration solution was loaded.

A COMSOL model has been simulated to show the concentration at the drug input, centre and output of a y-shaped microfluidic device when a realistic drug pulse is introduced. This drug concentration profile has been obtained in an experiment to determine the effect of the autoloader by comparing the detected intensity to the expected intensity when the drug flows through the detector without mixing such as in Figure 6-12. The channel positions simulated in COMSOL are shown in Figure 6-13 and the COMSOL results are shown in Figure 6-14. The results show the potential for flexible drug delivery using the system that can perform fast switching with varying drugs input.

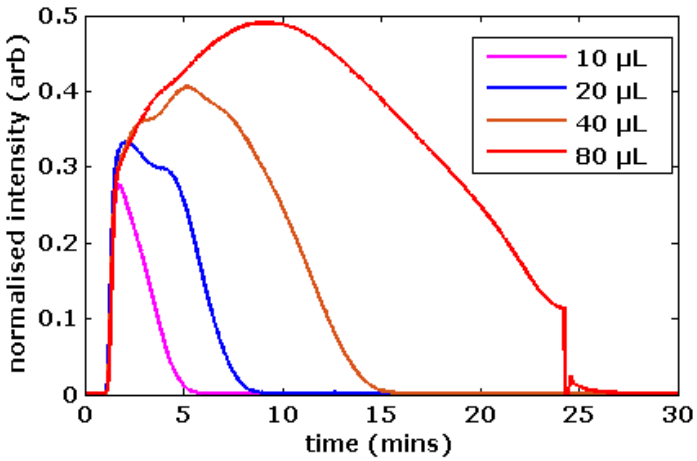

Figure 6-12: Typical preliminary data that is required to develop fully integrated system
The data shows intensity of loaded volumes using an autoloader normalised to the peak intensity obtained when flowing the same concentration through the detector. An extensive collection of this data is required to extract information such as arrival time, effective drug exposure over the possible flow rate regimes possible by the system and different tubing characteristics. The information can then be plugged back into the developed integrated software to provide better control of the drug delivery system.

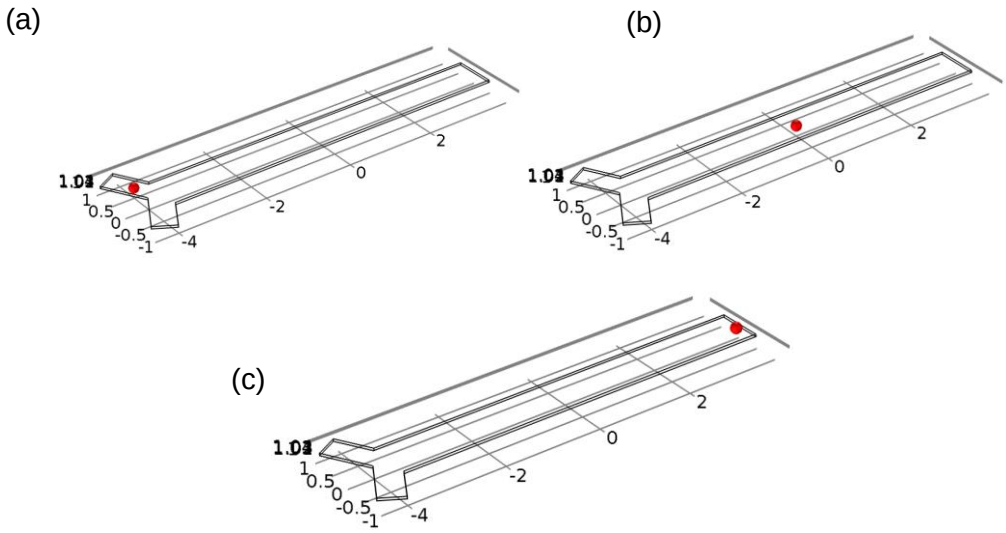

Figure 6-13: Simulated positions in a microfluidic device for combined liquid injection and interface sweeping in COMSOL

A Y-shaped microfluidic device was simulated in comsol to visualise the concentration profile in the channel when a drug is loaded with a realistic drug profile. The concentration profile was obtained for the positions (a) drug entry, (b) channel centre, and (c) output of the channel.

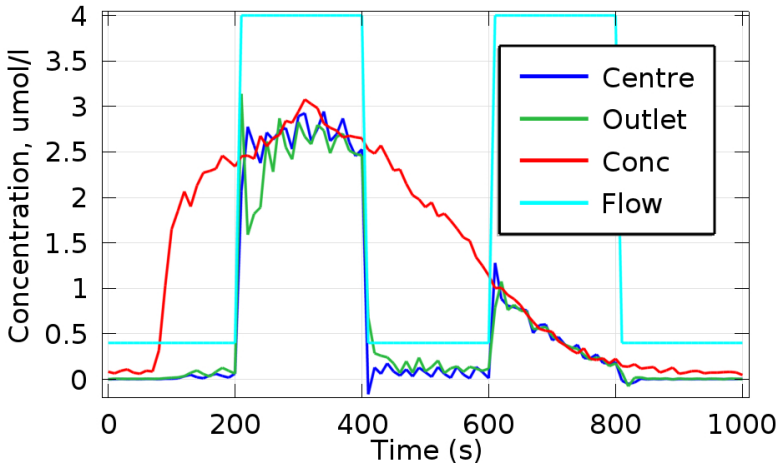

Figure 6-14: Rapid interface switching operation with realistic drug concentration input in COMSOL

Conc represents the actual drug concentration at the input of the drug input line. The Flow is the flow rate of the drug channel which is alternating between 8 and 80 nLs^{-1} while the media channel flow rate is alternated to maintain a total flow rate of 88 $nL.s^{-1}$.

6.4 Application Demonstrations

Some of the systems developed during the system development have been applied as liquid handling solutions. This includes the provision of a fully automated user interface for liquid transport, liquid loading and spatio-temporal control of drugs within a microfluidic device. Syringe driven flow and pneumatic pressure-driven liquid flow are currently being used in a series of collaborative experiments designed to identify optimised environments necessary for long term neuronal culture development in microfluidic devices. The pneumatic pressure-driven flow system was also used as a system that monitored response of hex cells to varying drug concentrations in a microfluidic device. The integration of the custom pneumatic pressure-driven flow and commercial autoloader for sequential reagent delivery was demonstrated in an immnunocytochemistry protocol. It is also being used in the lab as part of another collaborative work to identify neuronal culture distribution due to surface chemistry on the substrates used for the culture. Previous experiment had been undertaken to show the performance and it was only required to show that the cells could be stained with this method. Further work on an integrated software produced a system capable of utilising available commercial or custom-made components and subsystems to achieve spatio-temporal drug control in microfluidic devices as previously discussed in the Software Development section. This was demonstrated in an experiment that integrated the autoloader and the pneumatic pressure-driven flow control system allowing the user to change the drug applied to the system; change the target device for the drug and finally change the spatial distribution of the drug in the target device.

6.4.1 Optimisation of Neuronal Culture Environment

Efforts towards the optimisation of culture environment for neuronal cell culture is being undertaken in collaboration with other researchers (Hala Dowre, Houda Sahaf,

Alexander Johnstone). Chemically treated surfaces will be examined to identify optimised surfaces for neuronal culture growth and development in channels.

A liquid transport system is required to allow simultaneous reagent delivery for live-dead stain assay to six microfluidic devices containing neuronal cultures at 1 DIV, 5 DIV and 9 DIV. A five-way distribution valve has been developed on-chip using the hybrid fabrication technique with tape liquid layer discussed in the on-chip liquid handling system section and chemically bonded actuation layers. The experimental setup connects a Propidium-Iodide filled syringe and a Calcein AM filled syringe on two syringe drivers to inputs on the valve illustrated in Figure 6-15.

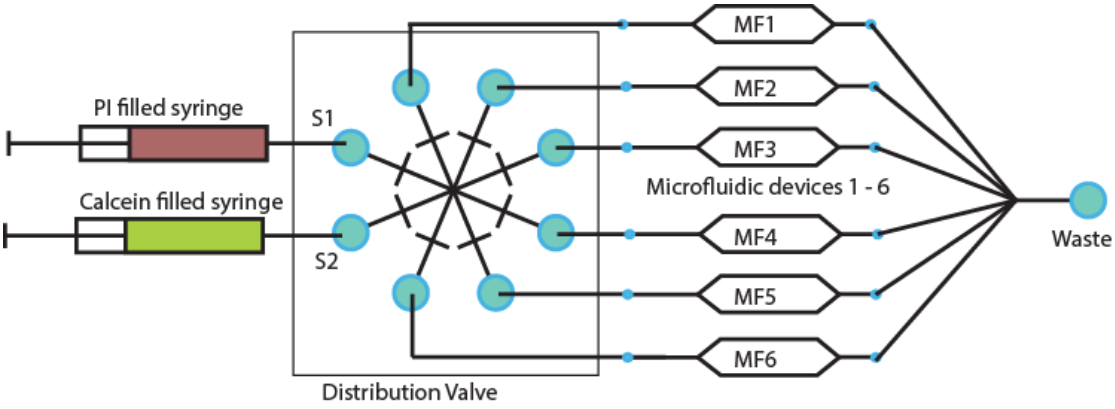

Figure 6-15: Experimental setup to load different reagents into different microfluidic devices.
Syringes containing Propidium-Iodide (PI) solution for dead-staining and Calcein AM for live-staining are connected to inputs of a distribution valve which also connects to six microfluidic devices with different chemically treated substrates.

The on-chip valves were actuated with a pneumatic solenoid valve (SMC SY series) connected to a pressure source. A Quick check showed that 1bar actuated a thin membrane with thickness of 200 μm sufficiently to seal a flow channel of 0.5 mm and height of 80mm. The solenoid valves are powered by 12V so a data acquisition device (NI 6008) was used to provide 5V digital trigger to an amplification circuit (same type used for controlling the proportional air valves for liquid control) to output the 12V required. The software defined control system is able to adapt to connected

components and can just as easily perform the operation with pneumatic pressure driven flow controllers replacing the syringe drivers. The software was modified to enable a timed sequence and output the digital signals to actuate respective on-chip valves. Users can define time dependent states for the flow at the inputs as well as the on/off status of the on-chip valves.

6.4.2 Immunocytochemistry

A simple labelling protocol was carried out to demonstrate the use of the integrated system for sequential agonist delivery to microfluidic devices. This was done to after extensive tests were done to show the capabilities of the loader for volume injection. The parameters used were defined using the drug exposure times required for an immunocytochemistry protocol shown in Table 6-1 and the effective drug exposure times calculated from the analysis of the sequential delivery of fluorescein concentrations in previous experiments. The parameters used defined the flow rates and volumes to be loaded and are shown in Table 6-2.

Table 6-1: Incubation times and steps used to obtain volume program for automated immunocytochemistry protocol

Step	Duration
Wash with phosphate buffered solution (PBS)	2 minutes
4% paraformaldehyde in PBS	20 minutes
3x wash with PBS	10 minutes
0.5% BSA with 0.1% Triton-X (blocking solution,BS)	30 minnutes
Primary antibodies in BS (1:200)	2.5 hours
3x wash with PBS	10 minutes
Secondary antibodies in BS (1:400)	1 hour
Wash with PBS	5 minutes

Table 6-2: Programmed Instructions to the autoloader and flow controller to achieve desired exposure times for immunocytochemistry protocol

Fluid	Volume (µl)	Flow rate (nl/s)	Estimated exposure time
Media	10	30	10
PBS	-	30	10
PFA	20	30	20
PBS	-	30	10
BS	30	30	30
Primary	60	15	120
PBS	-	30	10
Secondary	60	30	60
PBS	-	30	5

The images from the staining protocol are shown in Figure 6-16 which indicates the presence of astrocytes (red) and neurones (green) in the culture.

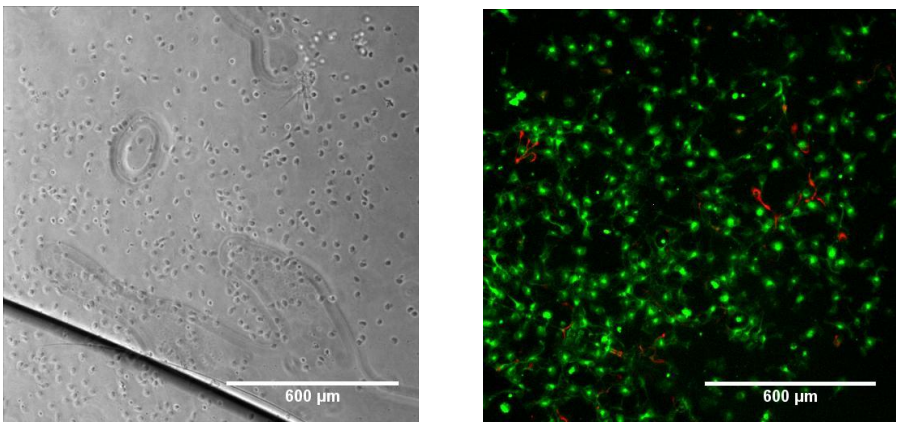

Figure 6-16: Imaging results of automated immnunocytochemistry protocol
Immunocytochemistry protocol was automated to label neurons and astrocytes in a microfluidic device. This was carried out to demonstrate the capabilities of the autoloader for sequential liquid injection. The images show x10 images of stained cells in a microfluidic device 7 DIV.

6.4.3 Calcium Signalling in Hek Cells

The software developed for liquid transport was used in an alternative agonist delivery application on cultured cells in a Y-shaped microfluidic device. The software development methods implemented resulted in a user-friendly and effective tool that was applied to dynamically control the concentration of receptor agonists delivered to Hek293 cells and cerebellar astrocytes.

The challenge was to assess how much information cells retain of temporal distribution of dynamic stimuli using neurotransmitters and hormones. A Y-shaped microfluidic device was employed with two flow control systems upstream. The flow controllers were used to deliver receptor agonists to cultures in the microfluidic device over varying time courses. The calcium signalling response to the delivery patterns were analysed to find out if the stimulus dynamics were encoded in the calcium spike patterns.

The limited temporal resolution in the spike train analysis for individual cells made it difficult to reconstruct the causal stimulus. However, a population analysis showed that the response could be used to efficiently track the temporal drug concentration patterns. This showed that the information from a cell network is likely to contain more information about signalling networks and information processing in the cells.

6.4.4 Combined Sequential Injection and Spatio-Temporal Drug Distribution

This example application connects the autoloader with the liquid transport system to a two-input microfluidic device as illustrated in Figure 6-17 and shown in Figure 6-18. The system is an improvement to the system used to examine Calcium signalling in Hek cells since any number of drugs can be input to the device. It also has the ability to run for hours without supervision.

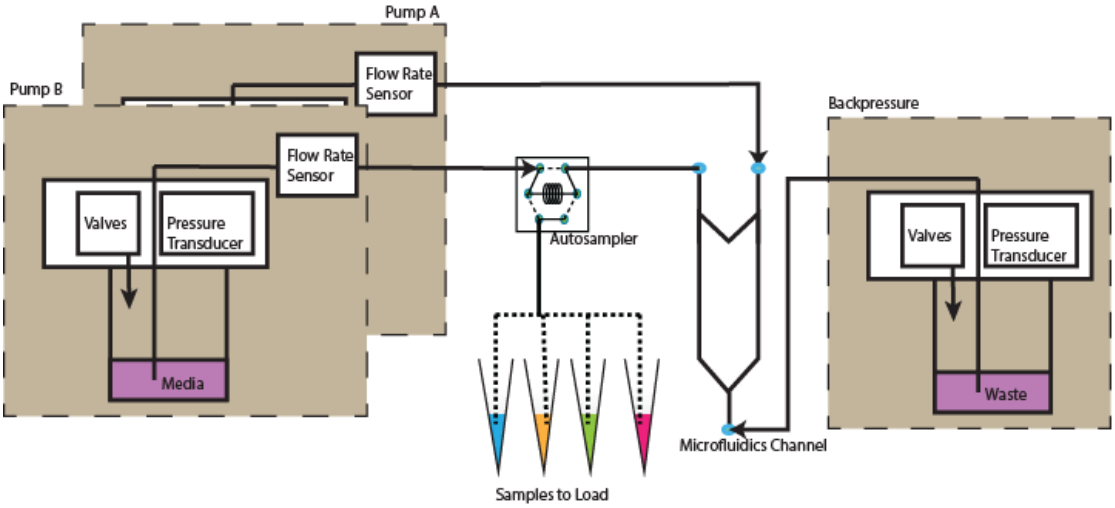

Figure 6-17: Combined Sample Loading with Spatio-Temporal Drug Delivery

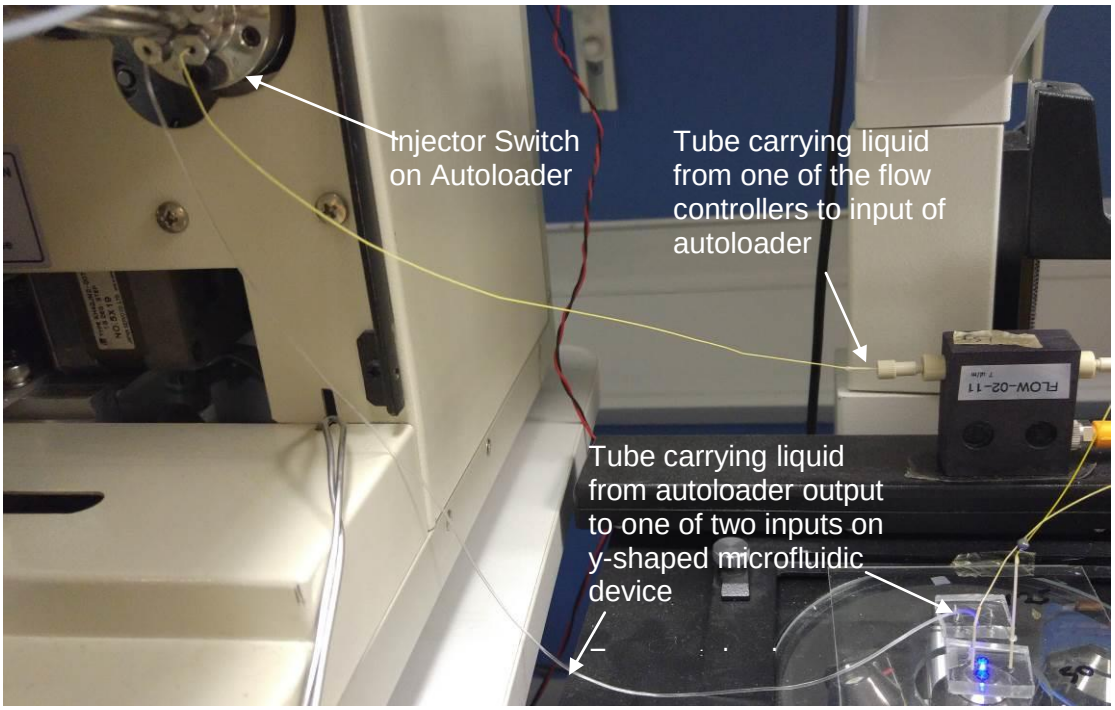

Figure 6-18: Image Showing Connection to One Input of Microfluidic Device Through Autosampler

This alternative system can be used to examine effects of different drugs, different concentrations of these drugs as well as the impact of the spatio-temporal distribution of the drugs in the microfluidic device. The biggest advantage of this setup is that all of these assessments can occur on the same culture without reconnections of the tubing which may introduce bubbles and kill the cells. It is however, more

complicated to make this possible in applications where the drug is only required for at specific time intervals since the line must be in continuous flow to get the drug to the input of the device. This challenge was solved by adding an alternative flow path at the drug inputs of the microfluidic device as illustrated in Figure 6-19. The alternative flow path is setup with on-chip valves system to allow flow bypass the microfluidic cell chamber.

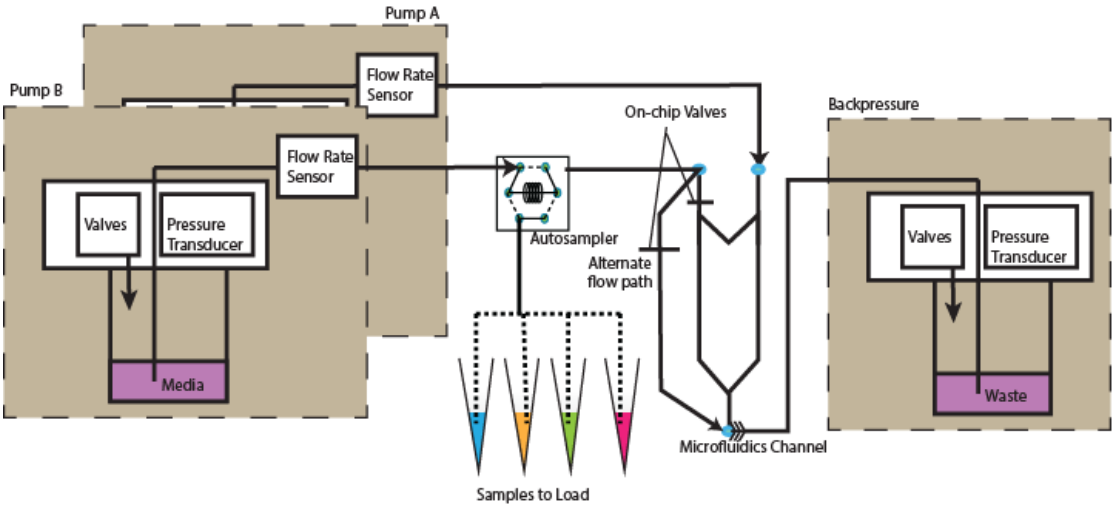

Figure 6-19: Alternate flow path added to microfluidic device

A script, similar to one in Figure 6-10 is used to determine system operation. The user is required to know the times required for the loaded drug to reach the drug input of the microfluidic device and put that into the script. The script includes settings to decide what flow path to use, flow rates of the Pump A and Pump B as well as back pressure settings. The script required for this operation is shown in Figure 6-20.

Pump A flow rate	Pump B flow rate	initial b.pressure	initial boundary position		
60	1	70	0.1		
f.controller operation	wait	boundary position	total flow rate	back pressure	delay
Autosampler operation	wait	vial	volume	flush	delay
Switch operation	wait	path (d/w)	n/a	n/a	n/a
swt	0s	w			
Pump A rate	60				
Pump B rate	100				
vol	0s	1	5	2	10m
Pump A rate	60				
Pumpt B rate	1				
swt	0s	d			
int	0s	0.1	60	70	1s
int	0s	0.9	60	70	1s
int	0s	0.1	60	70	1s
int	0s	0.9	60	70	1s
int	0s	0.1	60	70	1s
int	0s	0.9	60	70	1s

Figure 6-20: Improved script for integrated Transport and Loading System

This system will be applied to the delivery of neuromodulators at different concentrations within relevant time scales. However, this system also requires optimisation to reduce the amount of information the user needs to put into the script. It is currently able to load multiple sequences and switch as defined by the script but more work is required to abstract the operations so the users can define higher level functions. An example of such functions is the description of drugs used in each vial to allow the users continue the experiment with that knowledge rather than the vial number which may add confusion. This descriptions will be done at the start of the script. An example of a target script is described below.

*Script Start

*Parameters
Vial1 – 0. 5µM dopamine
Vial2 – 0.25µM dopamine
Vial3 – 0.125µM Charbacol
Pump A – Syringe Driver – Media
Pump B – Punematic – Media to loader
Loader type – Jasco

* Operation Start
load 0.5µM dopamine
delay 10 mins
switch drug to device
interface 90% drug 1s
interface 1 % drug 1s
*Operation End
*Script End

These examples are simple demonstrations of the integrated liquid handling system developed with an agile software design methodology. These demonstrations utilised the commercial autoloader. Integration of on-chip components for microfluidic applications will require more extensive software development process; however, it would be beneficial to investigate current trends adopted in the integration process of microfluidic subcomponents.

6.5 Microfluidic Systems Software Integration

Integration in microfluidics has been used to refer to the use of several on-chip valves (Thorsen, Maerkl et al. 2002) onto single microfluidic chips; combination of multiple micro components like mixers, multiplexers, filters onto a chip (Minhass, Pop et al. 2013); hardware design approaches in design of microfluidic systems (Melin and Quake 2007); software aided design of large scale microfluidic system based on well-established input-output properties (Melin and Quake 2007); and software programmable chips (Jensen, Bhat et al. 2010). The integration of microfluidic subcomponent systems allows for the automation of liquid handling functions to reduce errors from repetitive tasks.

Minimum attention has been given to software integration in the design of microfluidic components (Kong, Yuan et al. 2012). Several publications allude to its importance in the growth of microfluidics but there is little evidence that this is actively promoted in research environments. One reason may be that systems are often developed with the aim of solving specific functions within an environment as was the case with the integrated liquid handling system for neuromodulation of neuronal cultures.

Some work has been done to develop software solutions that could limit the software development time for these systems. A notable contribution to this effort is a website by Fordyce, et all linked from their characterisation of microfluidic features (Fordyce, Diaz-Botia et al. 2012). A valve-control-software based on Matlab was provided that can control individual valves or groups of valves. The user can pre-program a time-dependent sequence of valve actuations that can be performed unsupervised. This method of control is still described as manual (Minhass, Pop et al. 2012) since the user has to describe low level actions that result in high level functions. It is believed that the requirement for in-depth knowledge of the chip operation and control limits the pervasiveness of microfluidic applications (Fidalgo and Maerkl 2011). The words “automated” and “integrated” are loosely used in literature with minimal emphasis on the development process applied to realise the automation.

Continued usability of the developed integrated microfluidic systems depend on the ease of use for the system users; the abstraction of the low level functions; ease of redesign/changes; as well as the integration with other laboratory equipment.

Automation of laboratory equipment end-to-end processes of laboratory systems allow easy integration with other aspects of laboratory automation (Holzmüller-Laue, Göde et al. 2014). Suitable standards and interfacing must be established to ensure that the interaction with these systems and their output are transferrable across the wider research community. Research on the architectural descriptions of microfluidic systems have been undertaken to provide a more standardised method of designing

and controlling microfluidic systems (Fair 2007, Minhass, Pop et al. 2012). These research efforts do not address the exact problem scope of flow microfluidics with larger channel dimensions (~500 μm) but could provide insight towards control strategies for microfluidic system integration.

An ambitious top-down design approach for microfluidic development that allows users to concentrate on the applications of the chip rather with minimal fabrication knowledge was proposed (Minhass, Pop et al. 2012). It has been stated that manual control methodologies do not scale adequately as chips become more complex. Microfluidic component functionalities and interconnections between these functionalities were identified and a tool was developed to map user expectations of these functionalities to chip design. The proposed architecture is yet to be fully realised as implied in the conclusions of that research. Adoption of this research method would be an overkill on the integration efforts towards the integrated system.

In another example, set of fluidic functions like mixing, filtering, analysis, and transport have been identified (Fair 2007) based on typical high level biomedical applications like protein analysis, immune assays, and chemical separations that could be abstracted to serve as building blocks of the typical applications. The paper focuses on providing a high level architecture for controlling fluidic operations in droplet microfluidics but the theory can be applied to flow microfluidic chips.

The problem of integrated microfluidics is non-trivial as several specialties are required to realise the solution (Sabourin, Skafte-Pedersen et al. 2013). Physical integration has been identified as critical to the development of an architectural design of such system (Fair 2007). This constraint was accounted for in the design of the on-chip solution and the micro-components have been designed to be compatible or existing on the same substrate as recommended.

The integration in software is often ignored in literature as a manual methodology is typically adopted. However, this leads to an increased technical gap between the technologists developing the solutions and the end users. This has the effect of limiting the spread of microfluidics. It is believed that software abstraction will significantly increase the pervasive state of microfluidic devices (Fidalgo and Maerkl 2011). Further development of software-controlled chips may lead to increased user defined development patterns (“democratised development process”) (Leung, Zahn et al. 2012). It is most likely to happen when more responsibility is taken up by industry to provide over-the-shelf microfluidic tools allowing researchers take up higher level challenges like applying these tools to their research environments.

6.6 Discussion

The output of the software integration produced immediately usable software in LabVIEW that could be used to implement Liquid handling using the available lab tools such as syringe drivers, air-driven pneumatic flow controllers, proprietary autoloader, and a home-built on-chip valving system.

At the outset, it was proposed to develop a fully modular software system that would seamlessly or easily accept changes to the hardware. The design phase showed that extensive application development would be required to allow such additional features and an agile software development process was undertaken. This design methodology allowed rapid implementation of the software required to operate the available, fabricated and built components of the liquid handling system. A more extensive design methodology like water-fall would probably have resulted in an incomplete objective in terms of software development.

From this point, it is easy to add on small functionalities to the developed software systems to account for minor changes to application type but the software is not able

to cope with large changes to hardware configurations. The integrated system of commercial autoloader and liquid flow controller is able to transport media to cells in a microfluidic chamber; load up to 50 drug samples into the flow line; switch the media/drug interface in a dual input microfluidic device; rapidly introduce the drug to the cells in the device by rapidly switching the flow rates. Software programs have been written to account for different applications and some of the different hardware configurations. This system is being used in collaborative experiments within the lab and external to the primary lab in use which demonstrates its suitability for liquid handling solution in the wider research environment outside of neuroscience.

A future goal within this aspect of system integration the development of higher level functions that would abstract users from the low level functions. High level software architectures in LabVIEW are required to achieve this objective. The Actor Framework is an example architecture that steps away from a typical object-oriented design and is suitable for use where discrete controllers are interacting with physical plants operating concurrently and with different synchronisation requirements (Lee 2003, Lee and Neuendorffer 2004, Liu, Eker et al. 2004).

Another aspect of the software development that may hinder further application of this system is the proprietary nature of the software development environment (Laverty, Hastings et al. 2017). While LabVIEW presents a very versatile tool for developing large scale applications, its proprietary status prevents it from true widespread adoption as large license costs is often required to utilise the software (Barabas, Masullo et al. 2016). An alternative to this challenge is the development of a full windows application (*.exe) using LabVIEW development suite which would be comprised of all the libraries and tools in subfolders and does not require additional licensing on the part of the users of the software. This solution is not very elegant since the developed software will only be usable on specific OS versions and system specifications and also requires extensive development, debugging and testing time

that is not feasible within research environment. An open-source development environment, such as Python, presents an ideal solution(Barabas, Masullo et al. 2016). Open-sourcing the software system allows the possibility of community based support which has been shown to be successful in producing standard APIs and system frameworks.

7. Discussion, Conclusions and Future Work

7.1 Aims and Outcomes of the thesis

This work aimed at developing an integrated liquid handling system that could enable real time and deterministic drug signalling on cultures in microfluidic device. This was expected to be applied to primary neuronal cultures as part of a multidisciplinary research on learning paradigms and information encoding process in these cultures.

An essential element to achieve this was the development of hardware and software necessary to realise liquid flow control as well as volume injection and sampling to and from microfluidic devices for maintaining and performing long term assays on cell cultures in these devices. This was implemented by integration of macro liquid handling technologies for flow control and sequential agonist delivery to microfluidic devices. Modular off-chip liquid handling solutions were required to ensure and its ability to deliver required agonists and perform chemical switching patterns to any range of devices used with minor changes to hardware.

This development of this modular system has resulted in:

i. Development of a custom high precision liquid flow control system capable of rapid and steady flow control over the target range (1 – 100 $\mu L.s^{-1}$) for media and agonist transport; as well as spatio-temporal agonist delivery for drug signalling applications in single and dual input microfluidic devices.
ii. Characterisation and automation of commercial autoloader for sequential drug delivery into microfluidic devices.
iii. Attempts at design and fabrication of an alternative custom liquid injection system that could potentially allow sequential loading of agonists for a train of highly repeatable drug inputs upstream of the microfluidic device. This was also to enable downstream sampling of used media and drugs from the device for offline analysis.

iv. Preliminary Investigation of on-chip systems for modular implementation of liquid handling for microfluidic devices that employ rapid prototyping techniques. This would allow laboratories with limited resources to adopt microfluidics in their experimental setup.

v. Integration of a commercial autoloader with the high precision liquid flow transport for spatio-temporal drug delivery required for neuroscience study of chemical reward and signalling in neuronal cultures.

7.1.1 Macro Liquid Flow Control

Low latency in flow rate switching was necessary to enable fast flow switching times and high flow stability was necessary to avoid fluctuations of the interface formed between buffer and drug in a Y-shaped microfluidic device. The syringe driver was found to be lacking in the stability and latency requirements since it took several seconds to arrive at the target flow and oscillated at the desired flow rates. The need for a low cost solution further prevented the adoption of highly sophisticated off-the-shelf syringe drivers. This prompted the development of a pneumatic pressure control system in collaboration with Mr. Sorka Abanu and Johnstone Alexander. The system was developed as a pressure control system that regulated the air pressure over a liquid reservoir. Flow sensors were used to provide feedback to a software that performed the nested PID control algorithms necessary to control the flow in the system. The control system was further optimised to enable reliable fast flow switching and a switching time of 0.3 seconds was realised (rise time between 10 – 90% flow target). This was further characterised in a Y-shaped microfluidic device to demonstrate and apply the optimised flow control system. Drug signalling patterns like gradient control; interface shifting and rapid drug switching was realised with high stability where noise was recorded at 0.3 $nL.s^{-1}$ during stable flow control. This was useful for developing applications for drug concentration control using drug gradient

distribution by flowing at low flow rates while altering volume of drug to media. This has been developed further into a standalone application for a secondary laboratory investigating Hek cells and astrocyte cells.

7.1.2 Autoloader Characterisation and Automation

Off-chip liquid injection and sampling capabilities were also required for the microfluidic devices that would be independent of devices used. This was to provide a versatile tool that could be integrated with the liquid transport system to realise agonist delivery of several drug samples and concentrations within the same experiment. A commercial autoloader was characterised to identify its limits and automation software was developed to enable users perform sequential drug delivery to microfluidic devices. This was first integrated at hardware level only with the custom liquid flow control. Its limits were identified which included lack of sampling capabilities, non-deterministic operations, flow inconsistencies during operation and sample carryover from same needle use. The system was however developed to enable users describe long term experiments within a software defined graphic user interface (GUI). A demonstration of its use has been done with an immunocytochemistry protocol on a neuronal culture. This will be applied to future collaborative assays like immunocytochemistry for assessing effects of peptides on neuronal culture distribution of neurons and astrocytes during culture proliferation with Hala Dowre.

7.1.3 Development of Novel Liquid Injection System

The lack of sampling capabilities and other limitations of the commercial autoloader required a development effort towards realising an alternative solution to liquid injection and sampling for microfluidic devices. Such a system if successful could be applied to the sequential manipulation of reagents in a flow line in other fields not requiring a microfluidic device.

A design was produced for a novel injection system that allowed very small volumes (≈ 50 nL) to be injected into reservoirs drilled in a circular disc (rotor). This rotor could be rotated with a motor to align these reservoirs with the flow path of the carrier liquid to the microfluidic device which would then allow the ejection of the liquid from the reservoir. One of the advantages to the design was the high resolution of injected volumes since the smallest loadable volume was 50 nL. Another advantage was the non-disruptive flow injection that was incorporated into the design. However, the drawbacks identified such as the potential for damage to the disc due to combined action of the compressive forces required to maintain sealing and shear forces during the disc rotation. These forces would cause the inner section of the disc relative to the reservoir to shear against the outer section during rotation and cause damage. This prompted a redesign of the system using reservoirs on the disc surface. These reservoirs would intersect with through holes for liquid flow. A Prototype of the system was designed with reservoirs of different configurations to allow disruptive and non-disruptive switching. A torque of 0.4 N.m was required to rotate a similar commercially available switch by rheodyne. A motor capable of providing 1.87Nm holding torque was obtained to rotate the designed system.

The prototype was produced with some help from precision manufacturing group at the University of Nottingham who also advised on design modifications and optimal materials. The realised fabrication pieces were assembled and tested for leaks. It was found that a torque of 10 N.m was required to minimise leaks to less than $5nL.s^{-1}$. The motor also failed to rotate the discs at 5 N.m. The rotation at the lower torques ($T \leq 4$ N.m) unexpectedly sheared the reservoir surface which produced an uneven surface for interfacing with liquid transport ports. These issues which have been solved by industry would have required technical expertise and resources that were not available. This prompted a rethink of the original problem of modular liquid injection and the method applied to solve it.

7.1.4 Development of Modular On-chip

The rising trend of rapid prototyping and modular chip design was identified as a potential direction for realising the liquid loading and sampling capabilities required to realise the proposed integrated liquid handling system. This further raised the prospects of realising a very modular solution for liquid handling where fluidic components were assembled like Lego pieces. The ability to realise modular microfluidic setups is of particular interests to research laboratories to enable a multiplicity of tests to be achievable by selecting design elements that are required in the setup. Further to this is the need to realise these modular pieces using rapid prototyping techniques readily available to a non-microfluidics specialist laboratory.

The aim of this investigation was to identify what rapid-prototyping technologies would best allow the development of these components for scalable microfluidic adoption. The on-chip valves were identified as the basic unit of microfluidic liquid handling and an investigation was carried out on the feasibility of realising on-chip valves using low resolution Xurography techniques. This low resolution craft cutter may hold the best prospects for wider adoption when compared to more technically advanced techniques like laser cutting, micro-milling, SU-8 mold fabrication techniques.

PMMA-clamped tape devices, chemically functionalised PET sheets, and PDMS-to-PDMS glue bonding were characterised for bond strength with thin flexible PDMS films that will actuate over fluidic lines in on-chip valves. This high bond strengths realised from these methods make them suitable for use in the further development of an integrated liquid handling solution. Modular designs were also established that could be integrated with standalone microfluidic devices. More work will be required to optimise the development of devices using low resolution Xurography techniques that will be truly “cheap and easy to fabricate” devices. This forms the basis of future

work in promoting the wider adoption of microfluidics and solving liquid manipulation challenges in biomedical research.

7.1.5 Software Development Process

The ability to integrate a wide array of instrumentation devices and laboratory equipment with an integrated liquid handling system for chemical reward signalling was a constraint for software development. The choice of software to develop this liquid handling system was dependent on the ability to develop highly scalable functions that could easily be improved with added hardware as well as minimal software changes.

LabVIEW programming language provided this requirements. The graphical programming interface allowed faster implementation of the instrumentation systems necessary to develop the liquid flow control as well as syringe driven controls. Another requirement of the software development was the ability to use these laboratory equipment interchangeably with minimal software redesign. This along with the first objective of high scalability and integration with other laboratory equipment were considered when choosing an object oriented architecture for further development.

Object oriented programming provided a means to treat each system as an object and the functionalities as the properties of these objects. This programming methodology was considered while developing the task oriented structure for the low level tools like the pneumatic pressure-driven flow controller and syringe-driver pump system. However, agile software development methodologies were adopted for rapid application prototyping and so the applications were built as self-contained functions. One of such applications is the interface shifting application. This required the application to define the flow targets for two input pumps. A better developed

application with object-oriented design patterns would extend this functionality and allow the user increase the number of pumps required at runtime. This plug-and-play approach to software development will also allow many interchangeable lab equipment to be implemented in software to carry out the same function.

The flow control system was applied to an application with collaborators Tom Bellamy and Wayne Croft to steadily provide a concentration gradient using Gaba and Charbacol as agonists in two separate experiments. The software used applied design methodologies to provide a clean user interface for generic users as well ability to change system operations using the advanced interface.

7.1.6 Integration

COMSOL models were initially used to demonstrate the applicability of the flow controller to perform interface shifting and rapid interface sweeping. Models were also shown switching capabilities of an integrated system to perform more dynamic chemical signalling by switching loaded agonists. These range of applications were realised using an integrated system with the commercial autoloader despite the challenges. The integration of the commercial autoloader and flow control system was done to give a combined advantage of sophisticated chemical signalling patterns with several drug samples within the same experiment without physically changing the system. Up to 50 sample can be preloaded in the autoloader tray for use within the experiments. This integrated system will be used in future work for the long term assays requiring chemical stimulation of neuronal cultures towards understanding information processing in the brain.

7.2 Overall Conclusions

Systems like syringe drivers, vacuum pumps and peristaltic pumps have been established for performing flow control and generating drug delivery patterns in microfluidics as they are simple and suitable for many applications (Kuczenski, LeDuc et al. 2007, Author 2008, Chen, Feng et al. 2010, Sun, Chen et al. 2011). These systems do not scale well and on-chip valves have been used as well as part of integrated microfluidic systems to achieve microscale flow control (Melin and Quake 2007, Quake 2007). The development of these on-chip valves has enabled complex fluidic operations on cultures in microfluidic devices and increased throughput of biological assays (Sackmann, Fulton et al. 2014).

Some laboratories are unable to approach this sophisticated all-in-one solution due to technical or experimental challenges (Skafte-Pedersen, Sip et al. 2013). They may be unable to access the level of technical expertise, equipment or spaces required to develop these solutions. They may also require solutions that are more modular and interchangeable to continuously optimise other aspects of the microfluidic chip towards their target experiments. This was the case with the Neurophotonics laboratory that required the microfluidic chip surface to be independent of the fluidic controls. Such scenarios appeal to the implementations of off-chip liquid handling systems on passive microfluidic devices (Fair 2007, Skafte-Pedersen, Sip et al. 2013).

A modular approach was taken towards developing the microfluidic liquid handling solution. The liquid transport system was optimised to realise faster liquid flow rate switching time scales and liquid injection system was investigated to realise a usable liquid injection system that could be integrated.

A gas-driven-pressure flow controller was developed instead of syringe drivers and peristaltic pumps using pneumatic pressure manifolds, pressure sensors and flow

sensors. This was initially been developed as a simple liquid transport system and unable to perform fast flow switching to enable gradient generation applications. The fluid transport system has now been successfully optimised to enable rapid flow switching in microfluidic devices. This has yet to be successfully employed in fast switching experiments on neuronal cultures but will be employed when other constraints limiting its application like long term neuronal culture longevity under flow are solved by a collaborator, Mr. Nitzan Herzog. The abilities of the system in delivering steady interface shifts have been demonstrated and applied to an application with cultured HEK cells. Here, it was demonstrated to be capable of inducing precise spatial variation of a concentration gradient exposure and the overall concentration exposure to a cell network for many minutes. The liquid transport system is capable of utilising syringe driven and pressure driven flow control systems in achieving liquid transport objectives. This transport system is more advantageous to other systems in modularity, speed, feedback control for precision and usability of the control interface. A similar system to the pressure driven controller has subsequently been developed using a commercial pressure controller and used to achieve fast interface switching for multiple inputs by routing undesired volumes away from the target microfluidic device (Niman, Beech et al. 2013). The system, however, does not incorporate closed loop flow control but determines the flow obtained from simulations and calculations using fluorescence data. This open loop control will suffer from inaccuracies which may arise due to influence of bubbles rising in the system (Sung and Shuler 2009).

Although the novel fluid injection system (GSIS) was not successfully developed, the ability of a sequential injection system to deliver sequential volumes has been demonstrated with an autoloader that was characterised and used for an immunocytochemistry experiment. The issues affecting the development were not envisaged at the outset as these issues may have been solved by industry experts

with sufficient resources. Future requirements for custom macro liquid injection systems should adopt commercial injection switches to reduce the risks of failure at development. The developed system is comprised of an autoloader in line with a liquid transport system and is capable loading up to 50 agonists to the microfluidic device while employing sophisticated spatial and temporal delivery patterns using the flow control system. The flow inconsistency (Rogatsky, Braaten et al. 2009) is still an issue but its incorporation with a pneumatically driven closed loop flow control system ensures that this inconsistency is present for a short duration (< 1 second) before the flow control system corrects it.

The application of modular design methods and techniques for rapid prototyping of microfluidic components can indeed solve bridge the gap between microfluidic production and end users requiring off-chip liquid handling. While it may be ideal for commercial solutions to be developed, the lack of widespread adoption of microfluidics still makes this an economic challenge. The reverse may also be the case that lack of widespread adoption limits the availability of commercial solutions. The cost per microfluidic device is relatively high for some microfluidic devices (Au, Lee et al. 2014) which may be the result of patents registered tor these devices. It is expected that the prices will drop as more of these patents expire and this will increase competition making these devices readily available for wider adoption. Overcoming the immediate lack of pervasive microfluidic applications may result from development of easily assembled devices using cheap and relatively simple fabrication techniques.

The research into rapid-prototyping tools for liquid manipulation was aimed at developing modular designs that can be implemented using rapid-prototyping tools. Some development work realised that PMMA-clamping of microfluidic devices could provide device integrity but limit fluid flow when applied to development of multi-layered on-chip valve designs. The research also realised that oxygen-plasma

bonding of functionalised plastic to PDMS can provide device integrity with high pressure applications as well as PDMS-to-PDMS bonded devices. More work will be required to apply low resolution Xurography techniques to developing microfluidic liquid handling system. However, this has been integrated with applications to realise simple on-chip valves for a distribution valving system for flow into several microfluidic devices and a flow path selector in a dual-input microfluidic device.

7.3 Potential Future Directions

The work achieved here will be best implemented as a part of the larger project investigating learning paradigms in neuronal cultures *in vitro*. This should take the form of a high level object oriented software development process to describe the "objects" of the integrated system and the functions or properties of these objects. This systems that make up the larger project includes:

i. An electrical stimulation and recording equipment (for example, MEA)
ii. An optical stimulation equipment that can produce high spatiotemporal pixel patterns on a culture (Fu, B. and Johnstone, A. 2002).
iii. A high resolution optical recording equipment (imaging microscopy)
iv. Chemical reward system (Integrated Liquid Handling system)
v. Virtual Environment to simulate motor outputs from computations on neuronal activity and simulate sensory inputs 0for stimulation of the culture.

First, the challenge of sequential volume injection into the device must be solved. This should adopt modular on-chip components to realise these tasks. While the need for rapid-prototyping has been emphasised, this should not limit use of other techniques that enable development of on-chip fluid manipulation. An example is a Teflon actuated on-chip valve where Teflon has been used to replace PDMS as the flexible elastomer (Grover, von Muhlen et al. 2008). This implemented the use of

glass etching techniques which may be outsourced for rapid and high-precision development. The assembly process requires application of compression force and heat application which is easy to achieve in a laboratory.

The next step would be the development of the smart high-level software that can learn using information on neuronal activity gathered from sensing equipment. This software or framework for studying neuronal cultures will incorporate the integrated liquid handling system to provide chemical reward signals using the high level functions available to it like interface sweeping and volume loading. It could be developed to apply volume tracking that relies on the low level flow sensor data to maintain information on the volume of loaded reagents. It is tempting to view these function and others like interface sweeping and switching as a higher liquid manipulation function executed at the flow controller level. An added requirement may be to open-source the software solution. This can be done by adopting alternative programming languages like Python that have already been used extensively in research communities. An alternative hardware may be required for data acquisition for the flow control system but this may be realised by sophisticated micro-controllers that outperform simple Arduino platforms. A distributed system framework may also be beneficial by delegating specific tasks to specific hardware.

High level definition will enable a more fluid development process for the incorporated systems that are yet to be realised. This high level control system could be described using an actor framework, which sets up actions (functions) for actors (objects/equipment). This top-down approach to system development is expected to benefit the proposed system for investigating information encoding in neuronal cultures.

7.4 Relevance of this Work in the Field of Study

The later results with rapid prototyping and modular design approaches for developing on-chip liquid handling showed promise and could be key to improving widespread adoption of microfluidics in biomedical research. Many publications have cited the need for killer applications with microfluidics but it is clear that the real need is for quick and easy access to tools that improve use of microfluidics in biomedical research. The on-chip fabrication techniques developed during this thesis can be applied to realising this easy access.

The fluid handling system developed during this thesis can also be applied to other experimental questions that hold considerable implications if successfully implemented. This can allow researchers apply and remove precise drug pulses within a second with minimal concentration dilution except when intended with gradient applications.

8. References

Abgrall, P., L.-N. Low and N.-T. Nguyen (2007). "Fabrication of planar nanofluidic channels in a thermoplastic by hot-embossing and thermal bonding." Lab on a Chip **7**(4): 520-522.

Åkesson, B. M. and H. T. Toivonen (2006). "A neural network model predictive controller." Journal of Process Control **16**(9): 937-946.

Andersson, B., R. Andersson, L. Håkansson, M. Mortensen, R. Sudiyo and B. Van Wachem (2011). Computational fluid dynamics for engineers, Cambridge University Press.

Araci, I. E. and P. Brisk (2014). "Recent developments in microfluidic large scale integration." Curr Opin Biotechnol **25**: 60-68.

Aran, K., L. A. Sasso, N. Kamdar and J. D. Zahn (2010). "Irreversible, direct bonding of nanoporous polymer membranes to PDMS or glass microdevices." Lab Chip **10**(5): 548-552.

Aris, R. (1956). On the dispersion of a solute in a fluid flowing through a tube. Proceedings of the Royal Society of London A: Mathematical, Physical and Engineering Sciences, The Royal Society.

Arora, A., G. Simone, G. B. Salieb-Beugelaar, J. T. Kim and A. Manz (2010). "Latest developments in micro total analysis systems." Analytical chemistry **82**(12): 4830-4847.

Attia, U. M., S. Marson and J. R. Alcock (2009). "Micro-injection moulding of polymer microfluidic devices." Microfluidics and nanofluidics **7**(1): 1.

Au, A. K., H. Lai, B. R. Utela and A. Folch (2011). "Microvalves and Micropumps for BioMEMS." Micromachines **2**(4): 179-220.

Au, A. K., W. Lee and A. Folch (2014). "Mail-order microfluidics: evaluation of stereolithography for the production of microfluidic devices." Lab Chip **14**(7): 1294-1301.

Author, A. (2008). "Flow control in microfluidics: are the workhorse flows adequate?" Lab on a Chip **8**(3): 383-387.

Avila, K., D. Moxey, A. de Lozar, M. Avila, D. Barkley and B. Hof (2011). "The Onset of Turbulence in Pipe Flow." Science **333**(6039): 192-196.

Bae, A. J., C. Beta and E. Bodenschatz (2009). "Rapid switching of chemical signals in microfluidic devices." Lab Chip **9**(21): 3059-3065.

Balagaddé, F. K., L. You, C. L. Hansen, F. H. Arnold and S. R. Quake (2005). "Long-Term Monitoring of Bacteria Undergoing Programmed Population Control in a Microchemostat." Science **309**(5731): 137-140.

Bange, A., H. B. Halsall and W. R. Heineman (2005). "Microfluidic immunosensor systems." Biosensors and Bioelectronics **20**(12): 2488-2503.

Barabas, F. M., L. A. Masullo and F. D. Stefani (2016). "Note: Tormenta: An open source Python-powered control software for camera based optical microscopy." Review of Scientific Instruments **87**(12): 126103.

Barbati, A. C., C. Fang, G. A. Banker and B. J. Kirby (2013). "Culture of Primary Rat Hippocampal Neurons: Design, Analysis, and Optimization of a Microfluidic Device for Cell Seeding, Coherent Growth, and Solute Delivery." Biomedical microdevices **15**(1): 97-108.

Bartholomeusz, D., R. W. Boutté and J. D. Andrade (2005). "Xurography: rapid prototyping of microstructures using a cutting plotter." Microelectromechanical Systems, Journal of **14**(6): 1364-1374.

Becker, H. (2010). "One size fits all?" Lab on a Chip **10**(15): 1894-1897.

Becker, H. and U. Heim (2000). "Hot embossing as a method for the fabrication of polymer high aspect ratio structures." Sensors and Actuators A: Physical **83**(1): 130-135.

Beebe, D. J., G. A. Mensing and G. M. Walker (2002). "Physics and applications of microfluidics in biology." Annual Review of Biomedical Engineering **4**(1): 261-286.
Berthier, J., R. Renaudot, P. Dalle, G. Blanco-Gomez, F. Rivera, V. Agache and P. Caillat (2010). COMSOL assistance for the determination of pressure drops in complex microfluidic channels. Comsol Conference.
Bhargava, K. C., B. Thompson and N. Malmstadt (2014). "Discrete elements for 3D microfluidics." Proceedings of the National Academy of Sciences **111**(42): 15013-15018.
Bianchi, R. F., M. F. Panssiera, J. P. H. Lima, L. Yagura, A. M. Andrade and R. M. Faria (2006). "Spin coater based on brushless dc motor of hard disk drivers." Progress in Organic Coatings **57**(1): 33-36.
Blanco-Gomez, G., A. Glidle, L. M. Flendrig and J. M. Cooper (2009). "Integration of low-power microfluidic pumps with biosensors within a laboratory-on-a-chip device." Anal Chem **81**(4): 1365-1370.
Blume, P. A. (2007). The LabVIEW style book, Pearson Education.
Bodén, R., M. Lehto, J. Margell, K. Hjort and J.-Å. Schweitz (2008). "On-chip liquid storage and dispensing for lab-on-a-chip applications." Journal of Micromechanics and Microengineering **18**(7): 075036.
Boehm, B. (2006). "Some future trends and implications for systems and software engineering processes." Systems Engineering **9**(1): 1-19.
Bogusz, S., L. W. Hantao, S. C. G. N. Braga, V. d. C. de Matos França, M. F. da Costa, R. D. Hamer, D. F. Ventura and F. Augusto (2012). "Solid-phase microextraction combined with comprehensive two-dimensional gas chromatography for fatty acid profiling of cell wall phospholipids." Journal of separation science **35**(18): 2438-2444.
Bondi, A. B. (2000). Characteristics of scalability and their impact on performance. Proceedings of the 2nd international workshop on Software and performance, ACM.
Boon, J., S. Yip, J. Burgers, H. Van de Hulst, S. Chandrasekhar, F. Chen, C. De Loore, D. Frenkel and B. Smit (1988). "An introduction to fluid mechanics."
Bruus, H. (2007). Theoretical Microfluidics, OUP Oxford.
Buonocunto, P., A. Biondi and P. Lorefice (2014). Real-time multitasking in Arduino. Industrial Embedded Systems (SIES), 2014 9th IEEE International Symposium on.
Burry, R. W. (2010). Immunocytochemistry: a practical guide for biomedical research / Richard W. Burry, Springer.
C, S., A. N, J. Cui, J. Low and T. Che (2013). "Practical Considerations of Liquid Handling Devices in Drug Discovery."
Chamberlain, S., H. Sharp and N. Maiden (2006). Towards a framework for integrating agile development and user-centred design. International Conference on Extreme Programming and Agile Processes in Software Engineering, Springer.
Chang, S. T., E. Beaumont, D. N. Petsev and O. D. Velev (2008). "Remotely powered distributed microfluidic pumps and mixers based on miniature diodes." Lab Chip **8**(1): 117-124.
Chen, D. L. and R. F. Ismagilov (2006). "Microfluidic cartridges preloaded with nanoliter plugs of reagents: an alternative to 96-well plates for screening." Current opinion in chemical biology **10**(3): 226-231.
Chen, P., X. Feng, R. Hu, J. Sun, W. Du and B.-F. Liu (2010). "Hydrodynamic gating valve for microfluidic fluorescence-activated cell sorting." Analytica chimica acta **663**(1): 1-6.
Chen, Q., G. Li, Y. Nie, S. Yao and J. Zhao (2013). "Investigation and improvement of reversible microfluidic devices based on glass–PDMS–glass sandwich configuration." Microfluidics and Nanofluidics **16**(1-2): 83-90.
Chien, R.-L. and W. J. Parce (2014). "Multiport flow-control system for lab-on-a-chip microfluidic devices." Fresenius' Journal of Analytical Chemistry **371**(2): 106-111.

Christensen, A. M., D. A. Chang-Yen and B. K. Gale (2005). "Characterization of interconnects used in PDMS microfluidic systems." Journal of Micromechanics and Microengineering **15**(5): 928.
Chung, B. G., L. A. Flanagan, S. W. Rhee, P. H. Schwartz, A. P. Lee, E. S. Monuki and N. L. Jeon (2005). "Human neural stem cell growth and differentiation in a gradient-generating microfluidic device." Lab Chip **5**(4): 401-406.
Churski, K., J. Michalski and P. Garstecki (2010). "Droplet on demand system utilizing a computer controlled microvalve integrated into a stiff polymeric microfluidic device." Lab Chip **10**(4): 512-518.
Cockburn, A. and J. Highsmith (2001). "Agile software development, the people factor." Computer **34**(11): 131-133.
Cole, M. C., A. V. Desai and P. J. A. Kenis (2011). "Two-layer multiplexed peristaltic pumps for high-density integrated microfluidics." Sensors and Actuators B: Chemical **151**(2): 384-393.
Cooksey, G. A., C. G. Sip and A. Folch (2009). "A multi-purpose microfluidic perfusion system with combinatorial choice of inputs, mixtures, gradient patterns, and flow rates." Lab on a Chip **9**(3): 417-426.
Cosson, S., L. G. Aeberli, N. Brandenberg and M. P. Lutolf (2015). "Ultra-rapid prototyping of flexible, multi-layered microfluidic devices via razor writing." Lab on a Chip **15**(1): 72-76.
Cruz, P. P. and A. M. Gutiérrez (2010). LabVIEW for intelligent control research and education. E-Learning in Industrial Electronics (ICELIE), 2010 4th IEEE International Conference on, IEEE.
Cunningham, D. D. (2001). "Fluidics and sample handling in clinical chemical analysis." Analytica Chimica Acta **429**(1): 1-18.
Devaraju, N. S. G. K. and M. A. Unger (2012). "Pressure driven digital logic in PDMS based microfluidic devices fabricated by multilayer soft lithography." Lab on a Chip **12**(22): 4809-4815.
DIN, E. (1990). 28510-1: Adhesives–Peel test for a flexible-bonded-to-rigid test specimen assembly–Part 1: 90 peel, ISO.
Doktycz, M. J., J. E. Johnson and M. J. Cornett (2004). "Hybrid valve structure for high-throughput, low-volume liquid-handling applications." Journal of the Association for Laboratory Automation **9**(4): 250-256.
Douglas, J. F. (2005). Fluid Mechanics, Pearson/Prentice Hall.
Douglas, J. F., J. M. Gasiorek and J. A. Swaffield (1979). Fluid mechanics / J.F. Douglas, J.M. Gasiorek and J.A. Swaffield, Pitman.
Duffy, D. C., J. C. McDonald, O. J. Schueller and G. M. Whitesides (1998). "Rapid prototyping of microfluidic systems in poly (dimethylsiloxane)." Analytical chemistry **70**(23): 4974-4984.
Dunn, D. A. and I. Feygin (2000). "Challenges and solutions to ultra-high-throughput screening assay miniaturization: submicroliter fluid handling." Drug Discovery Today **5**(12, Supplement 1): 84-91.
Economou, A. (2005). "Sequential-injection analysis (SIA): A useful tool for on-line sample-handling and pre-treatment." TrAC Trends in Analytical Chemistry **24**(5): 416-425.
Eddings, M. A. and B. K. Gale (2006). "A PDMS-based gas permeation pump for on-chip fluid handling in microfluidic devices." Journal of Micromechanics and Microengineering **16**(11): 2396.
Eddings, M. A., M. A. Johnson and B. K. Gale (2008). "Determining the optimal PDMS–PDMS bonding technique for microfluidic devices." Journal of Micromechanics and Microengineering **18**(6): 067001.
Fair, R. B. (2007). "Digital microfluidics: is a true lab-on-a-chip possible?" Microfluidics and Nanofluidics **3**(3): 245-281.
Fardousi, M., M. Hossain, M. Islam and S. Ruslan (2013). "Cost-effective home-made spin coater for depositing thin films." J. Mod. Sci. Technol. **1**.

Feng, J., X. J. Yang, X. C. Li, H. Yang and Z. G. Chen (2011). "An automated fluid-transport device for a microfluidic system." Anal Sci **27**(10): 1057-1060.
Fidalgo, L. M. and S. J. Maerkl (2011). "A software-programmable microfluidic device for automated biology." Lab on a Chip **11**(9): 1612-1619.
Fiering, J., M. Mescher, E. L. Swan, M. Holmboe, B. Murphy, Z. Chen, M. Peppi, W. Sewell, M. McKenna and S. Kujawa (2009). "Local drug delivery with a self-contained, programmable, microfluidic system." Biomedical microdevices **11**(3): 571-578.
Fordyce, P. M., C. A. Diaz-Botia, J. L. DeRisi and R. Gomez-Sjoberg (2012). "Systematic characterization of feature dimensions and closing pressures for microfluidic valves produced via photoresist reflow." Lab Chip **12**(21): 4287-4295.
Foret, F. and P. Kusý (2006). "Microfluidics for multiplexed MS analysis." ELECTROPHORESIS **27**(24): 4877-4887.
Fuard, D., T. Tzvetkova-Chevolleau, S. Decossas, P. Tracqui and P. Schiavone (2008). "Optimization of poly-di-methyl-siloxane (PDMS) substrates for studying cellular adhesion and motility." Microelectronic Engineering **85**(5-6): 1289-1293.
Gao, J., M. L. Sin, T. Liu, V. Gau, J. C. Liao and P. K. Wong (2011). "Hybrid electrokinetic manipulation in high-conductivity media." Lab Chip **11**(10): 1770-1775.
Garstecki, P., A. Ganan-Calvo and G. Whitesides (2005). "Formation of bubbles and droplets in microfluidic systems." Technical sciences **53**(4).
Gatling, R. J. (1862). Improvement in revolving battery-guns, Google Patents.
Ghallab, Y. and W. Badawy (2004). "Sensing methods for dielectrophoresis phenomenon: from bulky instruments to lab-on-a-chip." Circuits and Systems Magazine, IEEE **4**(3): 5-15.
Go, J. S. and S. Shoji (2004). "A disposable, dead volume-free and leak-free in-plane PDMS microvalve." Sensors and Actuators A: Physical **114**(2-3): 438-444.
Graham, D. R. (1992). Incremental development and delivery for large software systems. Software Prototyping and Evolutionary Development, IEE Colloquium on, IET.
Grimes, A., D. N. Breslauer, M. Long, J. Pegan, L. P. Lee and M. Khine (2008). "Shrinky-Dink microfluidics: rapid generation of deep and rounded patterns." Lab on a Chip **8**(1): 170-172.
Griswold, R. E. and M. T. Griswold (1983). The Icon programming language, Prentice-Hall Englewood Cliffs, NJ.
Grover, W. H., R. H. Ivester, E. C. Jensen and R. A. Mathies (2006). "Development and multiplexed control of latching pneumatic valves using microfluidic logical structures." Lab Chip **6**(5): 623-631.
Grover, W. H., M. G. von Muhlen and S. R. Manalis (2008). "Teflon films for chemically-inert microfluidic valves and pumps." Lab Chip **8**(6): 913-918.
Gu, P., K. Liu, H. Chen, T. Nishida and Z. H. Fan (2011). "Chemical-Assisted Bonding of Thermoplastics/Elastomer for Fabricating Microfluidic Valves." Analytical Chemistry **83**(1): 446-452.
Guckenberger, D. J., T. E. de Groot, A. M. Wan, D. J. Beebe and E. W. Young (2015). "Micromilling: a method for ultra-rapid prototyping of plastic microfluidic devices." Lab Chip **15**(11): 2364-2378.
Haber, C., M. Boillat and B. van der Schoot (2004). "Flow sensor driven nanodispensing: The path to more reliable liquid handling operations." American laboratory **36**(21): 32-37.
Halldorsson, S., E. Lucumi, R. Gómez-Sjöberg and R. M. Fleming (2015). "Advantages and challenges of microfluidic cell culture in polydimethylsiloxane devices." Biosensors and Bioelectronics **63**: 218-231.
Harris, D. L. and M. Mutz (2006). "Debunking the myth: validation of fluorescein for testing the precision of nanoliter dispensing." Journal of the Association for Laboratory Automation **11**(4): 233-239.

Hashim, U., P. Diyana and T. Adam (2012). Numerical simulation of microfluidic devices. Semiconductor Electronics (ICSE), 2012 10th IEEE International Conference on, IEEE.
Hill, M. D. (1990). "What is scalability?" ACM SIGARCH Computer Architecture News **18**(4): 18-21.
Ho, C.-M. and Y.-C. Tai (1998). "Micro-electro-mechanical-systems (MEMS) and fluid flows." Annual Review of Fluid Mechanics **30**(1): 579-612.
Holzmüller-Laue, S., B. Göde, H. Fleischer and K. Thurow (2014). "Improved Compliance by BPM-Driven Workflow Automation." Journal of laboratory automation: 2211068214549626.
Hsieh, Y.-F., A.-S. Yang, J.-W. Chen, S.-K. Liao, T.-W. Su, S.-H. Yeh, P.-J. Chen and P.-H. Chen (2014). "A Lego®-like swappable fluidic module for bio-chem applications." Sensors and Actuators B: Chemical **204**(0): 489-496.
Huang, C.-W. and G.-B. Lee (2007). "A microfluidic system for automatic cell culture." Journal of Micromechanics and Microengineering **17**(7): 1266.
Huang, S., Q. He, X. Hu and H. Chen (2012). "Fabrication of micro pneumatic valves with double-layer elastic poly(dimethylsiloxane) membranes in rigid poly(methyl methacrylate) microfluidic chips." Journal of Micromechanics and Microengineering **22**(8): 085008.
Hung, P. J., P. J. Lee, P. Sabounchi, R. Lin and L. P. Lee (2005). "Continuous perfusion microfluidic cell culture array for high-throughput cell-based assays." Biotechnology and Bioengineering **89**(1): 1-8.
Iliescu, C., H. Taylor, M. Avram, J. Miao and S. Franssila (2012). "A practical guide for the fabrication of microfluidic devices using glass and silicon." Biomicrofluidics **6**(1): 16505-1650516.
Jang, Y. H., M. J. Hancock, S. B. Kim, S. Selimovic, W. Y. Sim, H. Bae and A. Khademhosseini (2011). "An integrated microfluidic device for two-dimensional combinatorial dilution." Lab Chip **11**(19): 3277-3286.
Javois, L. C. (1999). Immunocytochemical methods and protocols / edited by Lorette C. Javois, Humana Press.
Jensen, E. C., B. P. Bhat and R. A. Mathies (2010). "A digital microfluidic platform for the automation of quantitative biomolecular assays." Lab on a Chip **10**(6): 685-691.
Jensen, E. C., W. H. Grover and R. A. Mathies (2007). "Micropneumatic Digital Logic Structures for Integrated Microdevice Computation and Control." Microelectromechanical Systems, Journal of **16**(6): 1378-1385.
Kaigala, G. V., V. N. Hoang and C. J. Backhouse (2008). "Electrically controlled microvalves to integrate microchip polymerase chain reaction and capillary electrophoresis." Lab Chip **8**(7): 1071-1078.
Kamholz, A. E. and P. Yager (2001). "Theoretical Analysis of Molecular Diffusion in Pressure-Driven Laminar Flow in Microfluidic Channels." Biophysical Journal **80**(1): 155-160.
Kaur, R. and J. Sengupta (2013). "Software process models and analysis on failure of software development projects." arXiv preprint arXiv:1306.1068.
Kazuo, H. and M. Ryutaro (2000). "A pneumatically-actuated three-way microvalve fabricated with polydimethylsiloxane using the membrane transfer technique." Journal of Micromechanics and Microengineering **10**(3): 415.
Kenis, P. J., R. F. Ismagilov and G. M. Whitesides (1999). "Microfabrication inside capillaries using multiphase laminar flow patterning." Science **285**(5424): 83-85.
Kim, D., N. C. Chesler and D. J. Beebe (2006). "A method for dynamic system characterization using hydraulic series resistance." Lab on a Chip **6**(5): 639-644.
Kim, J., D. Chen and H. H. Bau (2009). "An automated, pre-programmed, multiplexed, hydraulic microvalve." Lab Chip **9**(24): 3594-3598.
Kim, J., R. Surapaneni and B. K. Gale (2009). "Rapid prototyping of microfluidic systems using a PDMS/polymer tape composite." Lab on a Chip **9**(9): 1290-1293.

Kim, L., Y.-C. Toh, J. Voldman and H. Yu (2007). "A practical guide to microfluidic perfusion culture of adherent mammalian cells." Lab on a Chip **7**(6): 681-694.
Kim, Y., B. Kuczenski, P. R. LeDuc and W. C. Messner (2009). "Modulation of fluidic resistance and capacitance for long-term, high-speed feedback control of a microfluidic interface." Lab on a Chip **9**(17): 2603-2609.
Konda, A., J. M. Taylor, M. A. Stoller and S. A. Morin (2015). "Reconfigurable microfluidic systems with reversible seals compatible with 2D and 3D surfaces of arbitrary chemical composition." Lab on a Chip **15**(9): 2009-2017.
Kong, F., L. Yuan, Y. F. Zheng and W. Chen (2012). "Automatic Liquid Handling for Life Science: A Critical Review of the Current State of the Art." Journal of Laboratory Automation **17**(3): 169-185.
Kovacs, G. T. (1998). Micromachined transducers sourcebook, WCB/McGraw-Hill New York.
Krauss, R. W. (2014). Evaluation of a Low-Cost Microcontroller for Real-Time Control Education and Prototyping. ASME 2014 Dynamic Systems and Control Conference, American Society of Mechanical Engineers.
Kuczenski, B., P. R. LeDuc and W. C. Messner (2007). "Pressure-driven spatiotemporal control of the laminar flow interface in a microfluidic network." Lab on a Chip **7**(5): 647-649.
Kuczenski, R. S., H. C. Chang and A. Revzin (2011). "Dielectrophoretic microfluidic device for the continuous sorting of Escherichia coli from blood cells." Biomicrofluidics **5**(3).
Kumamoto, J., H. Kitahata, M. Goto, M. Nagayama and M. Denda (2015). "Effects of medium flow on axon growth with or without nerve growth factor." Biochemical and Biophysical Research Communications **465**(1): 26-29.
Kundu, P. K., I. M. Cohen and D. R. Dowling (2012). Fluid mechanics, Waltham, MA Academic Press.
Lamberti, A., A. Sacco, S. Bianco, E. Giuri, M. Quaglio, A. Chiodoni and E. Tresso (2011). "Microfluidic sealing and housing system for innovative dye-sensitized solar cell architecture." Microelectronic Engineering **88**(8): 2308-2310.
Langelier, S. M., E. Livak-Dahl, A. J. Manzo, B. N. Johnson, N. G. Walter and M. A. Burns (2011). "Flexible casting of modular self-aligning microfluidic assembly blocks." Lab on a Chip **11**(9): 1679-1687.
Laverty, D. M., J. Hastings and X. Zhao (2017). An open source analogue to digital converter for power system measurements with time synchronisation. Instrumentation and Measurement Technology Conference (I2MTC), 2017 IEEE International, IEEE.
Leclerc, E., Y. Sakai and T. Fujii (2003). "Cell culture in 3-dimensional microfluidic structure of PDMS (polydimethylsiloxane)." Biomedical microdevices **5**(2): 109-114.
Lee, E. and S. Neuendorffer (2004). Classes and subclasses in actor-oriented design. Formal Methods and Models for Co-Design, 2004. MEMOCODE'04. Proceedings. Second ACM and IEEE International Conference on, IEEE.
Lee, E. A. (2003). Model-driven development-from object-oriented design to actor-oriented design. Workshop on Software Engineering for Embedded Systems: From Requirements to Implementation (aka The Monterey Workshop), Chicago.
Lee, J. N., C. Park and G. M. Whitesides (2003). "Solvent compatibility of poly (dimethylsiloxane)-based microfluidic devices." Analytical chemistry **75**(23): 6544-6554.
Lee, N. Y. and B. H. Chung (2009). "Novel Poly(dimethylsiloxane) Bonding Strategy via Room Temperature “Chemical Gluing”." Langmuir **25**(6): 3861-3866.
Leung, K., H. Zahn, T. Leaver, K. M. Konwar, N. W. Hanson, A. P. Page, C. C. Lo, P. S. Chain, S. J. Hallam and C. L. Hansen (2012). "A programmable droplet-based microfluidic device applied to multiparameter analysis of single microbes and microbial communities." Proc Natl Acad Sci U S A **109**(20): 7665-7670.

Li, N., C. H. Hsu and A. Folch (2005). "Parallel mixing of photolithographically defined nanoliter volumes using elastomeric microvalve arrays." Electrophoresis **26**(19): 3758-3764.
Li, Z., S. Y. Mak, A. Sauret and H. C. Shum (2014). "Syringe-pump-induced fluctuation in all-aqueous microfluidic system implications for flow rate accuracy." Lab Chip **14**(4): 744-749.
Lin, Y., X. Yu, Z. Wang, S.-T. Tu and Z. Wang (2012). "Laminar flow diffusion interface control in a microchannel with accurate Raman measurement." Chemical Engineering and Processing: Process Intensification **57-58**: 1-7.
Linder, V., S. K. Sia and G. M. Whitesides (2005). "Reagent-loaded cartridges for valveless and automated fluid delivery in microfluidic devices." Analytical chemistry **77**(1): 64-71.
Liou, D.-S., Y.-F. Hsieh, L.-S. Kuo, C.-T. Yang and P.-H. Chen (2010). "Modular component design for portable microfluidic devices." Microfluidics and Nanofluidics **10**(2): 465-474.
Liu, A.-l., F.-y. He, K. Wang, T. Zhou, Y. Lu and X.-h. Xia (2005). "Rapid method for design and fabrication of passive micromixers in microfluidic devices using a direct-printing process." Lab on a Chip **5**(9): 974-978.
Liu, C., J. Wu, J. Li, L. Ren, J. Tong and A. Arnell (2006). "Tribological behaviours of PA/UHMWPE blend under dry and lubricating condition." Wear **260**(1): 109-115.
Liu, J., J. Eker, J. W. Janneck, X. Liu and E. A. Lee (2004). "Actor-oriented control system design: A responsible framework perspective." IEEE Transactions on Control Systems Technology **12**(2): 250-262.
Liu, M., J. Sun and Q. Chen (2009). "Influences of heating temperature on mechanical properties of polydimethylsiloxane." Sensors and Actuators A: Physical **151**(1): 42-45.
Liu, Y. X., L. G. Chen and L. N. Sun (2009). "Design and Fabrication of a MEMS Flow Sensor and Its Application in Precise Liquid Dispensing." Sensors **9**(6): 4138-4150.
Ly, J., M. Masterman-Smith, R. Ramakrishnan, J. Sun, B. Kokubun and R. M. van Dam (2013). "Automated Reagent-Dispensing System for Microfluidic Cell Biology Assays." Journal of laboratory automation: 2211068213504758.
Mai, T. D., T. T. T. Pham, H. V. Pham, J. Sáiz, C. G. Ruiz and P. C. Hauser (2013). "Portable capillary electrophoresis instrument with automated injector and contactless conductivity detection." Analytical chemistry **85**(4): 2333-2339.
Marlin, T. E. and T. Marlin (1995). Process control: designing processes and control systems for dynamic performance, McGraw-Hill New York.
Marques, M. P. and P. Fernandes (2011). "Microfluidic devices: useful tools for bioprocess intensification." Molecules **16**(10): 8368-8401.
Martínez-López, J. I., H. Betancourt, E. García-López, C. A. Rodriguez and H. R. Siller (2017). "Rapid Fabrication of Disposable Micromixing Arrays Using Xurography and Laser Ablation." Micromachines **8**(5): 144.
Masters, B. R., P. T. So and W. W. Mantulin (2009). "Handbook of Biomedical Nonlinear Optical Microscopy." Journal of Biomedical Optics **14**(1): 9901.
McDonald, J. C. and G. M. Whitesides (2002). "Poly (dimethylsiloxane) as a material for fabricating microfluidic devices." Accounts of chemical research **35**(7): 491-499.
Meier, S. J., T. A. Hatton and D. I. C. Wang (1999). "Cell death from bursting bubbles: Role of cell attachment to rising bubbles in sparged reactors." Biotechnology and Bioengineering **62**(4): 468-478.
Melin, J. and S. R. Quake (2007). "Microfluidic large-scale integration: the evolution of design rules for biological automation." Annu Rev Biophys Biomol Struct **36**: 213-231.
Meyvantsson, I., J. W. Warrick, S. Hayes, A. Skoien and D. J. Beebe (2008). "Automated cell culture in high density tubeless microfluidic device arrays." Lab on a Chip **8**(5): 717-724.

Millet, L. J., M. E. Stewart, J. V. Sweedler, R. G. Nuzzo and M. U. Gillette (2007). "Microfluidic devices for culturing primary mammalian neurons at low densities." Lab Chip **7**(8): 987-994.
Minhass, W. H., P. Pop, J. Madsen and F. S. Blaga (2012). Architectural synthesis of flow-based microfluidic large-scale integration biochips. Proceedings of the 2012 international conference on Compilers, architectures and synthesis for embedded systems. Tampere, Finland, ACM**:** 181-190.
Minhass, W. H., P. Pop, J. Madsen and T.-Y. Ho (2013). Control synthesis for the flow-based microfluidic large-scale integration biochips. Design Automation Conference (ASP-DAC), 2013 18th Asia and South Pacific, IEEE.
Miró, M. and W. Frenzel (2004). "What Flow Injection has to Offer in the Environmental Analytical Field." Microchimica Acta **148**(1-2): 1-20.
Mohan, R., B. R. Schudel, A. V. Desai, J. D. Yearsley, C. A. Apblett and P. J. A. Kenis (2011). "Design considerations for elastomeric normally closed microfluidic valves." Sensors and Actuators B: Chemical **160**(1): 1216-1223.
Muller, L., M. Mohammed and J. W. Kimball (2015). Using the Arduino Uno to teach digital control of power electronics. Control and Modeling for Power Electronics (COMPEL), 2015 IEEE 16th Workshop on, IEEE.
Nam-Trung, N. and W. Zhigang (2005). "Micromixers—a review." Journal of Micromechanics and Microengineering **15**(2): R1.
Neuži, P., S. Giselbrecht, K. Länge, T. J. Huang and A. Manz (2012). "Revisiting lab-on-a-chip technology for drug discovery." Nature reviews Drug discovery **11**(8): 620-632.
Ng, A., U. Uddayasankar and A. Wheeler (2010). "Immunoassays in microfluidic systems." Analytical and Bioanalytical Chemistry **397**(3): 991-1007.
Nguyen, N.-T. and S. T. Wereley (2006). Fundamentals and applications of microfluidics / Nam-Trung Nguyen, Steven T. Wereley, Artech House.
Niman, C. S., J. P. Beech, J. O. Tegenfeldt, P. M. Curmi, D. N. Woolfson, N. R. Forde and H. Linke (2013). "Controlled microfluidic switching in arbitrary time-sequences with low drag." Lab on a Chip **13**(12): 2389-2396.
Oh, K. W. and C. H. Ahn (2006). "A review of microvalves." Journal of Micromechanics and Microengineering **16**(5): R13.
Piccin, E., D. Ferraro, P. Sartori, E. Chiarello, M. Pierno and G. Mistura (2014). "Generation of water-in-oil and oil-in-water microdroplets in polyester-toner microfluidic devices." Sensors and Actuators B: Chemical **196**: 525-531.
Pinto, E., V. Faustino, R. O. Rodrigues, D. Pinho, V. Garcia, J. M. Miranda and R. Lima (2014). "A rapid and low-cost nonlithographic method to fabricate biomedical microdevices for blood flow analysis." Micromachines **6**(1): 121-135.
Quake, S. R. (2007). "Versatile, fully automated, microfluidic cell culture system." Analytical chemistry **79**(22): 8557-8563.
Rane, T. D., H. C. Zec and T.-H. Wang (2012). "A Serial Sample Loading System Interfacing Multiwell Plates with Microfluidic Devices." Journal of Laboratory Automation **17**(5): 370-377.
Ranger, C. B. (1981). "Flow injection analysis. Principles, techniques, applications, design." Analytical Chemistry **53**(1): 20A-32A.
Ren, K., J. Zhou and H. Wu (2013). "Materials for microfluidic chip fabrication." Accounts of chemical research **46**(11): 2396-2406.
Rhee, M. and M. A. Burns (2008). "Microfluidic assembly blocks." Lab on a Chip **8**(8): 1365-1373.
Rogatsky, E., K. Braaten, G. Cruikshank, H. Jayatillake, B. Zheng and D. T. Stein (2009). "Flow inconsistency: The evil twin of column switching—Hardware aspects." Journal of Chromatography A **1216**(45): 7721-7727.
Rohde, C. B., F. Zeng, R. Gonzalez-Rubio, M. Angel and M. F. Yanik (2007). "Microfluidic system for on-chip high-throughput whole-animal sorting and screening

at subcellular resolution." Proceedings of the National Academy of Sciences **104**(35): 13891-13895.
Sabourin, D., P. Skafte-Pedersen, M. J. Soe, M. Hemmingsen, M. Alberti, V. Coman, J. Petersen, J. Emneus, J. P. Kutter, D. Snakenborg, F. Jorgensen, C. Clausen, K. Holmstrom and M. Dufva (2013). "The MainSTREAM component platform: a holistic approach to microfluidic system design." J Lab Autom **18**(3): 212-228.
Sackmann, E. K., A. L. Fulton and D. J. Beebe (2014). "The present and future role of microfluidics in biomedical research." Nature **507**(7491): 181-189.
Samuel, R., C. Thacker, A. V. Maricq and B. K. Gale (2014). "Simple and cost-effective fabrication of microvalve arrays in PDMS using laser cut molds with application to C. elegans manipulation in microfluidics." Journal of Micromechanics and Microengineering **24**(10): 105007.
Satyanarayana, S., R. N. Karnik and A. Majumdar (2005). "Stamp-and-stick room-temperature bonding technique for microdevices." Microelectromechanical Systems, Journal of **14**(2): 392-399.
Scott, A., A. K. Au, E. Vinckenbosch and A. Folch (2013). "A microfluidic D-subminiature connector." Lab on a Chip **13**(11): 2036-2039.
See, H. H. and P. C. Hauser (2014). "Automated Electric-Field-Driven Membrane Extraction System Coupled to Liquid Chromatography–Mass Spectrometry." Analytical chemistry **86**(17): 8665-8670.
Shaikh, K. A., K. S. Ryu, E. D. Goluch, J.-M. Nam, J. Liu, C. S. Thaxton, T. N. Chiesl, A. E. Barron, Y. Lu and C. A. Mirkin (2005). "A modular microfluidic architecture for integrated biochemical analysis." Proceedings of the National Academy of Sciences of the United States of America **102**(28): 9745-9750.
Sin, M. L., J. Gao, J. C. Liao and P. K. Wong (2011). "System Integration - A Major Step toward Lab on a Chip." J Biol Eng **5**: 6.
Skafte-Pedersen, P., C. G. Sip, A. Folch and M. Dufva (2013). "Modular microfluidic systems using reversibly attached PDMS fluid control modules." Journal of Micromechanics and Microengineering **23**(5): 055011.
Skoog, L. and E. Tani (2011). "Immunocytochemistry: an indispensable technique in routine cytology." Cytopathology **22**(4): 215-229.
Soe, A. K., S. Nahavandi and K. Khoshmanesh (2012). "Neuroscience goes on a chip." Biosensors and Bioelectronics **35**(1): 1-13.
Squires, T. M. and S. R. Quake (2005). "Microfluidics: Fluid physics at the nanoliter scale." Reviews of modern physics **77**(3): 977.
Stone, H. A. and S. Kim (2001). "Microfluidics: Basic issues, applications, and challenges." AIChE Journal **47**(6): 1250-1254.
Stone, H. A., A. D. Stroock and A. Ajdari (2004). "Engineering flows in small devices: microfluidics toward a lab-on-a-chip." Annu. Rev. Fluid Mech. **36**: 381-411.
Streets, A. M. and Y. Huang (2013). "Chip in a lab: Microfluidics for next generation life science research." Biomicrofluidics **7**(1): 11302.
Sui, G., W. Zhong, X. Ren, X. Wang and X. Yang (2009). "Structure, mechanical properties and friction behavior of UHMWPE/HDPE/carbon nanofibers." Materials Chemistry and Physics **115**(1): 404-412.
Sun, J., P. Chen, X. Feng, W. Du and B.-F. Liu (2011). "Development of a microfluidic cell-based biosensor integrating a millisecond chemical pulse generator." Biosensors and Bioelectronics **26**(8): 3413-3419.
Sundberg, S. A. (2000). "High-throughput and ultra-high-throughput screening: solution-and cell-based approaches." Current opinion in biotechnology **11**(1): 47-53.
Sung, J. H. and M. L. Shuler (2009). "Prevention of air bubble formation in a microfluidic perfusion cell culture system using a microscale bubble trap." Biomedical microdevices **11**(4): 731-738.
Tabeling, P. (2005). Introduction to microfluidics / Patrick Tabeling ; translated by Suelin Chen, Oxford University Press.

Takayama, S., E. Ostuni, P. LeDuc, K. Naruse, D. E. Ingber and G. M. Whitesides (2001). "Subcellular positioning of small molecules." Nature **411**(6841): 1016.
Taljaard, R. E. and J. Van Staden (1998). "Application of sequential-injection analysis as process analyzers." Laboratory Robotics and Automation **10**(6): 325-337.
Tan, A., K. Rodgers, J. P. Murrihy, C. O'Mathuna and J. D. Glennon (2001). "Rapid fabrication of microfluidic devices in poly (dimethylsiloxane) by photocopyingPresented at the 14th International Symposium on Microscale Separations and Analysis, Boston, January 13–18, 2001." Lab on a Chip **1**(1): 7-9.
Tang, L. and N. Y. Lee (2010). "A facile route for irreversible bonding of plastic-PDMS hybrid microdevices at room temperature." Lab Chip **10**(10): 1274-1280.
Tanzi, S., M. Matteucci, T. L. Christiansen, S. Friis, M. T. Christensen, J. Garnaes, S. Wilson, J. Kutchinsky and R. Taboryski (2013). "Ion channel recordings on an injection-molded polymer chip." Lab on a Chip **13**(24): 4784-4793.
Taylor, G. (1953). "Dispersion of Soluble Matter in Solvent Flowing Slowly through a Tube." Proceedings of the Royal Society of London. Series A. Mathematical and Physical Sciences **219**(1137): 186-203.
Teh, S.-Y., R. Lin, L.-H. Hung and A. P. Lee (2008). "Droplet microfluidics." Lab on a Chip **8**(2): 198-220.
Tehranirokh, M., A. Z. Kouzani, P. S. Francis and J. R. Kanwar (2013). "Microfluidic devices for cell cultivation and proliferation." Biomicrofluidics **7**(5): 051502.
Temiz, Y., R. D. Lovchik, G. V. Kaigala and E. Delamarche (2015). "Lab-on-a-chip devices: How to close and plug the lab?" Microelectronic Engineering **132**: 156-175.
Thompson, B. L., Y. Ouyang, G. R. Duarte, E. Carrilho, S. T. Krauss and J. P. Landers (2015). "Inexpensive, rapid prototyping of microfluidic devices using overhead transparencies and a laser print, cut and laminate fabrication method." Nature protocols **10**(6): 875-886.
Thompson, C. S. and A. R. Abate (2013). "Adhesive-based bonding technique for PDMS microfluidic devices." Lab on a Chip **13**(4): 632-635.
Thorsen, T., S. J. Maerkl and S. R. Quake (2002). "Microfluidic Large-Scale Integration." Science **298**(5593): 580-584.
Timoney, C. and R. Felder (1999). "Biochip Technology of the Future—Today!" Journal of the Association for Laboratory Automation **4**(4): 86-89.
Ting, H., J.-B. Hu, K.-T. Hsieh and P. L. Urban (2014). "A pinch-valve interface for automated sampling and monitoring of dynamic processes by gas chromatography-mass spectrometry." Analytical Methods **6**(13): 4652-4660.
Tsao, C.-W. and D. L. DeVoe (2008). "Bonding of thermoplastic polymer microfluidics." Microfluidics and Nanofluidics **6**(1): 1-16.
Unger, M. A., H.-P. Chou, T. Thorsen, A. Scherer and S. R. Quake (2000). "Monolithic microfabricated valves and pumps by multilayer soft lithography." Science **288**(5463): 113-116.
Urban, P. L. (2015). "Universal electronics for miniature and automated chemical assays." Analyst **140**(4): 963-975.
van Staden, J. K. F. (2015). "Application of phthalocyanines in flow-and sequential-injection analysis and microfluidics systems: A review." Talanta **139**: 75-88.
vanVarseveld, R. B. and G. M. Bone (1997). "Accurate position control of a pneumatic actuator using on/off solenoid valves." Ieee-Asme Transactions on Mechatronics **2**(3): 195-204.
Vekemans, K., L. Rosseel, E. Wisse and F. Braet (2004). "Immuno-localization of Fas and FasL in rat hepatic endothelial cells: influence of different fixation protocols." Micron **35**(4): 303-306.
Volpatti, L. R. and A. K. Yetisen (2014). "Commercialization of microfluidic devices." Trends in biotechnology **32**(7): 347-350.
Waldbaur, A., H. Rapp, K. Lange and B. E. Rapp (2011). "Let there be chip-towards rapid prototyping of microfluidic devices: one-step manufacturing processes." Analytical Methods **3**(12): 2681-2716.

Wang, B., S. Jedlicka and X. Cheng (2014). "Maintenance and Neuronal Cell Differentiation of Neural Stem Cells C17.2 Correlated to Medium Availability Sets Design Criteria in Microfluidic Systems." PLoS ONE **9**(10): e109815.
Wang, J. D., N. J. Douville, S. Takayama and M. ElSayed (2012). "Quantitative Analysis of Molecular Absorption into PDMS Microfluidic Channels." Annals of Biomedical Engineering **40**(9): 1862-1873.
Wang, X. B., J. Yang, Y. Huang, J. Vykoukal, F. F. Becker and P. R. Gascoyne (2000). "Cell separation by dielectrophoretic field-flow-fractionation." Analytical chemistry **72**(0003-2700 (Print)).
Wheeler, A. R., W. R. Throndset, R. J. Whelan, A. M. Leach, R. N. Zare, Y. H. Liao, K. Farrell, I. D. Manger and A. Daridon (2003). "Microfluidic device for single-cell analysis." Analytical chemistry **75**(14): 3581-3586.
White, F. M. (1991). Viscous Fluid Flow. New York, McGraw-Hill.
White, F. M. (2008). Fluid mechanics, McGraw-Hill Higher Education.
Whitesides, G. M. (2006). "The origins and the future of microfluidics." Nature **442**(7101): 368-373.
Wu, J. and N. Y. Lee (2014). "One-step surface modification for irreversible bonding of various plastics with a poly(dimethylsiloxane) elastomer at room temperature." Lab on a Chip **14**(9): 1564-1571.
Xiao, Z., M. Niu and B. Zhang (2012). "Droplet microfluidics based microseparation systems." Journal of separation science **35**(10-11): 1284-1293.
Yamada, A., Y. Katanosaka, S. Mohri and K. Naruse (2009). "A rapid microfluidic switching system for analysis at the single cellular level." NanoBioscience, IEEE Transactions on **8**(4): 306-311.
Yaxin, L., L. Chen, S. Lining and R. Weibin (2009). A self-adjusted precise liquid handling system. Robotics and Automation, 2009. ICRA '09. IEEE International Conference on.
Yetisen, A. K. and L. R. Volpatti (2014). "Patent protection and licensing in microfluidics." Lab on a Chip **14**(13): 2217-2225.
Young, E. W. and D. J. Beebe (2010). "Fundamentals of microfluidic cell culture in controlled microenvironments." Chemical Society Reviews **39**(3): 1036-1048.
Yuen, P. K. (2008). "SmartBuild-a truly plug-n-play modular microfluidic system." Lab Chip **8**(8): 1374-1378.
Yuen, P. K., L. J. Kricka and P. Wilding (2000). "Semi-disposable microvalves for use with microfabricated devices or microchips." Journal of Micromechanics and Microengineering **10**(3): 401.
Zeng, W., I. Jacobi, D. J. Beck, S. Li and H. A. Stone (2015). "Characterization of syringe-pump-driven induced pressure fluctuations in elastic microchannels." Lab on a Chip **15**(4): 1110-1115.
Zotou, A. (2012). "An overview of recent advances in HPLC instrumentation." Central European Journal of Chemistry **10**(3): 554-569.
Zurek, S., P. Marketos and A. J. Moses (2007). "LabVIEW as a tool for measurements, batch data manipulations and artificial neural network predictions." Przeglad Elektrotechniczny **83**(4): 114-119.

9. Appendices

9.1 Full consumables / equipment / software list

Chemicals used

Name	Company	Cat. No.
Neurobasal buffer solution	Invitrogen	21103-049
Neurobasal B27 supplement	Invitrogen	17504-044
Phosphate buffered saline (tablets)	Sigma Aldrich	
Poly-L-Lysine 0.01% (PLL)	Sigma Aldrich	P4707
Penicillin-Streptomycin	Sigma Aldrich	G1146
L-Glutamine growth factor	Sigma Aldrich	G7513
11-amino-1-undecanethiol (AUT)	Sigma Aldrich	674397
ACS grade anhydrous Ethanol	Sigma Aldrich	458-600
(3-mercaptopropyl) trimethoxysilane (MPTS)	Sigma Aldrich	175617
Anhydrous Toluene	Sigma Aldrich	244511
Fluorescein	Sigma Aldrich	F-6377
(3-Aminopropyl) trimethoxysilane **(APTMS)**	Sigma Aldrich	281778
(3-Glycidyloxypropyl) trimethoxysilane (GPTMS)	Sigma Aldrich	440167
Poly[dimethysiloxane-co-(3-aminopropyl)-methysiloxane]	Sigma Aldrich	480304
Paraformaldehyde	Sigma Aldrich	
Olive oil	Sigma Aldrich	
Mineral oil	Sigma Aldrich	
SU-8 2050 photoresist	Microchemicals GmbH	Ordered by physics cleanroom
SU-8 2005 photoresist	Microchemicals GmbH	
BPR100 photoresist	Shipley	
AZ6612 photoresist	Microchemicals GmbH	
AZ400K MIF developer	Microchemicals GmbH	
AZ5214E Image Reverse photoresist	Microchemicals GmbH	

Consumables used

Name	Company	Cat. No.
Glass coverslips 19mm, grade 1,5	Glaswarenfabrik Karl Hecht GmbH & Co KG	1001/19_15
Glass slides 25 x 75mm		
Glass slides 80 x 80mm x 1.2	Richardsons of Leicester	M2946
Poly(dimethylsiloxane)	Dow Corning	Sylgard 184
Polycarbonate porous membrane 0.1µm pore x 47mm	Whatman Cyclopore	7060-4701
Silicon Wafers [100]	Pi-Kem Ltd	n/a, to order

Oxygen N2 free	BOC Gases Ltd	UN1072
Nitrogen O2 free	BOC Gases Ltd	UN1066
CO2 vapour	BOC Gases Ltd	UN1013
5% CO2 / balance room air	BOC Gases Ltd	225742
Biopsy Punch	Harris Uni-Core	0.5, 1.5, 3mm

Components and equipment

Component	Company	Model / Cat. No.
Liquid Auto Sampler	Jasco	AS1150
Vacuum Pump	Becker	D-42279
	Pfiefer	DUO 2.5
	Spin coater	
Pressure Pump	Thorlabs	
	Clippard	EV-PM-05-6025
Proportional Air Flow valves	IMI Norgren Ltd	12-216C-04520 +EQIFIL+BED
Relief valves	IMI Norgren Ltd	1002/BM000
HPLC PEEK bulkheads	Thames Restek	VIZBU.5FPK
HPLC PEEK tubing	Kinesis	1568 / 1572
Pressure transducers	GE Druck	PMP 5074
Flow rate sensors	Elveflow, Elvesys	Mass flow sensor 2 (7µL/min)
	Sensirion AG	SLG1430-150
	IMI Norgren Ltd	RM1L-NND-NCV
Pressure regulators	IMI Norgren Ltd	11-818-100
	Proportion-Air	QVP1TFEE015
Air Solenoid Valves		
Air filter	IMI Norgren Ltd	F72G-2GD-QT1
Air filter 4mm adapter	IMI Norgren Ltd	C02250428
Air filter 6mm adapter	IMI Norgren Ltd	C02250628
Micro electrode arrays	Multi-Channel Systems	200/30iR-Ti
		200/30iR-Ti-gr
Stirrer		
Spin coater	SPS Europe	Spin150
Plasma Oven	Diener	Zepto
CCD Camera	Point Grey Research	Grasshopper 2
CCD Camera	Hamamatsu	Orca C11440-22CU
Inverted microscope	Brunel Microscopes	SP99F
Inverted microscope	Nikon, Tokyo	Eclipse Ti-U
Objective Lens	Olympus	
	Nikon, Tokyo	
Dissection microscope	Brunel Microscopes	IMXZ
Power supply	Thurlby Thandar Instruments (TTi)	TTi PL303QMD-P
Function Generator		
Oscilloscope		
Data Acquisition Card	National Instruments	USB-6259
	National Instruments	USB-6008 / 6009
Syringe Driver	Cole-Palmer	789210C
Temperature controller	Warner Instruments	TC-434B
Craft Cutter	Graphtec America	Silhouette Cameo

Software

Name	Company	Version
LabVIEW	National Instruments	2012
COMSOL Multiphysics	COMSOL	4.4
Inventor Professional	Autodesk	2013
ImageJ	National Institutes of Health	FIJI
Silhouette Studio	Silhouette America	-
MatLab	Mathworks	R2013a
Eagle PCB Design	CADSoft USA	6.1.0

9.2 Model Predictive Control

While PID algorithms provide a quick and easy way to implement control with minimal knowledge of the system, overshoot and settling times need to be optimised in real time since these may not be identical across the dynamic range of system outputs. The ability to predict the system output given a set of inputs can be applied to produce a set of inputs that produce an output. This is the foundation of model predictive control where a set of inputs are pre-calculated against an event horizon to reach the target system state. First the system model is required, usually as a transfer function or state-space model. This model can then be imported into a Model Predictive Controller (MPC) to realise inputs for targets. The benefit of such a controller is the ability to implement multi-input multi-output or multi-input single-output control with as much ease as single-input single-output. Another benefit is the ability of the controller to adapt in real time to the system dynamics.

System modelling provides information on the system for precise controls to be designed and optimised. Modelling from first principles may not account for system non-linearities and unaccounted dynamics. Also, the iterative steps of confirming the models with real systems make it time consuming for development of real world applications. These along with the presence of high speed acquisition system make it an inefficient method of modelling when compared to online or offline system identification tools available.

9.2.1 System Identification and Modelling

The tools for control design in MATLAB such as the system identification, model predictive controller design, PID tuner allowed quick system estimation, design and deployment of optimum controllers for the pressure control system.

System identification was required to obtain suitable model of the system which would allow an MPC provide faster control of the system. The data-driven system

identification method was preferred over classical mathematical models since the obtained information is based on the experimental data and is more accurate and descriptive of the physical system than models developed from classical approaches. It was also easy to view the changes to the system model caused by changes in the input conditions using this data-driven method.

System identification takes a set of inputs and corresponding outputs to develop a model of the system. A random number generator was used to generate 1000 samples (0 - 1). The numbers were scaled to produce a random sequence of between -100 and 100. This control sequence was introduced to the pressure control plant as an input at different update frequencies (16, 33, and 200 Hz). The algorithm changed this plant input to a corresponding duty cycle value with a minimum and maximum valve operating range set at 0.4 and 0.7 respectively for the pressurisation and depressurisation valves. The single valve control algorithm used to change only one valve at a time depending on the sign of the control signal. The resulting pressure from the plant and the control signal was logged at 200Hz.

The frequency of the input signal affected the response of the system and determined the output range measured when the control signal was applied in Figure 10-1. The models estimated from using the high frequency input output data set could not be used to verify the low frequency data sets. However, the low frequency data sets produced models that gave a good fit when verified against higher frequency data sets.

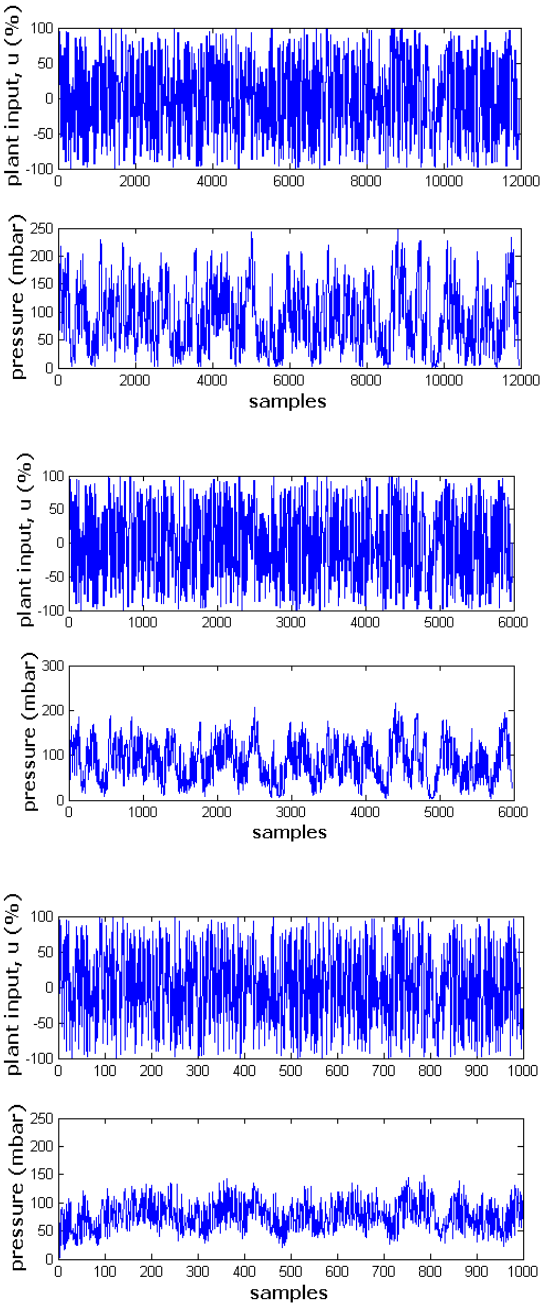

Figure 10-1: Different responses of the system from different input data frequencies
The frequency at which the system is disturbed affects the performance of the system and these frequencies are critical to system stability. The high frequency disturbance at 200Hz causes the system to operate within a small pressure range while the widest pressure range is seen when the 60Hz signal update is used. The input pressure to the plant was 300 mbar.

Further comparison of the effect of the frequency of the control signal was done by comparing the models from the different frequencies against the input output data from the range of frequencies examined. A set of scaled random numbers (n = 1000,

range = -100 to 100) were sent as control signals to the pressure control plant with the operational range of the valves set to (PV = 0.4 – 0.8; DV = 0.4 – 0.8) at an update interval (Δt = 5, 10, 20, 30, 40, 50, 60 ms). The input pressure to the system was set at 500mbar. The input output data was loaded into MATLAB for analysis of the plant model.

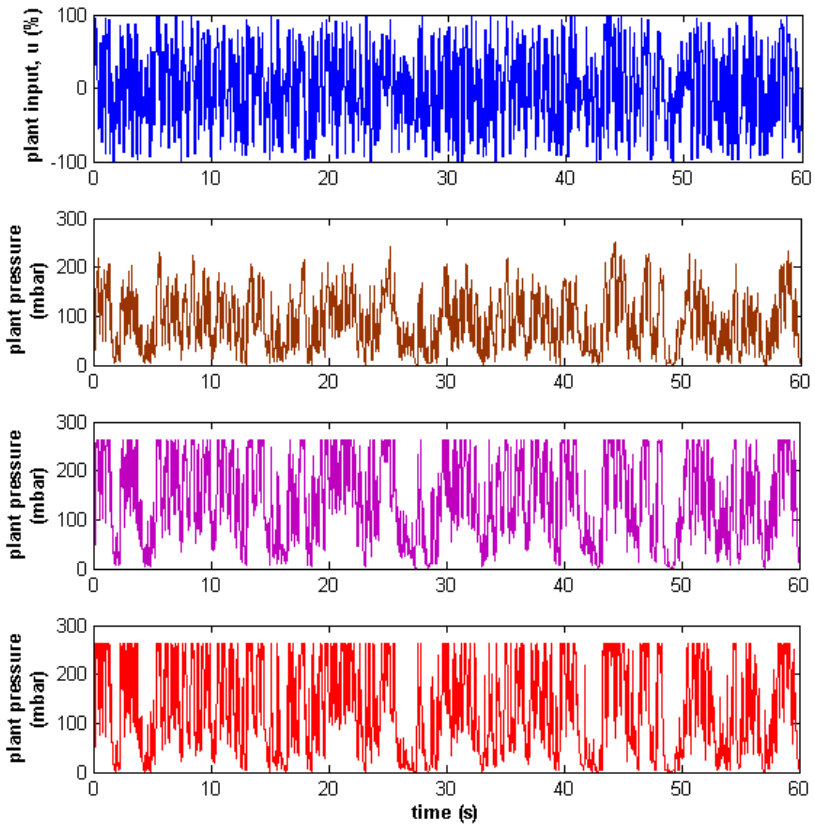

Figure 10-2: Response of the system from different input pressures

The transfer function of the input output data was estimated using the MATLAB system identification tool over different input frequencies and pressures. It was found that a setting of 4 poles and 3 zeros was sufficient to estimate the transfer function of the system for the various input configurations. Figure 10-2 shows the MATLAB system identification application with preloaded input-output data. Each data was dragged to the working data window and then analysed to give the estimated transfer

function models on the right hand side. These models were then compared to the validation data which was sourced by dragging the input output data to the validation data window.

The model fit comparison chart in Figure 10-4 shows how the identified models fit with other input output data used as validation data. Models obtained from lower frequency input output data models can fit the higher frequency verification data but the models from the higher frequency data below 20 ms interval fit poorly to the lower frequency verification data.

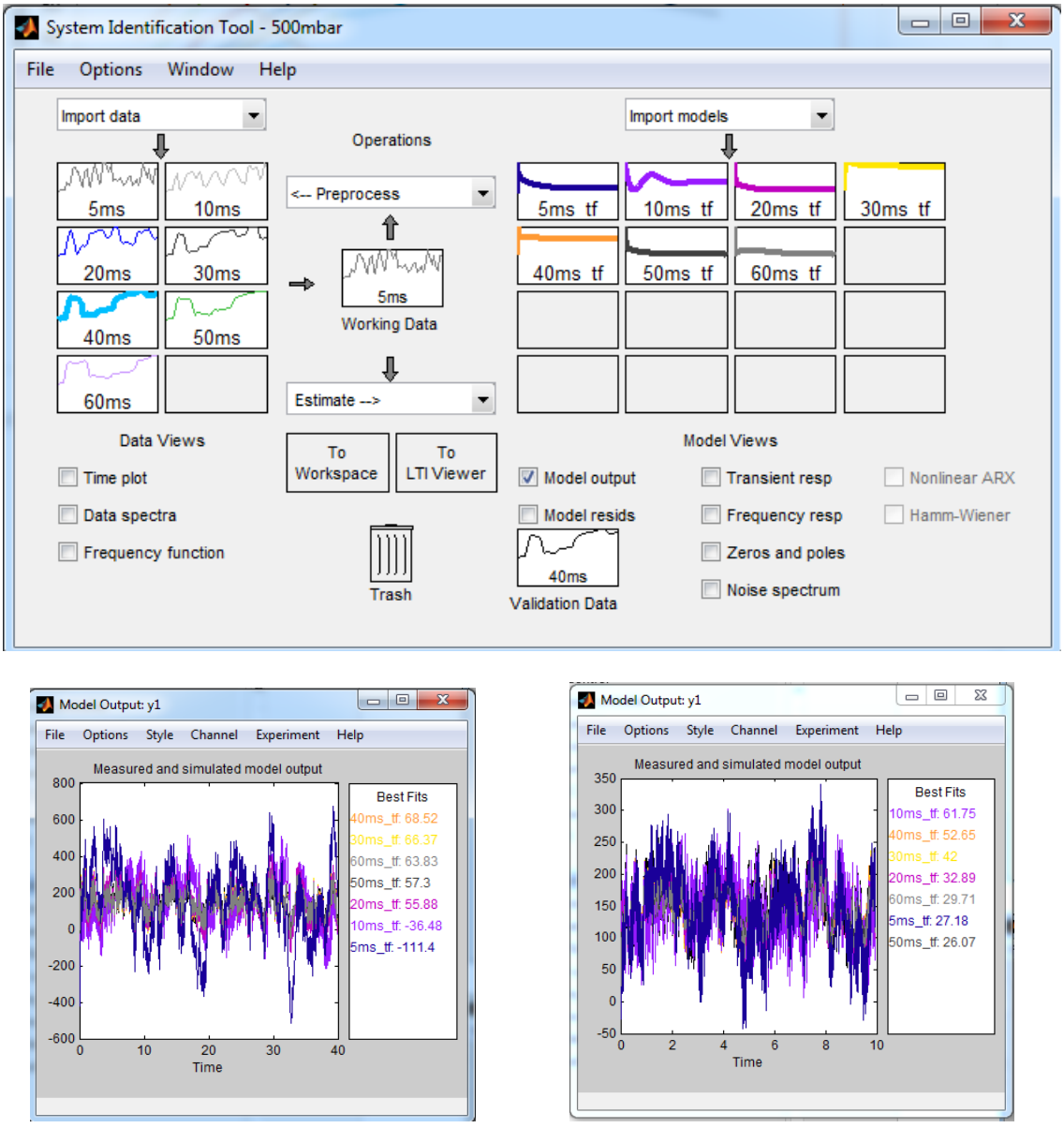

Figure 10-3: System Identification Tool and model output windows for estimation results

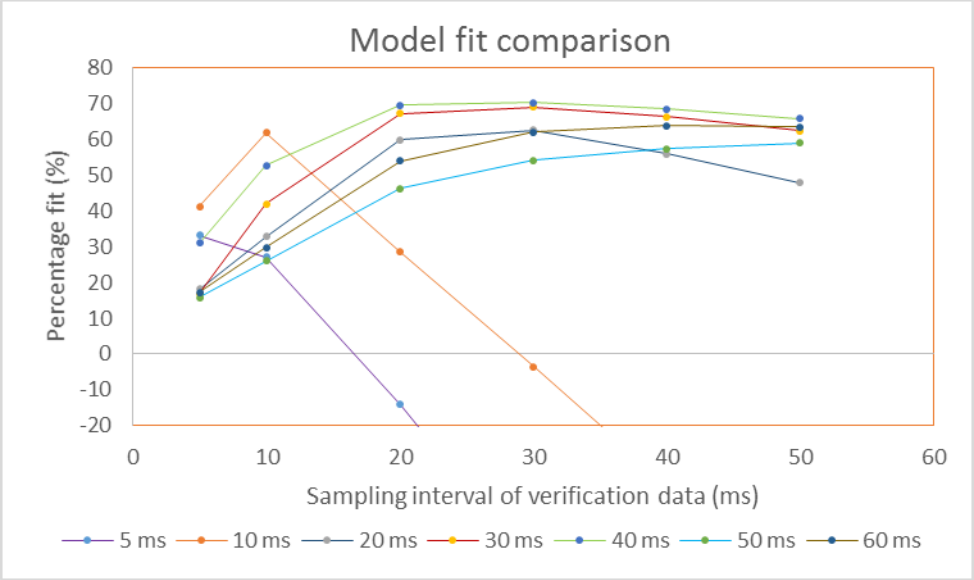

Figure 10-4: Comparison of the results from estimated transfer function models

$$\frac{-59.47\ s^3 + 9263\ s^2 + 3.16e05\ s + 1.96e04}{s^4 + 159.5\ s^3 + 2.034e04\ s^2 + 5.976e04\ s + 111.6}$$

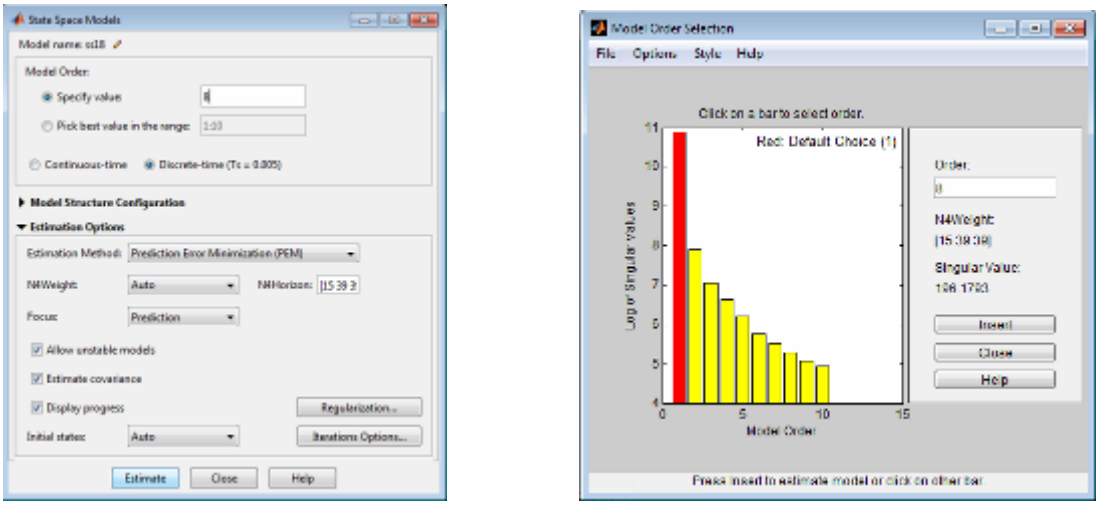

Figure 10-5: State-space model identification window settings
The left image shows settings used to get the best model fit and the right image shows the differences in the model order when the model order is set to pick best value in the range. The system was set as a discrete time model to enable subsequent use in model predictive control.

$$x(k+1) = \begin{bmatrix} 0.998088 & -0.0474113 & 0.0102177 & -0.0363815 & 0.0376604 & 0.0125381 & 0.0014898 & 0.0112643 \\ 0.0602891 & 0.394308 & 0.488594 & -0.443453 & 0.113057 & -0.112002 & 0.137757 & 0.0391205 \\ -0.00501791 & -0.619908 & 0.826618 & 0.237991 & 0.0123881 & 0.0334111 & 0.0061638 & 0.000731224 \\ -0.0521341 & 0.431193 & 0.333771 & -0.0257853 & 0.436153 & 0.277753 & -0.219396 & 0.0586227 \\ -0.0257542 & -0.0641423 & 0.123139 & -0.580122 & -0.690303 & 0.176565 & -0.140097 & -0.108124 \\ 0.0172596 & 0.0884406 & 0.00732308 & 0.152612 & -0.101309 & 0.846263 & 0.600029 & 0.41167 \\ -0.00538592 & 0.0558215 & 0.0253615 & -0.0579352 & 0.00747425 & -0.331536 & 0.357688 & 0.541019 \\ 0.0128676 & -0.00360356 & 0.0605693 & -0.00173005 & -0.0321317 & 0.0737688 & -0.504379 & 0.317376 \end{bmatrix} x(k) + \begin{bmatrix} -1.96627E\text{-}6 \\ -0.000232194 \\ -0.000172151 \\ 0.000437833 \\ 0.000457623 \\ -0.000206056 \\ 0.000170926 \\ 0.000158982 \end{bmatrix} u(k)$$

$$y(k) = \begin{bmatrix} 14412.5 & -54.6461 & 124.315 & -152.087 & 222.433 & 49.9421 & 41.176 & 79.3393 \end{bmatrix} x(k) + \begin{bmatrix} 0 \end{bmatrix} u(k)$$

Figure 10-6: 8th order state-space equation for type A manifold with 500mbar input and 40 ms control signal update rate.

The best state-space model to fit the input-output data was found to be a 9th order model. The procedure to apply the model predictive control requires inserting this model definition into the controller and adjusting the settings like maximum system output which in the case of pressure control is 250 mbar.

This system was not pursued further when good pressure control was realised by improving the loop rate of the system.

9.3 G-SIS Final Prototype Designs

The G-SIS final prototype was comprised of a motor, base stator, bearing, rotor, top stator, and stator clamp. The CAD designs are shown below.

9.3.1 Assembly

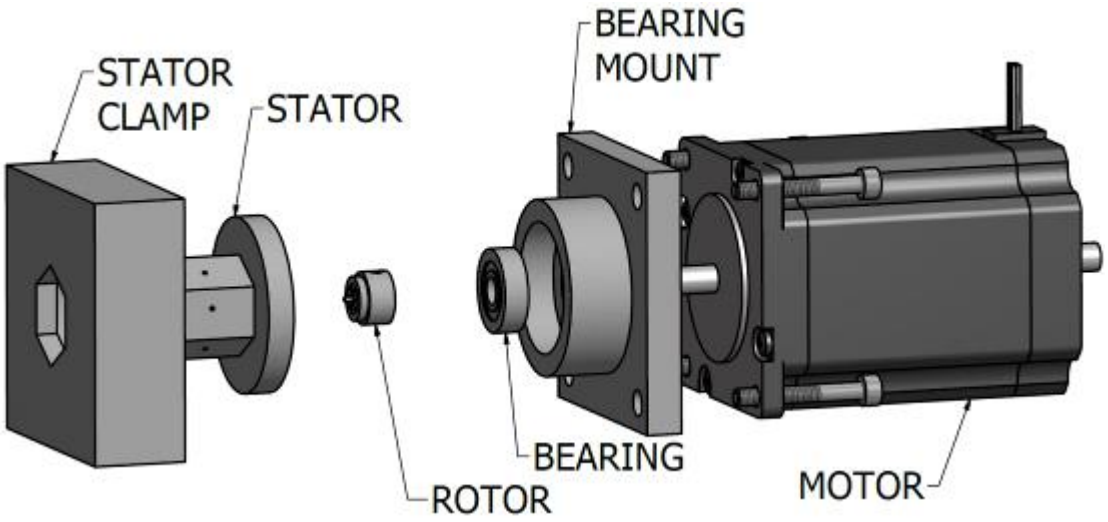

9.3.2 Bearing Mount

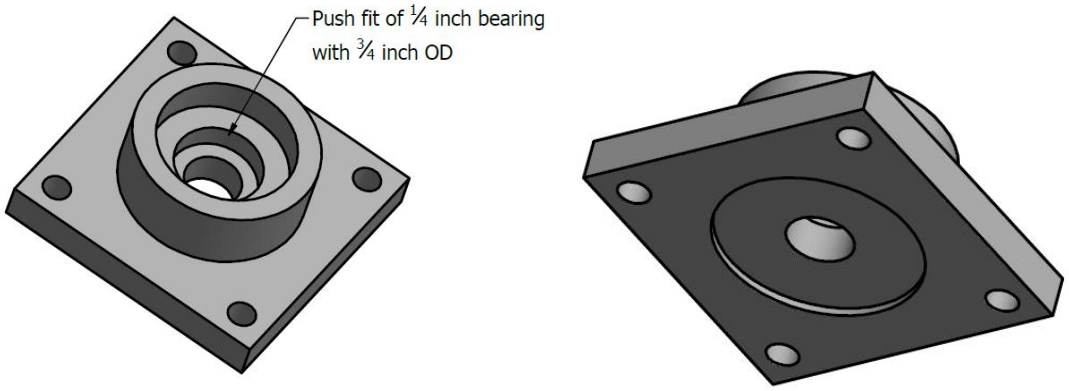

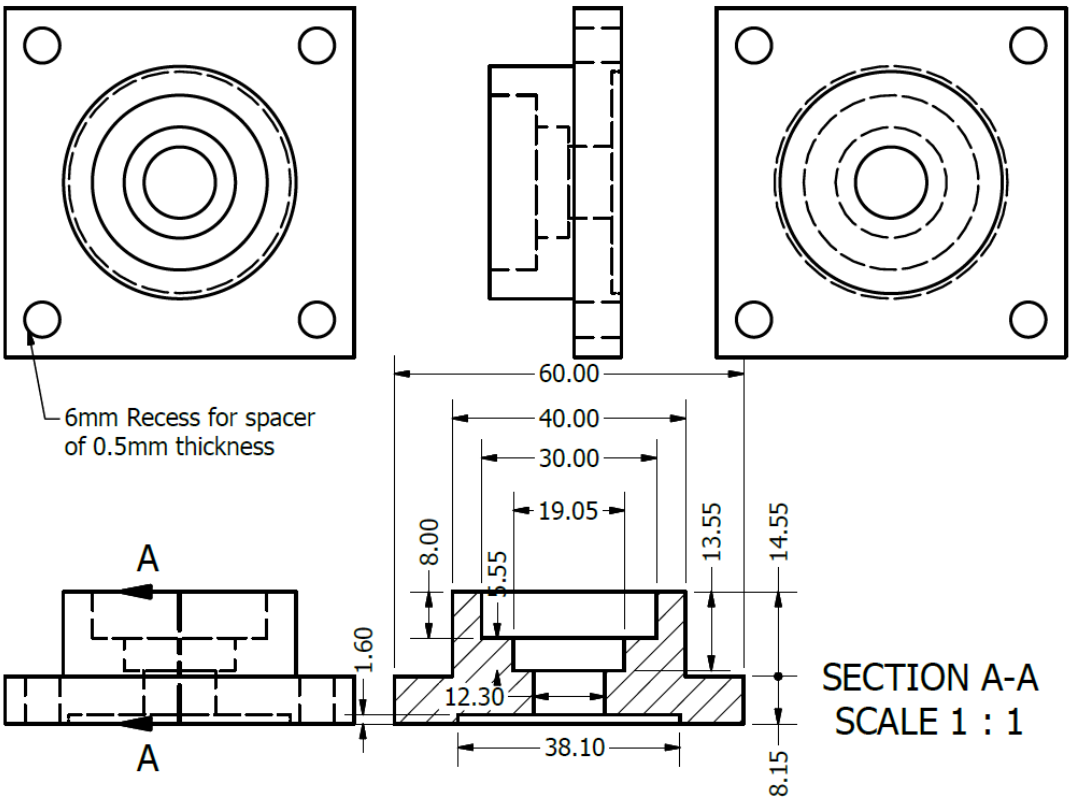

9.3.3 Bearing

RHP Bearings from RadioShack product ID 206-8339

9.3.4 Rotor

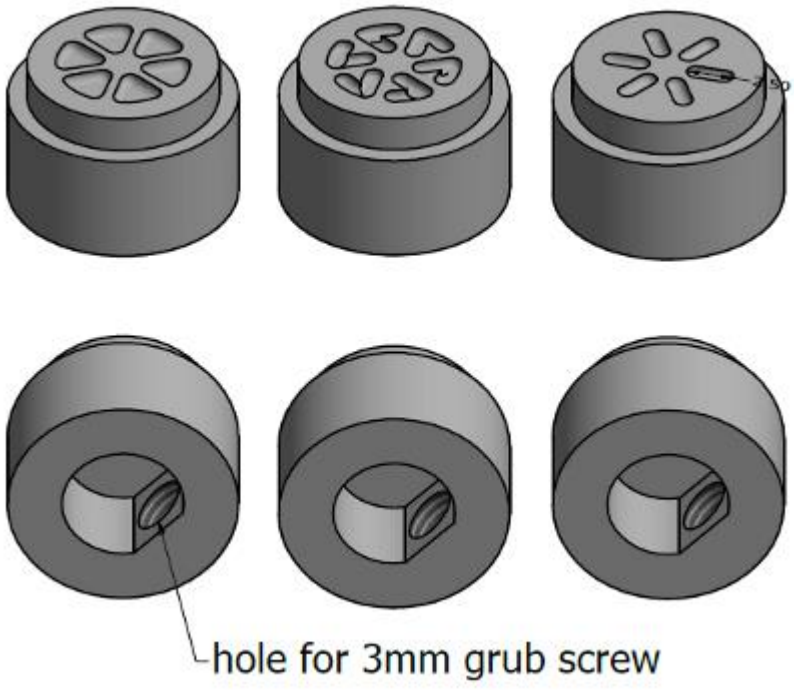

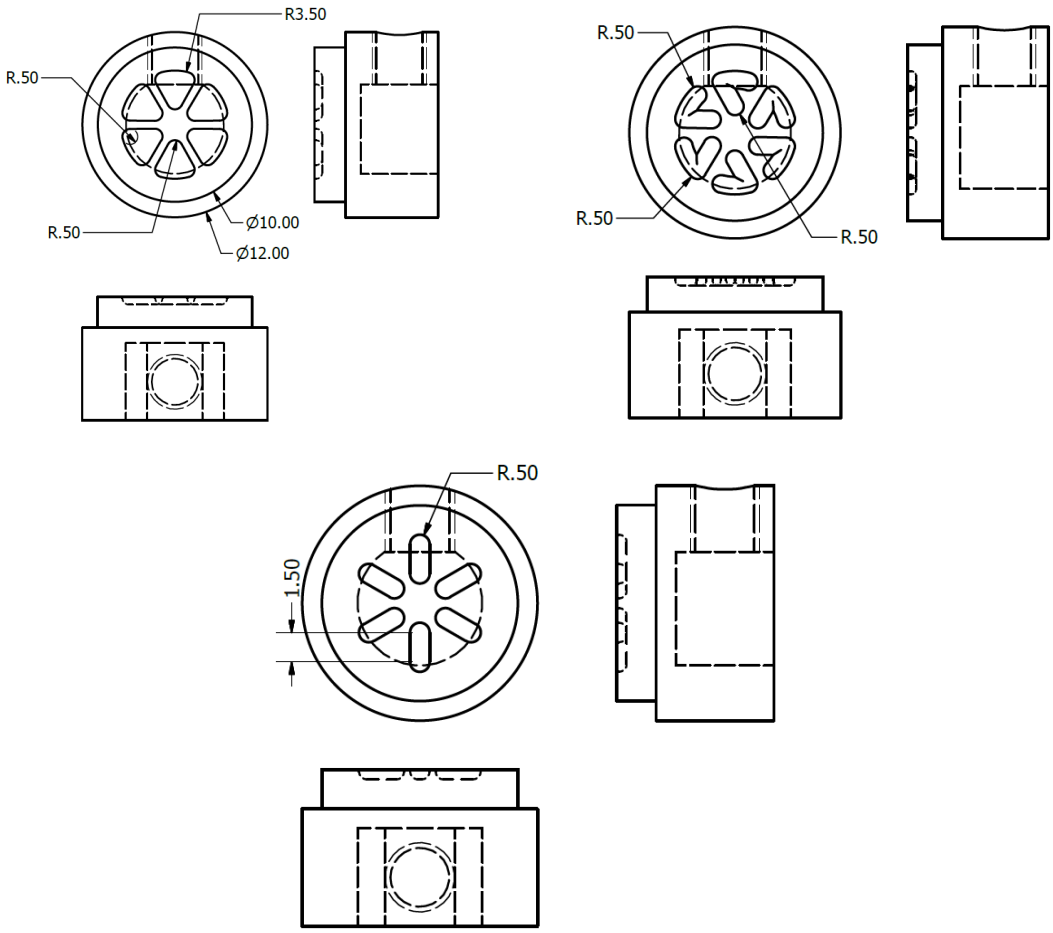

9.3.5 Stator

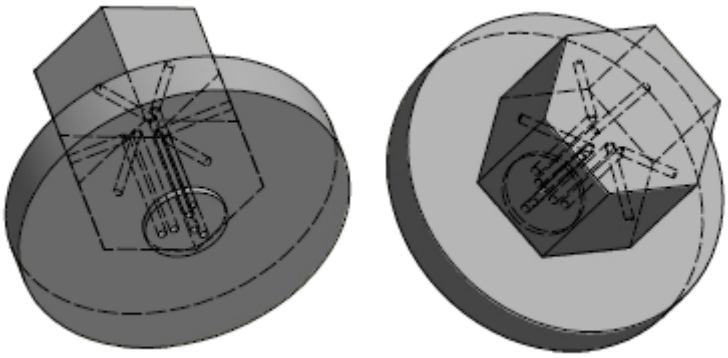

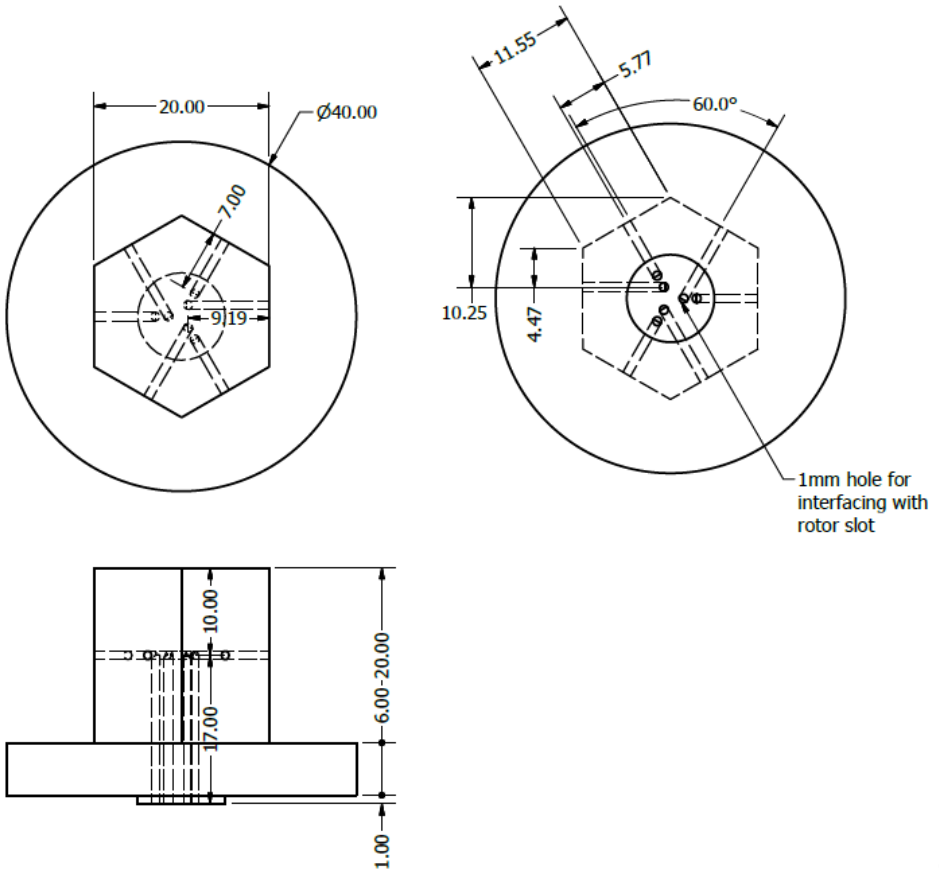

Ø

9.3.6 Stator Mount

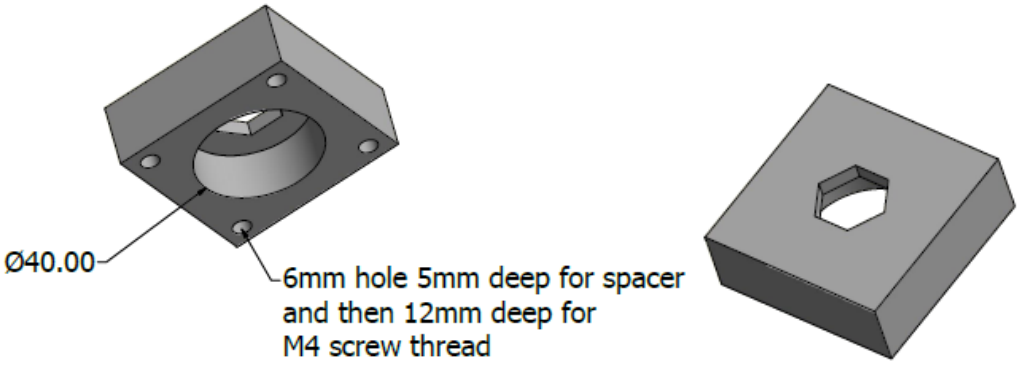

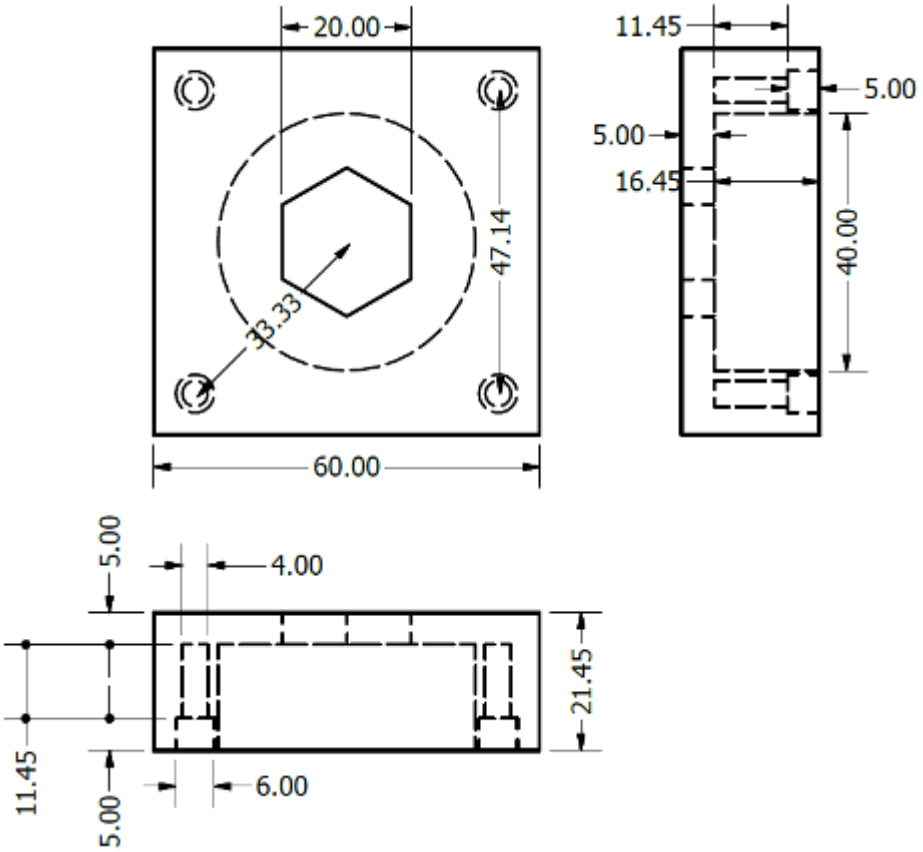
20.00
47.14
33.33
60.00
11.45
5.00
5.00
16.45
40.00
5.00
4.00
21.45
11.45
5.00
6.00